6 3 3 2

FTD-TT- 62-958

401729

TRANSLATION

TRANSACTIONS OF THE PHYSICS INSTITUTE

Edited By

D. V. Skobel'tsyn

FOREIGN TECHNOLOGY DIVISION

AIR FORCE SYSTEMS COMMAND

WRIGHT-PATTERSON AIR FORCE BASE

OHIO

Akademiya Nauk SSSR
Fizicheskiy Institut im. P. N. Lebedeva

TRUDY FIZICHESKOGO INSTITUTA

Vol. X

Izdatel'stvo Akademii Nauk SSSR
Moskva 1958

UNEDITED ROUGH DRAFT TRANSLATION

TRANSACTIONS OF THE PHYSICS INSTITUTE

EDITED BY: D. V. Skobel'tsyn

English Pages: 244

S/3851

THIS TRANSLATION IS A RENDITION OF THE ORIGINAL FOREIGN TEXT WITHOUT ANY ANALYTICAL OR EDITORIAL COMMENT. STATEMENTS OR THEORIES ADVOCATED OR IMPLIED ARE THOSE OF THE SOURCE AND DO NOT NECESSARILY REFLECT THE POSITION OR OPINION OF THE FOREIGN TECHNOLOGY DIVISION.	PREPARED BY: TRANSLATION SERVICES BRANCH FOREIGN TECHNOLOGY DIVISION WP-AFB, OHIO.

TABLE OF CONTENTS

TABLE OF CONTENTS CONTINUED

IN MEMORIAM

SEMEN ZAKHAROVICH BELEN'KIY

The well known theoretical physicist, head of the Theoretical Division of Physics Institute, Doctor of Physical and Mathematical Sciences Semen Zakharovich Belen'kiy died on 21 September 1956.

Semen Zakharovich was born in Moscow in 1916. Even before being graduated in 1938 from the Physics faculty of the Moscow State University he began scientific work in the field of theoretical physics. For many years the principal place in his activity was occupied by research into processes occurring in cosmic rays. The results he obtained in this field, expounded in his monograph "Cascade Processes in Cosmic Rays" (1948) and subsequently developed in many later articles, were highly praised and universally acknowledged in the world's literature. Semen Zakharovich also obtained original and interesting results in the field of hydrodynamics. He devoted much effort to the solution of important applied problems.

In 1954 a new stage began in his scientific activity, in that he embarked on research in the nuclear collisions of high-energy particles. This question, as is well known, is the center of attention of modern physics and is at the same time one of the most difficult problems. But here, too, Semen Zakharovich discovered new possibilities and arrived at important conclusions which are attracting ever-increasing attention both here and abroad.

Semen Zakharovich made far-reaching plans for research on the theory of collisions and multiple particle production, and this problem occupied him until his last days.

His services were rewarded with an Order of Lenin, the Papaleksi Prize, and the Stalin Prize. He took an active part in social life and was a member of the Communist Party of the Soviet Union since 1939.

Semen Zakharovich paid much attention to the training of youth. The work of a group of graduate students and the preparation of many dissertations were carried out under his guidance. As a leader he was most exacting and had a tendency to allow independence of work. He was able, without restricting the students' initiative, to help find the correct way with a few remarks.

Semen Zakharovich loved science, devoted all his efforts to it, was highly active and only a few knew how sick he was during the last years.

His associates, co-workers, and graduate students will never forget his high scientific principles, clarity of thought, directness of expression, and human qualities.

His untimely death struck particularly hard those who knew him closely and who marched on his side for many years. It is difficult to believe that we shall never see him again.

- Staff Members of the Theoretical Division

FROM THE EDITOR

The present volume contains two papers by S.Z. Belen'kiy. The article "Contribution to the Theory of Flow of Supersonic Gas Past a Wedge" was written in 1945, while the article "Hydrodynamic Equations with Account of Radiation" dates back to 1948.

Failure to publish these articles in time was accidental, and subsequently Belen'kiy, as far as was known, did not plan to publish them. Inasmuch, however, these articles contain interesting material, their publication in the Trudy of the Physics Institute in the form as they were found in Belen'kiy's papers seems advantageous.

The scientific activity of S.Z. Belen'kiy, which was only briefly touched upon in the obituary in the present volume, was delineated in detail in the journal "Uspekhi fizicheskikh nauk" for 1957, Vol. 61, where a bibliography of his scientific papers can be found.

CONTRIBUTION TO THE THEORY OF FLOW OF SUPERSONIC GAS PAST A WEDGE

S.Z. Belen'kiy

§1. INTRODUCTION

It is impossible to construct a continuous solution for the flow of a stream of gas at supersonic speed past a body. Indeed, if the front edge of the body is rounded off, the velocity at the edge itself should equal zero. At the same time, a small jet of gas impinging on the body should spread apart at the front edge. But if the velocity of the gas exceeds the velocity of sound, then upon expansion of the jet, as follows from the Bernoulli equation, the velocity of the gas increases and therefore cannot vanish. In order for the flow past the body to become possible, a discontinuity surface must arise in front of the body, a compression shock, the presence of which makes it possible to satisfy the boundary conditions on the surface of the body.

If the edge of the body is sharp, then the differential equations of gasdynamics lead to multiple-valued solutions in a definite region of space (one point in space corresponds to several values of the velocity), which is physically meaningless. Therefore a compression shock must be produced in front of the body, away from the sharp point, even at large tip angles.

Even if the contour of the body is such that the tangent to the contour at the forward point is parallel to the velocity of the incoming stream, and further on the contour bends smoothly, a unique solution may nevertheless be impossible and a compression shock arises at a certain

distance from the leading edge, in the forward direction relative to the stream. Because of the presence of discontinuity surfaces, the plotting of the flow past bodies in a supersonic stream is an exceedingly complicated problem which has been solved for only a few particular cases.

One such case is the flow past a dihedral angle (wedge). However, even in the investigation of this very simple problem we encounter the so-called "duality" of the solutions of gasdynamics for the discontinuities, a duality which has been subjected to many discussions.

If, by virtue of the streamlining conditions, the supersonic stream must turn through a certain angle which is smaller than 180°, then, according to the equations of gasdynamics, for specified stream velocity and turning angle, such a turn can be realized in two ways: 1) an oblique compression shock can be produced nearly normal to the velocity of the incoming stream, and the velocity behind this shock, as will be shown below, is always smaller than the velocity of sound; 2) an oblique shock farther away from the vertical than in the first case can arise, and the velocity behind it becomes subsonic or supersonic, depending of the velocity of the stream and the turning angle, but always larger than in the first case. In principle, both flow modes are possible. Usually the problem of the duality of the gasdynamic solution is considered applied to flow past a wedge, although of course it has a more general significance.

Experiment has shown that in flow past a wedge the mode realized corresponds to a high velocity behind the shock.

To explain this phenomenon theoretically, Roy [1] proposed that such flow can occur and be connected only with a minimum change in entropy, while Epstein [1] proposed to start from the minimum principle for the Hamiltonian. These criteria are quite arbitrary and can there-

fore not be regarded as convincing. Levinson [2] considers the stability of oblique shocks by the small oscillation method. The author reaches a conclusion that the only stable shocks are those for which the continuous velocity component parallel to the discontinuity (tangential) exceeds the velocity of sound ahead of the shock. It is easy to see that this conclusion contradicts the invariance of the gasdynamic equations under a Galilean transformation. Actually, it is always possible to change over to a coordinate system in which the tangential component of the velocity is smaller than the velocity of sound or is even equal to zero. It is obvious that in such a coordinate system the stability conditions cannot change. Thus, Levinson's work seems to be incorrect, since it contradicts the Galilean principle.

As regards the stability of compression shocks against small perturbations, this stability was investigated by Landau [3] for a straight shock, and it was shown that straight shocks are always stable (in agreement with experiment). This conclusion is valid, of course, for oblique shocks too.

In the case of flow around a wedge, the discontinuity has a sharp point, coinciding with the sharp point of the wedge. This case, strictly speaking, calls for an additional investigation of stability, which so far has not been performed by anyone. However, on the basis of the considerations which we shall develop in Section 3, it seems to us that such an investigation would not lead to new results.

Let us point out here that the problem of flow past a wedge, in the formulation used for its analysis so far, is of no interest from the physical point of view. One usually investigates a flow past an infinite dihedral angle and the solution obtained thereby is dual.

Any real body is finite, and the validity of the abstraction employed is far from obvious. Moreover, we believe that it is sufficient

to refine the formulation of the problem and to consider flow past a finite body, having a wedge-like end, in order to get rid of the duality of the solution. The necessary requirement that the boundary conditions be satisfied should lead to a unique choice of one of the possible solutions.

The derivation of a definite solution in the case of flow past a wedge does not mean at all that in all cases of turning of a supersonic flow this is precisely the solution obtained. To the contrary, we can point out examples in which a solution is obtained, for which the velocity behind the shock is smaller than the velocity of sound. Thus, in flow around a body with a rounded front end, the shock produced in front of the body bends in such a way, that the velocity behind it is smaller than the velocity of sound in some regions and larger in others.

It is obvious that by formulating a physically sensible problem concerning the flow around a body of arbitrary form, with account of conditions on the surface of the body and at infinity, we should always obtain a unique solution of the problem. At the present time unfortunately we cannot prove this premise as a rigorous mathematical theorem.

§2. OBLIQUE COMPRESSION SHOCK

Let us present a few relations from the theory of an oblique compression shock.

We shall designate with the index 1 quantities pertaining to the stream ahead of the shock, and with the index 2 quantities pertaining to the stream past the shock. The fundamental equations of gasdynamics, as applied to an oblique shock, are written in the following fashion:

$$\rho_1 v_{n_1} = \rho_2 v_{n_2} \tag{1}$$

$$p_2 - p_1 = \rho_1 v_{n_1}(v_{n_1} - v_{n_2}) \tag{2}$$

$$i_1 + \frac{v_1^2}{2} = i_2 + \frac{v_2^2}{2} = i_0. \tag{3}$$

Here ρ is the gas density, p the pressure, i the heat function, i_0 the "total" heat function, v_n the velocity component normal to the shock, v_t the velocity component parallel to the shock; this component does not experience a discontinuity. $v = \sqrt{v_n^2 + v_t^2}$

In Figure 1 the abscissa axis coincides with the direction of the velocity ahead of the shock, OD is the direction of the velocity past the shock, OB is the discontinuity line, OC is the Mach line of the flow ahead of the shock, OA is the Mach line of the flow past the shock, Φ is the angle between velocities, α_1 and α_2 are the Mach angles, and β is the angle between the shock and the direction of the velocity past the shock.

We shall consider the flow of a perfect gas (which does not limit the generality of the results obtained), and then $i = \gamma/(\gamma - 1)(p/\rho)$, where γ is the ratio of the specific heat at constant pressure to the specific heat at constant volume.

We introduce also the "critical velocity" c*, namely the stream velocity equal to the local velocity of sound

$$c^{*2} = \frac{2(\gamma-1)}{\gamma+1} i_0. \qquad (4)$$

The local velocity of sound c, defined by the relation $c^2 = dp/(d\rho)$, is

$$c^2 = \frac{\gamma+1}{2}\left(c^{*2} - \frac{\gamma-1}{\gamma+1} v^2\right) \qquad (5)$$

(for $c = v$, $v = c^*$).

It is seen from (5) that the velocity of a supersonic stream cannot exceed $v_{max} = \sqrt{(\gamma+1)/(\gamma-1)}\, c^*$.

Let us show that if the velocity past the shock exceeds the velocity of sound, then the discontinuity line is always situated between the Mach lines for the flows ahead of and behind the shock, and the discontinuity line makes a larger angle to the x axis than the Mach

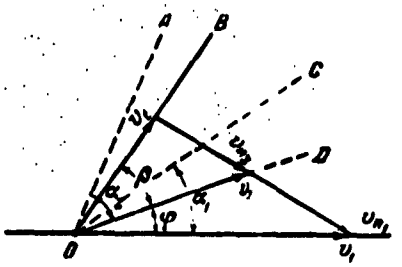

Fig. 1

line for the flow ahead of the shock, i.e.

$$\alpha_2 > \beta > \alpha_1 - \varphi. \qquad (6)$$

Eliminating p and ρ from (1),(2), (3) and using the relation (4), we obtain

$$v_{n_1} v_{n_2} = c^{*2} - \frac{\gamma-1}{\gamma+1} v_t^2 = c_t^{*2}. \qquad (7)$$

It is obvious that if $v_{n_1} > c_t^*$, then $v_{n_1} < c_t^*$ and vice versa. From (1) it follows that for a shock we have $v_{n_1} > v_{n_2}$ and consequently $v_{n_1} > c_t^*$. Let us set up the difference $c_1^2 - v_{n_1}^2$. Since in accordance with (5) and (7)

$$c_1^2 = \frac{\gamma+1}{2}\left(c_t^{*2} - \frac{\gamma-1}{\gamma+1} v_{n_1}^2\right),$$

we get

$$c_1^2 - v_{n_1}^2 = \frac{\gamma+1}{2}(c_t^{*2} - v_{n_1}^2). \qquad (8)$$

If $v_{n_1} > c_t^*$, then $v_{n_1} > c_1$.

An analogous relation occurs also for the flow past the shock:

$$c_2^2 - v_{n_1}^2 = \frac{\gamma+1}{2}(c_t^{*2} - v_{n_2}^2). \qquad (8')$$

Since $v_{n_2} < c_t^*$, we get $v_{n_2} < c_2$.

Therefore, the normal component of the velocity ahead of the shock always exceeds the velocity of sound, while the normal component of the velocity past the shock is always less than the velocity of sound.

From Figure 1 we get

$$\sin\beta = \frac{v_{n_1}}{v_2}, \quad \sin(\beta+\varphi) = \frac{v_{n_1}}{v_1}.$$

On the other hand, the angles between the Mach lines and the corresponding velocity directions (the Mach angles) are

$$\sin\alpha_2 = \frac{a_2}{v_2}, \quad \sin\alpha_1 = \frac{a_1}{v_1}.$$

Since $c_2 > v_{n_2}$, we get $\alpha_2 > \beta$, and since $c_1 < v_{n_1}$, we get $\beta > \alpha_1 - \phi$, q.e.d.

By transforming the relations (1) – (3) we can find a connection between the velocity components v_{2x} and v_{2y} past the shock for given volumes of v_1 and c*:

$$v_{2y} = \frac{(v_1 - v_{2x})^2\left(v_{2x} - \frac{c^{*2}}{v_1}\right)}{\frac{2}{\gamma+1}v_1 + \frac{c^{*2}}{v_1} - v_{2x}}. \qquad (9)$$

This curve has the form shown in Figure 2. The point A corresponds to the straight shock at which $v_{2y} = 0$, and $v_{2x} = c^{*2}/(v_1)$, where the point B corresponds to the absence of a shock ($v_{2y} = 0$, $v_{2x} = v_1$). The intersection of the line drawn from the origin at angle ϕ with the curve (9) makes it possible to determine the velocity occurring past the shock. We see that for a given angle of turn ϕ three values of the velocity are possible. One of them, F'', corresponds to a velocity past the shock exceeding the velocity ahead of the shock, that is, as follows from equation (1), it leads to a rarefaction shock. According to Zemplen's theorem, such shocks cannot be realized, so that the entire branch of the curve to the right of the point B has no physical meaning. The two other values of the velocity (F and F') are in principle equally valid. The point F' corresponds to the larger velocity past the shock, and F to the smaller velocity. The discontinuity line will make a smaller angle with the abscissa axis if the flow past the shock has the larger velocity. Indeed, let us write down the condition that the velocity component parallel to the direction of the shock remain continuous (Fig. 1):

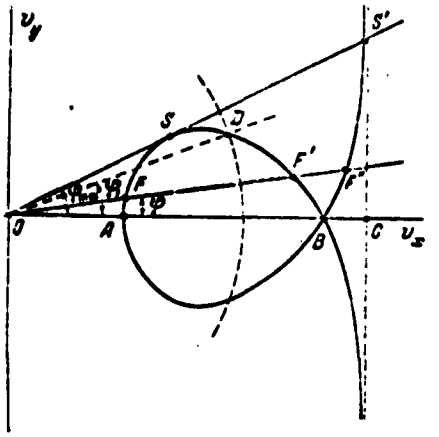

Fig. 2

$$v_1 \cos(\beta+\varphi) = v_{2x}\cos(\beta+\varphi) + v_{2y}\sin(\beta+\varphi).$$

Hence,

$$\operatorname{tg}(\beta+\varphi) = \frac{v_1 - v_{2x}}{v_{2y}}$$

or

$$\operatorname{tg}(\beta+\varphi) = \left(\frac{v_1}{v_{2x}} - 1\right)\frac{1}{\operatorname{tg}\varphi}. \qquad (10)$$

For specified v_1 and Φ the angle $\beta + \Phi$ will be the smaller, the larger the value of v_{2x}. * If the angle of turn Φ exceeds the limiting angle Φ_{max}, then a turn through a larger angle becomes impossible. This limiting angle is attained when the line drawn from the origin is tangent to the curve (the point S). Since the point B corresponds to supersonic velocity ($v_1 > c^*$), and the point A corresponds to subsonic velocity ($c^{*2}/(v_1) < c^*$), it is obvious that there is a point on the curve (9) corresponding to the velocity of sound past the shock. This point (D) is the point of intersection of the curve (9) with the circle $v_{2x}^2 + v_{2y}^2 = c^{*2}$. To the right of point D we have supersonic modes of flow past the jump, while to the left we have subsonic modes. Let us show that of the two possible values of the velocity past the shock (F and F'), not more than one corresponds to supersonic velocity and consequently at least one must be subsonic.

For this purpose it is sufficient to show that the point S always lies in the subsonic region.

Let us find the coordinate v_{xS} of the point S. The point S is the intersection of the curve defined by equation (9) with the line

$$v_y = \left(\frac{dv_y}{dv_x}\right)_S v_x. \qquad (11)$$

From this we have for the point S:

$$\left(\frac{d\ln v_{yS}}{dv_{xS}}\right)_S = 1. \tag{12}$$

Using equation (9), we determine d ln $v_{yS}/(dv_{xS})$:

$$\frac{d\ln v_{yS}}{dv_{xS}} = \frac{1}{v_1 - v_{xS}} + \frac{1}{2}\frac{1}{c_{xS} - \frac{c^{*2}}{v_1}} + \frac{1}{2}\frac{1}{\frac{2}{\gamma+1}v_1 + \frac{c^{*2}}{v_1} - v_{xS}}, \tag{13}$$

on the other hand

$$\frac{dv_a}{v} = -\frac{dp}{\rho v_a^2} \tag{13'}$$

Equating (13) and (13') we obtain after simple transformations the quadratic equation

$$\left.\begin{aligned} &v_{xS}^2 - Av_{xS} + B = 0, \\ &A = \frac{\gamma+1}{2\gamma v_1}\left(\frac{2}{\gamma+1}v_1^2 + 4c^{*2}\right), \\ &B = \frac{\gamma+1}{2\gamma v_1}c^{*2}\left(\frac{4}{\gamma+1}v_1 + 2\frac{c^{*2}}{v_1}\right). \end{aligned}\right\} \tag{14}$$

The point D corresponding to the velocity of sound is the point of intersection of the curve (9) with the circle $v_{2x}^2 + v_{2y}^2 = c^{*2}$. The coordinate v_{xd} is determined from the equation

$$c^{*2} - v_{xd}^2 = \frac{(v_1 - v_{xd})^2\left(v_{xd} - \frac{c^{*2}}{v_1}\right)}{\frac{2}{\gamma+1}v_1 + \frac{c^{*2}}{v_1} - v_{xd}}. \tag{15}$$

Transforming this equation, we obtain again a quadratic equation

$$\left.\begin{aligned} &v_{xd}^2 - A'v_{xd} + B' = 0, \\ &A' = \frac{\gamma+1}{2\gamma v_1}(3c^{*2} + v_1^2), \\ &B' = \frac{\gamma+1}{2\gamma v_1}c^{*2}\left(\frac{\gamma+3}{\gamma+1}v_1 + \frac{c^{*2}}{v_1}\right). \end{aligned}\right\} \tag{16}$$

Equation (14) has two solutions. One corresponds to the point S' where the line (11) is tangent to the curve (9). We denote it by $v_{xS}^{(1)}$. The second solution ($v_{xS}^{(2)}$) corresponds to the point where the line (11) crosses the branch of curve (9) pertaining to the rarefaction shocks (S').

Obviously, $v_{xd}^{(1)}$ is the smallest solution. Equation (16) also has two roots, $v_{xd}^{(1)}$ and $v_{xd}^{(2)}$, which corresponds to the presence in equation (9) of the quantity $(v_1 - v_{2x})^2$. It is easy to show that the point D corresponds to the larger of the roots $v_{xd}^{(2)}$.

Using the properties of quadratic equations, we write the obvious equations:

$$v_{xS}^{(1)} + v_{xS}^{(2)} - v_{xd}^{(1)} - v_{xd}^{(2)} = A - A' = \frac{c_1^2}{\gamma v_1}, \tag{17}$$

$$v_{xS}^{(1)} v_{xS}^{(2)} - v_{xd}^{(1)} v_{xd}^{(2)} = B - B' = \frac{c_1^2 c^{*2}}{\gamma v_1^2}, \tag{18}$$

where c_1 is the velocity of sound in front of the compression shock [see (5)].

We recall that $v_{xd}^{(2)} < v_1$ and $v_{xd}^{(1)} < v_{xd}^{(2)} < v_1$. On the other hand, $v_{xS}^{(2)} > v_1$. Thus, we always have $v_{xS}^{(2)} > v_{xd}^{(1)}$. The velocity v_1 of a supersonic stream can, as is well known, not exceed $v_{max} = \gamma + 1/(\gamma - 1)\ c^*$. For this valuc v_1 we get $c_1 = 0$. From (18) we obtain for this case

$$v_{xS}^{(2)} = v_{xd}^{(1)}.$$

Inasmuch as $v_{xS}^{(2)} > v_{xd}^{(1)}$, we also get $v_{xd}^{(2)} > v_{xS}^{(1)}$.

We have shown that for the maximum value v_1 (for specified c*) the point S is located in the region of subsonic velocities. Let us show now that this property is maintained for all supersonic values of the velocity v_1 of the incoming stream. Let us assume that there exist such values $v_1 > c^*$, for which $v_{xd}^{(2)} < v_{xS}^{(1)}$. Then, by virtue of the fact that v_{xd} and v_{xS} are continuous functions of v_1, there should exist such a value of v ($v_{max} > v_1 > c^*$) at which $v_{xS}^{(1)} = v_{xd}^{(2)}$. Equations (17) and (18) will be written for this value of v_1 in the following fashion:

$$v_{xd}^{(2)} - v_{xd}^{(1)} = \frac{c_1^2}{\gamma v_1},$$

$$v_{xd}^{(2)} - v_{xd}^{(1)} = \frac{c_1^2 c^{*2}}{\gamma v_1^2 v_{xd}^{(2)}}.$$ ( )

Hence $v_{xd}^{(2)} = c^{*2}/(v_1)$. But it follows from (9) that the coordinate v_y of the point with abscissa $c^{*2}/(v_1)$ is equal to zero. Thus, $v_{xd}^{(2)}$ is equal to the total stream velocity past the compression shock and is at the same time smaller than c*, since $v_1 > c^*$. This contradicts the condition that the point $v_{xd}^{(2)}$ should correspond to the velocity of sound.

We have reached a conclusion that over the entire interval of variation of v_1 (from c* to v_{max}) we have $v_{xS}^{(1)} < v_{xd}^{(2)}$ and thus the point S is always in the subsonic region.

If the angle of the turn in the velocity is $\Phi < \Phi_1$, where Φ_1 is the angle between the x axis and the line passing through the origin and through the point D, then one of the possible velocities past the discontinuity is supersonic, and the other is subsonic. If $\Phi > \Phi_1$, then both possible values of the velocity lie in the subsonic region.

§3. FLOW OF SUPERSONIC STREAM PAST A WEDGE

Let us consider the flow past an unbounded wedge with an aperture angle 2Φ, produced by a supersonic stream with velocity v_1 and critical velocity c*. If the angle Φ does not exceed the limiting value Φ_{max}, which is a function of v_1 and c*, then flow modes are possible, in which a shock wave initiates at the point of the wedge. Then, as follows from the foregoing section, two flow modes are possible in principle, one corresponding to a larger velocity behind the shock and the other corresponding to a smaller velocity. The angle between the discontinuity line and the surface of the wedge will in the former case (β) be smaller than in the latter case (β') (Fig. 3). Thus, in the case

of an infinite wedge we have two equally valid solutions, and we do not know how to choose between them.

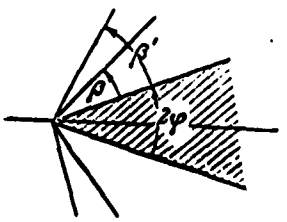

Fig. 3

Landau has shown [3] that any plane shock is stable relative to small perturbations, and that the singularity of the problem considered here lies only in the fact that the discontinuity has a kink (a sharp point). This case calls for an additional investigation from the point of view of stability. However, such an investigation does not seem to us to be fruitful. Indeed, were such an investigation to yield new results and were it to lead to the stability of one of the solutions, the solution more likely to be proved unstable is the one with the large kink in the shock, that is, with the larger velocity past the discontinuity. At large velocities of the incoming stream and at very small angles Φ, an oblique shock corresponding to a smaller velocity past the discontinuity is quite close to a straight shock and therefore has no kink whatever, whereas an oblique shock corresponding to the larger velocity has a considerable kink past the discontinuity. Yet experience shows that in the flow past a body, even at a small angle Φ, the solution realized corresponds to the larger velocity past the discontinuity.

The problem of flow past an unbounded wedge is a mathematical abstraction, the validity of which is not obvious beforehand. The physical formulation of the problem calls for flow around a finite body. We should therefore not be surprised at the duality of the solution for a case which is physically not realizable. We shall show that in the case of a finite body the two solutions are no longer equally valid.

Let us consider by way of an example the flow around a sharpened body with the contour as shown in Fig. 4. As will be shown below, the

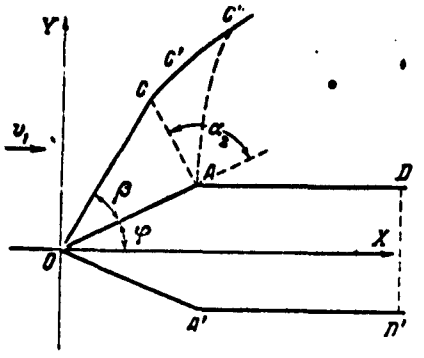

Fig. 4

choice of the specific form of the contour does not limit the generality of the conclusions.

Let us assume that when a supersonic stream flows past the body under consideration a compression shock starts on the point of the wedge, and that behind the shock the velocity remains supersonic (this is possible if $\Phi < \Phi_1$), that is, the solution corresponding to the larger velocity behind the discontinuity is realized.

Were the shock to extend to infinity without attenuating an intensity, then the resistance experienced by the body would be infinitely large (Fig. 4).

Actually, the entropy of the gas masses flowing around the body increases in the shock. As was shown by the author's paper [4], the resistance of the body is proportional to the expression $\int \Delta S dy$, where ΔS is the change in the entropy per unit length. Since ΔS is in our case a constant finite quantity, for an unbounded discontinuity the expression given above, and with it the resistance, become infinitely large. This does not occur, since perturbations that lead to the attenuation of the shock originate at the point A.

Because the velocity of the flow around the angle OAD exceeds the velocity of sound, the perturbations originating at the point A propagate along the Mach line. The solution corresponding to a plane oblique shock will be valid only to the point C, where the shock crosses the first Mach line (so-called weak discontinuity), making an angle a_2 with the direction OA. This crossing must occur, for in accordance with the proof given in the preceding section $\alpha_2 > \beta$. [illegible] round the

OAD, the stream expands, and, in accordance with the property of supersonic flows, the velocity will increase. Consequently the velocity of the stream in the region ACC' will exceed that in the region OCA, and therefore the discontinuity line should bend accordingly. It is obvious that the angle betweeen the discontinuity line and the x axis should decrease and approach the Mach angle of the flow ahead of the shock, since the difference between the velocities ahead of and behind the shock decreases. In the region AC'C" the velocity increases even more and the intensity of the shock becomes even less. At sufficiently large distances from the body, the intensity of the shock becomes as small as desired, and the discontinuity line merges with the Mach line. The expression $\int \Delta S dy$ is in this case finite, as is also the resistance of the body. The calculation (which can be carried out only if the angle Φ is small and the velocity of the incoming stream close to the velocity of sound) shows that the resistance calculated with the expression $\int \Delta S dy$ coincides exactly with the resistance calculated directly from the distribution of the pressure along OA and OA' (see [4]).

Let us assume now that a compression shock starts from the point of the wedge, and behind it the velocity becomes subsonic. In the case of subsonic flow past the angle OAD, the perturbation starting from the point A propagates in all of space and therefore the discontinuity line begins to bend immediately, starting from the vertex. Since the subsonic stream past the angle OAD expands, the perturbation starting from A leads to a decrease in the velocity, and the intensity of the shock should increase, while the discontinuity line should bend in such a way as to approach the y axis. Thus, in this case we shall have no section whatever in which the shock would be linear.

[From the foregoing qualitative analysis we should expect that in the flow past a pointed body the compression shock can be tangent to

the vertex only if the velocity behind the shock exceeds the velocity of sound. If the angle $\phi > \phi_1$, then, as shown in the preceding section, only one solution is supersonic and the problem is solved uniquely. If $\phi > \phi_1$, both solutions correspond to subsonic velocities and the shock cannot start from the vertex of the body. In this case the shock "jumps away" from the body, so that the real limiting angle at which the occurrence of discontinuity starting from the vertex is still possible is not ϕ_{max} but ϕ_1.] *

The criterion obtained by Levinson [2] on the basis of an incorrect theory differs greatly from ours. In place of the condition $v_2 > c_2$ (or $v_2 > c^*$) Levinson obtained a condition according to which the tangential velocity component is $v_t > c_1$. As can be seen from Fig. 11 of Levinson's paper, this condition differs from ours at all values of the velocities of the incoming stream.

In conclusion we point out that the criterion proposed is not at all universal for the flow around an arbitrary body. We recall that in flow past a rounded body there is produced a discontinuity line, the velocity behind which runs successively through all possible values from $c^{*2}/(v_1)$, corresponding to the point A on (curve 9) (see Fig. 2), to v_1, corresponding to the point B.

REFERENCES

1. Collection entitled "Gazovaya dinamika" [Gas Dynamics], ONTI [State Unified Scientific-Technical Publishers], 1939.
2. Ya. Levinson. Prikladnaya matematika i mekhanika [Applied Mathematics and Mechanics], 9, No. 2, 151 (1945).
3. L.D. Landau and Ye.M. Lifshits, Mekhanika sploshnykh sred [Mechanics of Continuous Media], Gostekhizdat [State Unified Publishing House for Technical and Theoretical Literature], 1944.
4. S.Z. Belen'kiy, Prikladnaya matematika i mekhanika, 8, 34 (1944).

From the editor: The paragraph enclosed in square brackets is included in the manuscript, but a note on its margin indicates that S.Z. Belen'kiy subsequently started to doubt the correctness of this conclusion. However inasmuch as the general conclusion that the two solutions are not equally valid in the case of a finite wedge is regarded at the present time as correct and was first made by S.Z. Belen'kiy, the publication of this article is fully justified.

Manuscript Page No.	[Footnotes]
11	It is easy to see that the direction of the oblique shock is perpendicular to the line F'B which joins the velocity vectors before and after the shock, that is, $\operatorname{ctg}(CBF') = v_{2y}/(v_1 - v_{2x})$. It is evident therefore that for a given v_1 the direction of the shock varies continuously and monotonically along curve (9) from $\pi/2$ to α_1.
14	To check the considerations advanced here, it would be desirable to carry out experiments with flow around a wedge at an angle Φ larger than Φ_1 but smaller than Φ_{max}.

HYDRODYNAMIC EQUATIONS WITH ACCOUNT OF RADIATION

S.Z. Belen'kiy

To solve many physical problems, particularly in astrophysics, it becomes necessary to take radiation into account in the hydrodynamic equations. In spite of the fact that the material equations of motion with account of radiation were derived many times, the question has not yet been fully clarified. In the present article we derive the fundamental equations in two different ways, and also discuss work by other authors.

1. We start from the laws of conservation of matter, momentum, and energy.

Let

$$f(v, r)\,dV\,d0 \tag{1}$$

be the number of particles in a three-dimensional volume $d0 = dxdydz$ with velocities in the interval at $(v_x, v_y, v_z, v_x + dv_x, v_y + dv_y, v_z + dv_z)$. Let, further,

$$N(n, r, \nu)\,d\nu\,d\omega\,d0 \tag{2}$$

be the number of photons in the three-dimensional volume d0 within the solid angle $d\omega$ and with energy lying in the interval $h\nu$, $h(\nu + d\nu)$, where ν is the radiation frequency and h is Planck's constant; the direction of propagation is characterized by a unit vector $\vec{n}$. The cosines of the angles between the vector $\vec{n}$ and the coordinate axis are denoted by α_i. The index i runs through three values corresponding to the angles with the x, y, and z axes.

We consider the change in an arbitrary component of the momentum:

$$-\int \frac{\partial}{\partial t}(P_{i\,\text{вещ}} + P_{i\,\text{изл}})\,d\Omega. \qquad (3)$$

Here $P_{i.\,veshch}$ is the density of the material component of the momentum equal to

$$P_{i\,\text{вещ}} = m\int f(v, r)\, v_i dV, \qquad (4)$$

where m is the mass of the particle. Were the particles of the material to be at rest in the reference frame considered, we would have $P_{i.veshch} = 0$. Actually, however, the particles move with macroscopic velocity $\vec{V}$. Thus, $\vec{v}_i = \vec{V}_i + \vec{v}_i'$, where $\vec{v}_i'$ is the microscopic particle velocity. Consequently,

$$P_{i\,\text{вещ}} = mV_i\int f(v, r)\,dV + m\int v_i' f(v, r)\,dV. \qquad (5)$$

But the quantity

$$m\int f(v, r)\,dV = \rho$$

is none other than the density of the material, and

$$\int v_i' f(v, r)\,dV = 0$$

The density of the radiation momentum component is

$$P_{i\,\text{изл}} = \frac{1}{c}\int N_{h\nu} s_i\, d\nu\, d\omega, \qquad (6)$$

since $h\nu/c$ is the momentum carried by the photon in a direction characterized by the vector $\vec{n}$. The change in momentum in the volume under consideration is determined by the momentum transferred by the particle and by the photons through the surface surrounding the volume.

The momentum transferred by the particles is

$$\left.\begin{aligned} m\oint f(v,\ r)\,v_i(vdS)\,dV = \\ = m\oint\int f(v,\ r)(V_i+v_i')(V_k+v_k')\,dS_k dV = \\ = m\oint\int f(v,\ r)(V_iV_k+v_i'V_k+v_k'V_i+v_i'v_k')\,dS_k dV = \\ = \oint \rho V_i V_k dS_k + m\int\int f(v,\ r)\,v_i'v_k'dV dS_k \end{aligned}\right\} \qquad (7)$$

where $d\vec{S}$ is the surface element, the absolute value of which is equal to the area of the element and whose direction is normal to the surface. From the macroscopic point of view, the quantitites under the surface-integral sign in the last term are the components of the pressure tensor P_{ik}

$$p_{ik} = m\int f(v,\ r)\,v_i'v_k'dV. \qquad (8)$$

If we neglect viscosity, then

$$p_{ik} = p\delta_{ik}, \qquad (8')$$

where p is the pressure of the material.

The momentum transferred by the photons is equal to

$$\oint\int N\frac{h\nu}{c}\alpha_i(c\alpha_k dS_k)\,d\omega d\nu = \oint\int Nh\nu\alpha_i\alpha_k d\omega d\nu dS_k. \qquad (9)$$

The quantities

$$p_{ik}' = \int Nh\nu\alpha_i\alpha_k d\omega d\nu \qquad (9')$$

form the tensor of radiant energy pressure.

The surface integrals (7) and (9) can be transformed in accord with the Gauss theorem into volume integrals:

$$\oint \rho v_i v_k dS_k + \oint p_{ik} dS_k = \int \frac{\partial}{\partial x_k}(\rho v_i v_k + p_{ik})\,dV, \qquad (10)$$

$$\int p_{ik}' dS_k = \int \frac{\partial p_{ik}'}{\partial x_k} dV. \qquad (11)$$

Equating expression (3) to the sum of (10) and (11), and taking into consideration the fact that the equality obtained must hold true for

an arbitrary volume dO, no matter how small, we obtain the following differential equation:

$$\frac{\partial}{\partial t}\left(\rho V_i + \frac{H_i}{c^2}\right) = -\frac{\partial}{\partial x_k}(\rho V_i V_k + p\delta_{ik} + p'_{ik}), \qquad (12)$$

where H is the vector of the radiant energy flux;

$$H_i = c\int N h\nu s_i \, d\nu d\omega.$$

Let us change over from the derivative of the velocity at a stationary point to the Lagrangian derivative D/Dt, and let us use the equations for the conservation of matter, which remain valid if pair production processes are neglected. Equation (12) can then be rewritten as:

$$\rho\frac{DV_i}{Dt} = -\frac{\partial p}{\partial x_i} - \frac{\partial p'_{ik}}{\partial x_k} - \frac{\partial}{\partial t}\left(\frac{H_i}{c^2}\right). \qquad (12')$$

The last two terms are due to the radiation.

Let us proceed now to the energy conservation equation. The change in the energy of a volume element per unit time is

$$-\int \frac{\partial}{\partial t}(W_{вещ} + W_{изл})\, d0, \qquad (13)$$

where W_{veshch} is the energy per unit material in a unit volume and W_{izl} is the radiation energy per unit volume;

$$W_{веш} = \int f(v, r)\left(\frac{mv_i^2}{2} + u\right)dV, \qquad (14)$$

where u is the potential energy of the particle in the field of the other particles. If the particles of the material move with macroscopic velocity $\vec{V}$, then

$$W_{веш} = \int f(v, r)\left(\frac{mV^2}{2} + \frac{mv'^2}{2} + mV_i v'_i\right)dV + \rho\varepsilon_u, \qquad (15)$$

where ε_u is the potential energy per unit mass of the material. Since

$$m\int f(v, r)\,dV = \rho, \quad \int f(v, r)\, v'_i dV = 0,$$

we get

$$W_{\text{полн}} = \frac{\rho V^2}{2} + \rho\varepsilon_k + \rho\varepsilon_u = \frac{\rho V^2}{2} + \rho\varepsilon \tag{16}$$

(ε_k is the kinetic energy of the microscopic motion of a unit mass of the material, and ε is the internal energy per unit mass of the material).

The radiation energy per unit volume is

$$W_{\text{изл}} = \int Nh\nu d\nu d\omega. \tag{17}$$

The change in the energy of the volume per unit time is due to two causes. First, the change of the energy is due to the flux of kinetic and internal energy of the material through the surface surrounding the volume:

$$\oint\left[\int f(\mathbf{v}, r)\left(\frac{mV_i^2}{2} + \frac{mv_i'^2}{2} + mV_i v_i'\right)dV + \rho\varepsilon_u\right]\cdot[(V_k + v_k')\,dS_k] = \\ = \oint\left(\frac{\rho V^2}{2} + \rho\varepsilon\right)(V_k dS_k) + \int f(\mathbf{v}, r)\, mV_i v_i' v_k' ds_k dV. \tag{18}$$

But

$$m\int f(\mathbf{v}, r)\, v_i' v_k' dV = p_{ik}.$$

The material energy flux is

$$\oint\left[\left(\frac{\rho V^2}{2} + \rho\varepsilon\right)V_k + V_i p_{ik}\right]dS_k. \tag{18'}$$

Second, the change in energy is due to the radiant energy flux:

$$\oint\int Nh\nu c\,(z_k dS_k)\,d\nu d\omega. \tag{19}$$

Equating the sum of the integrals (18') and (19) to expression (13) and changing over from surface integrals to volume integrals, we obtain, by taking a sufficiently small volume, the following equation:

$$\frac{\partial}{\partial t}\left(\frac{\rho V^2}{2} + \rho\varepsilon + W_{\text{изл}}\right) = -\frac{\partial}{\partial x_k}\left[\left(\frac{1}{2}\rho V^2 + \rho\varepsilon\right)V_k\right] - \frac{\partial H_k}{\partial x_k} - \frac{\partial V_k p}{\partial x_k}, \tag{20}$$

where H is the radiant energy flux vector. Using the equation for the conservation of matter and equation (12), we can rewrite (20) in the

form:

$$\frac{\partial W_{изл}}{\partial t}+\rho\frac{Dv_i}{Dt}-\frac{p}{\rho}\frac{D\rho}{Dt}=V_i\frac{\partial p'_{ik}}{\partial x_k}+V_i\frac{\partial}{\partial t}\left(\frac{H_i}{c^2}\right)-\frac{\partial H_k}{\partial x_k}. \qquad (20')$$

In the derivation of (12) and (20) we calculated the quantities determining the radiation in some "resting" coordinate frame. Yet it is convenient in many cases to calculate the radiation in a coordinate system that moves together with the matter. Let us assume that the velocity of a volume element of the matter is small compared with the velocity of light. On changing from the coordinate system in which the matter moves, to a system in which it is at rest, it is necessary to use the following formulas which take into account the Doppler effect and aberration:

$$\nu=\nu^*(1+\alpha_k^*\beta_k), \qquad (21)$$

$$\alpha_i=\frac{\nu^*}{\nu}(\alpha_i^*+\beta_i). \qquad (22)$$

Here $\beta = V_k/(c)$. The quantities designated with an asterisk refer to the coordinate frame in which the matter is at rest.

The values of W_{izl}, H and p'_{ik} in the two coordinate systems are related by:

$$W_{изл}=\int N h\nu d\omega d\nu=\int N^* h\nu^* d\omega^* d\nu^*\left(\frac{\nu}{\nu^*}\right)^2=\int N^* h\nu^* d\omega^* d\nu^*(1+\alpha_k^*\beta_k)^2. \qquad (23)$$

We obtain, with accuracy to terms of order v/c,

$$W_{изл}=W^*_{изл}+2\beta_k\frac{H_k^*}{c^2}=W^*_{изл}\frac{2\rho_k}{c^2}H^*_{\rho_k} \qquad (24)$$

$$H_i=c\int N^* h\alpha_i^*\nu^* d\nu^* d\omega^*+c\beta_k\int N^* h\nu^*\alpha_k^*\alpha_i^* d\nu^* d\omega^*+c\beta_k\int N^* h\nu^* d\nu^* d\omega^*=$$

$$=H_i^*+V_k p_{ik}^*+V_i W^*_{изл}. \qquad (25)$$

Finally,

$$p'_{ik}=p_{ik}^*+\frac{V_i}{c^2}H_k^*+\frac{V_k H_i^*}{c^2}. \qquad (26)$$

Substituting (24), (25), and (26) into equations (12) and (20), and neglecting terms of order v/c, we obtain ultimately that in this approximation equations (12) and (12') remain without change (if it is recognized that we neglect the term H_1/c^2), while equations (20) and (20') assume the following form:

$$\frac{\partial}{\partial t}\left(\frac{\rho V^2}{2}+\rho\varepsilon+W^*_{изл}\right)=-\frac{\partial}{\partial x_k}\left[\left(\frac{\rho V^2}{2}+\rho\varepsilon\right)V_k+H^*_k+\right.$$
$$\left.+V_i p^*_{ik}+V_k p+V_k W^*_{изл}\right], \qquad (27)$$

$$\frac{\partial W^*_{изл}}{Dt}+p\frac{D_1}{Dt}-\frac{p+W^*_{изл}}{\rho}\frac{D\rho}{Dt}=-p'^*_{ik}\frac{\partial v_i}{\partial x_k}-\frac{\partial H^*_k}{\partial x_k}. \qquad (28)$$

If the radiation is isotropic in the coordinate frame that moves together with the matter, then $H^*_k = 0$, and $p'^*_{ik} = p'^* \delta ik$.

Equation (28) is then written as:

$$\frac{DW^*_{изл}}{Dt}+p\frac{D_1}{Dt}-\frac{p+p'^*+W^*_{изл}}{\rho}\frac{D\rho}{Dt}=0. \qquad (29)$$

This equation expresses, as can be readily seen, the constancy of the entropy in a moving volume of liquid in which the radiation field is isotropic.

2. The hydrodynamic equations with account of radiation can be derived also by starting from the energy-momentum tensor for a system consisting of an aggregate of particles and radiation.

In a coordinate system with respect to which the given volume element of matter is at rest, this tensor has obviously the form:

$$T^*_{\alpha\beta}=-p\delta_{\alpha\beta}-p'^*_{\alpha\beta}, \qquad (30)$$

where, as usual, α and β run through the values from 1 to 3, p is the material pressure, and $p'^*_{\alpha\beta}$ is the radiation pressure;

$$T^*_{4\alpha}=T^*_{\alpha 4}=-\frac{i}{c}H^*_\alpha \qquad (30')$$

where H^*_α are the components of the radiant flux vector in the coordinate

system where the given material element is at rest;

$$T^*_{44} = W^p_{вещ} + W^*_{изл} \qquad (30'')$$

W^p_{veshch} is the density of the energy of the material, including the rest energy.

We now change over to a reference frame with respect to which the given element of matter moves with macroscopic velocity v. We assume that this velocity is directed along the x axis. The tensor T^*_{ik} is then transformed into the tensor T_{ik}. We confine ourselves to an examination of the one-dimensional problem, that is, we assume that $p^*_{\alpha\beta} = 0$, with the exception of p^*_{xx} and $H^*_y = H^*_z = 0$.

In this case

$$\left.\begin{aligned} T_{11} &= \frac{-(p+p^*_{xx}) - 2\frac{v}{c^2}H^*_z - \frac{v^2}{c^2}(W^p_{вещ}+W^*_{изл})}{1-\frac{v^2}{c^2}}, \\ T_{44} &= \frac{(W^p_{вещ}+W^*_{изл}) - 2\frac{v}{c^2}H^*_z + \frac{v^2}{c^2}(p+p^*_{xx})}{1-\frac{v^2}{c^2}}, \\ T_{41} = T_{14} &= \frac{-\frac{i}{c}H^*_z\left(1+\frac{v^2}{c^2}\right) - i\frac{v}{c}(W^p_{вещ}+W^*_{изл}+p+p^*_{xx})}{1-\frac{v^2}{c^2}}, \\ T_{22} &= T^*_{22},\ T_{33} = T^*_{33}, \end{aligned}\right\} \qquad (31)$$

the remaining components are $T_{ik} = 0$.

The equations of motion for the system under consideration are determined from the conditions $\partial T_{ik}/(\partial x_k) = 0$, which in our case reduce to the following relations:

$$\left.\begin{aligned} &\frac{\partial}{\partial x}\left(\frac{p+p^*_{xx}+2\frac{v}{c^2}H^*_z+\frac{v^2}{c^2}(W^p_{вещ}+W^*_{изл})}{1-\frac{v^2}{c^2}}\right)+ \\ &+\frac{\partial}{\partial t}\left(\frac{\frac{H^*_z}{c^2}\left(1+\frac{v^2}{c^2}\right)+\frac{v}{c^2}(W^p_{вещ}+W^*_{изл}+p+p^*_{xx})}{1-\frac{v^2}{c^2}}\right)=0, \\ &\frac{\partial}{\partial x}\left(\frac{H^*_z\left(1+\frac{v^2}{c^2}\right)+v(W^p_{вещ}+W^*_{изл}+p+p^*_{xx})}{1-\frac{v^2}{c^2}}\right)+ \end{aligned}\right\} \qquad (32)$$

$$+\frac{\partial}{\partial t}\left(\frac{(W^{r}_{\text{вещ}}+W^{\circ}_{\text{изл}})-2\frac{v}{c^2}H^{\circ}_{x}+\frac{v^2}{c^2}(p+p^{\circ}_{xx})}{1-\frac{v^2}{c^2}}\right)=0. \qquad (33)$$

Equations (32) and (33) are not complete without the condition for the conservation of the number of particles. For the relativistic case this equation is written as:

$$\frac{\partial}{\partial x}\left(\frac{nv}{\sqrt{1-v^2/c^2}}\right)+\frac{\partial}{\partial t}\left(\frac{n}{\sqrt{1-v^2/c^2}}\right)=0, \qquad (34)$$

where n is the number of particles per unit volume in the rest system.

Let $v \ll c$. The energy W^{p}_{veshch} can then be represented in the form of a sum of the "rest energy" of the matter and the internal energy of the matter per unit volume:

$$W^{r}_{\text{вещ}}=nmc^2+\rho\varepsilon, \qquad (35)$$

where $\rho = nm$. Equation (32) subject to the condition $v/c \ll 1$ assumes the form:

$$\frac{\partial}{\partial x}(p+p^{\circ}_{xx}+\rho v^2)+\frac{\partial}{\partial t}\left(\rho v+\frac{H^{\circ}_{x}}{c^2}\right)=0. \qquad (36)$$

Changing over to the nonrelativistic form of (33), we must take into account equation (34), which can be written, accurate to terms quadratic in v/c, in the form:

$$\frac{\partial}{\partial x}\left[nV\left(1+\frac{v^2}{2c^2}\right)\right]+\frac{\partial}{\partial t}\left[n\left(1+\frac{v^2}{2c^2}\right)\right]=0. \qquad (37)$$

Using (37), we find that when $(v/c) \ll 1$ equation (33) assumes the following form:

$$\frac{\partial}{\partial x}\left[\frac{\rho v^2}{2}v+v(\rho\varepsilon+p+p^{\circ}_{xx}+W^{\circ}_{\text{изл}})+H^{\circ}_{x}\right]+$$
$$+\frac{\partial}{\partial t}\left(\frac{\rho v^2}{2}+\rho\varepsilon+W^{\circ}_{\text{изл}}\right)=0. \qquad (38)$$

It is easy to see that equations (36) and (38) coincide with equations

(12) and (20) for the one-dimensional case.

The system of equations (12) and (20) or (12') and (20') must be supplemented not only with the continuity equation for the matter, but also by the transport equation for the radiation, which we shall not stop to discuss here.

3. We compare the equations obtained by us with the equations obtained by others, first of all with the equations of Milne, who prepared a review of the question considered by us.

If we neglect the term H/c^2 in our equations and the gravitational forces and internal energy sources in the Milne equations, then equation (12') coincides with the corresponding equation of Milne.

However, the equations that express the conservation of energy will be different.

Milne's equation in our notation has the following form:

$$\frac{\partial W_{\text{изл}}}{\partial t} + p\frac{Dv}{Dt} - \frac{p+p'}{\rho}\frac{D\rho}{Dt} = -\frac{\partial H_k}{\partial x_k}, \qquad (39)$$

here p' is the additional pressure due to the radiation. Let us compare equation (39) with (20'). They coincide only if we assume that tensor p'_{ik} has the form:

$$p'_{ik} = \delta_{ik}p',$$

and supplement the right half of (20') with the term

$$-\frac{\partial}{\partial x_k}(p'V_k).$$

This term is analogous to the term $-\partial(pV_k)/(\partial x_k)$, which is contained in (20) and has the physical meaning of the work done by the pressure forces. However, whereas the term $-\partial(pV_k)/(\partial x_k)$ follows directly from the transformation of the material energy flux, given in expression (18), no corresponding term arises for the radiation, as can be seen from (19). Milne's equation is therefore incorrect.

The equations of Jeans and Vogt for the energy has the following

form:

$$\frac{DW_{изл}}{Dt} - \frac{p+p'+W_{изл}}{3}\frac{Dv}{Dt} + p\frac{D\varepsilon}{Dt} = -\frac{\partial H_k}{\partial x_k}. \qquad (40)$$

Milne believes that it holds true under certain boundary condtions. Actually, the Jeans and Vogt equation is correct, as can be readily verified by comparison with (28), if, first, we assume that $p'_{ik} = p'\delta_{ik}$, and, second, the quantities characterizing the radiation are measured in a coordinate system with respect to which the given material element is at rest.

The use of the energy conservation equation in the form (28) is meaningful if the radiation field differs little from equilibrium with matter.

In conclusion, I am grateful to Professor I.Ye. Tamm for a discussion of this problem.

REFERENCES

1. V. Pauli, Teoriya otnositel'nosti [Relativity Theory], GTTI State Technical and Theoretical Editions], 1947.

2. Hd. d. Astrophys. [Handbook of Astrophysics], Vol. III, No. 2, 1930.

Manuscript Page No.

[List of Transliterated Symbols]

21 вещ = veshch = veshchestvo = material

21 изл = izl = izlucheniye = radiation

PRINCIPLES OF PROTON SYNCHROTRON THEORY

M.S. Rabinovich

FOREWORD

The development of accelerator technology acquired a particularly vigorous character after 1944, when V.I. Veksler [1-3] discovered the phenomenon of automatic phasing of particles in resonant accelerators, and new methods for obtaining high-energy particles were obtained on its basis.

Even by the end of 1945 it became possible to proceed to design and create installations, aimed at obtaining electrons and protons having energies of several million electron volts. For such energies, the most suitable accelerators turn out to be the synchrotron for electrons and the synchrocyclotron for protons, deuterons, and other particles.

It is obvious that the development of accelerator technology could advance only on the basis of well-developed theory, and indeed, in 1945 - 1947 the works of the author [4-8], S.M. Rytov [9], A.L. Burshteyn [10, 11], A.A. Kolomenskiy [13, 14] and others laid the groundwork for the theory of large resonant accelerators*.

In 1947, a synchrotron for 30 Mev was first started up at the Physics Institute of the USSR Academy of Sciences (FIAN), and two years later a synchrotron for 265 Mev (FIAN) and a synchrocyclotron for 550 Mev ** (Institute of Nuclear Physics Problems, Academy of Sciences USSR - IYaPAN) were constructed.

For nuclear physics to progress, it is very important to be able to attain even larger energies. The production of protons with energy

of 10,000 Mev would have made it possible to penetrate into the region of perfectly new phenomena, connected with the production of nucleons and heavier particles. The nuclear processes that occur at short distances attainable at such energies can change appreciably our notions concerning the nuclear forces.

In 1948 a group of theoreticians at the Physics Institute of the Academy of Sciences was charged with the problem of creating a complete and sufficiently exact theory that can serve as a basis for the design of an accelerator to produce protons with energy of 10,000 Mev (10 Bev).

At the present there exists only one type of accelerator with which the above-mentioned energy can be attained. Such an accelerator is the proton synchrotron with slotted magnet. The linear gaps are used to hold inflector plates, accelerating and signal electrodes, etc.

The colossal dimensions of the installation, the presence of linear gaps with impossibility of making the magnet gap sufficiently large, the injection of the particles into the accelerator chamber at relatively high energies, the need for exact correspondence between the values of the frequency and the magnetic field, and the influence of different fine effects on the motion of the particles, all these and many others have posed before the designers, particularly before the theoretical physicists, many new and complicated problems.

In 1948, when we embarked on the development of the theory of a proton synchrotron with slotted magnet, only one paper devoted to fast oscillations, that of Dennison and Berlin [32], was known. However, as will be shown in Chapter II, even this paper was not satisfactory. We therefore had to do the whole work from scratch.

During 1948–1950 the problem facing us was essentially completed [16–31]; some additional questions were worked up in 1951. However, even now practice poses before theory many new problems.

In the development of the theoretical problems, particular attention was paid to the applied aspect of the problem. We have therefore attempted to reduce the theory to a form that is convenient for direct use for practical purposes. To the contrary, practice kept urging on the theoreticians, raising new problems, making it possible to judge the validity of various assumptions.

On the basis of theoretical and experimental work it was shown that protons with energy of 10,000 Mev can be obtained; the basic parameters of the accelerator were chosen, the technical specifications for the individual units were formulated, and sketches and technical designs were prepared for two installations (a model for 180 Mev and an installation for 10,000 Mev).

The theory developed by the author and his co-workers served as the guiding material in the construction of the 10,000-Mev proton synchrotron. The correctness of some of the important conclusions of our theory was confirmed with a working model of a proton synchrotron operating at 180 Mev.

A description of the experiment made with this model and a comparison of the results with the theory was made in later papers by the author, I.S. Danilkin, L.P. Zinov'ev. and V.A. Petukhov.

In the present monograph are gathered the works of the author for 1948–1950, devoted to the theory of the proton synchrotron with slotted magnet. These works, naturally, do not cover all the problems in accelerator theory, but it seems to us that the main and principal problems are quite adequately represented.

Without changing the general plan of the exposition, we have made a few small additions in the course of preparing the manuscript for print, connected with the application of our theory to strong-focusing accelerators, based on work performed in 1953 [15].

The present work consists of six chapters.

In the first chapter we investigate slow, so-called radial-phase oscillations occurring when particles move in an accelerator with a slotted magnet. This chapter is a natural continuation and development of the author's earlier papers [16]. Using the method developed by us [8], we investigate the behavior of the particles on the phase plane, paying principal attention to many singularities of motion in an accelerator with slotted magnet, which are of practical significance.

We introduce a new stability criterion (I, 34) for the phase oscillations, connected with the presence of the straight-line gaps; the change in frequency of phase oscillations, the stability regions, the decrease in the oscillation amplitude and other quantities are determined for an accelerator with slotted magnet. The formulas obtained by us are of great significance for applications and for the theory of injection (Chapter V) and of resonances (Chapter IV).

In this chapter we investigated also acceleration in multiple resonance, that is, for an integral ratio of the frequency of the accelerating field to the frequency of revolution.

In the second chapter we consider fast particle oscillations. Unlike the known paper of Dennison and Berlin [32], we present here a correct account of the influence of the linear gaps on the injection and the capture of the particles in the acceleration mode, we determine the optimum angle of emission of particles from the injector, and introduce the concept of the envelope of the particle trajectory, with which it makes it possible to describe simply and illustratively the behavior of the particles in the accelerator. The motion of the particle is calculated for the first time with allowance for the presence of the magnetic field in the linear gaps.

In a real magnet there are always certain deviations of the mag-

netic field from the calculated value, which accelerate the orbit and consequently lead to an equivalent loss of part of the working region of the magnet. The presence of linear gaps in the magnet not only changes the character of the influence of the distortions, but also creates the possibility of occurrence of altogether new perturbations (for example, saturation of the edges of the magnet sectors facing the linear gaps).

It is clear from the foregoing that a clarification of the influences of the deviations of the magnetic field from the calculated value is one of the most important problems in the theory. Our own investigation [17], made in 1949 (together with A.M. Baldin and V.V. Mikhaylov), is still the only work devoted to this problem. The results of the third chapter, in which these calculations are presented, were already used not only in the designs but also in the processing of the measurements made on the 180-Mev proton synchrotron model and on individual blocks of the magnet of the large accelerator.

The fourth chapter treats an important and complicated problem of resonance phenomena between fast and slow oscillations. The resonance phenomena in accelerators with slotted magnets differ essentially from resonance phenomena in circular accelerators. This difference manifests itself, first, in the displacement of the resonant values of the characteristics of the magnetic field and, second, in the manifestation of multiple resonances. We have developed a special procedure for calculating with a high degree of accuracy the resonance phenomena in accelerators with slotted magnets. In spite of the complexity of the calculation, the final formulas are simple and admit of a clear physical interpretation. Along with the main calculation, we consider for the first time in the fourth chapter fast particle oscillations with account of the change of the magnetic field and the increase in the particle

energy.

Finally, we consider in the same chapter resonances between the high-frequency harmonics of the magnetic field and the phase oscillations. Using the method of Bogolyubov [33] and Mitropol'skiy [34], we succeeded in analyzing the resonance phenomena in the nonlinear approximation, which radically changes the results previously obtained and is quite important for practice. It turns out that in resonance the oscillation amplitude is limited not by "friction" and not by the speed of passage through the resonant region, but the very nonlinearity of the phase oscillations.

In the fifth chapter, injection theory is developed. After the detailed study of particle motion made in the first two chapters, it becomes possible to calculate the number of particles captured into the acceleration mode, and to choose the most effective and simplest method of injection. Numerous plots make it possible to estimate how the intensity is affected by various parameters of the accelerator and of the proton beam, by the error in the instant when the accelerating field is turned on, by the error in the angle of admission of the particles into the chamber, etc.

In the sixth chapter the envelope method is used for a theoretical investigation of the free oscillations in strong-focusing accelerators. This method turns out to be most fruitful in the solution of problems that arise in the design of a variety of strong-focusing accelerator types.

In our work, which was completed in March 1953, the significance of resonances in strong-focusing accelerators was pointed out for the first time. At the present time, there is an extensive literature devoted to this problem, so that we shall touch upon this question quite briefly.

Finally, in the sixth chapter we derive a phase equation for a strong-focusing accelerator by introducing a very convenient new quantity, n_{ef}.

On the whole, the sixth chapter develops the physical principles of strong-focusing accelerators quite sufficiently for a first introduction.

In conclusion, we shall stop to discuss some problems which for various reasons could not be treated in the present work.

First among them is the entire problem of the motion of the chamber from the linear accelerator-injector to the chamber of the 10 Bev proton synchrotron, considered in the paper by A.A. Kolomenskiy; another problem is that of extraction of the protons from the accelerator, developed by Sabsovich, Ganzhin, and others.

Finally, we did not consider scattering and charge exchange of the particles during the acceleration process, and also the problem of protection against radiation. All these problems are treated in a sufficient number of papers (see [31, 35, 36]).

The main deductions of the theory are always illustrated with the data on the 10 Bev proton synchrotron as examples, although they have a more general significance. Some of the methods developed by us were used to design accelerators of other types and of other dimensions, and in particular for accelerators intended to obtain both larger and smaller energies.

The magnet of the 10-Bev proton synchrotron consists of four sectors, separated by linear gaps, each eight meters long. The average radius of the magnet pole of the sector is 28 meters, the width of the pole is 2 meters, the height of the magnetic gap is 40 centimeters. The magnet section has an E-shape form. The maximum value of the magnetic field is 13,000 oersteds, which is reached within 3.2 seconds. At the

start of the acceleration, the rate of build-up of the magnetic field can change from 4,000 (normal value) to 12,000 oersteds per second (forced value). The magnetic field index lies in the greater part of the working region between 0.55 and 0.75 (average 0.65). The injection energy is W_1 = 10 Mev.

The present work could not be performed without close working contact with a large group of persons from the P.N. Lebedev Physics Institute of the USSR Academy of Sciences, the Scientific Research Institute for Electrophysical Apparatus of the Ministry of Electric Industry of the USSR, and the Radio Laboratory of the USSR Academy of Sciences, who participated in the design and production of the proton synchrotron of the USSR Academy of Sciences.

I am particularly indebted to the scientific director of all the work involved in the construction of the accelerator, V.I. Veksler, for continuous attention.

Manuscript Page No.

[Footnotes]

31 * The foreign literature of 1946–1947 also contains a large number of articles in which various problems connected with the construction, use, and theory of various types of accelerators are considered.

31 ** At the present time the proton energy attained in this synchrocyclotron is 680 Mev.

Manuscript Page No.

[List of Transliterated Symbols]

37 эФ = ef = effektivnyy = effective

LIST OF SYMBOLS

We list here the most frequently employed symbols, which are common to all the chapters of the present book. Along with them, separate symbols are introduced in each chapter, which apply only to the particular chapter.

The formulas in each chapter are numbered independently. Reference to formulas of other chapters is accompanied by indication of the number of the chapter. For example: (III, 15) denotes the fifteenth formula of chapter III, while (15) denotes the fifteenth formula of the same chapter in which the reference is found.

$\beta = v/c$ – ratio of particle velocity to the velocity of light.

$c = \cos\varkappa v$ (everywhere except in the first chapter).

c – velocity of light in the first chapter.

e – particle charge.

E – equilibrium value of the total energy of the particle.

E_a – proper energy of the particle.

ΔE – deviation of particle energy from the equilibrium value.

$F = 1 - (L/(2\pi R_0 + L)[n + \beta^2(1 - n)]$ – a coefficient.

F_c – amplitude of free oscillations.

$\vec{H}$ – magnetic field intensity vector.

H_r, H_0, H_z – intensity vector components.

H – axial component of the magnetic field.

$K = 1 + n/(1 - n)(1/\beta^2)$ – a coefficient.

$\kappa = \begin{cases} \sqrt{n} - \text{for vertical oscillations} \\ \sqrt{1-n} \text{ for radial oscillations.} \end{cases}$

L – length of all linear sections.

l – length of one linear section.

m – mass of particle.

m_0 – rest mass of particle.

4μ – frequency of free oscillations in the accelerator with slotted magnet, in dimensionless units.

n – index of magnetic field (see I, 6).

ν – angular dimension of magnet sector.

q – multiplicity, ratio of frequency of accelerating field to revolution frequency.

Π – orbit perimeter/2π.

$p = l\kappa/2R$.

r – radius in cylindrical coordinate system.

R – radius of instantaneous orbit.

R_0 – radius of equilibrium orbit.

ρ – deviation of particle radius from equilibrium value.

ρ_1 – distance from injector to equilibrium orbit.

$\bar{\rho}$ – maximum value of amplitude of radial-phase oscillations.

$s = \sin \kappa\nu$.

σ = length of path along instantaneous orbit/R

T – period of revolution of particle.

V_0 – sum of amplitudes of the voltages of the accelerating gaps.

W_1 – kinetic energy of the particle at the instant of injection into the chamber.

ϕ – phase of particle relative to the phase of the accelerating electric fields; $\phi = 0$ corresponds to maximum voltage on the

accelerating gap at the instant of passage of the particle.

ϕ_0 – phasing point (I, 21).

ϕ_1 – minimum value of the phase in the oscillations.

ϕ_2 – maximum value of the phase in the oscillations.

$\dot{\phi} = d\phi/(dt)$ – phase velocity.

ω – frequency of revolution of the particle in the magnetic field H.

ω_0 – frequency of accelerating field.

ω_1 – frequency of phase oscillations.

z – distance from particle to the central plane.

$$X = \begin{cases} \rho \text{ for radial oscillations.} \\ z \text{ for vertical oscillations.} \end{cases}$$

Chapter 1

RADIAL-PHASE MOTION OF PARTICLES

§1. INTRODUCTION

Motion of particles in an accelerator with slots differs essentially from the motion is a circular accelerator. In both cases, however, it can be broken up into three component motions.

A. Motion with resonant frequency along an orbit, with very slowly varying or even constant radius. This form of motion will be called motion along an equilibrium orbit.

B. Slow oscillations about the equilibrium orbit, which are called radial-phase oscillations and which are connected with the change in the particle energy due to the passage through the accelerating gap at different values of the phase of the alternating accelerating field. By way of an example we can point out that in the apparatus designed for the production of 10-Bev protons, the period of the phase oscillations ranges from 520 to 1450 microseconds. Inasmuch as the period of the phase oscillations is approximately 100 to 2,000 times larger than the period of revolution, the particle goes through many revolutions before the radius of the equilibrium orbit changes appreciably. Consequently the orbit of the particles that execute slow radial-phase oscillations is almost closed. This quasi-closed orbit will be called the instantaneous orbit.

C. Fast oscillations about the instantaneous orbit. These oscillations are also called free oscillations, since they are not connected, in first approximation, with the fluctuations of the particle energy as

the particle is accelerated. The period of the fast oscillations is usually on the order of the particle revolution. (In weak-focusing installations it is somewhat larger, and in strong-focusing installations it is 5–15 times smaller). Along with radial free oscillations, there exist vertical oscillations about the central plane of the magnet (the symmetry plane of the magnet). This is the only form of oscillations in the vertical direction.

Thus, the picture of the motion in the proton synchrotron is as follows: the instantaneous orbit (which is almost circular) executes slow oscillations (pulsates) about the equilibrium orbit. During the time of each oscillation, the particle has time to make many revolutions (from 100 to 2,000, depending on the particle energy). Fast free oscillations are produced about the instantaneous orbit, with a period that is 1.5 or 2 times larger than the period of revolution (the period of revolution is 7.5 microseconds at 4 Mev and 0.7 microseconds at 10 Bev). Superimposed on the above-described motion in the central plane are also vertical oscillations, with a period which likewise differs insignificantly from the period of revolution.

The resolution of a single motion into components is, of course, arbitrary, but it contains no inaccuracies or arbitrary assumptions. Our main statement is that these three types of motion can be regarded independently. Important exceptions are resonance phenomena and transients. These, however, will be considered separately. The connection between the free and phase oscillations manifests itself, in particular, in the so-called gap oscillations. The latter are due to the intermittent character of the manner by which the particle acquires energy. The basis for the possibility of considering these motions independently in the majority of cases is the large difference in the frequencies of the fundamental quantities that characterize the differ-

ent types of motion. A rigorous proof for this statement was derived by the author for circular accelerators [6, 8]. A similar proof was obtained in a different manner by S.M. Rytov [9]. The only one to touch upon this question in the foreign literature is Frank [37], who, however, made an error which was discussed in [8].

For accelerators with slots, the proof of this theorem is quite cumbersome, but it was made by A.A. Kolomenskiy [24] by the method of finite differences. A simpler proof can also be obtained, valid for small linear gaps (expansion parameter $L/2\pi R$, where L is the total length of all the linear gaps).

We can thus investigate henceforth each type of motion independently, making use of the calculations given above, and of the physical obviousness of the statement given above.

We shall henceforth use always, for each magnet sector, a cylindrical coordinate system with the plane $z = 0$ coinciding with the central plane of the magnet.

§2. EQUILIBRIUM ORBIT

By definition, the frequency of a revolution of a particle along an equilibrium orbit is equal to the frequency of the accelerating electric field $\omega_0(t)$. It is obvious that the radius R_0 of the equilibrium orbit is determined from the following conditions:

$$R_0 = \frac{\beta E}{eH(R_0, t)}; \quad \omega_0 = \frac{2\pi c\beta}{2\pi R_0 + L}; \quad \beta = \sqrt{1 - \left(\frac{E_0}{E}\right)^2}. \qquad (1)$$

where $\beta = v/c$, $E_0 = 938.1$ Mev is the proton's proper energy, L is the total length of all the linear gaps, and $H(R_0, t)$ is the vertical component of the magnetic field in the central plane at the radius R_0.

Eliminating E from the three equations, we obtain R_0 as a function of $H(R_0, t)$ and $\omega_0(t)$, that is, in final analysis, as a function of the time t. Combining the relation between H and ω_0 we can make the

radius R_0 of the equilibrium orbit vary in accordance with any prescribed law, and in particular, stay constant. Obviously, the latter case is the most typical for the proton synchrotron. Indeed, during the time of acceleration it is essential that the radius of the equilibrium orbit remain constant, in order that the dimensions of the apparatus be minimal, but it may turn out to be convenient during the time of injection to either increase or decrease the radius of the orbits.

Eliminating the energy E from equation (1) we obtain the connection between the frequency $\omega_0(t)$ of the accelerating field and the magnetic field $H_0(R_0, t)$, guaranteeing acceleration on an equilibrium orbit with radius R_0:

$$\omega_0 = \frac{2\pi c}{2\pi R_0 + L}\sqrt{1 - \frac{E_0^2}{E_0^2 + (eHR_0)^2}}; \qquad L = \sqrt{(eHR_0)^2 + E_0^2}. \tag{2}$$

Regarding R_0 in equation (2) either as constant or as dependent on the time, we obtain every time the required law relating the change in the frequency with the change in the magnetic field. To the contrary, knowing the dependence of the magnetic field and of the frequency of the accelerating field on the time, we can determine the time dependence of the radius R_0.

Let $\bar{\omega}_0(t)$ be such a law for the variation of the frequency as to make $R_0 = \bar{R}_0 = \text{const}$,

$$\omega_0(t) = \frac{2\pi c}{2\pi \bar{R}_0 + L} \frac{\bar{R}_0 eH(\bar{R}_0, t)}{\sqrt{E_0^2 + (e\bar{R}_0 H)^2}}. \tag{3}$$

Fig. 1 shows the dependence of the frequency $f = \bar{\omega}_0/(2\pi)$ on the value of the magnetic field for a 10-Bev proton accelerator.

Let the true frequency of the accelerating field $\omega_0(t)$ differ from the value required in accordance with (3)

$$\omega_0(t) = \bar{\omega}_0(t) + \Delta\omega_0(t). \tag{4}$$

Then the radius of the equilibrium orbit will likewise not be equal to $\bar{R}$.

$$R_0 = \bar{R}_0 + \Delta R_0. \qquad (5)$$

The connection between $\Delta\omega_0(t)$ and ΔR_0 is determined, accurate to the first powers of $\Delta\omega_0/(\omega_0)$ and $\Delta R_0/(R_0)$ from equation (3), in which we substitute relations (5) and (4):

$$\frac{\Delta R_0}{R_0} = -\frac{\Delta\omega_0}{F\omega_0}\frac{1}{n+\beta^2(1-n)}; \qquad F = 1 - \frac{L}{(2\pi R_0 + L)[n+\beta^2(1-n)]}, \qquad (6)$$

where $n = \partial \ln H/(\partial \ln R)$ is the index of the magnetic field.

In the nonrelativistic case formula (6) simplifies to

$$\frac{\Delta R_0}{R_0} = -\frac{\Delta\omega_0}{nF_0\omega_0}; \quad F_0 = 1 - \frac{L}{(2\pi R_0 + L)n}. \qquad (7)$$

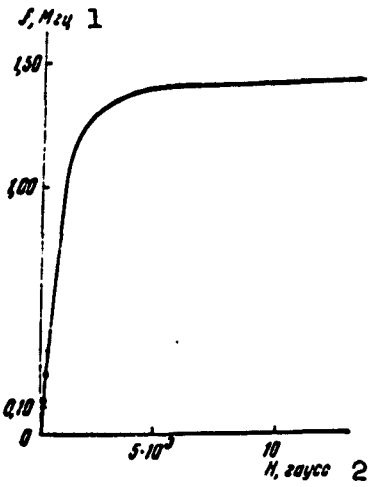

Fig. 1. Dependence of the frequency f of the accelerating field on the value of the magnetic field intensity H. The circles designate the values of the initial frequency at two injection energies, 4 Mev (H = 103 gauss) and 10 Mev (H = 163 gauss). 1) f, megacycles; 2) H, gauss.

The coefficient F is equal to unity if L = 0. In this case formulas (6) and (7) go over into the ordinary formula for a circular proton synchrotron. Since F < 1, it follows therefore that in a magnet with slots the radius of the equilibrium orbit is more sensitive to frequency deviations than is the case in circular accelerators. For example, a frequency error $\Delta\omega_0/(\omega_0) = \pm 0.2\%$ leads in the 10-Bev proton synchrotron to a displacement of $\pm$ 11.2 centimeters in the radius of the orbit, that is, decreases the employed working region by 22.5 centimeters (in a circular accelerator – by 16.8 centimeters).

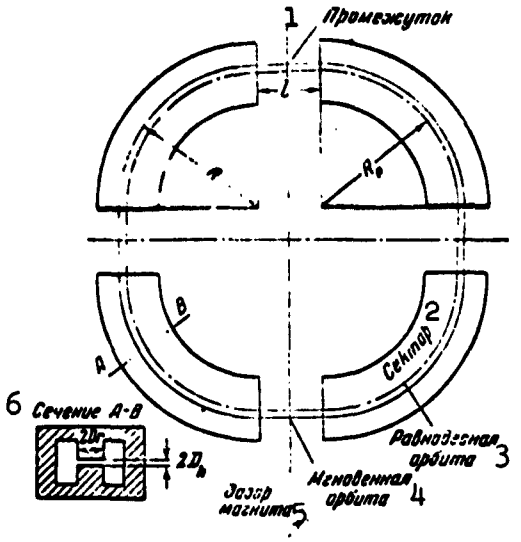

Fig. 2a. Diagram of accelerator. 1) Linear section; 2) sector; 3) equilibrium orbit; 4) instantaneous orbit; 5) magnet air gap; 6) section A-B.

§3. DERIVATION OF PHASE EQUATION

We shall call an "ideal accelerator with slots" an accelerator in which the magnetic field in the linear sections is exactly equal to zero, while in the sectors it corresponds to the field in a circular magnet with average radius R_0 (Fig. 2a). Such an idealization approximates quite accurately the true magnetic field in accelerators in which the ratio of the height of the air gap D_h in the circular sectors to the length of the straight-line sections $\underline{l}$ is sufficiently small. In the 10-Bev proton synchrotron the ratio is $D_h/\underline{l} = 0.0375$. For comparison we can state that in a 180-Mev proton synchrotron (the model of the accelerator) the ratio is $D_h/\underline{l} = 0.179$, that is, almost 5 times larger. Consequently in the model the magnetic field in the linear section plays a major role, but in the proton synchrotron for 10 Bev it plays an insignificant role. Consequently, it is meaningful to consider the motion in "ideal accelerator with slots" and only then take into account the influence of the magnetic field in the linear portions.

The phase equation can be derived by various means (see, for example, [18]. We choose a method which shows quite clearly all the assumptions and disregarded factors usually tacitly introduced in the derivation of the phase equation.

It might seem natural to consider the motion of particles in an accelerator with slots in a special coordinate system, shown in Fig. 2b.

The angle γ is measured along the oval trajectories, with

$$\gamma = \frac{s}{R\left(1 + \frac{L}{2\pi R}\right)}, \qquad (8)$$

where s is the length along the oval trajectory, reckoned from the chosen axis. Such a system, however, is not orthogonal, is convenient for the analysis of free oscillations but is not convenient for the analysis of radial-phase oscillations. At the same time, the introduction of the angle γ is a very useful device, facilitating the calculations. It is convenient, for example, to expand the accelerating

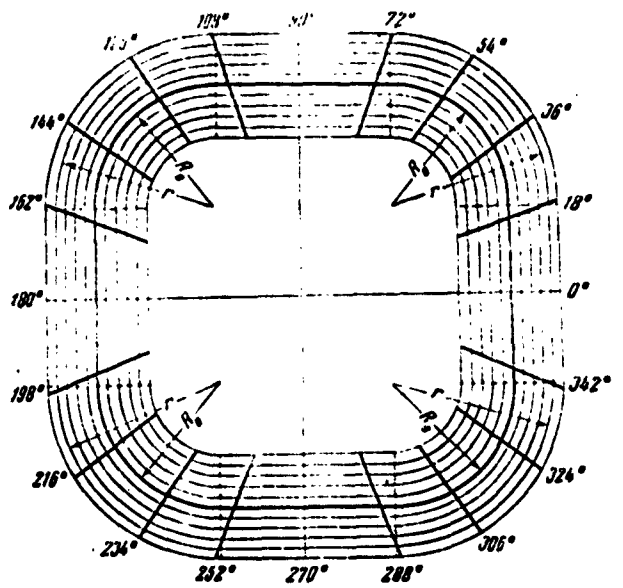

Fig. 2b. Coordinate system after formula (8).

electric field ε_γ in waves traveling in the direction of the angle γ:

$$\varepsilon_\gamma = \frac{V_0}{2\pi R H}\,\delta(\gamma)\cos\int^t \omega_0(t)\,dt, \qquad (9)$$

where $\delta(\gamma)$ is a periodic delta-function, period 2π; V_0 is the amplitude of the potential difference on the accelerating gap

$$H = 1 + \frac{L}{2\pi R} = \frac{\text{perimeter of orbit}}{2\pi R} \qquad (10)$$

We assume that we have two accelerating gaps at $\gamma = 0$ and $\gamma = \pi$, the accelerating field of which is in phase. Since $\mathcal{E}(\gamma)$ is a periodic function, we expand it in a Fourier series and obtain:

$$\mathcal{E}_1 = \frac{V_0}{2\pi H R} \sum_{k=-\infty}^{k=\infty} \cos\left[\int \omega_0 dt - (2k-1)\gamma\right] \tag{11}$$

Let us write down the equation of motion for the circular sectors. We know (see, for example, [8]) that in this case the equations assume the following simple form:

$$\left.\begin{aligned} &\frac{d}{dt}(m\dot{r}) = mr\dot{\varphi}^2 - \frac{er}{c}\dot{\varphi}H_z; \\ &\frac{d}{dt}\left(mr^2\dot{\varphi} - \frac{e\Phi}{2\pi c}\right) = e\mathcal{E}_1 R; \\ &\frac{d}{dt}(m\dot{z}) = \frac{e}{c}r\dot{\varphi}H_r, \end{aligned}\right\} \tag{12}$$

where

$$\Phi(r, t) = 2\pi \int_0^r H_z r dr.$$

For the linear sections, obviously, equation

$$\frac{d}{dt}(m\dot{r}) = 0; \quad \frac{d}{dt}(m\dot{s}) = e\mathcal{E}_1; \quad \frac{d}{dt}(m\dot{z}) = 0, \tag{13}$$

where s is the length reckoned along the trajectory, Fig. 2b.

Thus, in the linear section r and s are the ordinary Cartesian rectangular coordinates.

As the zero approximation we choose motion along an orbit with radius R_0, shown in Fig. 2b (heavy line).

The frequency of revolution on the equilibrium orbit is ω_0, while the speed is $v_0 = \omega_0 R_0 \Pi_0$.

We make use of the smallest of the quantities

$$\frac{R_0 - r}{R_0}, \quad \frac{\omega_0 - \dot{\varphi}}{\omega_0}, \quad \frac{v - v_0}{v} \tag{14a}$$

and carry out the calculations accurate to their first powers. The

largest among these three quantities is the last. We introduce the following notation:

$$\left.\begin{aligned} &r = R_0 + \rho;\quad \frac{\dot{\theta}}{\Pi} = \omega_0 - \dot{\varphi} = \frac{I}{mR^2};\\ &\Pi = \Pi_0\left[1 - \frac{\Pi_0 - 1}{\Pi_0}\frac{\rho}{R_0}\right];\quad \Pi_0 = 1 + \frac{L}{2\pi R_0};\\ &\frac{\dot{\theta}}{\Pi_0} = \omega_0 - \dot{\varphi} - \frac{\Pi_0 - 1}{\Pi_0}\frac{\rho}{R_0}\omega_0;\quad \frac{I}{R_0^2\Pi_0} = \omega_0 - \dot{\varphi} + \frac{1}{\Pi_0}\frac{\dot{\rho}}{R_0}\omega_0. \end{aligned}\right\} \qquad (14b)$$

The subscript 0 denotes all the quantities pertaining to the equilibrium orbit. The phase velocity $\dot{\Phi}$ shows the deviation of the revolution frequency of the particle along the oval trajectories from the equilibrium frequency ω_0.

It is clear from (8) and (14) that the angle γ is related with the phase Φ in the following fashion:

$$\gamma = \int (\omega_0 - \dot{\varphi})\,dt = \int \omega_0 dt - \varphi. \qquad (15)$$

We substitute relations (14) into equations (12) and (13) and expand each of the terms contained in it in powers of $\rho/(R_0)$ and $\dot{\Phi}/(\omega_0)$, for example

$$\left.\begin{aligned} &\Pi_0(r, t) = \Pi_0\left(1 - n\frac{\rho}{R_0}\right);\\ &\Phi(r, t) = \Phi_0(R_0, t) + 2\pi\Pi_0\frac{\rho}{R_0}R_0^2;\\ &E + \Delta E = E\left[1 + \frac{n^2}{1 - n^2}\left(\frac{1}{\Pi_0}\frac{\rho}{R_0} - \frac{\dot{\Phi}}{\omega_0}\right)\right];\\ &H_r = -n\Pi_0\frac{\dot{\rho}}{R_0}\ \text{etc.} \end{aligned}\right\} \qquad (16)$$

In the first order we obtain the following equations, which are simultaneously written out for the circular sector and the linear sections (R_0 = const):

$$\left.\begin{aligned} &\frac{d}{dt}\left[\frac{E}{1 - n^2}\frac{\dot{\rho}}{R_0}\right] - \frac{n^2}{1 - n^2}\left[\frac{\dot{\rho}}{R_0} - \frac{\dot{\Phi}}{\omega_0}\right] =\\ &= \frac{eV}{2\pi}\sum_{k=-\infty}^{k=\infty}\cos\left[\int \omega_0 dt - (2k-1)\gamma\right] -\\ &\quad - \left[\Pi_0 + \Pi_0\left(\frac{1}{\Pi_0} - g(\gamma)\right)\frac{\rho}{R_0}\right] \times\\ &\times \frac{d}{dt}\left[\frac{ER_0^2\Pi_0\omega_0}{c^2}\right] + \Pi g(\gamma)\frac{d}{dt}\left(\frac{eV_0}{2\pi c}\right); \end{aligned}\right\} \qquad (17)$$

$$\frac{d}{dt}(E\beta) = \frac{E\omega_0^2 R_0^2}{(1-\beta^2)}\left[\frac{2}{R}(1-n)\beta^2 kF - \frac{2}{\omega_0}\right]g(\gamma);$$

$$\frac{d}{dt}(E\lambda) = -E\omega_0^2 R_0^2 n\varepsilon g(\gamma);$$

$$K = 1 + \frac{n}{1-n}\frac{1}{\beta^2}, \qquad (17, \text{ cont'd})$$

where $g(\gamma)$ is equal to unity in the circular sector and to zero in the linear sections. The function $g(\gamma)$ for sectors can be represented in the form of the following series:

$$g(\gamma) = \frac{1}{\pi} - \frac{2}{\pi}\sin\frac{\pi}{\pi}\cos 4\gamma + \\ + \frac{1}{\pi}\sin\frac{2\pi}{\pi}\cos 8\gamma - \frac{1}{\pi}\sin\frac{3\pi}{\pi}\cos 12\gamma + \ldots \qquad (18)$$

We proceed to derive the phase equation. As was shown in [8, 24], of all the sum contained to the right in the first equation of (17), the term playing the principal role is the one with k = 1, since all other terms oscillate rapidly and yield zero upon averaging. A rigorous mathematical proof of the validity of the averaging method can be found in the work of N.N. Bogolyubov [33]. The component of the wave k = 1 propagates with a velocity equal to or close to the velocity of motion of the particles, and exerts a constant action on the particle. All remaining oscillating terms merely perturb the motion of the particles insignificantly.

We first neglect all the terms of the series in the first equation of (17), except one. Mathematically this means that we "spread out" the action of the two accelerating gaps over the entire oval orbit. In the same approximation, we can confine ourselves to only the zero term of the entire series in (18). This means that the action of the vortical electric field, which occurs in the circular sectors, is also "spread out" over the entire oval orbit.

Finally, inasmuch as the variation of the phase Φ is quite slow

compared with the revolution frequency, "without inertia," we can neglect in (16) the inertia force d/(dt)(mρ̇).

In this case we obtain from the second equation of (17)

$$\frac{\dot{\varphi}}{\omega_0} = \frac{\dot{\varphi}}{\omega_0(1-n)\gamma^2 KF}; \quad \frac{\Delta E}{E} = \frac{\dot{\varphi}}{\omega_0 FK}. \tag{19}$$

Substituting (19) into the first equation of (17), we obtain the principal phase equation:

$$\frac{d}{dt}\left(\frac{E}{\omega_0^2 FK}\frac{d\varphi}{dt}\right) - \frac{eV_0\cos\varphi}{2\pi} = -\frac{d}{dt}\left(\frac{ER_0^2\Pi_0^2\omega_0}{c^2} - \frac{e\Phi_0}{2\pi c}\right). \tag{20}$$

The left part of the phase equation (20) differs from the corresponding equation for the circular accelerator in the presence of the coefficient F [see (6)].

Let us determine the phase value $\varphi = \varphi_0$ for equilibrium motion. Since equilibrium motion is realized (by definition) with a resonant frequency ω_0, the $d\varphi/(dt)$ vanishes identically and

$$\cos\varphi_0 = \frac{2\pi}{eV_0}\frac{d}{dt}\left(\frac{ER_0^2\Pi_0^2\omega_0}{c^2} - \frac{e\Phi_0}{2\pi c}\right). \tag{21}$$

Thus, equilibrium motion can occur only for particles which have completely defined values of the phase ($\pm\varphi_0$). In other words, the equilibrium particles occupy completely defined places on the orbit.

The phase φ_0 has a remarkable and unique property: only this phase can, under certain definite conditions, remain constant all the time. For other phases, no such conditions exist. The quantity $eV_0/(2)\cos\varphi_0$ is equal to the energy acquired by the equilibrium particle from the electric field during one passage through the accelerating gap. For all other particles, $eV_0/(2)\cos\varphi_0$ (as will be shown below) is the energy acquired during one passage through the accelerating gap, averaged over the period of the phase oscillations. Of the two phase values $\pm\varphi_0$, only one is stable (in the cases of practical interest the phase $+\varphi_0$ is stable). Owing to the singular properties indicated above, the phase

Φ_0 is also called the "phasing point."

Expression (21) can be converted to a more convenient form. With the aid of the relation

$$R\omega_0 H_0 = c\mathcal{H}_0 \tag{22}$$

we readily obtain:*

$$eV_0 \cos\varphi_0 = \frac{(2\pi R_0 + L)eR_0H_0}{c}(1-\Delta), \tag{23}$$

where

$$\Delta = \frac{\dot{\Phi}_0}{2\pi R_0^2 H_0}\left[1 - \frac{L}{2\pi R_0 + L}\right]. \tag{24}$$

If $\Delta = 1$, then $\cos\varphi_0 = 0$. This means that in this case the average energy obtained by the protons from the electric field is equal to zero. The acceleration is only at the expense of the vortical electric field. By the same token we prove simultaneously that the condition

$$\Delta = \frac{\dot{\Phi}_0}{2\pi R_0^2 H_0}\left(1 - \frac{L}{2\pi R_0 + L}\right) = 1 \tag{25}$$

is indeed the condition for realization of betatron acceleration in an ideal accelerator with slots, and replaces the well-known betatron condition $\dot{\Phi}_0/(2\pi R_0^2 \dot{H}_0) = 1$ (the 2:1 condition). The phase equation (20) was derived by us for two accelerating gaps. It remains valid also for one or many gaps, if V_0 is taken to mean the sum of the amplitudes of the voltages on each of the gaps.

If we assume in equation (17) that there are no phase oscillations, that is, if we replace cos Φ by cos Φ_0 and neglect the intermittent character of the increase of the particle energy, that is, if we replace in the first equation $g(\gamma)$ by $1/\Pi$, we obtain the equations for the fast oscillations. Indeed, in this case we obtain from the first equation of (17):

$$\frac{\dot{\varphi}}{\omega_0} = \frac{1}{\Pi_0}\frac{\rho}{R_0}. \tag{26}$$

The integration constant is set equal to zero, for when $\dot{\Phi} = 0$ the deviation is $\rho = 0$. Substituting (26) in the second and third equations of (17) we readily obtain:

$$\frac{d}{dt}(E\dot{\rho}) + E\omega_0^2 H_0^2 (1-n)\rho g(\gamma) = 0;$$
$$\frac{d}{dt}(E\dot{z}) + E\omega_0^2 H_0^2 n z g(\gamma) = 0. \qquad (27)$$

The solution of equations (27) is the subject of Chapter 2. The separation which we made between fast and slow motions is physically obvious. In addition, a number of papers is devoted to a rigorous proof of this fact [6, 8, 24], so that this separation cannot raise any doubts whatever.

We note in conclusion that the phase equation for the accelerator with slots was first derived by us in the fall of 1948 and was used in the development of preliminary sketches and technical designs of the proton synchrotron of the USSR Academy of Sciences and its 180-Mev model.

§4. SOLUTION OF PHASE EQUATION IN THE FIRST APPROXIMATION

Equation (20) will be solved by the method which we developed [6, 8] for the solution of phase equations of cyclic accelerators.

We shall pay principal attention to the singularities of the phase equation for an accelerator with a slotted magnet as compared with the phase equation for a circular accelerator, since the latter was investigated in detail by the author [6, 8] and by others [9, 38], and is by now well known. In addition, in the present section we obtain several relations which will be used in chapters 4 and 5, devoted to the theory of resonance and injection theory.

The fundamental equation (20) can be rewritten, with the aid of the expression (23) for $\cos \Phi_0$, in the following simplest form:

$$\frac{d}{dt}\left(\frac{E}{KF\omega_0^2}\frac{d\varphi}{dt}\right) - \frac{eV_0}{2\pi}\cos\varphi = -\frac{eV_0}{2\pi}\cos\varphi_0. \qquad (28)$$

We recall that E, K, F, and $\omega_0(t)$ are specified functions of the time, which are calculated in fact from the following equations:

$$R_0 = \frac{3E}{M(R_0, t)}; \quad \beta = \sqrt{1 - \left(\frac{F_0}{E}\right)^2}; \quad F = 1 - \frac{n_0 - 1}{n_0^2 (1 - n) K}; \quad K = 1 + \frac{n}{1 - n} \frac{1}{\beta^2}. \tag{29}$$

In the first approximation all the coefficients of equation (28) can be regarded as independent of the time. In this case equation (28) is equivalent to the equation of an ordinary pendulum with external moment. As is known from pendulum theory, three types of motion are possible:

1) equilibrium motion, equivalent to the equilibrium position of the pendulum: $\varphi = \varphi_0$, $\dot{\varphi} = 0$;

2) oscillatory motion about the equilibrium motion, equivalent to oscillation of the pendulum about the equilibrium position. The phase velocity $\dot{\varphi}$ is equal to zero only in the mean. The phase φ varies within certain restricted limits;

3) nonresonant motion, which deviates gradually more and more from equilibrium. This case corresponds to rotation of the pendulum. The angular velocity $\dot{\varphi}$ increases on the average. The phase φ changes in one direction.

Let us carry a quantative calculation. Integrating (28) once (after first multiplying it by $\dot{\varphi}$) we get:

$$\dot{\varphi} = \omega_0 \sqrt{\frac{2 \omega_0 K F}{\pi E} |\sin \varphi - \varphi \cos \varphi_0 + a|}, \tag{30}$$

where a is the integration constant.

Let us find the range of values of the constant a, corresponding to oscillatory motion. The expression $D(\varphi) = \sin \varphi - \varphi \cos \varphi_0$ has a maximum when $\varphi = + \varphi_0$ and a minimum when $\varphi = - \varphi_0$. A plot of the function $D(\varphi)$ is shown in Fig. 3. The intersection of the plot of $D(\varphi)$ with the line $D = -a$ determines the values of the phases, at which $\dot{\varphi}$ vanishes.

In oscillatory motion, $\dot{\varphi}$ should vanish many times. For this purpose the line $D = -a$ should cross the curve $D(\varphi)$ at two points. The two crossing points merge into one at the maximum and minimum of the function $D(\varphi)$, and therefore

$$a_{max} = \sin\varphi_0 - \varphi_0\cos\varphi_0;$$
$$a_{min} = -\sin\varphi_0 + \varphi_0\cos\varphi_0.$$

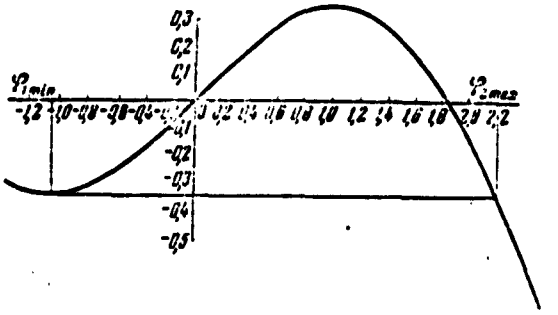

Fig. 3. Plot of the function $D(\varphi)$ for $\cos\varphi_0 = 0.5$.

Thus, the range of variation of the constant a is determined by the inequality

$$|a| \leqslant |\sin\varphi_0 - \varphi_0\cos\varphi_0|. \qquad (31)$$

As can be seen from the inequality (31), for the existence of a certain nonvanishing region of constant a, which would correspond to oscillatory motion, it is necessary to have $|\cos\varphi_0| < 1$. When $|\cos\varphi_0| > 1$ no phasing point φ_0 exists, and all the values of the constant a lead to nonresonant motion. Indeed, in this case $D(\varphi) = \sin\varphi - \varphi\cos\varphi_0$ is a monotonically decreasing function of φ, and for all values of the constant a the expression $\sin\varphi - \varphi\cos\varphi_0 + a$ can vanish only once. Consequently $\dot{\varphi}$ can likewise vanish only once, and in order to realize oscillatory motion $\dot{\varphi}$ should vanish many times.

We can express the constant a in terms of the initial conditions:

We recall that E, K, F, and $\omega_0(t)$ are specified functions of the time, which are calculated in fact from the following equations:

$$R_0 = \frac{3E}{M(R_0, t)}; \quad \beta = \sqrt{1 - \left(\frac{E_0}{E}\right)^2}; \quad F = 1 - \frac{n_0 - 1}{n_0^2 (1 - n) K}; \quad K = 1 + \frac{n}{1 - n} \frac{1}{\beta^2}. \tag{29}$$

In the first approximation all the coefficients of equation (28) can be regarded as independent of the time. In this case equation (28) is equivalent to the equation of an ordinary pendulum with external moment. As is known from pendulum theory, three types of motion are possible:

1) equilibrium motion, equivalent to the equilibrium position of the pendulum: $\varphi = \varphi_0$, $\dot{\varphi} = 0$;

2) oscillatory motion about the equilibrium motion, equivalent to oscillation of the pendulum about the equilibrium position. The phase velocity $\dot{\varphi}$ is equal to zero only in the mean. The phase φ varies within certain restricted limits;

3) nonresonant motion, which deviates gradually more and more from equilibrium. This case corresponds to rotation of the pendulum. The angular velocity $\dot{\varphi}$ increases on the average. The phase φ changes in one direction.

Let us carry a quantative calculation. Integrating (28) once (after first multiplying it by $\dot{\varphi}$) we get:

$$\dot{\varphi} = \omega_0 \sqrt{\frac{2 \cdot 3 KF}{\pi E} [\sin \varphi - \varphi \cos \varphi_0 + a]}, \tag{30}$$

where a is the integration constant.

Let us find the range of values of the constant a, corresponding to oscillatory motion. The expression $D(\varphi) = \sin \varphi - \varphi \cos \varphi_0$ has a maximum when $\varphi = + \varphi_0$ and a minimum when $\varphi = - \varphi_0$. A plot of the function $D(\varphi)$ is shown in Fig. 3. The intersection of the plot of $D(\varphi)$ with the line $D = -a$ determines the values of the phases, at which $\dot{\varphi}$ vanishes.

In oscillatory motion, $\dot{\varphi}$ should vanish many times. For this purpose the line D = −a should cross the curve D(φ) at two points. The two crossing points merge into one at the maximum and minimum of the function D(φ), and therefore

$$a_{max} = \sin\varphi_0 - \varphi_0\cos\varphi_0;$$
$$a_{min} = -\sin\varphi_0 + \varphi_0\cos\varphi_0.$$

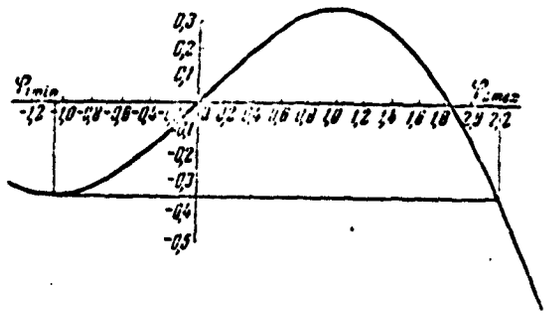

Fig. 3. Plot of the function D(φ) for cos φ_0 = 0.5.

Thus, the range of variation of the constant a is determined by the inequality

$$|a| \leq |\sin\varphi_0 - \varphi_0\cos\varphi_0|. \qquad (31)$$

As can be seen from the inequality (31), for the existence of a certain nonvanishing region of constant a, which would correspond to oscillatory motion, it is necessary to have $|\cos\varphi_0| < 1$. When $|\cos\varphi_0| > 1$ no phasing point φ_0 exists, and all the values of the constant a lead to nonresonant motion. Indeed, in this case D(φ) = sin φ − − φ cos φ_0 is a monotonically decreasing function of φ, and for all values of the constant a the expression sin φ − φ cos φ_0 + a can vanish only once. Consequently $\dot{\varphi}$ can likewise vanish only once, and in order to realize oscillatory motion $\dot{\varphi}$ should vanish many times.

We can express the constant a in terms of the initial conditions:

the initial phase velocity $\dot{\varphi}_{nach}$ and the initial phase φ_{nach}. From (30) we get:

$$a = \left(\frac{\dot{\varphi}_{nach}}{\omega_0}\right)^2 \left(\frac{\pi E}{el\omega_0 K F}\right) - \sin\varphi_{nach} + \varphi_{nach}\cos\varphi_0.$$

According to the foregoing relation, the initial conditions should satisfy the following inequality:

$$\left|\left(\frac{\dot{\varphi}_{nach}}{\omega_0}\right)^2 \left(\frac{\pi E}{el\omega_0 K F}\right) - \sin\varphi_{nach} + \varphi_{nach}\cos\varphi_0\right| \leqslant \sin\varphi_0 - \varphi_0\cos\varphi_0. \qquad (32)$$

Fig. 4 shows the region of initial conditions for different values of cos φ_0, satisfying inequality (32). If we replace the inequality sign of (31) by an equal sign, we obtain the separatrix curve, which separates the region of initial conditions that lead to oscillatory motion from the region of initial conditions that lead to rotary non-resonant motion.

We see that the separatrix encloses the maximum area when cos φ_0 = = 0 and contracts to a point when cos $\varphi_0 = 1$.

Of the two singular points $\pm \varphi_0$ on the phase plane, one is a center and the other is a saddle. If KF > 0, then it is obvious that the stable phase is $\varphi = \varphi_0$, and the unstable one is $\varphi = -\varphi_0$ (Fig. 5).

If KF > 0, then the character of the singular points changes. The stable phase is $\varphi = -\varphi_0$, and the unstable phase is $\varphi = +\varphi_0$.

The coefficient K > 0, if n < 1, and K < 0, if n > 1. Inasmuch as it is necessary for the stability of the fast oscillations in accelerators with ordinary focusing that n be smaller than unity (see below), the case K < 0 will be considered only in Chapter 6.

The coefficient F is a monotonic function of the energy (Fig. 5); it has a minimum when $\beta \sim 0$ and a maximum when $\beta = 1$.

$$\left.\begin{aligned} F_{max} &= 1 - \frac{L}{2\pi R + L}; \\ F_{min} &= 1 - \frac{L}{n(2\pi R + L)}. \end{aligned}\right\} \qquad (33)$$

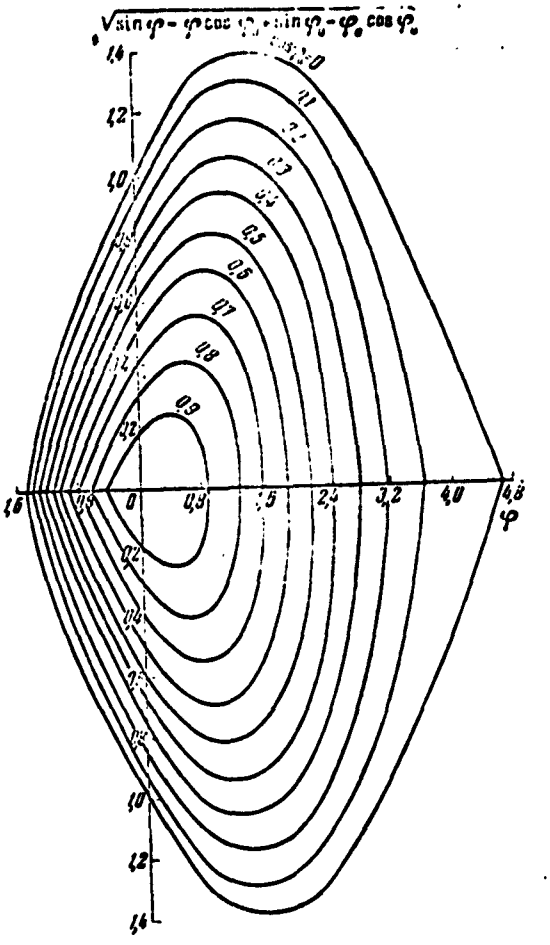

Fig. 4. Phase plane and separatrices for different cos φ_0.

We see that F_{max} is always larger than zero. F_{min} may prove to be smaller than zero if the length of the linear sections is sufficiently large or n is sufficiently small. In this case the stable phasing point is $-\varphi_0$ and the unstable one $+\varphi_0$. Of course, it is immaterial for the operation of the accelerator which of the two points is stable. It is sufficient that one of them be stable. However, for relativistic particles ($\beta \approx 1$), $F_{max} > 0$; hence if $F_{min} < 0$, then $F = 0$ at some instant in acceleration to relativistic energies. At that instant there exists no phasing point at all, and the phase pattern becomes changed. Large par-

ticle losses are possible then, for the two stability regions overlap only in part.

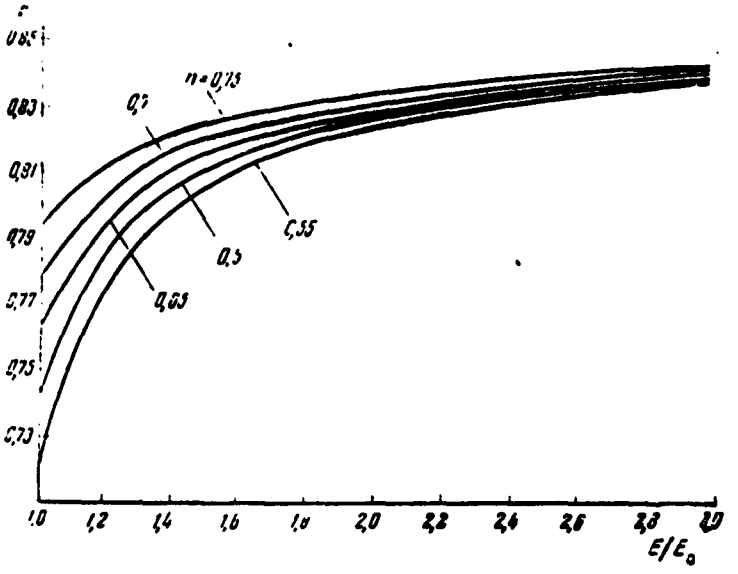

Fig. 5. Plot of F as a function of the energy for different values of n.

Therefore, for an installation such as the 10 Bev proton synchrotron, in which the particle velocity varies over a wide range, we should stipulate that F_{min} be larger than zero:

$$F_{min} > 0 \text{ or } \frac{1}{R} < \frac{n}{1-n}. \qquad (34)$$

The condition (34) must of course be satisfied with a margin, since, as will be shown below, small values of F_{min} are not desirable.

The condition (34) affords, generally speaking, a great freedom in the choice of the length of the linear portions, but it is nevertheless a more stringent limitation (in the region of values of n of interest to us) than the condition which will be derived below for the stability of the fast oscillations.

Usually a condition (34) is satisfied with a 6 to 10-fold margin. For example, for the 10 Bev proton synchrotron, $F_{min} = 0.77$ and condition (34) is satisfied with a 9-fold margin.

The occurrence of stability of the phasing point – φ_0 for a sufficient length of the linear sections, and the rearrangement of the phase region during the acceleration process, can be illustratively interpreted. We can state that an accelerator with slots presents a combination of annular and linear accelerators. It is known that in linear accelerators the stable point is – φ_0, and in annular ones it is + φ_0. The reason for it is that in linear accelerators the transit time between two passages through the accelerating slot decreases with increasing velocity, while in annular ones it increases. When the length of the linear sections is sufficiently great, the phase properties of the linear accelerator predominate over the phase properties of the annular accelerator. However, when $\beta \to 1$ the phase stability of the linear accelerator disappears, that is, the transit time ceases to depend on the energy, and therefore, no matter what the length of the linear sections, when $\beta \sim 1$ the phase properties of the annular accelerators prevail.

The concept of critical energy E_{kr}, which we were the first to introduce, and at which the phase region changes and phase stability is lost, has particular significance for accelerators with strong focusing. We have subsequently also shown how to eliminate the critical energy. In ordinary accelerators with weak focusing, the critical energy is eliminated by suitable choice of the index n. Concerning strong focusing, see Chapter 6.

Let us determine the amplitude of the phase oscillations. Let $\varphi_1 < \varphi_0$ and $\varphi_2 > \varphi_0$ be the extreme points, between which the phase oscillations are carried out. At these points $\dot{\phi}$ vanishes:

$$\frac{\dot{\phi}}{\omega_0} = \sqrt{\frac{eU_0 K F}{\pi E}} [\sin \varphi - \varphi \cos \varphi_0 - \sin \varphi_1 + \varphi_1 \cos \varphi_0] \qquad (35)$$

We obtain the value of φ_2 by drawing from the following trans-

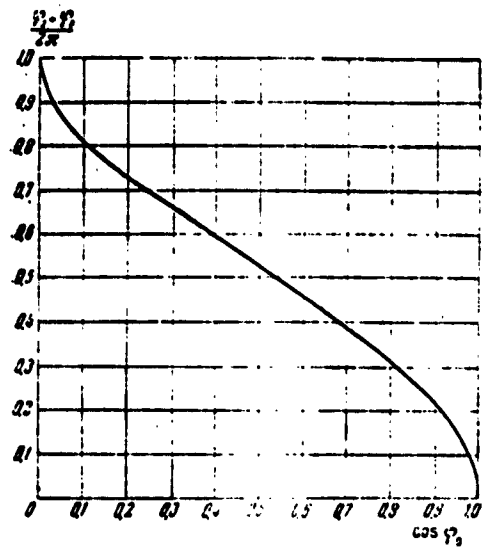

Fig. 6. Ratio of maximum region of stability with respect to φ, for different values of cos φ_0, to the stability region when cos φ = 0 and for values of cos φ_0 from 0 to 1 in steps of 0.05; the values of $\varphi_2 + \varphi_0/(2\pi)$ are respectively equal to: 1,000; 0.873; 0.815; 0.768; 0.729; 0.691; 0.656; 0.622; 0.589; 0.557; 0.524; 0.492; 0.459; 0.424; 0.389; 0.352; 0.312; 0.268; 0.217; 0.152; 0.

cendental equation:

$$\sin\varphi_2 - \varphi_2\cos\varphi_0 - \sin\varphi_1 + \varphi_1\cos\varphi_0 = 0. \qquad (36)$$

Inasmuch as sin φ − φ cos φ_0 has a minimum at the point $\varphi = -\varphi_0$, it is obvious that the smallest value of the phase is $\varphi_1 = -\varphi_0$. The largest value of φ_2 is obtained from (36) by putting $\varphi_1 = \varphi_0$:

$$\varphi_{2\max} - \frac{\sin\varphi_{2\max}}{\cos\varphi_0} = \operatorname{tg}\varphi_0 - \varphi_0. \qquad (37)$$

Thus, the greatest swing in the phase oscillations is $\varphi_{2_{max}} + \varphi_0$. Figure 6 shows a plot of the dependence of $(\varphi_{2_{max}} + \varphi_0)/2\pi$ on cos φ_0, obtained with the aid of numerical calculations. The radial oscillations connected with the phase oscillations (the radial-phase oscillations) can be determined from Eqs. (19) and (30):

$$\frac{\rho}{R} = \sqrt{\frac{eV_0}{\pi KFE^2(1-n)^2}(\sin\varphi - \varphi\cos\varphi_0 + a)}. \qquad (38)$$

Figures 7 and 8 show the trajectories of the radial-phase oscillations against the background of the chamber dimensions. The trajectories shown can be treated (when $\beta^2 \ll 1$) as prevailing in a coordinate system moving together with the equilibrium particle (of course, free oscillations are disregarded).

The amplitude of the radio oscillations is obtained from (38), by putting $\varphi = \varphi_0$:

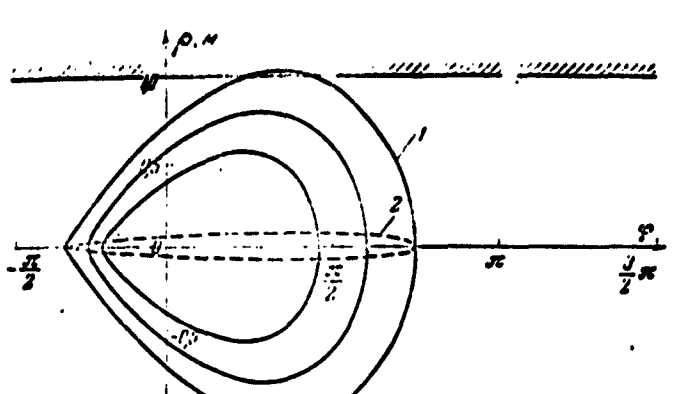

Fig. 7. Phase region at the start of acceleration (W_1 = 4 Mev) at a voltage V_0 = = 8 kv in variables ρ and φ: 1) Separatrix at the start of acceleration; 2) separatrix at the end of acceleration.

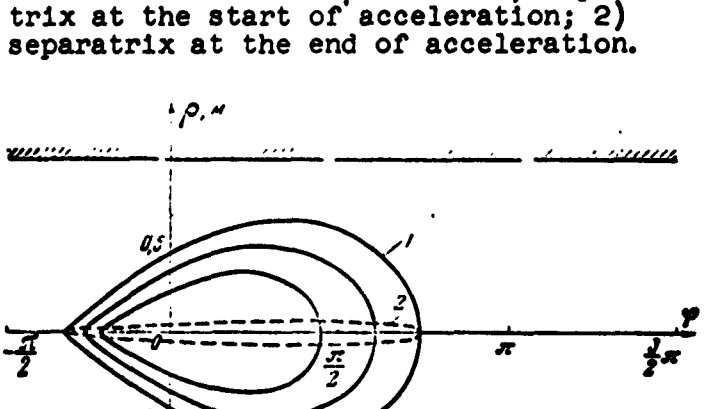

Fig. 8. The same phase region as in Fig. 7, but for a different injection energy (W_1 = 10 Mev).

$$\frac{\rho_A}{R_0} = \sqrt{\frac{eV_0}{\pi K E_0 \beta^2 (1-n)}} (\sin\varphi_0 - \varphi_0\cos\varphi_0 + a), \qquad (39)$$

$$a = -\sin\varphi_1 + \varphi_1\cos\varphi_0.$$

where ρ_A denotes the amplitude of the radial-phase oscillations. The greatest amplitude of radial oscillations will be denoted by $\bar{\rho}$. The value of $\bar{\rho}$ is obtained from (39) by putting $\varphi_1 = -\varphi_0$:

$$\frac{\beta}{\beta_0} = \sqrt{\frac{2\varepsilon_1 \omega_0 \sin\varphi_0}{\pi K F E (1-\beta_0^2)}\left(1 - \frac{\varphi}{\varphi_0}\cos\varphi_0\right)}. \quad (40)$$

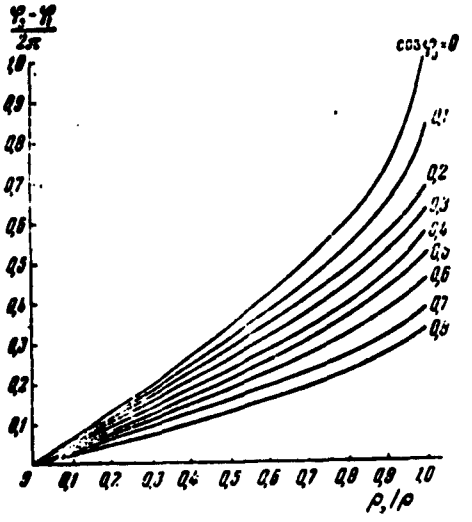

Fig. 9. Connection between the amplitude of the radio-phase oscillations ρ_A and the relative swing of the phase oscillations $(\varphi_2 - \varphi_1)/2\pi$, at different values of cos φ_0. In motion along the separatrix we have $\rho_A = \bar{\rho}$.

Figure 9 shows the dependence of the relative amplitude of the phase oscillations $(\varphi_2 - \varphi_1)/2\pi$ on the relative amplitude of the radial-phase oscillations $\rho_A/\bar{\rho}$ for different values of cos φ_0.

With the aid of Eqs. (16), (19), and (30) we can find the energy scatter of the particles ΔE:

$$\frac{\Delta E}{E} = \sqrt{\frac{\varepsilon_1 \omega_0}{\pi K F E}(\sin\varphi - \varphi\cos\varphi_0 + a)}. \quad (41)$$

The amplitude of the energy fluctuations $(\Delta E)_A$ and the largest amplitude $\Delta\bar{E}$ is determined in the same manner as used for the radial-phase oscillations.

Integrating (30) once more we obtain

$$\int_0^t \sqrt{\frac{\varepsilon_1 \omega_0 K F}{\pi E}}\,\omega_0 dt = \int_0^{\varphi} \frac{d\varphi}{\sqrt{\sin\varphi - \varphi\cos\varphi_0 + a}}.$$

The integration can be carried out in the general case only numerically. However, the expression obtained enables us to determine the frequency ω_1 of the phase oscillations. During one period of the phase oscillations $T_1 = 2\pi/\omega_1$ we can assume that ω_0, K, F, and E are constant, and then

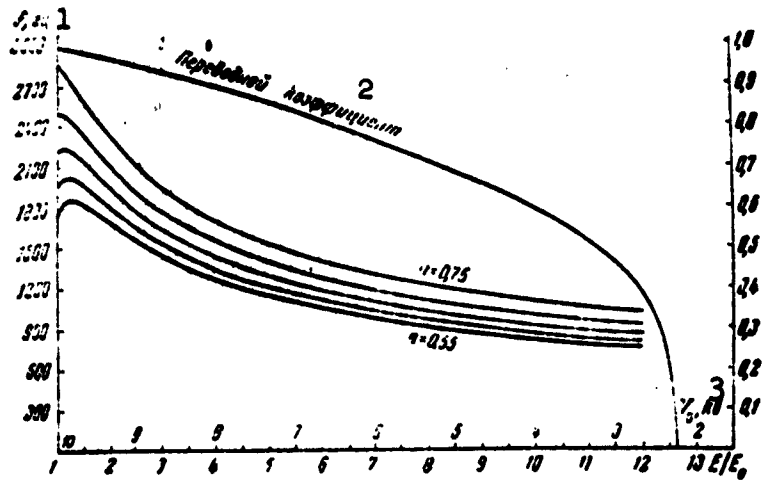

Fig. 10. Frequency (in cycles per second) of the phase oscillations; V_0 = 10 kv (vertical scale) and different values of the magnetic field index n (from n = 0.75 for the upper curve and n = 0.55 for the lower one with interval 0.05). The same figure shows the conversion coefficient for the calculation of the frequency of the phase oscillations for other values of V_0 (right-hand scale). 1) cps; 2) conversion coefficient; 3) kv.

$$T_1 = \frac{2}{\omega_0}\sqrt{\frac{\pi h}{eV_0 \sin\varphi_0}}\int_{\varphi_1}^{\varphi_2}\frac{d\varphi}{\sqrt{\sin\varphi - \varphi\cos\varphi_0 + \alpha}}, \qquad (42)$$

where $\varphi_1 < \varphi_0 < \varphi_2$. The phases φ_1 and φ_2 determine, as already mentioned, the amplitude of the phase oscillations.

Figure 11 shows a plot of the values of the integral contained in (42). So long as $|\varphi_1 - \varphi_0| \ll 1$, the value of this integral is constant. As $|\varphi_1 - \varphi_0|$ increases, the integral also begins to increase. When $\varphi_1 \to -\varphi_0$ the integral tends to infinity.

We introduce in place of the phase φ_1 the deviation α_{max} from the phasing point: $\alpha_{max} = \varphi_0 - \varphi_1$. The Integral (42) can be evaluated analytically, if we assume that $\alpha_{max} \ll 2\varphi_0$. In this case* (see Fig.

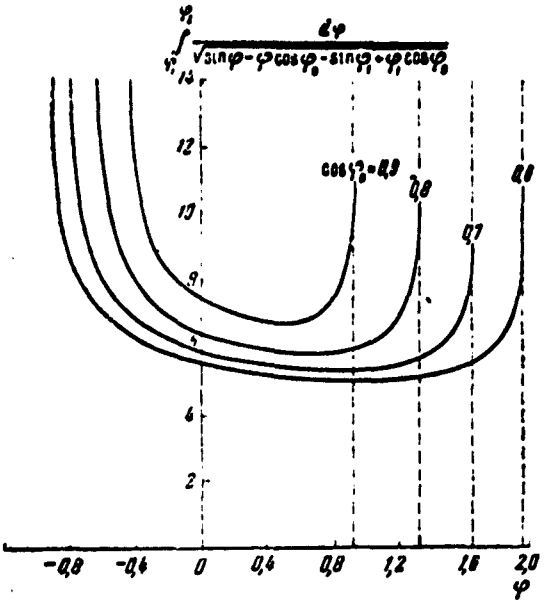

Fig. 11. Value of the integral

$$\int_{\varphi_1}^{\varphi_2} \frac{d\varphi}{\sqrt{\sin\varphi - \varphi\cos\varphi_0 - \sin\varphi_1 + \varphi_1\cos\varphi_0}}$$

as a function of φ_1 and φ_2. The value of φ_0 for each curve is marked by lines and arrows ($\varphi_1 < \varphi_0$; $\varphi_2 > \varphi_0$).

10) we have

$$\omega_1 = \omega_0 \sqrt{\frac{\dots}{2\pi L}} \left[1 - \frac{\dots}{16} \left(1 - \frac{5}{3}\cos^2\varphi_0 \right) + \frac{\dots}{\dots} + \dots \right]. \qquad (43)$$

Thus, the frequency of the phase oscillations in an accelerator with slots differs by a factor $\sqrt{F}$ from the frequency in an ordinary proton synchrotron (disregarding the fact that ω_0 is Π_0 times smaller than in a circular accelerator).

The results of this section serve also to prove the correctness of the assumptions which we have made in the derivation of the phase equation. Indeed, it is easy to show, for example, the correctness of

Relations (14) when $W_1 \gg eV_0$, which is always the case.

§5. SOLUTION OF PHASE EQUATION IN SECOND APPROXIMATION

We now proceed to determine the second approximation, which should take into account the influence of the changes in the coefficients of Eq. (20) on the change of the particle phase.

The solution given in the preceding section is valid only when the parameters are constant. But if the magnetic field, the frequency, and other parameters of the apparatus change sufficiently slowly, then the particle motion can be described as being successive transitions from one trajectory, obtained in the preceding section, to the next trajectory, that is, from motion with one integration constant $\underline{a}$ and several values of the parameters K, F, E, and ω_0, to motion with another constant and other values of the parameters. The integration constant and the parameters change here so slowly, that at each given instant the motion can be described in the same manner as before. In other words, at each given instant we can regard the motion as occurring on a definite trajectory calculated in the preceding section.

The law governing the variation of the integration constant or, what is the same, the law governing the variation of the oscillation amplitude, is determined with the aid of adiabatic invariants. The adiabatic invariant of a system with one degree of freedom is the integral $\oint pdq$, taken over the entire period of oscillation. In our case the role of $\underline{q}$ is assumed by the phase φ, and the role of $p = mq$ is assumed by the quantity $E\dot{\varphi}/\omega_0^2 K F$, since $E/\omega_0^2 K F$ plays in Eq. (20) the role of the mass (or the moment of inertia).

The adiabatic invariant (apart from the constants) can be written in the following form:

$$I_{adv} = \int \sqrt{\frac{E_{n+1}}{\omega_0^2 K F}} \oint \sqrt{\sin\varphi - \varphi_0 \cos\varphi_0 + a}\, d\varphi. \qquad (44)$$

From this we obtain the dependence of a on the time. In the general case the Integral (44) cannot be evaluated in terms of elementary functions. Figure 12 shows a plot of the function

$$\sqrt{U(\cos\varphi_0;\ \alpha_1;\ \alpha_2)} = \int_{\varphi_1=\varphi_0-\alpha_1}^{\varphi_2=\varphi_0+\alpha_2} \sqrt{(\sin\varphi-\sin\varphi_1)-(\varphi-\varphi_1)\cos\varphi_0}\,d\varphi.$$

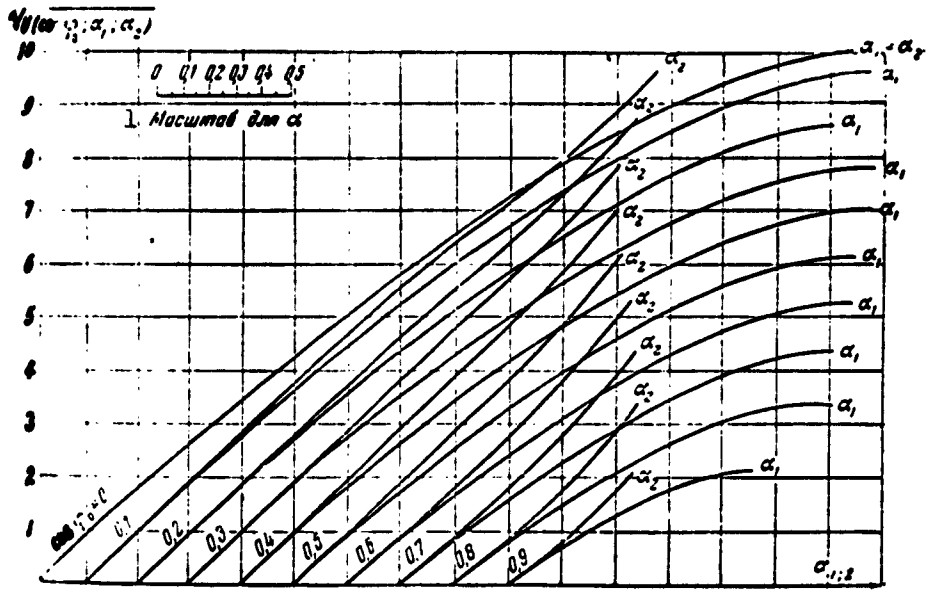

Fig. 12. Plot for the calculation of the variation of the phase-oscillation amplitudes upon change in the accelerator parameters. 1) Scale for α.

The use of the graph in Fig. 12 is very simple. A horizontal line crossing any curve gives the initial values of α_1 and α_2. For convenience, each pair of curves pertaining to different values of cos φ_0 starts from different points. Therefore the values of α_1 and α_2 (in radians) should be reckoned for each curve from its own origin. The ordinates of the curve yield the values of the integral $\sqrt{U}$.

When the parameters are changed, the product $\sqrt[4]{\frac{E\Gamma_0}{\omega_0^3 KF}}\sqrt{U(\cos\varphi_0;\ \alpha_1;\ \alpha_2)}$ should remain unchanged. Therefore the horizontal line is displaced to such an extent, that the indicated product remains constant. The new points of intersection determine new values of α_1 and α_2. When varying

cos φ, it is necessary to move horizontally to a second curve, corresponding to the new value of cos φ_0, and the intersections again determine the new values of α_1 and α_2.

The graph presented should be used only for sufficiently large oscillation amplitudes. Let us assume that the oscillations occur only in the vicinity of φ_0. We make a change of variable $\varphi = \varphi_0 + \alpha$ and carry out the calculation with accuracy to α^2. In this case

$$\alpha_{max} \sim \sqrt{\frac{\kappa F \omega_0^2}{\omega_0 \sin \varphi_0 \cdot E}}. \qquad (45)$$

In the relativistic case K, F, and ω_0 are constant, while the energy E is proportional to H, and therefore (when V_0 = const) α_{max} = $= (\varphi_0 - \varphi_1)$ is proportional to $H^{-1/4}$. In the nonrelativistic case it is necessary to take into account the time dependences of K, ω_0, and F, and the result will depend on the value of the magnetic field index n.

Figure 13 shows the dependence of $\alpha_{max}/(\alpha_{max})_{nach}$ on the particle energy for constant values of V_0 and sin φ_0, and for different values of the index n. Let V_0, R_0, and φ_0 remain unchanged during the acceleration process. We stipulate that under these conditions α_{max} must decrease all the time, that is, we require that the inequality $d\alpha/dt_{max} < 0$ be fulfulled. This requirement is equivalent to the condition $(d/dt)(K F \omega_0^2/E) < 0$. In carrying out the differentiation we take account of the fact that $\omega_0 = \omega_c \beta$ where ω_c = const. As a result we get

$$\frac{d^2\alpha_{max}}{dt} = b^2\left[2(1-\beta^2) - K\beta^2 + \frac{L}{(2\pi R_0 + L)(1-n)}\right] < 0, \qquad (46)$$

where b^2 is a positive quantity. The expression in the left half of the inequality decreases with increasing β^2. Therefore, if this inequality is satisfied when $\beta^2 = 0$, it will be satisfied for all other values of β^2. We thus obtain

$$n > \frac{2}{3} + \frac{L}{3(2\pi R_0 + L)} = n_{кр}. \qquad (47)$$

The Condition (47) replaces the condition n > 2/3 which we derived in 1946 [4] for a circular accelerator.

If $n < n_{kr}$, then the amplitude of the phase oscillations will first increase and then decrease. In the cases of practical interest this increase in amplitude is small. The increase in amplitude continues up to a certain energy value E_{kr}. We obtain the value of E_{kr} from (46) by replacing the inequality sign by an equal sign. Indeed, the vanishing of (46) denotes the reversal of the sign of $d\alpha_{max}/dt$:

$$E_{кр} = E_0 \sqrt{3(1-n)\,H_0}. \qquad (48)$$

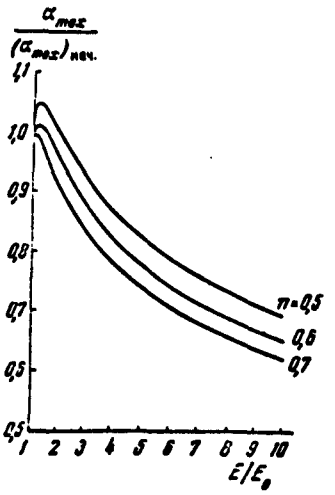

Fig. 13. Dependence of $\alpha_{max}/(\alpha_{max})_{nach}$ on the energy for the 10-Bev proton synchrotron data ($L/R_0 = 8/7$).

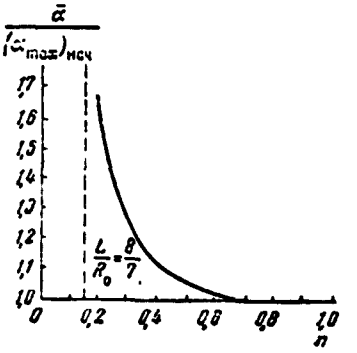

Fig. 14. $\bar{\alpha}/(\alpha_{max})_{nach}$ as a function of the values of n for the 10-Bev proton synchrotron parameters ($L/R = 8/7$).

It is obvious that the amplitude of the phase oscillations has a maximum when $E = E_{kr}$. Let us calculate the ratio of the largest amplitude $\bar{\alpha}$ of the phase oscillations to the initial value:

$$\frac{\bar{\alpha}}{(\alpha_{max})_{nach}} = \sqrt[4]{\frac{2}{3n\sqrt{3}(1-n)\Pi_0^{1/4}F_{min}}}. \qquad (49)$$

The ratio $\bar{\alpha}/(\alpha_{max})_{nach}$ as a function of n is plotted in Fig. 14 for a definite value of L/R_0.

§6. PHASE EQUATION WHEN THE MAGNETIC FIELD SPILLS OVER INTO THE LINEAR SECTIONS

The phase equation for the case when a magnetic field exists in the linear section is derived in perfect analogy with the case of the "ideal accelerator" (without a field in the linear section). In the derivation it is necessary to take into account the distinguishing features of the "nonideal accelerator" with slotted magnets. We shall therefore start to discuss these singularities, without obtaining the entire derivation.

Let us consider by way of an example the case of a field H, which is constant in the gap in the x and y directions (see Fig. 15). As will be shown in the next chapter, if a field is present in the linear portion, the magnet sectors will subtend not an angle $\pi/2$, but $\pi/2 - \delta_0$, where δ_0 is the angle through which the particle trajectory is turned in the linear section. We shall measure the lengths of the linear sections from the points A and B, in which the field is only slightly different (at the accuracy which interests, say by 1%) from the field inside the gap.

If the particle moves not along an equilibrium orbit, but is displaced as a result of the radial-phase motion, then the center of curvature will shift from the point C to the point O and the tangent to the particle trajectory will turn not through an angle δ_0, but an angle α (Fig. 15). Considering the Triangles ACB and AOB, we can find the connection between the angles α and δ_0:

$$\alpha = \frac{r_0 + \rho}{r_1}\delta_0.$$

The length of the circular trajectory of the particle in the linear portion is:

$$\frac{L}{4} = r_1\alpha = r_0\delta_0 + \rho\delta_0 = \frac{L_{эф}}{4} + \rho\delta_0.$$

Consequently, the perimeter of the orbit can be written in the following form:

$$R(2\pi - 4\delta_0) + L_{эф} + 4\rho\delta_0 = \\ = 2\pi R + L_{эф} - 4\delta_0(R - \rho).$$

Putting $L_{эф} - 4R_0\delta_0 = L^*$, we write for the perimeter of the orbit: $2\pi R + L^*$

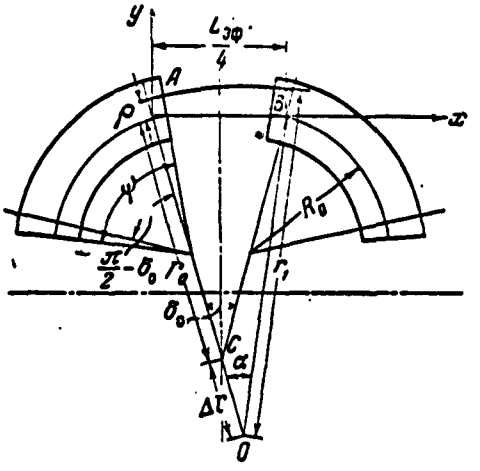

Fig. 15. Diagram explaining the symbols.

Thus, the coefficient Π, defined by Eq. (10), assumes the following form:

$$\Pi^* = 1 + \frac{L^*}{2\pi R}. \qquad (50)$$

In analogy with the foregoing, the magnetic flux Φ* (R,t) through the orbit of radius R also changes, since it is necessary to take into account the magnetic flux in the linear sections. The coefficient F is likewise changed:

$$F^* = 1 - \frac{\Pi^* - 1}{\Pi^* 2\pi k_0 [n - \nu^2(1-n)]}.$$

After going through all the steps for the derivation of the phase equation, we can show that the form of the phase equation does not change if Π, F, Φ, and L are replaced by Π*, F*, Φ*, and L*. Indeed, Eqs. (17) for the circular part of the magnet obviously remain the same. Nor are the equations for the straight line portions changed

we write for $g(\gamma)$ in the linear portions $H_1/H_0(R_0)$ and put $\overline{g(\gamma)}^{sr} = 1/\Pi^*$.

In radial accelerators, however, the magnetic field is not constant along the particle trajectory. But it is clear from the foregoing arguments that the decisive role is played by the angle of turn of the particle trajectory in the linear section, and not the form of $H_1(x)$. Therefore, if H_1 depends on x, then all the formulas will contain the average quantity $\overline{H} = \frac{1}{l}\int_0^l H_1(x)\,dx$, since this is the quantity responsible for the turning of the particle trajectory (see Chapter 2, §4). The law governing the variation of H_1 along the y axis has been shown by detailed calculations to influence little the motion of the particles under rather broad assumptions concerning the magnitude of the change in the field.

We have assumed in the preceding calculations that the presence of the field in the linear portions is taken into account in the construction of the magnet. The sectors have been made smaller by an angle δ_0, so that the equilibrium trajectory in the round sectors is part of a circle of radius R. If the correction for the angle δ_0 has not been made or has been made inaccurately, then, as shown in Chapters 2 and 3, the particle trajectory becomes distorted, but its length remains constant, accurate to $(\rho/R_0)^2$.

§7. ACCELERATION IN MULTIPLE RESONANCE

As will be shown in Chapters 4 and 5, it may be convenient to use multiple resonance between the revolution frequency and the accelerating-field frequency. For example, it will be shown in Chapter 5 that under certain conditions the intensity of injection increases in multiple resonance. It is indicated in Chapter 4 that it is possible to avoid the undesirable resonance between the high frequency pertuba-

tions of the magnetic field and the slow phase oscillations with the aid of multiple resonance.

In addition, in multiple resonance the accelerating system with two gaps and a single linear section operates more effectively.

A detailed investigation of the multiple-resonance conditions (for a round accelerator) was made in considerable detail in [39]. In the present section we touch briefly only upon the general and principal problems of the multiple acceleration mode. As far as we know, our investigations are the only theoretical work devoted to this problem. The first actual multiple acceleration mode was realized by A.M. Prokhorov [40].

Let us assume that the frequency of the accelerating electric field is q times larger than the frequency of revolution of the equilibrium particle:

$$\omega_0(t) = q\dot{\varphi}.$$

If we have accelerating gaps in only one linear portion, then q can assume arbitrary integral values.

In what follows it would be convenient to use the following notation: φ denotes, as before, the phase of the particle in degrees of the high-frequency accelerating field; ψ is the phase in degrees of the particle trajectory (at angles γ). If $q = 1$, then φ and ψ coincide. They are obviously connected by

$$\psi = \frac{\varphi}{q} + 2\pi\frac{N}{q}; \quad \dot{\psi} = \frac{\dot{\varphi}}{q}, \tag{51}$$

where N is an integer smaller than q. In multiple resonance, the motion of the particle is in resonance not with the first but with the q-th harmonic of the expansion (11) of the accelerating field in a series of traveling waves. For this purpose we must obviously satisfy the condition $2K - 1 = q$ [see (11)] or $K = (q + 1)/2$. From this fol-

lows, incidentally, also the condition that q must be odd in the case of two accelerating gaps, since K is an integer. In the derivation of the phase equation only the relations between the frequency of the accelerating field and the particle revolution frequency change. Thus, for example, Eqs. (14) and (15) are now rewritten in the form

$$\left.\begin{aligned} q\frac{\dot{\varphi}}{H} &= \omega_0 - \dot{\varphi} \quad \text{or} \quad q\left(\frac{\dot{\varphi}}{H} + \dot{\varphi}\right) = \omega_0; \\ q\gamma &= \int \omega_0 dt - \varphi = \int \omega_0 dt - q\varphi + 2\pi N. \end{aligned}\right\} \tag{52}$$

Consequently, if ω_0 is replaced in Eqs. (17), (20), and (28) by ω_0/q, and $\dot{\Phi}$ is replaced by $\dot{\varphi}/q$, we obtain the phase equation for the case of multiple resonance. For example, in place of (28) we write

$$\frac{d}{dt}\left[\frac{Eq}{\omega_0^2 FK}\frac{d\varphi}{dt}\right] - \frac{eV_0\cos\varphi}{2\pi} = -\frac{eV_0\cos\varphi_0}{2\pi}. \tag{53}$$

Equation (53) differs from (20) and (28) in that the first term on the left has a constant coefficient q.

Let us integrate (53). In analogy with the foregoing we obtain:

$$\frac{\dot{\varphi}}{\omega_0} = \sqrt{\frac{eV_0 K^2 F}{\pi q E}(\sin\varphi - \varphi\cos\varphi_0 + a)}. \tag{54}$$

Comparing with (30), we see that $\dot{\varphi}/\omega_0$ decreases by a factor $\sqrt{q}$. Inasmuch as Relation (19), which connects the radial deviation ρ with $\dot{\varphi}/\omega_0$, remains unchanged, in the case of multiple resonance (but other conditions remaining equal) the amplitude of the radio oscillations decreases by a factor $\sqrt{q}$. The amplitude of the energy oscillations $(\Delta E)_A$ also decreases by a factor $\sqrt{q}$ [see Eqs. (38)-(41), whose right half should be divided in our case by $\sqrt{q}$].

Let us find the frequency of the phase oscillations by the method of §4 [see (43)]:

$$\omega_1 = \omega_0 \sqrt{\frac{eV_0 K^2 F \sin\varphi_0}{2\pi q E}}. \tag{55}$$

Thus, the ratio ω_1/ω_0 is $\sqrt{q}$ smaller than before, but ω_1 is ob-

viously larger by the same amount. It is obvious that this circumstance can be used if ω_1 must be changed in order to avoid some undesirable resonance (see Chapter 4).

The stability region can be determined from equations of the type (32):

$$\left|\left(\frac{\dot{\varphi}_{max}}{\omega_0\sqrt{q}}\right)^2 \frac{\pi E}{eV_0 kF} - \sin\varphi_{max} + \varphi_{max}\cos\varphi_0\right| \leqslant \sin\varphi_0 - \varphi_0\cos\varphi_0. \qquad (56)$$

We see from this equation that the stability region, plotted in the coordinates $(\dot{\varphi}, \varphi)$, remains the same if the φ scale is left unchanged, but $\dot{\varphi}$ is multiplied by $\sqrt{q}$. In the ordinary scale, all the dimensions in the direction of the $\dot{\varphi}$ axis are contracted by a factor $\sqrt{q}$, while in the direction of the φ axis they remain unchanged.

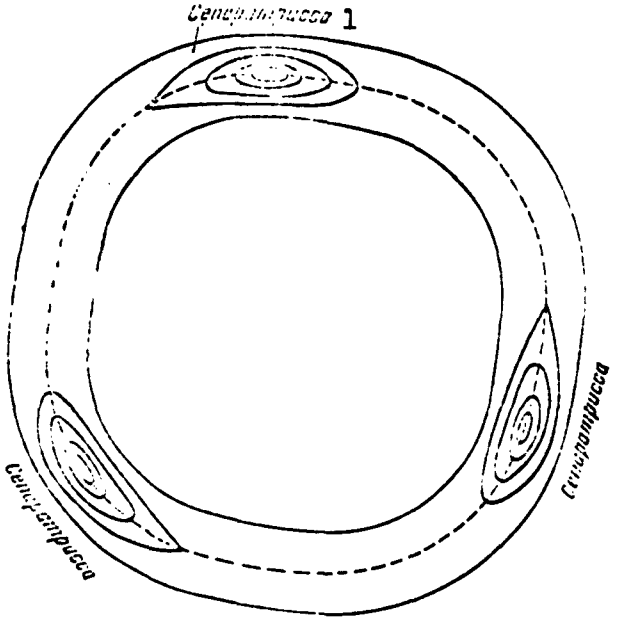

Fig. 16. Phase plot for $\cos\varphi_0 = 0.6$ and multiplicity $q = 3$ against the background of the accelerator chamber. 1) Separatrix.

In place of the $\dot{\varphi}$ we introduce the axis ρ, using the fact that ρ is proportional to $\dot{\varphi}$ [see (19)]. In this case (56) is rewritten in the

form

$$\left|\left(\frac{\rho_{max}}{R_0\sqrt{q}}\right)^2 \frac{\pi E'}{eV_0} K F_0^2 (1-n)^2 - \sin\varphi_{min} + \varphi_{min}\cos\varphi_0\right| < \sin\varphi_0 - \varphi_0\cos\varphi_0. \qquad (57)$$

On going over from degrees φ of the high frequency field to degrees of the particle trajectory, we make use of the first formula of (51) which signifies a change in scale along the φ axis by a factor g, and a transfer of the origin by an amount $2\pi N/q$. When the phase φ varies between 0 and 2π, the phase Ψ varies between 0 and $2\pi/q$. Inasmuch as (57) is periodic in φ with period 2π, the period in Ψ is $2\pi/q$. Consequently, the separatrix separating the stable region (57) from the unstable one, is contracted by a factor g on changing from φ in degrees to Ψ in degrees, and is repeated g times in identical fashion over the extent of the interval $0 < \Psi < 2\pi$, as shown in Fig. 16.

Thus, in g-fold resonance we have q particle beams in the accelerator. It is easy to see that the total area g of the separatrixes, in the case of g-fold resonance, is $q^{1/2}$ smaller than the area of one separatrix in ordinary resonance.

When the intensity is calculated in Chapter 5, it is necessary to know the connection between the amplitudes of the phase and radial oscillations. Figure 9 shows the dependence of $(\varphi_2 - \varphi_1)/2\pi$ on $\rho_A/\overline{\rho}$ for $q = 1$, where φ_1 and φ_2 are the extreme points of the phase oscillations. When $q \neq 1$ we are interested in the sum $\frac{1}{2\pi}\sum (\Psi_{2i} - \Psi_{1i})$, where Ψ_{21} and Ψ_{11} are the extreme points of the phase oscillations in the i-th beam. It is easy to see that as a result of (51)

$$\varphi_2 - \varphi_1 = \sum (\Psi_{2i} - \Psi_{1i}).$$

Thus, the plot in Fig. 9 can be used also in the present case. It must be remembered, however, that, other conditions being equal, the maximum permissible deviation $\overline{\rho}$ in the case of g-fold resonance is $\sqrt{q}$

times smaller than usual.

Multiple resonance has the same effect on the magnitude of the radial oscillations as a reduction in the amplitude of the accelerating voltage. But a reduction in the amplitude of the accelerating voltage simultaneously decreases the region of stability with respect to the coordinate ψ. At the same time, the transition to multiple resonance does not change the region of stability with respect to ψ. The influence of multiple resonance on the intensity will be investigated in Chapter 5. It can be stated here that the "convenience" or "inconvenience" of multiple resonance depends on the dimensions of the separatrix and on the dimensions of the accelerating chamber. It therefore turns out that in the 180-Mev model, where the separatrix is very small, multiple resonance is harmful. In the 10-Bev proton synchrotron, at an injection energy of 4 Mev, it is convenient to use multiple resonance. An increase in the injection energy by g times affects the stability region in exactly the same manner as g-fold resonance. Therefore, at large injection energies (20 Mev) it is "inconvenient" to use multiple resonance. In addition, multiple resonance can be used for certain physical experiments, in which it is essential to obtain short particle pulses striking a target.

[Footnotes]

Manuscript Page No.

53 It is easy to show with the aid of Relation (21) that if $\dot{R}_0 \neq 0$, then

$$eV_0 \cos\varphi_0 = \frac{(2\pi R_0 + L)\, e H_0 f}{c}(1-\Delta) + (1-n)\,\psi^2 R^2 T \frac{\dot{R}_0}{R_0}. \qquad (23')$$

64 ω_1 is calculated with accuracy to α^4_{max} in Chapter 4 [see (4, 84)].

Manuscript Page No.

[List of Transliterated Symbols]

57 нач = nach = nachal'nyy = initial

69 кр = kr = kriticheskiy = critical

71 эф = ef = effektivnyy = effective

72 ср = sr = sredniy = average

Chapter 2

FAST OSCILLATIONS OF PARTICLES

§1. Introduction

Fast oscillations in accelerators with slotted magnets were investigated in [32, 38]. However, as will be shown below, the calculation made by Dennison, Berlin, et al did not make it possible to actually estimate how the linear portion really influenced the operation of the accelerator. Moreover, the criterion of the influence of the linear portion as introduced by Dennison and Berlin is the so-called quantity r^2, the ratio of the maximum to the minimum oscillation amplitude, which, as will be shown below, has no physical meaning. These calculations did not make it possible to estimate the influence of the presence of the linear sections on the particle intensity. All these questions were completely solved again in the works of the author together with A.M. Baldin and V.V. Mikhaylov [17-19, 22] in 1949-1950.

The present chapter is devoted to the motion of particles in the so-called theoretical magnetic field, which will be defined below. Other important questions concerning the motion of particles, which were not at all discussed in the literature, namely the motion of the particles when the magnetic field deviates from theoretical and resonance phenomena in the motion of the particles, will be developed in Chapters 3 and 4. An account of the influence of the linear sections on the intensity of the accelerated beam is also investigated in Chapter 5.

In the present chapter we consider the motion in a constant mag-

netic field; an account of the variation of the magnetic field is given in Chapter 4 (§§2 and 3). This question is treated separately in Chapter 4 in order to avoid repetition. In Chapter 4, in considering the passage through resonance, we are forced all the same to regard the parameters of the equation (the magnetic field, the index n, and others) as variable quantities.

§2. Calculation of Particle Trajectories in an Ideal Accelerator with Slots

We must solve Eqs. (I, 27) which were obtained in the preceding chapter. In the first part of our calculation we use the method proposed by Dennison and Berlin [32]. Namely, we solve the equations (I, 27) separately for the circular sectors and for the linear portions, and then "join" these solutions.

The fast motions in the circular sectors have been thoroughly investigated. The basic results are universally known. We formulate only those premises, which will be used later on.

We write down the fast oscillations in the circular sectors in the form

$$\chi = A \sin \omega t + B \cos \omega t, \tag{1}$$

where χ denotes either ρ or z, and

$$\omega = \omega_0 = \frac{\omega}{R},$$

$\kappa = \sqrt{1 - n}$ for radial oscillations and $\kappa = \sqrt{n}$ for vertical oscillations.

The amplitudes of oscillations A and B decrease with varying magnetic field in proportion to $H^{-1/2}$. Inasmuch as the fast oscillations can be regarded independently of the radial-phase oscillations U, the principal results can be obtained by means of an analysis in a constant magnetic field, independently of the increase in energy. We therefore assume in the present chapter H = const.

As in the case of slow oscillations, we consider first a motion in an ideal accelerator with slots. In this case we can write an equation of the type (12) for each sector.

For example, for the k-th sector:

$$\chi_k = A_k \sin \omega t_k + B_k \cos \omega t_k \qquad (2)$$

For convenience we measure the time for each sector from the instant that the particles enter in it (therefore we use t_k in place of t in (2)).

Let us find the connection between the amplitudes (A_k, B_k and A_{k+1}, B_{k+1}) in two neighboring sectors of the magnet. In the linear section of an ideal accelerator with slots, there is no magnetic field. Therefore the particle will move along a straight line. This means that $\dot{\chi}$ does not change during the time of flight, and χ changes by an amount $\dot{\chi} l/v$, where l is the length of one gap and $v \approx R_0\omega$ is the velocity. Taking these considerations into account, we readily obtain

$$\begin{aligned} A_k \cos\tfrac{2\pi\varkappa}{N} - B_k \sin\tfrac{2\pi\varkappa}{N} &= A_{k+1}, \\ A_k \sin\tfrac{2\pi\varkappa}{N} + B_k \cos\tfrac{2\pi\varkappa}{N} &= -\tfrac{\dot{\chi}_k(v)\, l}{v} + B_{k+1}. \end{aligned} \qquad (3)$$

Here $\dot{\chi}_k(v)$ is the value of $\dot{\chi}_k$ at the end of the k-th sector

$$\dot{\chi}_k(v) = \omega\varkappa \left[A_k \cos\tfrac{2\pi\varkappa}{N} - B_k \sin\tfrac{2\pi\varkappa}{N} \right]; \qquad (4)$$

N is the number of sectors.

We introduce the notation

$$\varkappa = \tfrac{2\pi\varkappa}{N}, \quad p = \tfrac{l\varkappa}{2R_0}, \quad s = \sin\tfrac{2\pi\varkappa}{N}, \quad c = \cos\tfrac{2\pi\varkappa}{N}. \qquad (5)$$

Then Eq. (3) assumes the form

$$\left.\begin{aligned} A_k c - B_k s &= A_{k+1}, \\ A_k (s + 2pc) + B_k (c - 2ps) &= B_{k+1}. \end{aligned}\right\} \qquad (6)$$

From the system of the two first-order difference equations (6) we eliminate B_k and B_{k+1}, thereby increasing the order of the equation

$$A_{k+2} + A_k - 2A_{k+1}(c - ps) = 0. \qquad (7)$$

We seek the solution of (7) in the form

$$A_k = De^{i\mu k}.$$

Substituting $De^{i\mu k}$ in (7) and canceling $De^{i\mu(k+1)}$ out, we obtain

$$e^{i\mu} + e^{-i\mu} = 2(c - ps)$$

or

$$\cos\mu = c - ps. \qquad (8)$$

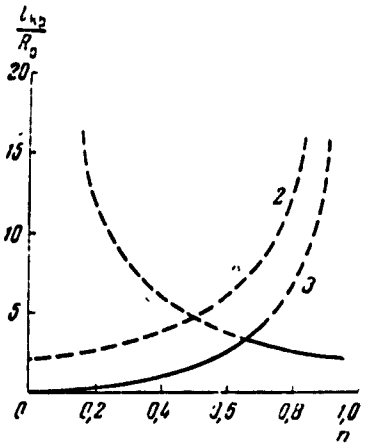

Fig. 17. Permissible values of 1/R, obtained from the requirement that the phase and fast oscillations be stable at different values of n. The solid curve shows the permissible values of 1/R for simultaneous stability of both oscillations. 1) Vertical fast oscillations; 2) radial fast oscillations; 3) phase oscillations.

From Eq. (8) we obtain two values of μ, which are of opposite sign. We shall henceforth assume μ to be positive. When $p = 0$ we get $\mu = \kappa\nu$; when $p \ll 1$ we readily obtain

$$\mu \approx \kappa\nu + p - \frac{p^2 c}{2s} + p^3\left(\frac{1}{6} + \frac{c^2}{2s^2}\right) + \ldots \qquad (9)$$

The general solution of (7) assumes the form

$$A_k = De^{i\mu k} + D^* e^{-i\mu k} = D_1 \cos\mu k + D_2 \sin\mu k; \qquad (10)$$
$$D = \frac{1}{2}(D_1 - iD_2).$$

The asterisk following a letter denotes here the complex conjugate. In order not to have growing terms in the solution, the following inequality must be satisfied

$$|\cos\mu| = |c - ps| < 1. \qquad (11)$$

Condition (11) imposes certain requirements, which are generally speaking not stringent, on relation $1/R_0$. Figure 17 shows the dependence of the limiting values of $1/R_0$ on the magnetic field index for the vertical and radial motions.

We determine B_k from the first equation of (6):

$$B_k = \frac{A_k c - A_{k+1}}{s} = A_k d; \qquad (12)$$

$$d = \frac{c - e^{i\mu}}{s}.$$

Thus, the values of B_k differ from A_k by a constant factor, so that we can write

$$B_k = D_k d e^{i\mu k} + D_k^* d^* e^{-i\mu k} = c_1 \cos \mu k + c_2 \sin \mu k. \qquad (13)$$

The quantities c_1, c_2, D_1, and D_2 are not independent. The connection between them is established with the aid of (12).

The constant D, and also D_1 and c_1 can be readily expressed in terms of the initial conditions (the initial deviation and the initial velocity). Let, for example, the injector be located at the start of the sector, and let at the instant t = 0 the deviation be $\chi = \chi_0$ and the velocity k = 0.

Then we must put in (2)

$$\gamma_0 = B_0 = Dd + D^* d^* = c_1; \qquad (14)$$

$$\gamma_0' = \omega_z A_0 = \omega_z (D + D^*) = \omega_z D_1. \qquad (15)$$

The constant D, as well as D_2 and c_2, can be readily obtained from (12), (14), and (15)

$$D = \frac{\frac{\gamma_0'}{\omega_z} d^* - \gamma_0}{d^* - d}; \quad D_2 = \frac{s}{\sin \mu} \left[\frac{\gamma_0'}{\omega_z} p - \gamma_0 \right]; \qquad (16)$$

$$c_2 = \frac{1}{\sin \mu} \left[\frac{\gamma_0'}{\omega_z} (s + 2ps) - ps\gamma_0 \right].$$

The general solution of the equations (I, 27) has the form

$$\gamma_k = (De^{i\mu k} + \text{c. c.}) \sin \omega_z t_k + (dDe^{i\mu k} + \text{c. c.}) \cos \omega_z t_k. \qquad (17)$$

In [32, 38] the solution (17) was interpreted as follows: the fast oscillations are produced in an accelerator with slotted magnet with the same frequency $\kappa\omega$ as in a circular accelerator with radius R_0, but the oscillation amplitude is modulated with frequency μ. No actual investigation of (17) was made, and all attention was focused on the behavior of the oscillation amplitudes [Eqs. (10) and (13)].

However, such an analysis has several shortcomings. Indeed, the "modulation" frequency μ turns out to be larger than the frequency of the oscillations (in the same units) $2\pi\kappa/N$, so that the concept "modulation" does not apply in Formula (17). In addition, in the investigation of the motion we are interested, of course, not in the amplitude of the oscillations but in the maximum deviation χ.

In the papers cited the authors identify the maximum deviation in a given sector with the amplitude, although, as will be shown below, this is not true for all azimuths.

For the calculation of the intensity in accelerators, the main problems are collisions with the injector and with the chamber walls. It is therefore necessary to determine the maximum and minimum deviations at the injector azimuth and the azimuths in which the deviations are maximum and minimum.

As a rule, no such determinations were made, and the ratio of the maximum to minimum amplitude was introduced instead as a characteristic of the "imperfection" of the slotted accelerator as compared with the circular accelerator.

We have obtained a simpler and physically clearer expression for the free oscillations, with the aid of which we can answer the foregoing questions and present a more complete and clear description of the motion of particles in an accelerator with slots.

We introduce the dimensionless length

$$\sigma = \frac{\varkappa S}{R_0}, \qquad (18)$$

where S is the length of the path along the equilibrium orbit. It is obvious that $\kappa\omega t_k = \sigma_k$, where σ_k is the dimensionless length of the path covered by the particle in the $\underline{k}$-th sector. Therefore the deviation in (17) can be regarded as a function of σ_k and $\underline{k}$. The discrete

variable $\underline{k}$ is connected with the particle revolution number M by the relation

$$k = N \cdot M, \tag{19}$$

Equation (17) can obviously be rewritten in the form

$$\chi_M = (D \sin\sigma + dD\cos\sigma)\, e^{i\mu k} + \text{c.c.} = F_c(\sigma)\cos(NM\mu + \alpha(\sigma)), \tag{20}$$

where

$$F_c = 2\,|D\sin\sigma + dD\cos\sigma|;$$
$$\alpha = \operatorname{Arg}|D\sin\sigma + dD\cos\sigma|. \tag{21}$$

We have written σ without the subscript $\underline{k}$ in Formula (20), since this formula holds true for any $\underline{k}$. With such an expression for the deviation χ_M, it is natural to regard $F_c(\sigma)$ as the oscillation amplitude at the azimuth σ. This amplitude is constant* for a given value of the azimuth σ, for specified initial conditions, and for the chosen injector position. Thus, by fixing the value of σ in the formula for $F_c(\sigma)$, we obtain an expression for the maximum deviation at the given location in the sector. It is obvious that in order to find the extremum of (20) it is sufficient to seek the extremum of F_c.

Substituting in (21) the expressions for D and $\underline{d}$ from (12) and (16), we get

$$F_c^2 = 4DD^*\left[1 + \frac{2p\cos s\cos(s_v - \sigma)}{s}\right] =$$
$$= \frac{s\,[s + 2p\cos s\cos(s_v - \sigma)]}{\sin^2 s}\left[\chi_0^2 + \frac{\dot{\chi}_0^2}{\omega^2}\left(1 + 2p\,\frac{\sigma}{s}\right) - 2p\chi_0\frac{\dot{\chi}_0}{\omega}\right], \tag{22}$$

where $\sigma_v = 2\pi\kappa/N$ is the length of one sector in dimensionless units (18). As can be seen from (22), F_c^2 consists of two factors, one dependent only on σ and the other on the initial conditions (the parameters of the accelerator with slots are assumed to be specified). Thus, the curves $F_c^2 = F_c^2(\sigma)$ on the (σ, F_c^2) plane are identical for all sectors and are symmetrical relative to the centers of the sectors. For different initial conditions, one curve goes over into another by multiplying all ordinates by a constant factor.

The condition $dF_c/d\sigma = 0$ yields

$$\sigma_{max} = \frac{\sigma_\nu}{2}; \quad \sigma_{min} = \frac{\sigma_\nu \pm \pi}{2}, \qquad (23)$$

where σ_{max} and σ_{min} are the azimuths, on which F_c is maximal and minimal. From (23) it follows that F_c has a maximum always at the center of the sector, while no minimum is produced within the sector, since σ_{min} always lies outside the sector. Indeed, even in the case of two linear spaces, in accordance with (18), the angular dimension of the sector is in our units $\sigma_\nu < \pi$. Therefore σ_{min} is either smaller than zero, or larger than π, although by definition $0 < \sigma < \sigma_\nu$.

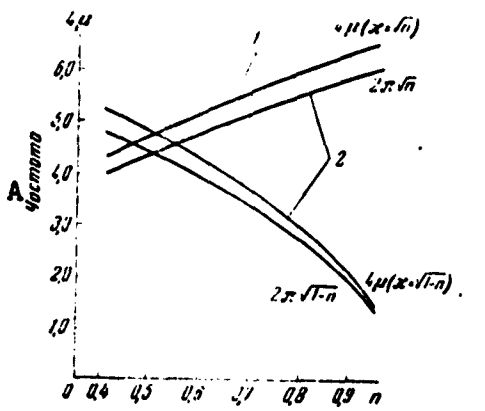

Fig. 18. Dependence of the frequency of the fast oscillations in dimensionless units on the index n in a circular accelerator and in the 10-Bev proton synchrotron ($1/R_0 = 2/7$): 1) accelerator with slots; 2) circular accelerator. A) Frequency.

The maximum and minimum values of F_c^2 coincide with the maximum and minimum of $A_k^2 + B_k^2$ obtained previously by the other cumbersome method, using the concept of "modulation" of the oscillations. In addition, however, we proved here that the maximum of the oscillations occurs only at the center of the sector, and no minimum is produced in the sector. Thus, it becomes particularly clear that the characteristic introduced by Dennison and Berlin, referred to above, has no phys-

ical meaning.

The dimensionless oscillation frequency is, according to (20), equal to $N\mu$ in lieu of $2\pi\kappa$ for the circular accelerator. Figure 18 shows the dependence of 4μ on $\underline{n}$ for the parameters of the proton synchrotron of the USSR Academy of Sciences. For comparison, we show also plots for the frequency $2\pi\kappa$.

The $F_c(\sigma)$ curve for the specified initial conditions limits the region of the sector in which the oscillations take place, and, as can be seen from (20), the deviation at the given azimuth σ reaches a value F_c, but nowhere exceeds it. Therefore F_c can be called the envelope of the particle trajectories for specified initial conditions. The value of the envelope is also important for the calculation of intensity.

We note that the dependence of F_c on σ can be regarded as "spatial modulation" of the amplitude of the oscillations occurring with frequency $N\mu\omega/2\pi$. This modulation is produced in such a way, that the distribution of the amplitudes is constant in time. By way of illustration we can point out the analogy between Formula (20) with the equation of a standing wave, in which the amplitudes are likewise different at different points. In the standing wave, however, the oscillations occur at all points either in phase or out of phase. In our case, the phase of the oscillations varies from point to point like in a traveling wave.

So far we have considered oscillations of particles in any place in the magnet sector. Let us consider now the oscillations of the particles in the linear section. The deviation of the particle from the equilibrium orbit in the $\underline{k}$-th linear section will be denoted by χ_k^{pr}. Obviously,

$$\chi_k^{пр} = \chi_k(\sigma_\nu) + \dot{\chi}_k(\sigma_\nu)\frac{\sigma_{пр}}{\varkappa\omega}, \qquad (24)$$

where $\chi_k(\sigma_\nu)$ and $\dot{\chi}_k(\sigma_\nu)$ are the deviation and its time derivative at

the end of the k-th sector, and σ_{pr} is the length reckoned in the linear section from the sector, along the equilibrium orbit, in the dimensionless units (18).

Indeed, $\sigma_{pr}/\omega\kappa = t_{pr}$ is the time reckoned from the instant that the particle enters into the k-th linear section. The length of the linear section in dimensionless units is equal to 2p. We note that Formula (24), which we have obtained for an "ideal accelerator with slots," remains valid under certain assumptions also for a "nonideal accelerator with slots," i.e., for an accelerator with a magnetic field in the linear section (see §4).

Using (17), we obtain

$$\begin{aligned}\chi_k^{np} &= [D_2(s+c\sigma_{np}) - c_2(s\sigma_{np}-c)]\sin\mu k + \\ &+ [D_1(s+c\sigma_{np}) - c_1(s\sigma_{np}-c)]\cos\mu k = \\ &= F^{np}(\sigma_{np})\cos[\mu k + \psi(\sigma_{np})]. \end{aligned} \tag{25}$$

The value of $F^{pr}(\sigma_{pr})$ is obtained with the aid of (15) and (16). After simple transformations we obtain

$$|F^{np}|^2 = \frac{s^2+2pcs+c_{np}s^2(\sigma_{np}-2p)}{\sin^2\mu}\left\{\gamma_0^2 - 2p\gamma_0\frac{\gamma_0}{\varkappa\omega} + \left(1+2p\frac{c}{s}\right)\frac{\gamma_0^2}{\varkappa^2\omega^2}\right\}. \tag{26}$$

It is natural to call the function $F^{pr}(\sigma_{pr})$ the envelope of the particle trajectory in the linear section. All the statements made above concerning the envelope inside the circular sector apply, obviously, also to the function $F^{pr}(\sigma_{pr})$. The function $F^{pr}(\sigma_{pr})$ also consists of two factors, one dependent only on σ_{pr} and the other on the initial conditions. The dependence on the initial conditions coincides here with the dependence of $F_c(\sigma)$ on the initial conditions [see (22)]. This, incidentally, is obvious from the very outset from Eq. (22), and was used to carry out the calculations.

The function $F^{pr}(\sigma_{pr})$ is symmetrical with respect to the center of the linear section (in the center of the section $\sigma_{pr} = p$) and has a minimum at this point. This is directly clear from (26). Thus,

$$[F^{pr}_{min}]^2 = \chi_0^2 - 2p\chi_0 \frac{\chi_0}{\pi\mu} + \left(1 + 2p\frac{c}{s}\right)\frac{\chi_0^2}{\pi^2\mu^2}. \qquad (27)$$

On the boundaries of the sectors, the functions $[F^{pr}]^2$ and F_c^2 as well as their derivatives coincide. Indeed, the only difference between $[F^{pr}]^2$ and F_c^2 lies in the fact that the expression $f_1 = 2ps \cos\sigma \cos(\sigma_\nu - \sigma)$ is replaced by $f_2 = 2pcs + \sigma_{pr}(\sigma_{pr} - 2p)$. But $f_1(0) = f_1(\sigma_\nu) = f_2(0) = f_2(2p) = 2pcs$. In addition $f'_2(2p) = f'_2(0)$ and $f'_2(0) = f'_1(\sigma_\nu)$, where the prime denotes differentiation with respect to σ or σ_{pr}.

It follows from these calculations that it is possible to introduce a single envelope, which is continuous (together with its derivative), for the particle trajectories both in the sector and in the linear section. Thus, the deviation from the equilibrium orbit for any case can be written in the form

$$\chi = F^{pr}(s)\cos(qk + \varphi(s)),$$

where σ is the length in dimensionless units (18), reckoned from a certain point along the equilibrium orbit.

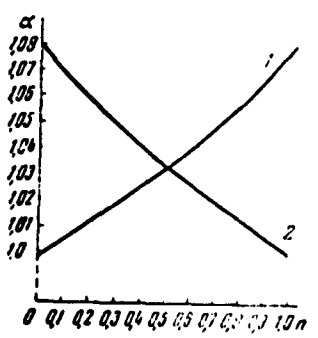

Fig. 19. Dependence of the coefficient α on the magnetic field index n for the vertical (1) and radial (2) oscillations.

The maximum of the function F_c^{pr} is located at the center of the sector and is equal to

$$[F_c^{pr}(s)]^2_{max} = \frac{s^2 - p^2(1+c)}{\sin^2\pi\mu}\left[\chi_0^2 + \left(1 + 2p\frac{c}{s}\right)\frac{\chi_0^2}{\pi^2\mu^2} - 2p\chi_0\frac{\chi}{\pi\mu}\right]. \qquad (28)$$

The minimum of the function $F_c^{pr}(\sigma)$ is located in the center of the linear section and is determined by Formula (27). We note that the minimum of the function $F_c^{pr}(\sigma)$ does not coincide with the minimum of the function $F_c(\sigma)$, which, as shown above, is not realized. The ratio of the maximum of F_c to the minimum of F_c^{pr} is independent of the initial conditions and is

equal to

$$\alpha = \frac{\sqrt{n^2 + \mu^2(1-n)}}{\sin \mu} = \sqrt{\frac{s + pc + p}{s + 2pc - p^2 s}}. \qquad (29)$$

Unlike the value of the "depth of modulation" $\Gamma = \sqrt{\frac{s+pc+p}{s+pc-p}}$, introduced by Dennison and Berlin [32], the quantity α has a perfectly defined physical meaning. For the proton synchrotron of the USSR Academy of Sciences, $\alpha = 1.022$ for the radial motion and $\alpha = 1.048$ for the vertical motion. The dependence of α on $\underline{n}$ is shown in Fig. 19 (for $L/\Gamma = 4/7$). The smallness of α for $L/R = 4/7$ shows that the spatial modulation of the oscillation amplitudes is not large.

§3. Some Singularities of Injection in an Accelerator with Slotted Magnet

Let us consider the singularities of the injection of particles in an accelerator with slotted magnet. For this purpose we express the quantities χ_0 and $\dot{\chi}_0/\kappa\omega$, which pertain to the start of the sector, by χ_1 and $\dot{\chi}_1/\kappa\omega$, which pertain to an arbitrary azimuth at which the injector is located. Putting $k = 0$ and $\kappa\omega t_k = \sigma_1$ in (17), we obtain

$$\begin{aligned} \chi_i &= \frac{\dot{\chi}_0}{\kappa\omega} \sin \sigma_i + \chi_0 \cos \sigma_i; \\ \dot{\chi}_i &= \dot{\chi}_0 \cos \sigma_i - \chi_0 \omega \kappa \sin \sigma_i. \end{aligned} \qquad (30)$$

In the calculation of the collisions with the injector, it is necessary to know the deviation of the particle from the equilibrium orbit at the location of the injector. Using (30), we obtain $F_c^2(\sigma)$ at the azimuth of the injector

$$[F_c(\sigma_i)]^2 = \chi_i^2 + \left[\frac{\chi_i p \sin(2\sigma_i - \sigma_1) + \frac{\dot{\chi}_0}{\kappa\omega}(s + 2p\cos\sigma_i \cos(\sigma_1 - \sigma_i))}{\sin \mu}\right]^2. \qquad (31)$$

It is seen from (31) that for a specified deviation of the injector, χ_1, from the instantaneous orbit and for a specified position of the injector, σ_1, there exists a certain optimum value of the velocity $\dot{\chi}_1^{opt}$ at which the two components in the square bracket of (31) cancel each other out. If the particle is emitted from the injector with $\dot{\chi}_1 =$

$= \dot{\chi}_1^{opt}$, then it is obvious that the amplitude of the oscillations is minimal at the location of the injector and is equal to χ_1.

The expression for $\dot{\chi}_1^{opt}$ follows directly from (31):

$$\frac{\dot{\chi}_1^{opt}}{\chi_{m0}} = \frac{\gamma_i p \sin(\sigma_v - 2\sigma_i)}{s + 2p\cos\sigma_i \cos(\sigma_v - \sigma_i)}.$$

Unlike the circular accelerator, $\dot{\chi}_1^{opt}$ does not vanish and is a function of χ_1 and σ_1. The velocity $\dot{\chi}_1$ can be expressed in terms of the angle γ between the direction of emission and the tangent to the equilibrium orbit at the plate where the injector is located:

$$\gamma = \frac{\dot{\chi}_i}{\omega R_0}. \tag{32}$$

We denote the optimum angle by γ_{opt}

$$\gamma_{opt} = \frac{\dot{\chi}_i^{opt}}{\omega R_0} = \frac{\gamma_i}{R_0} p \frac{\sin(\sigma_v - 2\sigma_i)}{s + 2p\cos\sigma_i \cos(\sigma_v - \sigma_i)}. \tag{33}$$

In this notation, Formula (31) assumes the simple and physically clear form:

$$F_i^2(\sigma_i) = \chi_i^2 + f_i \frac{R_0^2}{\nu^2}(\gamma - \gamma_{opt})^2, \tag{34}$$

where

$$f_i = \frac{s + 2p\cos\sigma_i \cos(\sigma_v - \sigma_i)}{\sin^2 \sigma_v}. \tag{35}$$

If we let the lengths of the linear sections approach zero ($p \to 0$), then $f \to 1$ and $\gamma_{opt} \to 0$, so that we arrive at the ordinary formula for circular accelerators:

$$F_i^2(\sigma_i) = \chi_i^2 + \frac{R_0^2}{\nu^2}\gamma^2. \tag{36}$$

Comparing (33) and (34), we conclude that in our case the injection differs from the injection in circular accelerators in two respects. First, the optimum angle does not vanish and, what is more important, varies during the injection process, owing to the variation of χ_1. Second, the deviation from maximum angle leads in our case to a stronger increase in the oscillation amplitude. This amplitude will be

the same as in a circular accelerator, but not with radius R_0, but with radius $f_1 \cdot R_0$. Figure 20 shows the dependence of γ_{opt} on the injector position. For the proton synchrotron of the USSR Academy of Sciences, γ_{opt} varies from 0 to 3', while $f_1 = 1.063$ for the radial motion and $f_1 = 1.042$ for the vertical motion.

To calculate the collisions with the chamber walls we must know the amplitude of the oscillations not only at the injector azimuth (σ_1), but also at arbitrary azimuth (σ). Using (22), we write

$$\frac{F_c^2(\sigma_1, \sigma)}{F_c^2(\sigma_1)} = \frac{s + 2p\cos s\cos(\sigma_1 - \sigma)}{s + 2p\cos s\cos(\sigma_1 - \sigma_1)}, \qquad (37)$$

where $F_c(\sigma_1, \sigma)$ is the amplitude of the oscillations at azimuth σ, when the ejector is located at azimuth σ_1. The value of $F_c^2(\sigma_1)$ is determined from Formula (34).

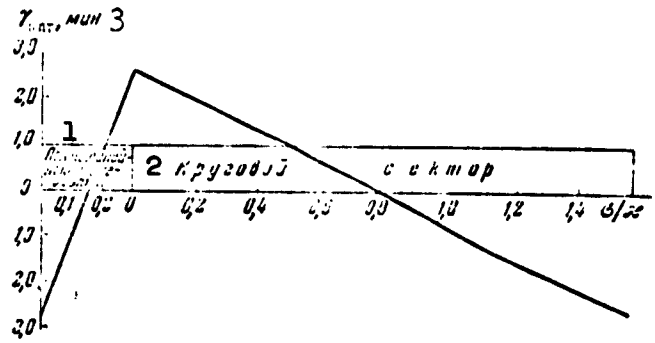

Fig. 20. Optimum angle γ_{opt} at $\chi_1 = 50$ cm in the 10-Bev proton synchrotron ($R_0 = 28$ m, $l/R_0 = 2/7$) as a function of the point of injection. 1) Linear section; 2) circular sector; 3) γ_{opt}, min.

So far we have assumed that the injector is located in the sector. If it is located in the linear section, the formulas will differ somewhat from (34) and (37). Let us establish the connection between the values of χ_0 and $\dot{\chi}_0/\kappa\omega$, referred to the start of the sector, with χ_1 and $\dot{\chi}_0/\kappa\omega$, referred to the point $(\sigma_{pr})_1$ inside the linear section:

$$\chi_{0\omega} = \chi_{1\omega} - \dot{\chi}_{1\omega} - \ldots \frac{1}{\chi_{1\omega}} \quad \dot{\chi}_{0\omega} = \dot{\chi}_{1\omega}. \qquad (38)$$

Substituting (38) in (26) and (22) and carrying out a series of analogous calculations, such as separation of the optimum angle, determination of f_{pr}, etc., we obtain an expression for the amplitude of the oscillations at any point σ_{pr} and at any azimuth σ, if the injector is located at the point $(\sigma_{pr})_1$:

$$[F^{np}(\sigma_{np}, \sigma_{np})_i]^2 = \frac{s + 2pc + s(\sigma_{np} - 2p)\sigma_{np}}{s + 2pc + s[(\sigma_{np})_i - 2p](\sigma_{np})_i}\left[\chi_i^2 + f_{np}^2 \frac{R_0^2}{\varkappa^2}(\gamma - \gamma_{opt}^{np})^2\right];$$

$$[F_s(\sigma; (\sigma_{np})_i)]^2 = \frac{s + 2p\cos\sigma\cos(\sigma_i - \sigma)}{s + 2pc + s[(\sigma_{np})_i - 2p](\sigma_{np})_i}\left[\chi_i^2 + \right.$$

$$\left. + f_{np}^2 \frac{R_0^2}{\varkappa^2}(\gamma - \gamma_{opt}^{np})^2\right], \qquad (39)$$

where

$$f_{np} = \frac{s + 2pc + s[(\sigma_{np})_i - 2p](\sigma_{np})_i}{\sin\mu};$$

$$\gamma_{opt}^{np} = \frac{\gamma_i \varkappa s}{R_0}\frac{(\sigma_{np})_i - p}{s + 2pc + s[(\sigma_{np})_i - 2p](\sigma_{np})_i}. \qquad (40)$$

Comparing Formulas (33), (35), and (37) with Formulas (39) and (40), we see that we can write the expression for the envelope in general form, i.e., for arbitrary location of the injector on the orbit:

$$[F_s^{np}(\sigma, \sigma_i)]^2 = \frac{f(\sigma)}{f(\sigma_i)}\left[\chi_i^2 + \frac{R_0^2}{\varkappa^2} f^2(\sigma_i)(\gamma - \gamma_{opt})^2\right], \qquad (41)$$

where

$$f(\sigma) = \begin{cases} \frac{s + 2p\cos\sigma\cos(\sigma_i - \sigma)}{\sin\mu} & \text{for } \sigma \text{ in the sector} \\ \frac{s + 2pc + s(\sigma - 2p)\sigma}{\sin\mu} & \text{for } \sigma \text{ in the linear section,} \end{cases} \qquad (42)$$

and

$$\gamma_{opt} = \frac{1}{2}\frac{\gamma_i \varkappa}{R_0}\frac{d\ln f(\sigma)}{d\sigma}\Big|_{\sigma=\sigma_i}. \qquad (43)$$

In practice, the parameter $p \ll 1$, so that the expression for $f(\sigma)$ and γ_{opt} can be simplified

$$f(\sigma) = \begin{cases} 1 + p\frac{\cos(2\sigma - \sigma_i)}{s} & \text{for } \sigma \text{ in the sector,} \\ 1 + p\frac{c}{s} + (\sigma - 2p)\sigma & \text{for } \sigma \text{ in the linear section,} \end{cases} \qquad (42')$$

$$\gamma_{opt} = \begin{cases} -p\frac{\gamma_i \varkappa}{R_0}\frac{\sin(2\sigma_i - \sigma)}{s} & \text{for } \sigma \text{ in the sector,} \\ \frac{\gamma_i \varkappa}{R_0}(\sigma_i - p) & \text{for } \sigma \text{ in the linear section.} \end{cases} \qquad (43')$$

In the calculation of $f(\sigma)$ in the linear section it is necessary to bear in mind that the third term in (42) is of order p^2, whereas we carry out our calculation everywhere with accuracy to the first power of p. We retained this term because its order decreases upon differentiation.

As was shown above, the function $f(\sigma)$ is continuous, together with its derivative (see also Figs. 20 and 21). Figure 21 shows a plot of $f(\sigma)$ for vertical ($\kappa = \sqrt{n}$) and radial ($\kappa = \sqrt{1-n}$) oscillations at different values of the index n. It is seen from the figure that $f(\sigma)$ has a minimum in the middle of the linear section and a maximum in the middle of the sector.

Formula (43) clarifies the physical meaning of the optimal angle γ_{opt}. It turns out that if we draw an envelope through the injector, then γ_{opt} coincides with the direction of the tangent to the envelope. Physically this is obvious from the very definition of the envelope. Indeed, if the direction of emission of the particle crosses the envelope passing through the point of injection, this means that at the trajectory of the particle there exists an envelope which passes above the point of injection, which contradicts the definition of the optimal angle. This statement can be verified directly by differentiating (41) with respect to the length of the trajectory $\sigma R_0/\kappa$.

It is clear from (41) that the amplitude of the oscillations at the place where the injector is located (for arbitrary location of the injector along the orbit), is equal to

$$F_c^{np}(\sigma_i, \sigma_i) = F_c^{np}(\sigma_i) = \sqrt{\chi_i^2 + \frac{R_0^2}{\kappa^2} f^2(\sigma_i)(\gamma - \gamma_{opt})^2}.$$

Thus, in calculating the collisions with the injector, the entire singularity of the accelerator with slots manifests itself in the appearance of the quantities γ_{opt} and $f(\sigma_i)$, which are functions of the

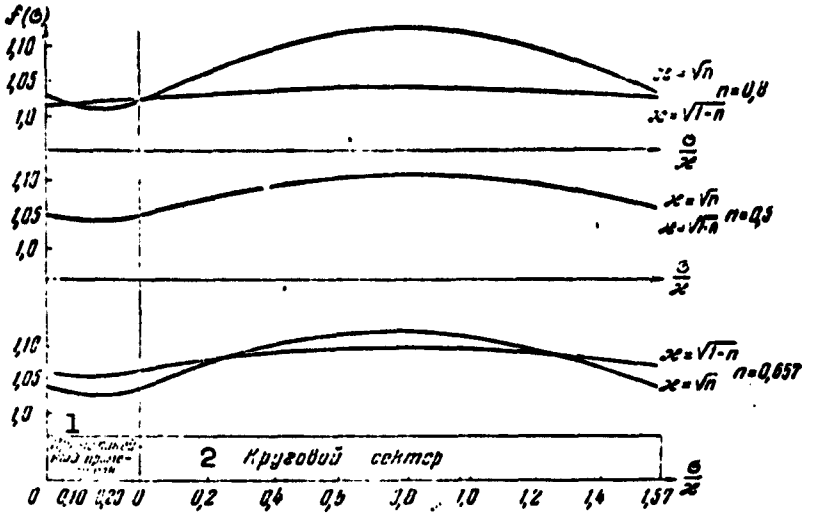

Fig. 21. The function $f(\sigma)$ for different values of n for radial and vertical oscillations. 1) Straight line section; 2) circular sector.

injector position. It is clear from the plot of Fig. 21 that $f(\sigma_1)$ has a minimum at the middle of the linear section. Therefore, in order to reduce the probability of the particle striking the injector, it is most convenient to place the latter in the middle of the linear portion. However, as is clear from Formula (41), the coefficient preceding the square bracket will assume in this case a maximum value. This means that this injector position increases the probability of collision with the chamber walls. The practical choice of the injector position is determined by design considerations and by the convenience with which the high-energy particles can be admitted into the chamber. Therefore the length of the linear section should not be very large, so that $f(\sigma)$ differs little from unity. This is precisely the situation in the proton synchrotron of the USSR Academy of Sciences.

The envelope method developed above has a wide range of application. The properties of the free oscillations, which were derived here, are general properties of solutions of equations with periodic coefficients. It is known that if the oscillations are described by an equa-

tion of the type

$$\rho'' + g(\sigma)\rho = 0,$$

where $g(\sigma)$ is the periodic function with period σ_0, then, with the exception of several cases (resonances, edges of the stability regions), the solution can be written in the form

$$\rho(\sigma) = \mathrm{Re}\, De^{i\frac{\mu}{\sigma_0}\sigma}\varphi(\sigma),$$

where $\varphi(\sigma)$ is the complex periodic Floquet function and μ is the characteristic exponent. We normalize the Floquet functions in such a way that the Wronskian of the functions

$$\varphi(\sigma) = e^{i\frac{\mu}{\sigma_0}\sigma}\varphi(\sigma) \text{ and } \varphi^*(\sigma) = e^{-i\frac{\mu}{\sigma_0}\sigma}\varphi^*(\sigma)$$

is equal to $-2i$. Then the oscillations of the particles at the azimuth σ can be written in the form

$$\rho(\sigma) = A_i(\sigma)\cos[N\mu k - \alpha(\sigma)],$$

where N is the number of periods of the function $g(\sigma)$ contained in the entire orbit, and

$$A_i = \sqrt{\frac{\beta_i}{f(\sigma_i)}}\sqrt{\varepsilon_x}\cos\varphi_i + \frac{\alpha_i}{\sqrt{\beta_i f(\sigma_i)}}\sqrt{\varepsilon_x}\sin\varphi_i;$$

The function $f(\sigma)$ is the modulus of the Floquet function

$$f(\sigma) = \varphi(\sigma)\varphi^*(\sigma).$$

The quantity κ in the expression for the amplitude is in this case an arbitrary number, introduced in the definition of the dimensionless quantity σ.

The derivation of these formulas, and also the application of this method to a strong-focusing accelerator, will be given in Chapter 6.

§4. Calculation of Particle Trajectories with Account of a Magnetic Field in the Linear Sections

So far we have disregarded the presence of a magnetic field in the linear section. As shown by estimates, even in the 10 Bev proton synchrotron, where the ratio of the height of the magnet gap to the

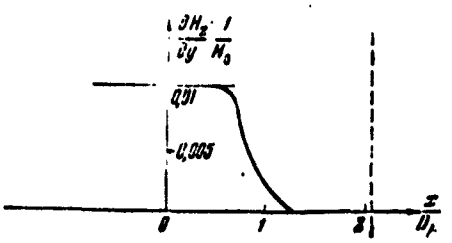

Fig. 22. Characteristic of magnetic field $\partial H_z/\partial y \cdot 1/H_0$ near the edge of a straight magnet, as given by model measurements.

length of the linear sections is small, failure to take into account the magnetic field in the sections would lead to a loss of part of the working region of the magnet (~12 cm).

As will be shown below, if the penetration of the magnetic field into the linear sections is taken into account in the design of the magnet, it is possible to avoid noticeable losses of the working region of the magnet due to this cause (at least at the instant of injection).

The magnetic field in the linear sections should be measured with models. By the time the work was outlined, we had only the results of measurements on models (solid iron, direct current), carried out at the Physics Institute of the Academy of Sciences [17, 42] in 1949, and also the results of measurements made in 1951 and 1952 on the magnetic field of the proton synchrotron model.* In addition, an approximate theoretical calculation was made. On the basis of these measurements it can be concluded that the decrease in the field in the direction of the y axis in the equilibrium-orbit zone (see Fig. 24) is quite small. We shall therefore assume in the present section $\partial H_z/\partial y = 0$. Actually this condition is not a limitation: $\partial H_z/\partial y$ influences little the character of the motion, since on the average $\partial H_z/\partial y \cdot y$ is considerably smaller than $H_0 - H_z$. This can be verified by direct calculation of

the orbit, as was indeed done [22]. Figure 22 shows a plot of $\partial H_z/\partial y$ x x $1/H_0$ in the linear section. The abscissas represent the lengths in units of magnet airgap. Thus, the magnetic field in the linear section depends only on the coordinate x.

The results of measurements on the proton-synchrotron model have shown that the dependence of the magnetic field on the x coordinate is different in a solid magnet from that in a laminated one. This is caused by the existence of an air gap between the steel laminations. Therefore the effect of the edges of the magnet facing the linear portions on the magnetic field inside the sector is much stronger. We shall not use the plot of Fig. 23 for quantitative calculations. Qualitatively, the plot of Fig. 23 (obtained with the aid of measurements on a solid magnet) describes correctly the variation of the field in the linear section.

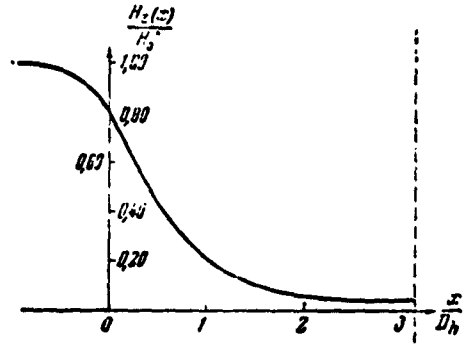

Fig. 23. Characteristic of magnetic field $H_z(x)/H_0$ at the edge of a straight-line magnet according to model measurements.

The formulas of the present chapter and of the next chapter were used successfully to calculate the trajectories and to choose the geometrical dimensions of the 180 and 10,000 Mev installations.

To investigate the motion of the particles in the linear section, we make use of the following procedure.

The equation of motion (I, 27) in the central plane of the linear section has the form

$$\frac{d^2y}{dt^2} = -\omega \frac{H_z}{H_0} \cdot \dot{x},$$

where $\omega = eH_0/mc$ is the frequency of revolution in the magnetic field H_0 of the circular sectors. Integrating the equation, we obtain

$$\dot{y} = \dot{y}(0) - \omega \int_0^t \frac{H_z}{H_0} \frac{dx}{dt} dt.$$

Changing from the variable t to the variable x in accordance with the following approximate relation (which is valid with accuracy to within y^2)

$$dx = \omega R_0 dt, \tag{44}$$

we obtain

$$y'(x) = y'(0) - \frac{1}{H_0 R_0} \int_0^x H_z(\xi)\, d\xi, \tag{45}$$

where the prime denotes differentiation with respect to x.

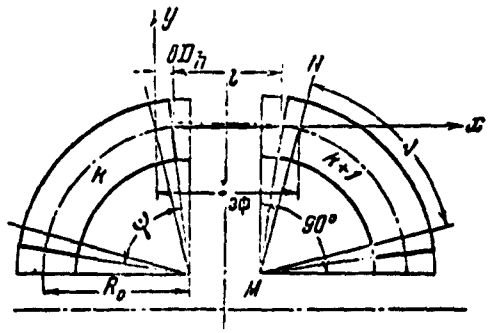

Fig. 24. Diagram illustrating the notation.

Equation (45) will be used to join the solutions of the type (2) in two neighboring sectors. The magnetic field in the sector, on the boundary with the linear section, amounts to only 78-84% of the field inside the sector. Thus, this boundary cannot be used as the line for joining the solutions of type (2), unless azimuthal asymmetry is intro-

duced.

Let us introduce the concept of effective length of the linear section

$$l_{эф} = l + 2bD_h, \tag{46}$$

where l is the length of the linear section and D_h is the height of the magnet gap. The quantity 2b ranges from 1.5 to 2.5, depending on the construction of the magnet. Thus, we add to the geometrical length of the linear section, on each side, a length bD_h. We shall assume that on the boundary defined by l_{ef} the magnetic field differs from H_0 by less than 1-5%.

Let us integrate (45) over the effective linear section:

$$y(l_{эф}) = y(0) + y'(0)\, l_{эф} - \frac{1}{H_0 R_0}\int_0^{l_{эф}} dx \int_0^x H_z(\xi)\, d\xi. \tag{47}$$

We denote the deviation ρ from equilibrium orbit at the start of the sector by $\rho(l_{ef})$, and at the end of the orbit by $\rho(0)$. Let the effective angle of the sector be ν (Fig. 24) and let it differ from $\pi/2$ by δ_0. Then, obviously (Fig. 25),

$$y(l_{эф}) = \rho(l_{эф})\cos\frac{\delta_0}{2} = \rho(l_{эф}) - \rho(l_{эф})\frac{\delta_0^2}{2}.$$

We neglect the second term ($\delta_0 < 0.02$-0.06) and obtain

$$y(l_{эф}) = \rho(l_{эф}); \quad y(0) = \rho(0). \tag{48}$$

With the same degree of accuracy, we get

$$\left.\begin{aligned} y'(0) &= \frac{\frac{\dot\rho(0)}{v} + \operatorname{tg}\frac{\delta_0}{2}}{1 - \frac{\dot\rho(0)}{v}\operatorname{tg}\frac{\delta_0}{2}} = \frac{\dot\rho(0)}{v} + \frac{\delta_0}{2}; \\ y'(l_{эф}) &= \frac{\dot\rho(l_{эф})}{v} - \frac{\delta_0}{2}. \end{aligned}\right\} \tag{49}$$

With the aid of (48) and (49) we rewrite (45) and (47):

$$\rho(l_{эф}) = \rho(0) + \frac{\dot\rho(0)\, l_{эф}}{v} + \eta, \tag{50}$$

$$\dot\rho(l_{эф}) = \dot\rho(0) + \delta\omega R_0,$$

where

$$\eta = \frac{\ldots}{2} - \frac{\ldots}{\ldots} \int_0^{\ldots} \ldots H_x(\xi)\, d\xi;$$

$$\delta = \delta_0 - \frac{1}{H_0 l_0} \int_0^{l_{sep}} H_x(\xi)\, d\xi.$$

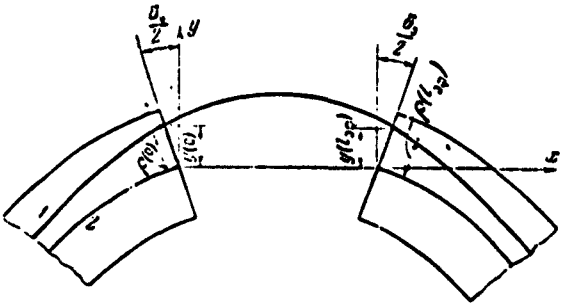

Fig. 25. Diagram illustrating the notation: 1) particle trajectory; 2) instantaneous orbit.

Equation (50) differs from the analogous equation for the "ideal accelerator" with slotted magnet in the presence of the terms δ and η. We therefore obtain in lieu of Eq. (6)

$$\begin{aligned} \varepsilon + A_k c - B_k s &= A_{k+1}; \\ \eta + A_k (s + 2pc) + B_k (c - 2ps) &= B_{k+1}, \end{aligned} \tag{51}$$

where

$$\varepsilon = \frac{\delta l_0}{\varkappa}; \quad c = \cos\sigma_\nu; \quad s = \sin\sigma_\nu; \quad p = \frac{\varkappa l_{sep}}{2l_0}; \quad \sigma_\nu = \varkappa\nu;$$

σ_ν is the effective length of the sector in the dimensionless units (18). Thus, we use the same notation as in the preceding section, except that all the geometrical dimensions are replaced by effective ones. Apart from this, Eq. (51) differs from (6) in the presence of the free terms ε and η.

The general solution of (51) is the sum of the general solution of the corresponding homogeneous equation [i.e., Eq. (51) without η and ε] and the particular solution of the complete equation. We have obtained a solution for the homogeneous equation in the preceding section. The particular solution can be readily obtained, since the free

terms are constants. With this remark taken into account, we readily obtain

$$B^* = \frac{\gamma(1-\alpha)+\varepsilon(s+2\rho c)}{2(1-\alpha+\rho s)};$$
$$A^* = \frac{\varepsilon(1-\alpha+2\rho s)-\gamma s}{2(1-\alpha+\rho s)}. \qquad (52)$$

Thus, the motion in the k-th sector will be described by the following equation:

$$\rho_k = (D_1\cos\mu k + D_2\sin\mu k + A^*)\sin\omega x t_k + (C_1\cos\mu k + C_2\sin\mu k + B^*)\cos\omega x t_k, \qquad (53)$$

The constants D_1, D_2, C_1, and C_2 are not, as already shown, independent but are related by the two equations in (14). The constants C_1 and D_1 can be readily determined with the aid of the initial conditions

$$C_1 + B^* = \rho_{max}$$
$$(D_1 + A^*)\omega x = \dot{\rho}_{max} \qquad (54)$$

The constants C_2 and D_2 can be determined from Formula (14)

$$D_2 = \frac{s}{\sin\mu}\left[\rho\left(\frac{\dot{\rho}_{max}}{\omega x} - A^*\right) - (\rho_{max} - B^*)\right],$$
$$C_2 = \frac{1}{\sin\mu}\left[\left(\frac{\dot{\rho}_{max}}{\omega x} - A^*\right)(s+2\rho c) - (\rho_{max} - B^*)\rho s\right]. \qquad (55)$$

If we make the following change of variables:

$$\rho' = \rho_k - \rho_k^* = \rho_k - A^*\sin\omega x t_k - B^*\cos\omega x t_k, \qquad (56)$$

then Eqs. (53), (54), and (55) become similar to Eqs. (15), (16), and (17), obtained for the "ideal accelerator with slots." Thus, the presence of a field in the linear section changes the instantaneous orbit (and also the equilibrium one), with respect to which we measure the coordinate ρ. If ρ is measured from the new instantaneous orbit, then all the results of the preceding section remain in force.

The equation of this new orbit can be readily written down:

$$\rho_k^* = A^*\sin\sqrt{1-n}\theta + B^*\cos\sqrt{1-n}\theta, \qquad (57)$$

where $\theta = \omega t$ is the azimuth of the particle, reckoned every time from the start of the sector (line MN on Fig. 24). Inasmuch as the new orbit

is not a part of a circle even in the sector, not all the working region can be utilized. In order to determine the value $\Delta\rho^*$ of the unused working region, we must calculate $\Delta\rho^* = \rho^*_{max} - \rho^*_{min}$. If we substitute the numbers for the accelerator of the USSR Academy of Sciences, we obtain $\Delta\rho^* = 12$ cm.

One can in general eliminate the losses in the working region due to the presence of the magnetic field in the linear sections (at least during the injection period) by choosing in suitable manner the angle subtended by the magnet sectors. Indeed, in order to avoid distortion of the orbit, we require that

$$A^* = B^* = 0.$$

This condition is equivalent to the conditions

$$\tau_1 = \frac{\delta_0 l_{sep}}{2} - \frac{1}{H_0 l_0}\int_0^{l_{sep}} dx \int_0^x H_z(\xi)\,d\xi = 0, \qquad (58)$$

$$\delta = \delta_0 - \frac{1}{H_0 l_0}\int_0^{l_{sep}} H_z(\xi)\,d\xi = 0.$$

Equations (58) can be satisfied in some cases by suitably choosing the angle subtended by the sector:

$$\psi = \pi - \frac{2bD_x}{l_0} = \frac{\pi}{2} - \frac{1}{H_0 l_0}\int_0^{l_{sep}} H_z(\xi)\,d\xi + \frac{2bD_x}{l_0}. \qquad (59)$$

If the magnetic field is symmetrical with respect to the center of the linear section, then

$$\int_0^{l_{sep}} dx \int_0^x H_z(\xi)\,d\xi = \int_0^{l_{sep}} H_z(\xi)(l_{sep} - \xi)\,d\xi = \frac{l_{sep}}{2}\int_0^{l_{sep}} H_z(\xi)\,d\xi.$$

Introducing the notation

$$H_{sep} = \frac{1}{l_{sep}}\int_0^{l_{sep}} H_z(\xi)\,d\xi,$$

we rewrite (58) in the simpler form

$$\delta = \delta_0 - \frac{l_{sep}}{l_0}\frac{H_{sep}}{H_0} = 0,$$

$$\eta = \frac{l_{ef}}{2} \lambda = p\pi = 0. \qquad (60)$$

Thus, in the case of a symmetrical field the second equation in (58) and (60) is the consequence of the first. The angle subtended by the sector is

$$\psi = \frac{\pi}{2} + \frac{\delta D_0}{R_0} - \frac{l_{ef}}{R_0} \frac{H_{cp}}{H_0}. \qquad (61)$$

Thus, for example in the proton synchrotron of the USSR Academy of Sciences, the sectors must be made to subtend an angle not $\pi/2$, but somewhat less. The exact value of ψ can be determined only after model measurements. One must bear in mind, however, that owing to saturation and to other factors H_{sr} and l_{ef} do not remain constant, but change during the course of acceleration. Therefore Eqs. (60) can be satisfied only within a certain time interval.

With the aid of (60) we can also simplify Relation (52):

$$A^* = \frac{\varepsilon}{2} = \frac{R_0 \lambda}{2\pi}; \quad B^* = \frac{1+\varepsilon}{\varepsilon} \cdot \frac{\varepsilon}{2}. \qquad (62)$$

If Condition (60) is satisfied, then Relation (50) coincides with the analogous equation for the "ideal accelerator with slots," and Eq. (51) coincides with Eq. (6). The only difference lies in the fact that in place of the geometrical length of the linear section it is necessary to take the effective length.

If the magnetic field is asymmetrical with respect to the center of the linear section, then in general it is impossible to choose an angle ψ such that A* and B* vanish simultaneously, and consequently, that the orbit does not become distorted.

Manuscript Page No.

[Footnotes]

85 We recall that we are not considering here the attenuation due to the increase in the magnetic field.

97 Magnetic measurements made on the 10-Bev proton synchrotron magnet have essentially confirmed our calculations and the validity of the assumption made later on.

Manuscript Page No.

[List of Transliterated Symbols]

87 пр = pr = promezhutok = section

91 опт = opt = optimal'nyy = optimal

96 нач = nach = nachal'nyy = initial

99 эф = ef = effektivnyy = effective

103 ср = sr = sredniy = average

Chapter 3

EFFECT OF DEVIATION OF THE MAGNETIC FIELD FROM THEORETICAL ON THE MOTION OF THE PARTICLES

§1. Introduction

Certain deviations from the theoretical magnetic field are always observed in a real magnet. By theoretical field in the magnet sectors we mean a field independent of the azimuth θ within the angle ν (see Fig. 24) and uniform in all the sectors. In addition, we assume that all sectors have the same symmetry plane. In the linear sections, the theoretical field is regarded to be one which causes the coefficients δ and η to vanish, in accordance with (II, 60). Another important assumption is that all four sectors are similar to one another.

If we realize the theoretical field, then the instantaneous orbits of the particles (i.e., the orbits about which the fast oscillations are executed) have inside the sectors the form of a circular arc, located symmetrically with respect to the chamber walls. Any deviation of the magnetic field from theoretical will lead to a distortion of the instantaneous particle orbit, which is equivalent to the loss of a certain fraction of the working region of the magnet. This is illustrated in Fig. 26. The distorted orbit (solid line) deviates from the theoretical one (dashed line) by $\pm\Delta_1/2$. In order for the particles not to strike the chamber walls (or the injector), it is necessary that their maximum oscillation amplitude be smaller by $\Delta_1/2$ than the oscillation amplitude permissible in the theoretical magnetic field. As will be shown in detail in Chapter 5, the intensity of the particle

beam is directly connected with the permissible swing of the oscillations about the equilibrium orbit. Thus, the shaded area in Fig. 26 is in fact not used to produce an intense beam of accelerated particles. The smaller the deviations of the magnetic field from the theoretical value, the less distorted the orbit and consequently the larger the intensity of the particle beam for a specified dimension of magnetic gap. At sufficiently large deviations from the theoretical field, the acceleration of the particles becomes impossible at all.

Along with distortion of the equilibrium and instantaneous orbits, the deviations of the magnetic field from the theoretical can cause in some cases an increase in the oscillation amplitude. Such an increase in the amplitude has a resonant character* and can occur for certain fully defined values of the magnetic field index n. Therefore the value of n in the main part of the working region of the magnet is chosen such that it does not correspond to resonance. The resonance phenomena will be investigated in detail in the next chapter.

It is clear from the foregoing that a clarification of the influence of the deviations of the magnetic field from theoretical is one of the most important problems in accelerator theory.

In an accelerator with a slotted magnet, the influence of disturbing phenomena on the motion of the particles is much stronger than in circular accelerators. Moreover, the presence of the linear portions makes it possible for entirely new disturbances to arise (inaccuracy in the installation of the sectors, shift of the symmetry planes of the magnetic field in the sectors, inaccuracies in the angular dimensions of the sectors and in the length of the linear sections, difference between the average fields in different sectors, etc.).

Usually the deviations of the fields' from theoretical are divided into a statistical part and into an instantaneous part, in accord with

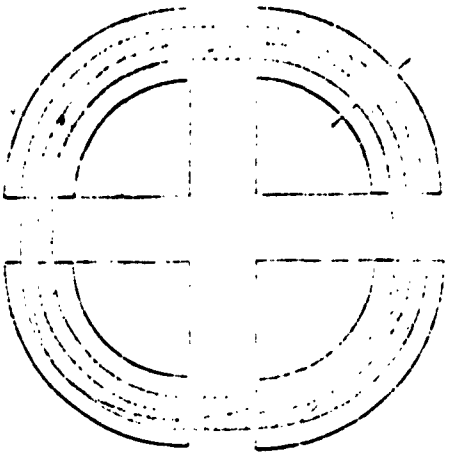

Fig. 26. Distorted orbit. The shaded region is the actually lost portion of the radial gap of the magnet.

the measurement method used in circular synchrotrons and in betatrons. We shall not do this, and use the term deviation to denote everywhere the total deviation.

Our investigation [17], carried out in 1949 (together with A.M. Baldin and V.V. Mikhaylov) is indeed the only one devoted to this question. It served as the basis for the design and to the choice of tolerances for the 10-Bev proton synchrotron of the USSR Academy of Sciences and for the 180-Mev model.

We shall consider in succession several deviations of the magnetic field from theoretical, assuming these deviations to be small quantities. Obviously, only this case is of practical interest. Each of the inhomogeneities will make its own contribution to the distortion of the equilibrium orbit. In view of the smallness of the deviations, it is natural to assume that the total distortion of the orbit is the sum of the partial distortions, each considered separately.

§2. Calculation of the Perturbed Orbit

In the presence of various types of perturbations in circular accelerators, the motion of the particles in the vertical and radial di-

rections are described by the following differential equation:

$$\frac{d}{d\theta}(H\dot{\chi}) + Hx^2\chi = Hxg(\Theta), \qquad (1)$$

where the dot denotes differentiation with respect to the azimuth Θ. The function $g(\Theta)$ is periodic in Θ with period 2π. The general solution of (1) can be written in the form

$$\chi = A\sin x\Theta + B\cos x\Theta + \frac{1}{2\sin x\pi}\int_{\Theta}^{\Theta+2\pi} g(\xi)\cos x(\Theta - \xi + \pi)\,d\xi;$$

$$\chi^*(\Theta) = \frac{1}{2\sin x\pi}\int_{\Theta}^{\Theta+2\pi} g(\xi)\cos x(\Theta - \xi + \pi)\,d\xi. \qquad (2)$$

The function $\chi^*(\Theta)$ has a period 2π and can be regarded as the equation for the distorted orbit.

An analogous expression can be obtained also for the accelerator with slotted magnet, by using the solution of the homogeneous equation, investigated in detail in Chapter 2, to determine the periodic solution of the equation with right half.

It is sometimes convenient to introduce the effective angle subtended by the sector, $\nu < \pi/2$, as was done in the preceding chapter. Then during one revolution the azimuth Θ increases by $4\nu < 2\pi$, if it is assumed that the azimuth Θ does not change in the linear portions. In this case the equation of the distorted orbit has the form

$$\chi^*(\Theta) = \frac{1}{2\sin 2x\nu}\int_{\Theta}^{\Theta+4\nu} g(\xi)\cos x(\Theta - \xi + 2\nu)\,d\xi. \qquad (3)$$

We introduce the following notation:

$$g_1(\Theta) = g(\Theta);\quad g_2(\Theta) = g(\nu + \Theta);\quad g_3(\Theta) = g(2\nu + \Theta),\ \text{etc.} \qquad (4)$$

$$\chi_1^*(\Theta) = \chi^*(\Theta);\quad \chi_2^*(\Theta) = \chi^*(\nu + \Theta),\ \text{etc.}$$

As in the preceding chapter, we assume that the angle is measured from the start of each sector and varies from 0 to ν.

The equation of the distorted orbit in the sectors is sought in the form

$$\chi_N = A_N \cos \varkappa (\nu - \theta) - B_N \cos \varkappa \theta + \chi^*(\theta) \qquad (5)$$

with supplementary periodicity conditions

$$A_{N+4} = A_N, \quad B_{N+4} = B_N, \qquad (6)$$

where N is the number of the sector ($1 \leq N \leq 4$).

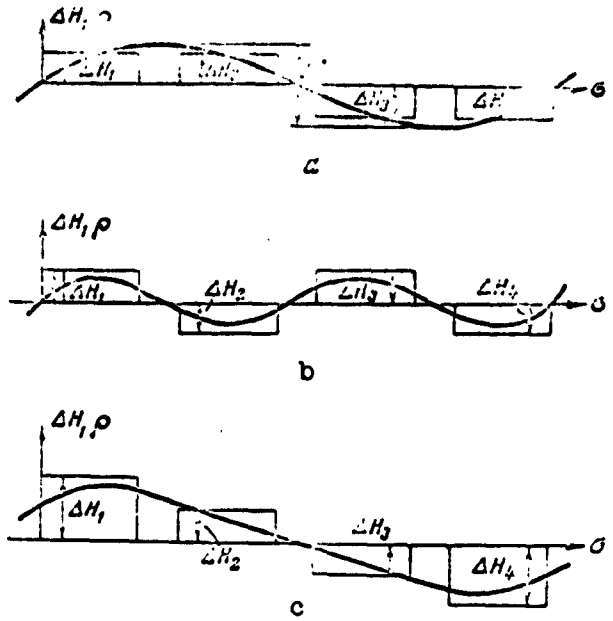

Fig. 27. Distortions of field and form of distorted orbit.

Equation (5) with supplementary conditions (6) can be regarded as the equation for the new distorted orbit. The oscillations of the particles about the distorted orbit will occur in exactly the same manner as about the symmetrical orbit. Indeed, if we measure the deviation χ_N from the new orbit, we obtain an oscillation equation which coincides exactly with the homogeneous equations of the preceding chapter.

It is easy to obtain the equation relating A_N and B_N with A_{N+1} and B_{N+1}:

$$B_N = A_{N+1} - \frac{\varepsilon_N}{s},$$
$$A_N - B_N c + 2p\left[B_N s + \frac{\gamma_N(\nu)}{\quad}\right] = A_{N+1} c - B_{N-1} - \gamma_N, \qquad (7)$$

where the notation of the preceding chapter [see (50, 51)] is used for

ε_N and η_N. Unlike the previously considered cases, we assume that the quantities ε_N and η_N do not have the same values in the different linear sections. Thus, the quantities $\varepsilon_N = \varepsilon_N R_0/\kappa$ and η_N pertain to the linear section between the N-th and the N + 1-st sectors.

We seek the solution of (7) in the form

$$A_N = D_N e^{i\mu N} + D_N^* e^{-i\mu N}, \tag{8}$$

where D_N is an unknown function of number N, satisfying the equation

$$\left.\begin{aligned} D_{N+1} - D_N &= \frac{e^{-i\mu(N+1)}}{2i\sin\mu} f_N; \\ f_N &= \frac{-\varepsilon_N s - \varepsilon_N (c - 2\rho s) + \varepsilon_{N+1}}{s} - \frac{2\rho \cdot s}{\varkappa} z'_N(\nu). \end{aligned}\right\} \tag{9}$$

With the aid of (9) we can readily obtain the periodic solution for A_N, which satisfies simultaneously Relations (6) and (7). For this purpose it is necessary to use the periodicity of the function f_N. As a result of the calculations we obtain

$$\left.\begin{aligned} A_N &= \frac{f_N \cos\mu + f_{N+1} + f_{N+2}\cos\mu - f_{N+3}\cos 2\mu}{2\sin\mu\sin 2\mu}, \\ B_N &= A_{N+1} - \frac{\varepsilon_N}{s}. \end{aligned}\right\} \tag{10}$$

Thus, the problem is completely solved.

By way of an example, Fig. 27 shows the distorted orbit for different values ΔH of the deviation of the average field in the magnet sectors from the theoretical value. The ordinates represent the deviation of the orbit from the average position in the chamber. The vertical dimension of the direct angles is equal to the change in the radius of curvature of the particle trajectory in the given sector, due to the deviation of the magnetic field from the average value.

Figure 28 shows the orbit in the 180-Mev proton synchrotron, calculated in accordance with the derived formulas and the magnetic-measurement data.

§3. Motion of Particles in Vertical Direction

The motion of the particles in the vertical direction should be

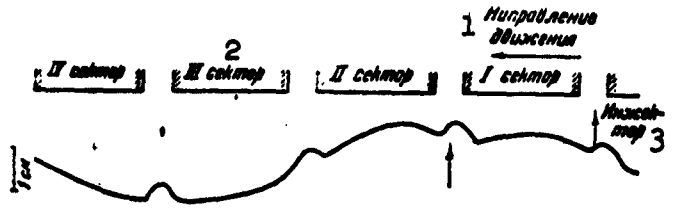

Fig. 28. Orbit in 180-Mev proton synchrotron as obtained by magnetic-measurement data. The arrow indicates the linear section with magnetic field different from theoretical. 1) Direction of motion; 2) sector; 3) injector.

examined with particular care. Indeed, the region accessible for particle motion in the vertical direction is 5-7 times smaller than that in the radial direction. It is usually assumed that the inhomogeneities arising in the magnetic field do not give rise to additional oscillations in a vertical direction. In fact, however, in an accelerator with slotted magnet, unless special measures are adopted, additional vertical oscillations with large amplitude can be produced. Connected with this phenomenon is a very dangerous resonance between the vertical oscillations and the revolution frequency, which occurs in the 10-Bev proton synchrotron, unlike in the circular accelerator, at $n = 0.84$, which lies within the stability region.

Owing to the structural features of slotted magnets, the "central magnetic plane" in such magnets is actually not a plane.

The reason for it is, first, that inaccuracies are possible in the installation of the individual sectors relative to one another, as a result of which the "average magnetic planes" of the different sectors may be situated at different levels; second, each sector is made up of 48 blocks, so that the "central plane" will not be a plane even within a single sector; third, the geometrical central plane may not coincide with the central magnetic plane, and the position of the latter is influenced by many factors (in particular, the location of the

magnet windings).

Assume that the equation of the surface on which $H_r = 0$ can be written in the form

$$z = \frac{z^{(0)}}{\varkappa} = \Delta z_\nu + \sum_{k=1}^{\infty} z_k \sin(k\theta + \alpha_k^\nu) \qquad (11)$$
$$1 \leqslant \nu \leqslant 4,$$

where the coordinate z is measured from the central plane, chosen such that $\sum_{\nu=1}^{4} \Delta z_\nu = 0$. To solve the problem of interest to us we can use the results of §2, if we assume $\kappa = \sqrt{n}$; $\chi = z$; $\varepsilon_N = \eta_N = 0$. Without stopping for the self-evident calculations, we shall consider a few important cases.

We assume that the central magnetic planes of the sectors are shifted parallel to one another, and then all the z_k in (11) are equal to zero. Formulas (3) and (10) are valid in our case if we assume

$$g_\nu = \sqrt{n}\,\Delta z_\nu \qquad (12)$$

and replace $\sqrt{1-n}$ by $\sqrt{n}$.

Before we write out the theoretical formulas, let us call attention to the fact that in the case of the vertical motion we have a relation, which has a high degree of accuracy, fully adequate for the calculations on the 10-Bev proton synchrotron,

$$\cos\mu = 0{,}84 - n. \qquad (13)$$

For example, when n = 0.55 Eq. (13) yields for cos μ a value 0.29. Exact calculation leads to 0.298. When n = 0.95, the exact value of cos μ is 0.1, while the approximate value is 0.09.

Then, according to (10) and (3),

$$A_\nu = \frac{(2{,}68 - 2n)(\Delta z_\nu - \Delta z_{\nu-1}) - (\Delta z_{\nu+2} - \Delta z_{\nu+1})}{4(0{,}84 - n)(1{,}84 - n)}; \qquad (14)$$
$$z_\nu = A_\nu \cos\varkappa(\nu - 0) - A_{\nu+1}\cos\varkappa\theta + \Delta z_\nu.$$

Along with the coordinate z_N, which is measured from the central plane defined above, we introduce a coordinate z'_N, measured from the

central magnetic plane of the N-th sector. Obviously, $z'_N = z_N - \Delta z_N$.

Let us consider three particular cases, shown schematically in Fig. 29:

1) $\Delta z_1 = \Delta z_2 = a$; $\Delta z_3 = \Delta z_4 = -a$;
2) $\Delta z_1 = \Delta z_3 = a$; $\Delta z_2 = \Delta z_4 = -a$;
3) $\Delta z_1 = -\Delta z_4 = 2a$; $\Delta z_2 = -\Delta z_3 = a$.

Let us calculate the maximum deviation from the central magnetic plane z'_{max}:

$$1)\ z'_{max} = \frac{a}{0{,}84 - n};\qquad 2)\ z'_{max} = \frac{2a\cos\mu\frac{\nu}{2}}{1{,}84 - n};$$

$$3)\ z'_{max} = \frac{0{,}16 - 0{,}84c - n(1+c)}{2(0{,}84 - n)(1{,}84 - n)}. \qquad (15)$$

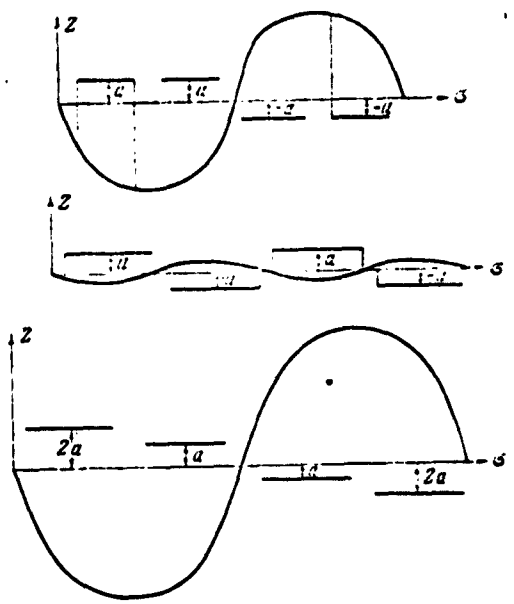

Fig. 29. Distortions of central magnetic plane and form of section of central plane of vertical oscillations.

As can be seen from (15), in cases 1) and 3) the value of z'_{max} exceeds a by many times and becomes infinite when $\cos\mu = 0$ (i.e., when $n = 0.84$). This is connected with the fact that when $\cos\mu = 0$ resonance sets in between the vertical oscillations and the perturbations of the central magnetic plane (see Chapter [illegible]).

Thus, when the magnetic planes are shifted parallel to one another, we obtain curvilinear surfaces, the projections of which on the vertical plane are shown in Fig. 29. It is precisely near these surfaces that the free vertical oscillations are now executed. We can therefore call them the effective central "planes." It is clear that owing to the distortion of the central "planes" we are unable to use part of the magnet gap, equal to $2z'_{max}$. For example, if the inaccuracy in the installation of the sectors is ± 3 mm, then we lose 34 mm in the vertical gap of the magnet when $n = 2/3$ and 130 mm when $n = 0.75$.

Let all the ΔZ_N be equal to zero, and then we can use Formula (5) to calculate the coordinates of the effective central "plane," after making in this formula the following obvious substitutions:

$$A_N = -\frac{l}{R_0}\sum_{k=1}^{\infty}\frac{kz_k}{k^2-\varkappa^2}\cdot\frac{\cos\alpha_k^N}{2\left(\cos k\frac{\pi}{2}-\cos\pi\varkappa\right)};$$

$$z_N = A_N\cos\varkappa(\nu-0)-A_{N+1}\cos\varkappa\theta+\sum_{k=1}^{\infty}\frac{z_k}{k^2-\varkappa^2}\sin(k\theta+\alpha_k^N). \qquad (16)$$

We see that the effect of the odd harmonics exceeds that of the even ones. The reason for it is that for vertical oscillations $\cos\mu$ is quite close to zero. In other words, in the region of the values of the index n of interest to us we are close to resonance between the revolution frequency and the vertical oscillations.

Let us consider some odd harmonics in Expression (16).

We readily obtain

$$z_N^k(\theta) = \frac{z_k}{k^2-\varkappa^2}\left[\frac{kl}{R}\frac{\cos\alpha_k^N\cos\varkappa(\nu-0)-(-1)^{\frac{k+1}{2}}\sin\alpha_k^N\cos\varkappa\theta}{2(0{,}84-n)}+\right.$$
$$\left.+\sin(k\theta+\alpha_k^N)\right]. \qquad (17)$$

In (17) the greatest contribution is made by the first two terms, whose maximum value is

$$\frac{kl}{R}\frac{z_k}{k^2-\varkappa^2}\frac{\sqrt{1+c}}{2(0{,}84-n)}.$$

We shall assume that the maximum of (32) occurs at the same values of α_k^N and θ as for the first two terms. This is true if cos $\mu \ll kl/2R$. In this case we obtain

$$(z_y^k(0))_{max} = \frac{s_k}{k^2 - \nu^2}\left[\frac{\sqrt{1+e}}{2\cos\mu}\cdot\frac{kl}{R} + \delta_k\right], \qquad (18)$$

where $\delta_k = 1$ if $(k + 1)/2$ is even and $\delta_k = 0$ if $(k + 1)/2$ is odd.

As is seen from (18), the effect of the first harmonic is approximately five times larger in amplitude when n = 2/3, and 8.5 times larger when n = 0.75. The effect of the third harmonic (when n = 2/3) is approximately 8 times smaller, and that of the fifth harmonic 15 times smaller than the effect of the first harmonic. The effect of the second harmonic is 25-30 times smaller than the effect of the first harmonic.

§4. Conclusion

In the preceding sections we investigated in detail the motion of particles under the action of various disturbing phenomena. We have shown that if we disregard resonance effects, then the action of any kind of perturbation reduces to a distortion of the equilibrium orbit or the surface about which the oscillations are executed, and does not affect the character and magnitude of these oscillations.

The forms of orbit distortion have a relative stability, since the disturbing phenomena are in themselves relatively stable. During the acceleration process, the form of the orbit changes very slowly. In the 10-Bev proton synchrotron there will be two periods during which the form of the distorted orbit changes apparently at a relatively larger speed. The first is the initial period of acceleration, as the magnetic field increases from 150 to 1000 oersted. The remanent magnetization, which plays a large role at 150 oersteds, ceases to influence the form of the orbit at 1000 oersteds. Second, at the very end

of acceleration, starting with a field of 11,500-12,000 oersteds, the saturation phenomena increase sharply and influence the form of the orbit. Of course, the most important is the form of the orbit at the start of the acceleration.

If the orbit were to be known beforehand, suitable changes in the construction of the chamber and of the magnet could help avoid losses in the working region of the magnet, similar to the account of the deviation of our orbit from circular due to the presence of the linear sections. Thus, the losses in the employed portion of the working region are due to the fact that the magnet and the chamber are designed for an orbit consisting of four arcs joined by straight lines, whereas the actual orbit assumes a different complicated form.

On the basis of the foregoing formulas it becomes possible to do the following: 1) calculate the form of the particle trajectory for any distortions; 2) estimate beforehand the orbit distortion brought about by some particular deviation of the field from theoretical; 3) ascertain what types of distortion are the most dangerous; 4) choose methods for mutual cancellation of the distortions; 5) choose (with account of the results of Chapter 4) the value of the magnetic field index n in the main part of the working region of the magnet; 6) determine the required accuracy of the magnetic measurements; 7) determine the required accuracy of manufacture and erection of the magnet (angular dimensions of the sectors, lengths of the linear sections, etc.); 8) choose (with account of the results of Chapter 5) the dimensions of the magnet cross section.

Manu-
script
Page
No.

[Footnote]

107 Resonant phenomena may also not be connected with deviations of the magnetic field from theoretical, but, as will be shown in the next chapter, such resonances in annular magnets with weak focusing hardly play any role.

Chapter 4

RESONANT PHENOMENA IN ACCELERATOR WITH SLOTTED MAGNET

§1. Introduction

The various possible resonant phenomena in accelerators should be the subject of a special analysis. In the first three chapters we have investigated in detail the free and radial-phase oscillations. All the calculations were made in the linear approximation. Usually such an analysis is satisfactory, and inclusion of the second and higher approximations is of no practical use. This holds true, however, only away from resonance between the different modes of oscillation. Resonant phenomena between the fast oscillations in circular accelerators were considered in many papers (see, for example, [43-45, 56, 57]).

Resonant phenomena in an accelerator with slots were first investigated in detail by the author [25, 27]. As will be shown below, the resonant phenomena in accelerators with slotted magnet differ essentially from resonant phenomena in a cyclic accelerator. This difference manifests itself primarily in the fact that several resonant values of the magnetic field index n are strongly changed even when the lengths of the linear sections are small.* This is particularly significant when the resonant shift of the index is from the region of values of n lying outside the working region of the magnet to the inside of this region. This is clear from the fact that the frequency of the free oscillations in accelerators with slotted magnets (as can be seen from Fig. 18) changes and this causes a change in the index n at which reso-

nance with the revolution frequency sets in. The resonant value of $\underline{n}$ hardly shifts at all in the case of nonlinear resonance between free oscillations, for so long as $p = l\kappa/2R$ is small, the frequencies of the vertical and radial oscillations in accelerators with slots vary in proportion to each other. Therefore the well-known resonance occurring at $n = 0.2$ between the vertical and radial oscillations occurs in an accelerator with a slotted magnet at practically the same value of the magnetic field index $\underline{n}$. Another distinguishing feature is that in an accelerator with slotted magnet there occur, in addition to the ordinary resonances, also multiple resonances, i.e., resonances with the external force having a frequency not equal to the natural oscillation frequency, but to a multiple of this frequency, i.e., larger or smaller by an integral number of times. The theory of such resonances was first developed in general form in the classical paper of Mandel'shtam and Papaleksi [49]. The reason for the occurrence of multiple resonances lies in the anharmonicity of the fundamental oscillatory process.

Unlike the synchrocyclotron, the microtron, and annular accelerators, the principal role is played by the magnetic field in the region where $n > 0.2 \sim 0.3$. According to the technical specifications, $0.55 < n < 0.75$ in the main part of the working region. It is therefore meaningless to consider the well-known resonance at $n = 0.2$, and also the resonance at $n = 0.25$ (the value of $\underline{n}$ is given for the circular accelerator), etc. In annular accelerators with slots the principal role is assumed by resonances between the radial oscillations and the revolution frequency, brought about by the presence of deviations of the magnetic field from the theoretical, and resonances between the vertical oscillations and the revolution frequency, brought about by the distortion of the central magnetic plane (Fig. 30).

In addition to resonances with the free oscillations, resonances

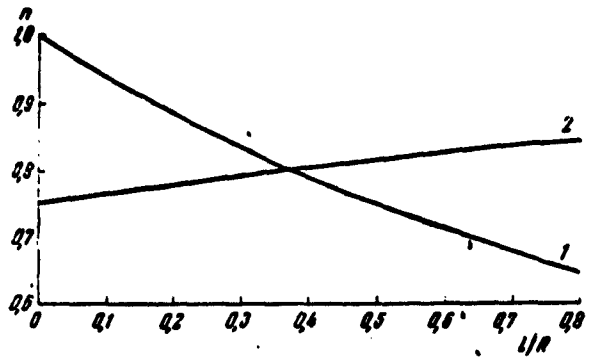

Fig. 30. Resonant values of n as a function of 1/R for vertical (1) and radial (2) oscillations.

with the phase oscillations can occur in the accelerator. This question was raised for the first time in the summer of 1950 in a discussion of the power supply for the magnets of the 180-Mev and 10,000-Mev proton synchrotrons, held at the Scientific Research Institute for Electrophysical Apparatus of the Ministry of Electric Industry, USSR. It turned out that the magnetic field will contain small harmonic components with frequencies lying in the range of variation of the phase-oscillation frequency. Calculations which we made at that time indicated that in spite of the exceedingly small amplitude of these harmonics (~0.02 gauss), this phenomenon may prove dangerous in some cases. In addition, we called attention to the danger of exceedingly small oscillations in the frequency and amplitude of the accelerating electric field.

§2. Generalization of the Averaging Method

In solving ordinary differential equations with slowly varying coefficients or with small nonlinearities, and also in the investigation of the passage of a system through resonance, the "method of averaging," which was established on a solid mathematical foundation in the papers of N.N. Bogolyubov [33], plays an important role. This method is particularly convenient if we are interested in first-

approximation calculations, as is usually the case. From the mathematical point of view the changeover from the circular accelerator to an accelerator with slotted magnet denotes the changeover from differential equations to difference equations or from equations with constant coefficients to an equation with periodic coefficients. This averaging method can also be generalized to include the present case.

The motion of the particles in the circular sector can be described by Eq. (III, 1). It is possible to change over from the second-order differential equation (III, 1) to two first-order equations in the two variables $A(\theta)$ and $B(\theta)$, using the following transformation

$$\begin{aligned} \chi &= A(\theta)\sin\int_0^\theta \varkappa d\theta + B(\theta)\cos\int_0^\theta \varkappa d\theta; \\ \dot{\chi} &= \varkappa\left[A(\theta)\cos\int_0^\theta \varkappa d\theta - B(\theta)\sin\int_0^\theta \varkappa d\theta\right], \end{aligned} \tag{1}$$

where the angle θ varies from 0 to ν. Substituting (1) in (III, 1), we obtain differential equations for A and B:

$$\begin{aligned} \dot{A}(\theta) &= \frac{g(\theta)}{\varkappa}\cos\alpha - \frac{\dot{\varkappa}}{2\varkappa}A(\theta) - \frac{\dot{\varkappa}}{2\varkappa}[A(\theta)\cos 2\alpha - B(\theta)\sin 2\alpha]; \\ \dot{B}(\theta) &= -\frac{g(\theta)}{\varkappa}\sin\alpha - \frac{\dot{\varkappa}}{2\varkappa}B(\theta) + \frac{\dot{\varkappa}}{2\varkappa}[A(\theta)\sin 2\alpha + B(\theta)\cos 2\alpha], \end{aligned} \tag{2}$$

where $\alpha = \int_0^\theta \varkappa d\theta$ and $\varkappa = \sqrt{H \cdot H\kappa^2}$. Were the angle θ to vary without limit, then, on averaging the equations in (2), we would find that the terms in the square brackets vanish. For example, if $g = 0$, we obtain directly the known law governing the variation of the amplitude of free oscillations in a circular accelerator. Indeed, in this case $A(\theta) \sim \sqrt{\varkappa} = \sqrt{H\kappa}$. For an accelerator with slots, such an averaging yields nothing, since θ varies within a limited range. It is obvious, however, that in this case, too, the expression in the square brackets in (2) should play no role.

We mark the quantities A, B, χ, and κ with the index $\underline{k}$, which indicates the number of the sector. In addition, we introduce

$$\left.\begin{aligned} H_k(0)\varkappa_k(0) &= y_k^0;\ A_k(0) = A_k^0;\ A_k(\nu) = A_k \\ H_k(\nu)\varkappa_k(\nu) &= y_k;\ B_k(0) = B_k^0;\ B_k(\nu) = B_k \end{aligned}\right\} \qquad (3)$$

and "join" the solutions in two neighboring sectors with the aid of Relation (1):

$$\left.\begin{aligned} y_k(A_k c - B_k s) &= A_{k+1}^0 y_{k+1}^0; \\ A_k s + B_k c + 2p(A_k c - B_k s) &= B_{k+1}^0. \end{aligned}\right\} \qquad (4)$$

Here

$$\left.\begin{aligned} c &= \cos\int_0^{\nu} \varkappa d\theta;\ s = \sin\int_0^{\nu} \varkappa d\theta; \\ p &= \frac{l\varkappa_k}{2R}. \end{aligned}\right\} \qquad (5)$$

The first equation in (4) expresses the equality of the radial or vertical components of the particle momentum at the end of the k-th and the beginning of the k + 1-st sectors. The radial or vertical momentum is in our case equal to $H\chi$, apart from constants, so that the right and left halves of (4) contain the value of the magnetic field at the instant when the particle leaves the k-th sector and at the instant when the particle enters the k + 1-st sector.

Equations (4) and (2) are the exact equations of the investigated problem, and should be solved simultaneously. However, the systems (4) and (2) can actually be solved if we assume that the variations of $A(\theta)$; $B(\theta)$; $\kappa(\theta)$; $H(\theta)$, etc. are slow compared with the variation of the angle θ. Let us integrate in this approximation the equation (2) with respect to θ from 0 to ν. In integrating between these limits, we can assume that A and B, which are contained in the right half of (2), do not depend on θ within the confines of a single sector. As a result we obtain

$$\left.\begin{aligned} A_{k+1} - A_{k+1}^0 &= \int_0^{\nu} \frac{\varepsilon_{k+1}(\theta)}{\varkappa} \cos\alpha d\theta - h_k A_{k+1} - h_k\left[A_{k+1}\varkappa c - B_{k+1}s^2\right]; \\ B_{k+1} - B_{k+1}^0 &= -\int_0^{\nu} \frac{\varepsilon_{k+1}(\theta)}{\varkappa} \sin\alpha d\theta - h_k B_{k+1} + h_k\left[A_{k+1}s^2 + B_{k+1}\varkappa c\right], \end{aligned}\right\} \qquad (6)$$

where

$$h_k = \frac{\Delta\nu}{2\pi} = \frac{\nu}{2}\frac{d\ln(H\varkappa)}{d\theta}. \qquad (7)$$

Substitution of (6) in (4) yields the first difference equation of the problem under consideration:

$$A_k c - B_k s = \frac{y_{k+1}^*}{y_k}\left\{(1+h_k)\,i_{k+1} + \frac{\varepsilon h_k}{\varkappa}\left[A_{k+1}c - B_{k+1}s\right] - \right.$$
$$\left. - \int_0^{\theta} \frac{\varepsilon_{k+1}(\theta)}{\varkappa}\cos\alpha\, d\theta\right\}, \qquad (8)$$

$$A_k(s+2pc) + B_k(c-2ps) = (1+h_k)\,B_{k+1} - \frac{\varepsilon h_k}{\varkappa}\left[A_{k+1}s + B_{k+1}c\right] +$$
$$+ \int_0^{\theta} \frac{\varepsilon_{k+1}(\theta)}{\varkappa}\sin\alpha\, d\theta.$$

In order to be able to apply the averaging method to (8), we must separate in A_k and B_k the rapidly oscillating part, similar to what is done for differential equations. Therefore in place of the actual variables A_k and B_k, we introduce the complex variable D_k, which turns into a constant when $h_k = 0$ and $g_k = 0$:

$$A_k = D_k e^{i\Sigma_k} + D_k^* e^{-i\Sigma_k}, \qquad (9)$$
$$B_k = d_k D_k e^{i\Sigma_k} + d_k^* D_k^* e^{-i\Sigma_k},$$

$$d_k = \frac{c - e^{i\mu_{k+1}}}{s} = p - i\frac{\sin\mu_{k+1}}{s}; \qquad (10)$$

$$\Sigma_k = \sum_{l=1}^{l=k}\psi_l;\quad \cos\mu_{k+1} = c - ps.$$

It is easy to verify that if D_k and d_k are regarded as constant, then (9) is a solution of the corresponding homogeneous equation (8) when the parameters are constant. According to (9), we obtain

$$A_{k+1} = D_k e^{i\Sigma_{k+1}} + \Delta D_k e^{i\Sigma_{k+1}} + \text{c.c.}; \qquad (11)$$
$$D_{k+1} = D_k d_k e^{i\Sigma_{k+1}} + (d_k\Delta D_k + D_{k+1}\Delta d_k)\,e^{i\Sigma_{k+1}} + \text{c.c.}$$

Substituting (11) in (8), we obtain two linear equations with respect to the two unknowns ΔD and ΔD^*:

$$\Delta D_k e^{i\Sigma_{k+1}} + \Delta D_k^* e^{-i\Sigma_{k+1}} = (\Psi_1 e^{i\Sigma_{k+1}} + \text{c.c.}) - \frac{\varepsilon_k}{\varkappa_{k+1}}\int_0^{\theta}\frac{\varepsilon_{k+1}}{\varkappa}\cos\alpha\, d\theta;$$

$$d_k\Delta D_k e^{i\Sigma_{k+1}} + d^*\Delta D_k^* e^{-i\Sigma_{k+1}} = (\Psi_2 e^{i\Sigma_{k+1}} + \text{c. c.}) + \frac{1}{1+h_k}\int_0^{\varphi}\frac{g_{k+1}}{u}\cos u\,d\varphi. \quad (12)$$

where Ψ_1 and Ψ_2 are slowly varying functions of the number $\underline{k}$. In the solution of (12) we encounter terms of the form

$$\Psi_1^* e^{-2i\Sigma_{k+1}};\ \Psi_2^* e^{-2i\Sigma_{k+1}},\ \text{etc.}$$

Upon averaging they yield zero, and consequently the average solution (12) has the form

$$\Delta D_k = \frac{\Psi_1 d_k^* - \Psi_2 + \frac{\bar{I}^{cp}}{1+h_k}}{d_k^* - d_k}, \quad (13)$$

where

$$\Psi_1 d_k^* - \Psi_2 = -\frac{h_k}{1+h_k} D_k + \frac{D_{k+1}\Delta d_k}{d_k^* - d_k}\left[1 - \frac{h_k e^{-i\mu_{k+1}}}{(1+h_k)^2}\right] - D_k d_k^*\left(1 - \frac{y_k}{y_{k+1}^*}\right); \quad (14)$$

$$I_k = e^{-i\Sigma_{k+1}}\int_0^{\varphi}\left(g_{k+1}\sin z + \frac{y_k}{y_{k+1}^*} d_k^* g_{k+1}\cos z\right)d\varphi. \quad (15)$$

If we regard Δd_k and h_k as small quantities, the squares and products of which can be neglected, then Eq. (13) assumes the following final form:

$$D_{k+1}\left(1 + h_k + \frac{i\Delta d_k s}{2\sin\mu_{k+1}}\right) - D_k\left[1 - \frac{1}{2}\left(1 - \frac{ips}{\sin\mu_{k+1}}\right)\left(1 - \frac{y_k}{y_{k+1}^*}\right)\right] = \frac{s\bar{I}_k^{cp}}{2i\sin\mu_{k+1}}. \quad (16)$$

Equation (16) is fundamental to our theory. Its derivation is somewhat cumbersome because we are taking into account the changes in the system parameters, with an aim toward obtaining later the law governing the variation of the amplitude of the free oscillations in an accelerator with a slotted magnet. In the investigation of the passage through resonance, one can generally speaking disregard the variations of the parameters, since the resonance plays usually an important role for a short time interval. In this case Eq. (16) simplifies to

$$D_{k+1} - D_k = \frac{\varepsilon T^{cp}}{2i \sin \mu_{k+1}}. \qquad (17)$$

Equations (16) and (17) are a generalization of the abbreviated equations of averaging theory to include the case of difference equations.

§3. Adiabatic Variation of the Amplitude of Free Oscillations

In order to solve Eq. (16) it is first necessary to solve the corresponding homogeneous equation. A solution of this last problem is simultaneously equivalent to a determination of the adiabatic varia-

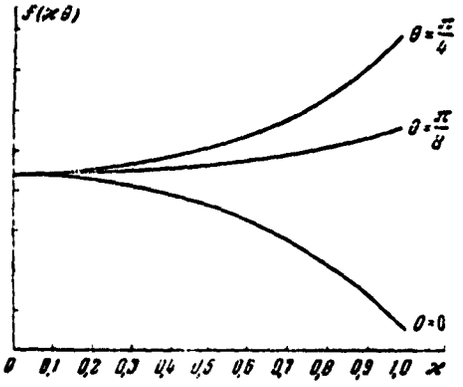

Fig. 31. Dependence of the function $f(\kappa\theta)$ on κ for three values of θ and for the parameters of the proton synchrotron of the USSR Academy of Sciences ($1/R = 2/7$).

tion of the amplitude of the oscillations in accelerators with slotted magnets. Solving (16), we obtain in first approximation (in φ_k and Δd_k),

$$\ln D_k = -\sum_{i=1}^{k} \left\{ \left[\varphi_k + \frac{1}{2}\left(1 - \frac{y_k}{y^0_{k-1}}\right)\right] + \right.$$
$$\left. + \frac{is}{2 \sin \mu_{k+1}} \left[\Delta d_k - p\left(1 - \frac{y_k}{y^0_{k+1}}\right)\right]\right\} + \ln D_0. \qquad (18)$$

Replacing summation by integration, we obtain

$$D_k = D\left(\frac{\nu H \sin\mu}{s}\right)^{-1/2} e^{-\frac{1}{2}\int_0^{\theta}\frac{\left[4p-p\left(1-\frac{y_k}{y_{k+1}}\right)\right]}{s\ln\mu}d\theta} \qquad (19)$$

The square of the oscillation amplitude at the azimuth σ is determined from Formula (II, 22):

$$F_\sigma^2 = \frac{4DD^*}{\nu H}\frac{s}{\sin\mu}\left[1+\frac{2p\cos\frac{\pi}{2}\cos(\sigma_0-\sigma)}{s}\right] = \frac{4DD^*}{\nu H} f(\sigma), \qquad (20)$$

where f(σ) is defined in (II, 42). It is seen from Formula (20) that if κ is constant, then the law governing the variation of the amplitudes of the free oscillations in an accelerator with slotted magnet coincides with the law governing the variation in a circular accelerator. However, if κ changes, as is usually the case on going through resonance, then certain singularities appear, present only in an accelerator with slotted magnet: first, the change in the oscillation amplitude is different in different azimuths; second, the rate of attenuation itself changes.

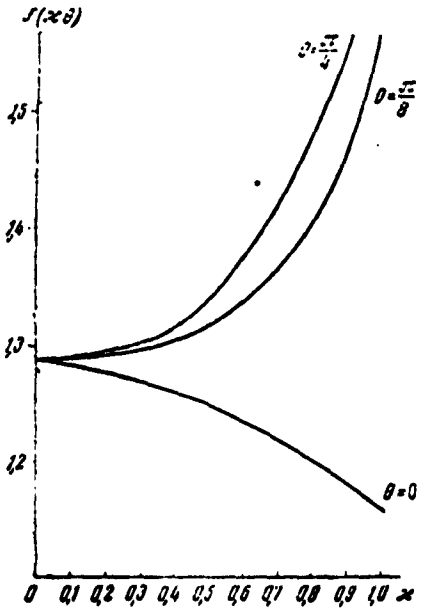

Fig. 32. Dependence of the function f(κθ) on κ for three values of θ and for 1/R = 1.

Figures 31 and 32 show the function $f(\sigma)$ for three different azimuths: $\theta = 0$ (edge of the sector), $\theta = \pi/4$ (middle of the sector), and $\theta = \pi/8$ (intermediate points), and for two values of L/R, namely 8/7 (the proton synchrotron of the USSR Academy of Sciences) and 4. We see from these figures that when κ increases the amplitude at the center attenuates more slowly, and on the edge it attenuates more rapidly, than in a circular accelerator.

From Formula (19) we can determine the change in the phase of the oscillations due to changes in the parameter κ and in H. We assume that κ = const. Then

$$\frac{D_{k_1}(H_2)}{D_{k_1}(H_1)} = \left(\frac{H_1}{H_2}\right)^{\nu_r} e^{i\frac{L\kappa}{4\pi R\sin\mu}\ln\frac{H_2}{H_1}}.$$

Thus, the change in the phase of the oscillations is logarithmic, i.e., rather slow. For example, in the proton synchrotron of the USSR Academy of Sciences, the phase of the oscillations changes by approximately 30° during the entire acceleration time.

§4. Resonance when n = 0.84

In the 10-Bev proton synchrotron when n = 0.84 the frequency of revolution and the frequency of the vertical oscillations coincide and cos μ = 0. The value of cos μ in the vicinity of n = 0.84 can be found from Formula (III, 32). The value of the index n, at which resonance takes place, can be calculated from the following approximate formula, which usually gives an accurate result:

$$n = 1 - 2b + 3b^2 - 2{,}4b^3 + \ldots, \qquad (21)$$

where $b = 1/\pi R$. Formula (21) is a solution of the equation

$$\cos\frac{\pi\sqrt{n}}{2} - \frac{1\sqrt{n}}{2!!}\sin\frac{\pi\sqrt{n}}{2} = 0,$$

which is expanded in powers of b.

The magnetic field index n in the main part of the chamber is, of course, chosen to be much smaller than 0.84 and on the average its

value is 0.66. According to the technical specification, at the instant of injection from a working region measuring 160 cm, $\underline{n}$ lies in approximately 140 cm between 0.55 and 0.75. It is desirable, however, to use the entire working region of the magnetic field, up to $n = 1$. In addition to the trivial desire for making full use of the magnet gap, this is connected with two other factors: first, when $n \sim 1$ the orbit is compressed more rapidly, which can increase the injection efficiency; second, when the particle beam is extracted from the accelerator chamber, it is necessary to use the region $n \sim 1$, in order to increase the pitch of the unwinding spiral along which the particle moves. It is therefore important that we be able to calculate the single or multiple passage of the particles through the resonant region.

The resonance at $n = 0.84$ will occur if a vertical force acts with the period of particle revolution. Such a force, in particular, is the distortion of the central magnetic plane of the magnet, considered in §3 of the preceding chapter. Such a force is also the vertical component of the electric field of the injection plates (injector). In short, any local constant force having a vertical component due to the rotation of the particle, acts on the particle with the period of revolution. When $n = 0.84$ there is also parametric resonance in the case when the index $\underline{n}$ depends on the azimuth. The principal role will then be played by the second harmonic of the variation of $\underline{n}$.

Let us investigate first the resonance phenomenon in the case of a parallel shift of the magnetic planes of the individual sectors. This corresponds to the first case considered in §3 of the preceding chapter which, apparently, corresponds most accurately to the actual situation in the proton synchrotron of the USSR Academy of Sciences. After substituting (III, 12) into (15), we obtain

$$I_k = e^{-i\Sigma_{k+1}\Delta z_{k+1}}\left[(1-c)+d_k^* s\right]; \qquad (22)$$

$$g_k = \Delta z_k^*.$$

We average I_k in the following fashion:

$$I_k = \Delta z_{k+1} e^{-i\left[\Sigma_{k+1}-\frac{\pi}{2}(k+1)\right]} e^{-i\frac{\pi}{2}(k+1)}\left(1-e^{i\mu_{k+1}}\right) =$$

$$= \left(\Delta z_{k+1} e^{-i\frac{\pi}{2}(k+1)}\right) e^{i\psi_k}\left(1-e^{i\mu_{k+1}}\right).$$

The quantity $\psi_k = -\left[\Sigma_{k+1} - \frac{\pi}{2}(k+1)\right]$ changes little during the course of the resonance, and upon averaging it can be regarded constant, just like μ_{k+1}. The quantity $(\Delta z_{k+1} e^{-i\pi/2(k+1)})$ is a periodic function of $\underline{k}$ with period 4. It is therefore sufficient to average it over one period, changing $\underline{k}$ from 0 to 3. As a result we obtain

$$I_k^{cp} = \frac{-ie^{i\psi_k}\left(1-e^{-i\mu_{k+1}}\right)}{4}\left[(\Delta z_1 - \Delta z_3) - i(\Delta z_2 - \Delta z_4)\right]. \qquad (23)$$

Let us use Eq. (17), i.e., let us disregard the change in the oscillation amplitude due to the change in the parameters during the time of passage through resonance. In this case

$$D_k = D_0 + \sum_0^k \frac{s I_k^{cp}}{2i\sin\mu}. \qquad (24)$$

We replace the summation in (24) by integration and take the resultant integral by the method of steepest descent at the point of exact resonance. As a result we obtain the value of D_k after passage through resonance in the form:

$$D_k = D_0 + \frac{(1+i)s}{8}\sqrt{\frac{2\pi i}{\mu'}}\left[(\Delta z_4 - \Delta z_2) + i(\Delta z_3 - \Delta z_1)\right] e^{i\psi_k}. \qquad (25)$$

It is clear from (25) that the addition to D_0 has a maximum when $\Delta z_k \cdot \Delta z_{k+2} < 0$, i.e., if the alternation of the signs of the shifts of the central planes occurs every other sector. Here (and henceforth) we shall calculate the resultant amplitude obtained after passage through resonance. Of course, it is easy to calculate with the aid of the Fresnel integrals the entire process whereby the oscillation amplitude

builds up (see Figs. 33 and 34). The value of the square of the amplitude $D_k D^*_k$ depends essentially on the relation between the phases of the initial and final oscillations. If we average over all the phases, we obtain

$$\overline{D_m D_m^*} = D_0 D_0^* + \frac{\pi s}{16\mu'}\left[(\Delta z_1 - \Delta z_2)^2 + (\Delta z_3 - \Delta z_1)^2\right], \tag{26}$$

where

$$\mu' = \frac{d\mu}{dk} = \left(s + pc + \frac{p}{\pi\nu}s\right)\frac{\pi}{16\sqrt{n}}\Delta n, \qquad \mu' \approx \frac{\pi\Delta n}{16}\left(1 + \frac{4p}{\pi}\right). \tag{27}$$

Δn is the change in n during one complete revolution of the particle.

According to (II, 22), the amplitude of the oscillations F_c^2 is

$$\overline{F_c^2} = \overline{4D_k D_k^*}\left[1 + \frac{2p\cos\varepsilon\cos(\alpha_1 - \varepsilon)}{s}\right].$$

Let us consider one example. Let

$$\Delta z_1 = \Delta z_2 = -a; \quad \Delta z_3 = \Delta z_4 = a.$$

If $\Delta n = 0.01$, then the amplitude of the vertical oscillations F_c exceeds a by almost 60 times.

In conclusion we note that in order to calculate the passage through resonance during the instant of injection it is not essential to replace the sums by integrals, since a numerical calculation by means of Formula (24) does not entail great difficulty. Indeed, the number of revolutions during which the resonance is significant is on the order of 15-25. Figures 33 and 34 show a comparison of numerical calculation with the method of steepest descent.

Let us consider further the resonance phenomenon for a random deviation of the central magnetic plane from the geometrical plane. Let $g_1(\theta)/\kappa$; $g_2(\theta)/\kappa$; $g_3(\theta)/\kappa$, and $g_4(\theta)/\kappa$ be the deviations of the central magnetic plane in the first, second, etc. sectors of the magnet. We expand this deviation, as in §3 of the preceding chapter, in a Fourier series [see (III, 11)], and investigate the effect of the j-th

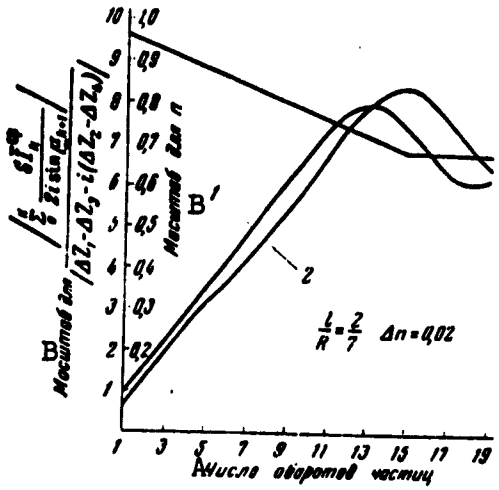

Fig. 33. Comparison of numerical calculations with the calculation by the method of steepest descent: 1) numerical calculation; 2) calculation by the method of steepest descent. A) Number of particle revolutions; B) scale for.

harmonic:

$$z_j \sin(j\theta + \alpha_{j,k}) = \frac{z_j\left(e^{ij\theta}e^{i\alpha_{j,k}} - e^{-ij\theta}e^{-i\alpha_{j,k}}\right)}{2i}. \qquad (28)$$

In calculating I_k^{sr} by Formula (15) we must average the following quantities:

$$1)\ e^{-i\sum_{k+1}+i\alpha_{j,k+1}}, \qquad (29)$$

$$2)\ e^{-i\sum_{k+1}-i\alpha_{j,k+1}}, \qquad (30)$$

where

$$\alpha_{j,k+1} = \alpha_{j,0} + \frac{\pi}{2} j(k+1),$$

$$\sum_{k+1} = i\left[\frac{\pi}{2}(k+1) + \sum_{1}^{k-1}\left(\mu_k - \frac{\pi}{2}\right)\right]. \qquad (31)$$

Let us consider first the exponent in (29). According to (31), we obtain

$$i\left[(k+1)\left(-\frac{\pi}{2} + \frac{\pi}{2}j\right) + \alpha_{j,0} - \sum_{1}^{k+1}\left(\mu_k - \frac{\pi}{2}\right)\right]. \qquad (32)$$

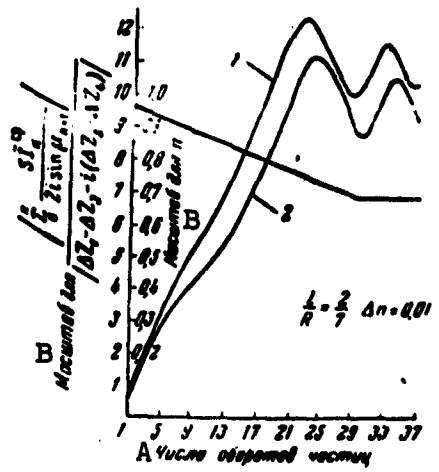

Fig. 34. Comparison of numerical calculations with the calculation by the method of steepest descent (case of slower variation of the magnetic field index n than on Fig. 33). 1) Numerical calculation; 2) calculation by the method of steepest descent. A) Number of particle revolutions; B) scale for.

The last two terms in (32) are almost constant (since $\mu_k \sim \pi/2$) and the first term can, generally speaking, vary rapidly. In this case, the value of (29) vanishes on averaging. However, if $(-\pi/2 + \pi j/2)$ is equal to zero or is a multiple of 2π, then the average value of (29) will be different from zero. This latter case occurs when

$$j = 4q + 1,$$

where $q = 0, 1, 2, 3, 4$, etc.

An analogous analysis of Expression (30) leads to the conclusion that it does not vanish on averaging if

$$j = 4q - 1,$$

where $q = 1, 2, 3, 4$, etc.

Thus, in our case all the odd harmonics of the shift of the magnetic plane resonate. We have carried out the derivation for an accelerator with four linear sections. Obviously, if we have not four but M

sections, the following numbered harmonics will resonate:

$$j = Mq \pm 1. \tag{33}$$

For example, in a circular accelerator only the first harmonic resonates, while in an accelerator with four linear sections all odd harmonics resonate, and in an accelerator with six linear sections the resonating harmonics are numbers 1, 5, 7, 11, 13, etc. This phenomenon is very simple to explain. The eigenfunctions of the oscillation equations are harmonic, and when the eigenfunction of the lowest period is expanded in a Fourier series, we obtain harmonic components of the indicated period.

Thus, we should consider the action of all the odd harmonics. It must be borne in mind here that if j is contained in the exponent (28) with a plus sign, we consider the harmonics numbered 1, 5, 9, 13, 17, etc., while if j has a minus sign, we consider the harmonics numbered 3, 7, 11, 15, 19, etc. It is therefore sufficient to consider only one of the expressions contained in (28):

$$g_k^j(0) = \frac{Z_j e^{i j \theta_0} e^{i \alpha_{j,k}}}{2i} \varkappa;$$

$$J_k^{cp} = \frac{\varkappa Z_j e^{i(\alpha_{j,0} + \psi_k)}}{2i} \int_0^{\pi} e^{ij\theta} (\sin \varkappa\theta + d_k^* \cos \varkappa\theta)\, d\theta; \tag{34}$$

$$D_k = D_0 + \frac{1}{2i} \int_0^k \frac{s I_k^{cp}}{\sin \mu_{k+1}}\, dk; \quad \psi_k = -\int_0^k \left(\mu - \frac{\pi}{2}\right) dk.$$

We replace the summation in (34) by integration, since the integrand changes very little after a change by unity. Carrying out the calculations indicated in (34), we obtain

$$D_k = D_0 + \frac{l Z_j \varkappa p s e^{i \alpha_{j,0}}}{2i (j^2 - \varkappa^2)} \int_0^k e^{i\psi_k} dk, \tag{35}$$

$$\int_0^k e^{i\psi_k} dk = \sqrt{\frac{2\pi}{i\mu'}}\, e^{i\psi_0},$$

where ψ_0 is the phase of ψ_k at the resonance point.

If all the harmonics are present, we should sum their action. As a result we obtain

$$D_k = D_0 - \sum_{j=0}^{\infty} \sqrt{2\pi} \frac{\pi \rho_0 (2j+1) Z_{2j+1}}{2 [(2j+1)^2 - \varkappa^2] \sqrt{\beta^*}} e^{i\psi_0} e^{i(-1)^j \varepsilon_{2j+1,1}}. \qquad (36)$$

It is easy to calculate the sum contained in (36). Indeed

$$\sum_{j=0}^{\infty} \frac{(2j+1) Z_{2j+1}}{(2j+1)^2 - \varkappa^2} e^{i(-1)^j \varepsilon_{2j+1,1}} =$$

$$= \frac{\varepsilon}{4\varepsilon\varkappa} \int_0^{\frac{\pi}{2}} [(g_1 - g_3) - i(g_2 - g_4)] \left[\sin \varkappa\theta + \frac{(i+c)}{s} \cos \varkappa\theta \right] d\theta. \qquad (37)$$

Inasmuch as (i + c)/s is equal to the value of d^*_k at resonance [see (10)], we can regard [sin $\kappa\theta$ + d^*_k cos $\kappa\theta$] as the solution of the complex-conjugate homogeneous difference equation for the resonant κ. In spite of the apparent simplicity of the right half of (37) compared with the left half, it is more convenient to use the left half, for there are ready-made methods for expansion in a Fourier series (templates, analyzers, etc.), and the series converges rapidly. For the same reasons, for example, one does not use in practice the "simple" expression (III, 2) for the distorted orbit in the central plane, it being preferable to expand (III, 2) in a Fourier series.

We note that the right half of (37) can of course be obtained also directly (without resorting to the Fourier series) in the calculation of I^{sr}_k by means of Formula (15), as we did in the derivation of Formula (23). For this purpose it is necessary to use the following relation, obtained in analogy with (23):

$$\overline{e^{-i\Sigma_{k+1} g_{k+1}}}^{op} = \frac{e^{i\psi_k}}{4i} [(g_1 - g_3) - i(g_2 - g_4)].$$

In the cases of practical interest, the series (36) converges well and usually its first term exceeds appreciably all the others.

Expression (36) can be simplified by assuming 1/R to be a small

quantity

$$D_k = D_0 - \frac{e^{i\mu_{2m}}(1+i)}{2\sqrt{\Delta n}}\left\{\left(1-\frac{3}{2}b\right)Z_1 e^{i\mu_{1,1}} + \right.$$

$$\left. + b\sum_{j=1}^{\infty}\frac{2j+1}{2j(j+1)}Z_{2j+1}e^{i[(-1)^j\mu_{2j+1,1}]}\right\}; \quad b=\frac{1}{\pi R}. \qquad (38)$$

It is seen from (37) that the action of the first harmonic is $(1 - 3b/2)/(3b/4) \approx 12.5$ times stronger than that of the third harmonic, and 22.5 times stronger than that of the fifth harmonic, etc.

As is seen from (38), the magnitude of the resonance is greatly influenced by the value of Δn. Apparently it will be on the order of 0.01-0.02.

So far we have carried out the calculations using the simplified equation (17) in place of Eq. (16). It is easy to get rid of this limitation. The solution of the homogeneous equation (16) is given in §3. Applying to this solution the method of varying the constant, we easily obtain the desired solution. Let F_k be the solution of the homogeneous equation [see (19)], then

$$D_k = F_k\sum_{0}^{k}\frac{sT_k^p}{2i\sin\mu_{k+1}F_{k+1}}. \qquad (39)$$

In summing (39) we use the method of steepest descent. Consequently,

$$D_k = \frac{F_k}{F_{k_0+1}}D'_k, \qquad (40)$$

where F_{k_0+1} is the value of F_k at the saddle point k_0, while D'_k is the solution obtained above. In other words, past the saddle point, the amplitude D_k varies in accordance with the usual rules considered above in §3. Parametric resonance at $n = 0.84$ can be analyzed by the method developed in the next section.

§5. Parametric Resonance at n = 0.79

When $n = 0.79$, a well-known resonance between the first harmonic of the azimuthal asymmetry and the radial oscillations is produced in

the proton synchrotron of the USSR Academy of Sciences. In this resonance, the frequency of the radial oscillations (8) is equal to half the revolution frequency 2π, i.e.,

$$\mu=\frac{\pi}{4};\quad \cos\frac{\pi}{2}\sqrt{1-n}-\frac{1\sqrt{1-n}}{2R}\sin\frac{\pi}{2}\sqrt{1-n}=\frac{\sqrt{2}}{2};$$
$$n=0{,}75+0{,}5b-0{,}95b^2+1{,}7b^3-\ldots; \qquad (41)$$
$$b=\frac{l}{\pi R}.$$

The effect of this resonance is proportional to the product of the small deviations from the theoretical field and from the equilibrium orbit. This resonance is therefore referred to as a second-order resonance.

Assume that the vertical components of the magnetic field can be represented in the following form [see (III, 14)]:

$$H_z(r,\theta)=H_0(r)[1+h_k(r,\theta)],$$

where H_0 does not depend on the azimuth θ and on the number of the sector $\underline{k}$, while $h_k(r, \theta)$ is small and yields zero when averaged over $\underline{k}$ and θ: $\overline{h_k(r,\theta)}^{cp}=0$. We then must write in lieu of (III, 1)

$$\frac{d}{d\theta}(H_0\beta)+H_0(1-n_k'(\theta))\rho=-H_0h_k(R,\theta);$$
$$n_0=-\frac{R}{H_0}\frac{\partial H_0}{\partial r};\quad n_k'(\theta)=n_0(1+h_k)-R\frac{\partial h_k}{\partial r}-2h_k=n_0+n_k(\theta). \qquad (42)$$

The customarily employed quantity $n_k(\theta)$ is small compared with the constant quantity n_0.

The influence of the term $-H_0h_k(R, \theta)$ on the motion of the particles was already investigated in the preceding section.

The term $-n_k(\theta)\rho$ usually does not play an essential role. But if $n \approx 0.79$, then this term, which is small in magnitude, resonates in the 10-Bev proton synchrotron with the frequency of the radial oscillations and in some cases may cause a noticeable increase or decrease in the oscillation amplitude.

Let us expand $n_k(\theta)$ in a Fourier series

$$n_k(\theta) = \frac{1}{2}\sum_{j=-\infty}^{j=+\infty} a_j e^{i\left(j\theta + \frac{\pi}{4}jk\right)}. \qquad (43)$$

The sign in front of the phase α_j is plus if j is positive and minus if j is negative. We use Eq. (17). It contains the quantity I_k^{av} [see Formula (15)]:

$$\overline{I_k^{cp}} = \frac{D_{k+1}}{\pi}\int_0^{\pi} n_{k+1}(\theta)\,|\sin\varkappa\theta + d_k\cos\varkappa\theta|^2\,d\theta + \overline{}^{cp}$$

$$+\frac{D_{k+1}^*}{\pi}e^{-2i\sum_{k+1}}\int_0^{\pi} n_{k+1}(\theta)(\sin\varkappa\theta + d_k^*\cos\varkappa\theta)^2\,d\theta =$$

$$= (i\psi_1 D_{k+1} + \psi_2 e^{i\varphi_k} D_{k+1}^*)\frac{2i\sin\mu_{k+1}}{\varepsilon}, \qquad (44)$$

where $n_k(\theta)$ is the value of $n'(\theta) - n_0$ in the k-th sector, and $\varkappa = \sqrt{1 - n_0}$ (we recall that θ changes from 0 to $\pi/2$). In averaging (44) we shall assume that $\varphi_k = -2\sum_{k+1} + \frac{\pi}{2}(k+1)$ is a slow function of k. Equation (17) assumes the form:

$$D_{k+1}(1 - i\Psi_1) - D_k = \Psi_2 D_{k+1}^* e^{i\varphi_k} \qquad (45)$$

The values of Ψ_1 and Ψ_2 are readily determined from (44):

$$\Psi_1 = -\frac{\varepsilon}{8\varkappa\sin\mu_{k+1}}\int_0^{\pi}(n_1 + n_2 + n_3 + n_4)\,|\sin\varkappa\theta + d_k\cos\varkappa\theta|^2\,d\theta;$$

$$\Psi_2 = -\frac{\varepsilon}{8\varkappa\sin\mu_{k+1}}\int_0^{\pi}[(n_1 - n_3) - i(n_2 - n_4)](\sin\varkappa\theta + d_k^*\cos\varkappa\theta)^2\,d\theta, \qquad (46)$$

where n_1, n_2, n_3, and n_4 is the value of $n(\theta)$ in the first, second, etc. sectors. From the expansion (43) we readily obtain

$$(n_1 + n_2 + n_3 + n_4) = 4\sum_{j=1}^{\infty} a_{4j}\cos(4j\theta + \alpha_{4j})$$

$$(n_1 - n_3) - i(n_2 - n_4) = 2\sum_{j=0}^{\infty} a_{2j+1}e^{i[(-1)^j((2j+1)\theta + \alpha_{2j+1})]}. \qquad (47)$$

Thus, the quantity Ψ_2 is connected with the odd harmonics of $n_k(\theta)$, while the quantity Ψ_1 depends on the values of the harmonics that are multiples of four.

Let us first investigate the effect of the oscillations of the term Ψ_1 on the amplitude. We note that its action is not connected with

the existence of the resonance under consideration, and does not depend directly on n_0. Calculation by means of Formulas (46) and (47) yields (when $a_0 = 0$)

$$\Psi_1 = \frac{\rho}{2\sin\pi\nu_{z0}} \sum_{j=1}^{\infty} \frac{a_{2j}\cos\varepsilon_{2j}}{(2j)^2 - \nu^2}. \qquad (48)$$

In this case the solution (45) is equal to

$$D_k = D_0 e^{i\int_0^k \Psi_1 dk}. \qquad (49)$$

Inasmuch as Ψ_1 is a real quantity, the amplitude of D_k remains constant. The phase of D_k changes monotonically. Thus, Ψ_1 can be regarded as a correction to the frequency of the free oscillations, brought about by the azimuthal variation of the magnetic field index.

Substituting (47) in (46), let us calculate Ψ_2 for the resonant value n_0. The derivations will be carried out for all the terms, except the one corresponding to the first harmonic, with accuracy to p^2. The influence of the first harmonic will be determined accurate to p. After cumbersome but straightforward calculations we obtain

$$\Psi_2 = p \sum_{j=0}^{\infty} \frac{a_{2j+1} e^{\pm i\varepsilon_{2j+1}}}{(2j+1)^2 - 4\nu^2} \left[1 - \frac{2\nu}{2j+1} + i\frac{2j-1}{\nu} - p\right]. \qquad (50)$$

As indicated in the preceding chapter, an appreciable fraction of the azimuthal asymmetry is brought about by the difference between the levels of the magnetic field in the sectors of the magnet. Using the notation introduced there (see Fig. 27) we write, in accord with (42) and (47):

$$n_0(0) = (n_0 - 2)\, h_0 = (n_0 - 2)\, \Delta_0 H;$$

$$\Psi_1 = (n_0 - 2)\left[\frac{\rho_0 (c^2 - s^2)}{2\nu^2 \sin\mu} - \frac{\pi (s + \rho c)}{4\nu \sin\mu}\right] \Delta H_{sp}; \qquad (51)$$

$$\Psi_2 = \frac{(1-i)(n_0-2)}{16(1-n_0)} [1 - p(1-\pi\nu) - p^2] [(\Delta_1 H - \Delta_3 H) - i(\Delta_2 H - \Delta_4 H)].$$

Let us proceed to a study of the resonance and let us put $\Psi_1 = 0$.

We shall henceforth be interested principally in the change of the amplitude of the free oscillations. We therefore write the equation for $|D_k|$, defined by the formula:

$$D_k = |D_k| e^{i\gamma_k}.$$

In place of (45) we obtain (accurate to the first power of $\Delta\gamma_k$) the two equations:

$$\begin{aligned} |D_{k+1}| - |D_k| &= |\Psi_2||D_{k+1}|\cos(\psi_2 - 2\gamma_k + \psi_2); \\ \Delta\gamma_k &= -|\Psi_2|\sin(\psi_2 - 2\gamma_k + \psi_2), \end{aligned} \qquad (52)$$

where ψ_2 is the phase of Ψ_2.

We first integrate the first equation in (52):

$$\begin{aligned} |D_k| &= D_0 e^{\int_0^k |\Psi_2|\cos u\, dk}; \\ u &= \psi_2 - 2\gamma_k + \psi_2. \end{aligned} \qquad (53)$$

The integral contained in (53) can be taken by the method of steepest descent, assuming the phase γ_k to be constant. Indeed, the saddle points for the two equations will be the same. Consequently, $\Delta^2\gamma_k$ is equal to zero at the saddle point. Therefore

$$u'' = \psi_2'' + \psi_2'' = -2\mu' + \psi_2''.$$

The prime denotes here differentiation with respect to $\underline{k}$. We can neglect the quantity ψ''_2, since it is of the next (higher) order of smallness compared with μ'. The position of the saddle point is determined from the condition

$$u' = \psi' - 2\Delta\gamma_k + \psi_2' = -\left(2\mu - \frac{\pi}{2}\right) - 2\Delta\gamma_k + \psi_2' = 0.$$

The shift of the saddle point from the resonance point $2\mu - \pi/2 = 0$ is usually not very considerable, and we shall neglect it henceforth. This introduces, of course, an uncertainty in our calculations. For the cases of practical interest, however, the initial amplitude of the oscillations in the proton synchrotron of the USSR Academy of Sciences is sufficiently large compared with the additional amplitude due to the

resonance. We can therefore solve Eq. (46) in practice rather simply by successive approximations, taking as the zero-th approximation the initial value of D_{κ}. At any rate, the method which we are using yields perfectly satisfactory results for our case. In addition, as we have already noted, it is not difficult to carry out a numerical summation of (46) which, as shown by experiment, consumes only a few hours per trajectory.

After passing through resonance, the integral in (53) is equal to

$$\int_0^k |\Psi_s| \cos u dk = |\Psi_s^{res}| \sqrt{\frac{\pi}{\mu'}} \sin\left(\frac{\pi}{4} - u_0\right), \qquad (54)$$

$$|\mu'| = \frac{\pi \Delta n}{2}\left[1 + 2b - \frac{3\pi}{8} b^2\right], \quad b = \frac{l}{\pi R},$$

where u_0 is the value of the phase u at the saddle point and Δn is the change in n_0 during one revolution of the particle.

As can be seen from (50) and (51), the correction introduced by the linear sections will not play an appreciable role, if the first harmonic is not one order of magnitude smaller than the third, fifth, etc. harmonics. A more important circumstance is that the presence of the linear sections shifts the resonant value of n_0.

As it executes radial-phase oscillations, the particle may pass through the resonant region many times, and the point of maximum deviation of the frequency can lie in the resonant region. In this latter case Expression (54) is not valid, for $\mu' = 0$ at the point of maximum deviation. Courant [44] proposed to use as the stationary phase the phase at this point (which we designate by the number 2 to distinguish it from point 1, where resonance takes place).

We shall essentially follow Courant from now on, with one exception: in place of the Bessel function we shall use the Airy functions [50]. This enables us to simplify noticeably the final formulas and combine three cumbersome expressions into a single simple one.

At the point 2 the derivative is $u'' \cong 2\mu' = 0$. Therefore

$$u = u_0 + u'(k-k_2) + \frac{'u'''(k-k_2)^3}{6} + \dots; \qquad (55)$$

$$\lim \int_0^{\Delta k} \cos u\, dk = \frac{2^{1/6}\sqrt{\pi}}{(u''')^{1/3}} v\left(\frac{2^{1/3}u'}{(u''')^{1/3}}\right) \cos u_0,$$

where v(x) is the Airy function (in the notation of V.A. Fok [50]);

$$u' = -\pi(1+2b)\Delta B\left(\frac{\partial n_0}{\partial r}\right)_1, \qquad (56)$$

$$u''' = -\frac{\pi(1+b)A\Omega_r^2}{2v_2}\left(\frac{\partial n_0}{\partial r}\right)_2,$$

where ΔB is the distance from the point at which $n_0 = 0.79$ to the point of maximum deviation of the particle which executes radial-phase oscillations with amplitude A and with frequency

$$\Omega_r = \frac{\pi}{2}\frac{\omega_1}{\omega_0} = \frac{\pi}{2}\sqrt{\frac{e|e|KF\sin\varphi_0}{2\pi E}}. \qquad (57)$$

It can be shown that at sufficiently large ΔB Formula (55) goes over into (54) with accuracy to within the difference $\sqrt{\pi} - 2^{3/4}$.

§6. Significance of Resonances of Fast Oscillations to the Operation of the Accelerator

The role and the significance of the resonance at $n = 0.79$ is essentially different from the role and significance of the resonance at $n = 0.84$.

Let us consider two stages of accelerator operation: the injection process and the acceleration process. The resonance at $n_0 = 0.84$ is harmful and dangerous only during the period of injection, for during the time of acceleration the radial oscillations rapidly decrease and move the particle away from the resonant region.

The resonance at $n = 0.79$ is not dangerous during the time of injection. To the contrary, in some cases it may prove useful. Indeed, as can be seen from (53), (54), and (55), depending on the value of the phase the amplitudes of the oscillations can both increase and decrease. The particles in which the amplitude decreases can become ef-

fectively captured in the acceleration mode. Barden [51] considered a similar case of injection in the betatron. He assumed the index n to be independent of the radius and close to its resonant value. His variable was the azimuthal asymmetry.* However, Barden's case is far from reality in either the betatron or in particular in the heavy-particle accelerator. Apparently, our case is of great significance for all types of cyclic accelerators, when the injection is from a region where n is close to unity. The influence of the investigated resonance on the injection in a betatron was considered in detail in a paper by A.B. Kuznetsov [52].

Let us apply our formulas to the 10-Bev proton synchrotron of the USSR Academy of Sciences. Let $\Delta n = 0.02$; $h_1 = h_3 = h_0$; $h_2 = h_4 = -h_0$. Then Eq. (53) assumes with the aid of (54) the following form

$$D_k = D_0 e^{|\kappa h_0| \cos \varphi_0} \qquad (58)$$

Since in this case h_0 does not exceed 0.003, the increase during the time of passage through resonance is not more than 5% of D_k. This quantity is on the order of the pitch of the turning orbit during the time of injection. At the start of acceleration the amplitude of the radial oscillations attenuates over the period of the phase oscillations by the same amount. Thus, if $\Delta n = 0.02$ or more, the resonance under consideration hardly influences the injection process.

The resonance plays an entirely different role during the acceleration period. If the amplitude of the radial-phase oscillations is so large that the instantaneous orbit falls into the resonant region, then oscillations can build up gradually owing to the multiple passage through resonance. In order for such a buildup not to occur, it is necessary that the amplitude of the oscillations be attenuated by the increase in the magnetic field during the period of the phase oscillations more than it increases as a result of resonance.

Let us consider an example. Let $\Delta B = 0$; $eV_0 = 6$ kev; $W_1 = 10$ Mev; $R(\partial n_0/\partial R) = 100$; $A/R_0 = 0.02$. Then

$$D_k = D_0 e^{\cdots \cos u}. \qquad (59)$$

The exponents turn out to be approximately twice as large as in (57). This is understandable, for in our example the radial velocity changes direction at the resonance point. The orbit of the particle is therefore in the resonance region for a relatively long time. However, if $\Delta B/R_0 \cong 0.001$, i.e., $\Delta B \cong 3$ cm, then the exponent in (58) decreases by 16 times. Thus, the resonance at $n_0 = 0.79$ is quite peaked. Of course, the sharpness of the resonance (and to a smaller degree its magnitude) depends on the value of $R(\partial n_0/\partial R)$.

We see from the foregoing analysis that in the proton synchrotron of the USSR Academy of Sciences free radial oscillations of the particles can actually build up if the amplitude of the radial-phase oscillations is sufficiently large. But if the resonant value n_0 is sufficiently close to the edge of the magnet pole, then it is always possible to make the percentage of the lost particles negligibly small. Indeed, as shown in Chapter 5, during the accelerating mode the particles captured are essentially those with small amplitudes of the radial-phase oscillations. Moreover, we shall show that the optimal injection mode occurs at $V_0 = 4$-6 kev, when the radial-phase oscillations occupy only one half the region between the average orbit and the injector. Therefore if the resonant value n_0 is located at a large distance, the effect under consideration will not play any role.

During the time of acceleration it is expected that the pole piece will become saturated and the points $n_0 = 0.79$ and $n_0 = 0.84$ will shift into the magnet. However, the attenuation of the radial-phase oscillations is much faster.

Thus, by taking suitable measures, it is possible to avoid the in-

fluence of these harmful resonances.

The influence of other possible resonances in the higher orders can be considered in analogous fashion. However, an analysis of all the possibilities shows that in the region from 0.55 to 0.75 there is no danger of resonances. Consequently, the technical specifications of the magnet stipulate specially that n_0 lie within these limits in an appreciable portion of the working region (140 out of 160 cm).

The correctness of our statement is confirmed also by the successful operation of betatrons and synchrotrons with n ranging from 0.6 to 0.75.

§7. Different Cases of Resonance with Slow Phase Oscillations

Resonances with slow phase oscillations are usually not considered in accelerator theory for the following reasons: a) the frequency of the phase oscillations is hundreds and thousands of times smaller than the frequency of revolution and the frequency of the fast free oscillations; b) the frequency of the phase oscillations changes sufficiently strongly during the acceleration process; c) the frequency of the phase oscillations is usually much larger than the commercial frequencies (the frequency of the magnetic field, etc.).

We shall now show that item "c" does not hold true in the proton synchrotron of the USSR Academy of Sciences. Indeed, owing to the large dimensions of the installation, all the frequencies, and particularly the cyclic frequency of the phase oscillations, are considerably reduced.

Figure 10 shows the variation of the frequency of the phase oscillations $f_1 = \omega_1/2\pi$ during the time of acceleration for a voltage $V_0 = 8000$ volts and a multiplicity $q = 1$.

The frequency f_1 changes from ~2000 to ~700 cps. If multiple resonance is used, then the frequency f_1 is increased by a factor $\sqrt{g}$.

The increase in V_0 also increases the frequency of the phase oscillations approximately as $\sqrt{V_0}$. The frequency f_1 is considerably influenced by the value of the index n (in the relativistic case $f_1 \sim 1/(\sqrt{1-n})$, and in the nonrelativistic case

$$f_1 \sim \sqrt{\frac{n-\left[\frac{L}{2\pi R+L}\right]}{1-n}}.$$

The magnet windings are fed from a 12-phase rectifier. Consequently, the magnetic field will contain a certain component with nominal frequency 600 cps, and also harmonics with frequencies 1200, 1800, 2400 cps, etc.

An estimate and the experience with the 180-Mev proton synchrotron have shown that the amplitude of these components is quite small (on the order of several hundredths of a gauss). But if the frequency of the phase oscillations is equal at some instant to one of the frequencies indicated above, then harmonic field components of small amplitude can play a considerable role.

The magnetic field can be written in the form

$$H(t)=H_0(t)+\sum_{j=1}^{\infty} h_j \sin(j\Omega t+\psi_j), \qquad (60)$$

where $\Omega = 2\pi$ 600 radian/sec, and H_0 a slowly varying function of the time.

Let us consider several possible cases.

1. The frequency of the accelerating field does not follow the high-frequency oscillations of the magnetic field. In the right half of the phase equation there appears an oscillating term, which we now calculate. If our magnetic field exceeds the theoretical value by ΔH, then the particle energy increases, for a specified revolution frequency, by an amount

$$\Delta E_1=\frac{E\Delta H}{H(1-n)K^2}. \qquad (61)$$

Substituting the value of ΔE in the first equation of (I, 17), we obtain

$$\frac{d}{dt}\left(\frac{E}{\omega_0^2 KF}\frac{d\varphi}{dt}\right)-\frac{eV_0\cos\varphi}{2\pi}=-\frac{eV^0\cos\varphi_0}{2\pi}+M_1;$$

$$M_1=-\frac{E}{\omega_0 H(1-n)KFH_0}\sum_{j=1}^{\infty}h_j j\Omega\cos(j\Omega t+\psi_j); \qquad (62)$$

$$\frac{d\Delta H}{dt}=\sum_{j=1}^{\infty}h_j j\Omega\cos(j\Omega t+\psi_j).$$

Here and henceforth we neglect the terms of the form $E\Delta H$; $\omega_0\Delta H$, etc., assuming them to be negligibly small.

2. Frequency of accelerating field changes so that the radius of the equilibrium orbit remains constant. In order to obtain the oscillating time in this case, it is sufficient to separate the oscillating part in the expression for cos φ_0. For this purpose, we substitute (61) in (I, 23) and obtain

$$M_1=\frac{2eK_0^2H_0}{c}(1-\delta)\frac{d\Delta H}{dt}. \qquad (63)$$

In addition to the cases considered above, other factors can also lead to resonance. For example, if the supply of the generator of the accelerating field is from a rectifier, then the amplitude may oscillate for the same reasons as the magnetic field:

$$V_0'=V_0\left(1+\sum_{j=1}^{\infty}b_j\cos(j\Omega t+\psi_j)\right). \qquad (64)$$

The frequency control system may also cause the frequency of the accelerating field to oscillate:

$$\omega_0'=\omega_0+\sum_{j=1}^{\infty}c_j\sin(j\Omega t+\psi_j). \qquad (65)$$

We are considering a discrete spectrum only. (It is not difficult to consider also a continuous spectrum.) Let us calculate the coefficients M.

3. Amplitude oscillations. By direct substitution of (64) into

the phase equation we obtain:

$$M_3 = \frac{eV_0 \cos\varphi_0}{2\pi} \sum_{j=1}^{\infty} b_j \cos(j\Omega t + \psi_j). \qquad (66)$$

4. Frequency oscillations. If an amount $\Delta\omega$ is added to the frequency, then $\dot{\psi}$ increases by $\Delta\dot{\psi} = \Delta\omega$. Therefore the additional term in the phase equation is

$$M_4 = -\frac{d}{dt}\left(\frac{E}{\omega_0^2 KF}\Delta\omega\right) =$$

$$= -\frac{E}{\omega_0^2 KF} \sum_{j=1}^{\infty} C_j j\Omega \cos(j\Omega t + \psi_j). \qquad (67)$$

§8. Calculation of the Passage Through Resonance in the Linear Approximation

We make the following change of variables in the phase equation:

$$\varphi = \varphi_0 + \alpha \qquad (68)$$

and assume that φ_0 is a constant or slowly varying function of the time, while the deviation α is a small alternating quantity, the square of which can be neglected. As a result we obtain

$$\frac{d}{dt}(m_{\varphi\varphi}\dot{\alpha}) + k_{\varphi\varphi}\alpha = \sum_{j=1}^{\infty} A_j \cos(j\Omega t + \psi_j), \qquad (69)$$

where

$$m_{\varphi\varphi} = \frac{E}{\omega_0^2 KFq}, \quad k_{\varphi\varphi} = \frac{eV_0 \sin\varphi_0}{2\pi},$$

and the quantities A_j will have their own values for each of the four cases considered in §7. For example, in case (1) [see (62)] we have

$$A_j^{(1)} = -\frac{m_{\varphi\varphi} h_j j\Omega\omega_0}{H(1-n)\Pi_0} = -\frac{Eh_j \cdot j\Omega}{\omega_0 H(1-n)KF\Pi_0}. \qquad (70)$$

In cases (2), (3), and (4):

$$A_j^{(2)} = \frac{2eR_0^2\Pi_0}{e}(1-\delta)h_j \cdot j\Omega; \qquad (71)$$

$$A_j^{(3)} = \frac{eV_0}{2\pi}\cos\varphi_0 \cdot b_j; \quad A_j^{(4)} = -m_{\varphi\varphi} j c_j \Omega.$$

Let us assume that at the instant t_j the frequency of the phase

oscillations is $\omega_1 = \sqrt{k_{ef}/m_{ef}} = j\Omega$, then only the j-th term will be of significance in the entire sum in the right half of Eq. (69). We can therefore neglect all the other terms of the sum. The solution of the corresponding homogeneous equation (68) is known:

$$\alpha = \sqrt[4]{\frac{m_{nom}}{m_{\text{эф}}(t)}}\left[c_1 e^{i\int \omega_1 dt} + c_2 e^{-i\int \omega_1 dt}\right].$$

The particular solution of the complete equation (68) is determined by the well-known method of varying the constant. The increasing part of this solution is

$$\alpha = \frac{A_j e^{i\psi_1(t)}}{2im^{1/4}_{\text{эф}}(t)}\int_0^t \frac{e^{i[\psi_1(t)-\psi_1(t)]}}{m^{1/4}_{\text{эф}}(t)\dot{\psi}_1}dt, \qquad (72)$$

where

$$\psi_1 = \int_0^t \omega_1(\tau)\,d\tau; \quad \psi_2 = \int_0^t j\Omega d\tau.$$

The amplitude value of α after passage through resonance can be determined, as usual, by the method of steepest descent, and the character of the increase in the amplitude can be determined with the aid of the Fresnel integrals. As a result of simple calculations we obtain

$$\alpha_{max} = \left|\frac{\sqrt{\pi}\,A_j}{\sqrt{2|\dot{\omega}_1|}\,m_{\text{эф}}(t_j)\,\omega_1}\right|. \qquad (73)$$

Substituting in (73) the values of A_j from (70) and (71) we obtain an expression for α_{max} in the cases under consideration. Before we discuss the obtained result and give numerical examples, we call attention to two circumstances. First, if the frequency Ω is not constant, then Formula (73) will contain, obviously, in place of the quantity $|\dot{\omega}_1|$ the quantity $|\dot{\omega}_1 - \dot{\Omega}|$; second, the use of Formula (73) is permissible if α_{max} resulting from the numerical calculation is smaller than unity.

In the 10-Bev proton synchrotron $\dot{\omega}_1$ is a small quantity when $\beta \sim$ ~ 1, and when $\beta \sim 0$ the frequency ω_1 is practically constant. Therefore

even very small harmonic components of the magnetic field and of the frequency may exert during the time of resonance a very strong influence on the amplitude of the phase oscillations.

Let us give two numerical examples.

1. The resonances with frequency 600 and 1800 cps can be eliminated, if necessary, by varying V_0 during the time of operation of the machine. Therefore, let us consider resonance with frequency 1200 cps. The value of $\dot{\omega}_1$ depends essentially on the magnetic field index $\underline{n}$ and on the value of eV_0. This dependence is particularly strong, especially at low energies (up to 1 Bev):

$$\dot{\omega}_1 \approx -2\pi \cdot 600$$

for $\omega_1 = 2\pi \cdot 1200$; $n = 2/3$; $V_0 = 6000$ v; $H = 4000$ oersted. Substituting the values obtained in (73) we get

$$|\alpha^{(1)}_{max}| = 120h_2; \quad |\alpha^{(2)}_{max}| = 240h_2, \qquad (74)$$

where h_2 is in oersted. Thus, a value of h_2 on the order of 0.01 oersted can result in large phase oscillations. In this case h_2 is only 0.00025% of H, but $h_2 \cdot j\Omega$ amounts to about 2% of dH/dt.

From the foregoing example it is clear that even when $h_2 = 0.01$ oersted it is necessary to take into account the nonlinearity of the phase equation.

2. Six-phase rectification in the generator supply system leads to oscillations of V_0; the amplitude of this oscillation is 0.3% and the frequency is 300 cps. Higher harmonics of the fundamental frequency also appear. The amplitude α_{max} is in the worst case ($\omega_1 = 2\pi \cdot 600$; $\dot{\omega}_1 = 2\pi \cdot 100$)

$$\alpha_{max} = \left| \sqrt{\frac{\pi}{2}} \cdot b_j \cdot \operatorname{ctg} \varphi_0 \frac{\omega_1}{\sqrt{\dot{\omega}_1}} \right| = 100 b_j.$$

If b_j amounts to 0.5%, then $\alpha_{max} = 0.5$.

3. Let us consider the oscillations of the frequency of the ac-

celerating field. In this case

$$\alpha_{max} = \sqrt{\frac{\pi}{2}} \frac{\varphi_j}{\sqrt{\dot{\omega}_1}}.$$

If $\alpha_{max} = 1$, then $C_j = \sqrt{2\dot{\omega}_1/\pi} \approx 15 \sim 50$ cps.

Thus, small perturbations at resonant frequency can cause sufficiently large phase oscillations, which again leads to the need for taking into account the nonlinearity of the problem, which turns out to be quite appreciable.

§9. Calculation of Passage Through Resonance with Account of the Nonlinearity of the Oscillations

We are not in position at present to solve the nonlinear problem completely. However, the existing methods, and primarily the averaging method, enable us to solve the problem by assuming the nonlinearity to be small. This essentially makes the results of the preceding section more accurate, since the rate of passage through resonance is small and therefore even a small nonlinearity changes the results appreciably. Indeed, in the linear approximation, when $\dot{\omega}_1 \to 0$, the amplitude of the forced oscillations tends to infinity for all values of A_j [as can be seen from (73)]. At the same time, when the nonlinearity is small and the values of A_j small, the amplitude of the phase oscillations remains finite in the case of interest to us even when $\dot{\omega}_1 \approx 0$.

The physical reason for this phenomenon has been explained long ago [53]. When the amplitude of the phase oscillations increases, the frequency of the oscillations decreases, so that the particle goes out of resonance.

In the proton synchrotron of the USSR Academy of Sciences the frequency ω_1 of the small phase oscillations decreases very slowly during the course of acceleration. However, during the passage through the resonance the amplitude of the phase oscillations increases, which rapidly brings the system out of resonance. N.M. Krylov and N.N. Bogol-

yubov [53] called such systems actively nonlinear, to distinguish them from passively nonlinear systems, which do not limit the amplitude in the absence of damping.

We shall show that the direction of passage through resonance is very important here. If the time and amplitude dependence of the frequency of the phase oscillations act in one direction (i.e., $(\partial\omega_1/dt)(\partial\omega_1/\partial\alpha_{max}) > 0$), then the nonlinearity itself assumes the role of "effective friction." This is precisely the case during the entire time of acceleration in accelerators. The account of the small nonlinearity enables us to obtain not only a qualitative but also a quantitative result. This method, however, does not enable us to consider the passage of the particle through the separatrix on the phase plane. The latter question can be treated only qualitatively.

For the calculation we used the work of Yu.A. Mitropol'skiy [34], who developed and mathematically justified the use of the averaging method for systems with slowly varying coefficients.

We introduce in the phase equation (62) the dimensionless time

$$\tau = \int_0^t \omega_1 dt, \qquad (75)$$

where ω_1 is the frequency of the small phase oscillations [see (69)], and carry out expansion in powers of α [see (68)]. As a result we obtain

$$\alpha'' + \alpha = -\varepsilon\left(\frac{\alpha^2}{2}\operatorname{ctg}\varphi_0 - \frac{\alpha^3}{6} - D\sin\eta\right) + \varepsilon^2\left[\frac{\alpha^4}{24}\operatorname{ctg}\varphi_0 - \frac{\alpha^5}{120} - \delta\alpha'\right], \qquad (76)$$

where ε is a smallness parameter, which in the final answer must be set equal to unity, while the prime denotes differentiation with respect to τ and

$$\delta = \frac{d\ln\omega_1 m_{\text{эф}}}{d\tau}; \quad D = \frac{A_1 2\pi}{eV_0\sin\varphi_0}; \quad \frac{d\tau_1}{d\tau} = \frac{f\Omega}{\omega_1}; \qquad (77)$$
$$\frac{d\eta}{d\tau} = \xi = \xi_0 + \varepsilon\xi_1\tau.$$

Let us estimate the dimensionless quantities contained in (77), for the parameters used in (74):

$$\delta = 0{,}7 \cdot 10^{-4}; \quad D = \sqrt{\frac{2}{\pi}}\, a^{(max)}_{max} \frac{\sqrt{\omega_1}}{\omega} \approx h_j; \qquad \xi_1 = \delta = 0{,}7 \cdot 10^{-4}, \tag{78}$$

where h_j is expressed in oersteds. Thus, D is on the order of several hundredths or less.

We seek the solution of (76) in the form [34]:

$$\begin{gathered} a = a\cos\gamma + \varepsilon u_1(\varepsilon\tau;\ a;\ \eta;\ \gamma) + \varepsilon^2 u_2 + \ldots; \\ \gamma = \eta + \psi; \\ \frac{da}{d\tau} = \varepsilon a_1(\varepsilon\tau;\ a;\ \psi) + \varepsilon^2 a_2 + \ldots; \quad \frac{d\psi}{d\tau} = 1 - \xi + \varepsilon b_1(\tau;\ a;\ \psi) + \varepsilon^2 b_2 + \ldots. \end{gathered} \tag{79}$$

Substituting (79) in (76) we obtain the equations in the first and second approximation for u_1 and u_2. The left halves of these equations will contain expressions $u''_1 + u_1$ or $u''_2 + u_2$. From the right half it is necessary to eliminate the terms with cos γ and sin γ in order that the solution contain no secular terms. Equating the coefficients of cos γ and sin γ to zero, we obtain the equations for the determination of a_1, a_2, b_1, and b_2.

In place of the procedure indicated above, which is well known in oscillation theory [53], we can multiply the initial equation (76) first by cos γ and then by sin γ, and integrate within the limits from 0 to 2π with account of (79).

Both methods yield the following first-approximation equation

$$\begin{aligned} (1-\xi)\frac{\partial a_1}{\partial\psi} - 2ab_1 &= \frac{a^3}{8} - D\sin\psi; \\ (1-\xi)\,a\frac{\partial b_1}{\partial\psi} + 2a_1 &= -D\cos\psi. \end{aligned} \tag{80}$$

Solving (80), we obtain

$$\begin{aligned} a_1 &= -\frac{D\cos\psi}{1+\xi}; \quad b_1 = -\frac{a^2}{16} + \frac{D}{a}\sin\psi; \\ u_1 &= -\frac{a^2}{4}\left(1 - \frac{1}{3}\cos 2\gamma\right)\operatorname{ctg}\varphi_0 - \frac{a^3}{192}\cos 3\gamma. \end{aligned} \tag{81}$$

We analogously find the second-approximation equation

$$(1-\xi)\frac{\partial a_2}{\partial\psi}-2ab_2=-\frac{Da^2\sin\psi}{16(1+\xi)}-\frac{D\cos\psi}{1+\xi}\frac{d\xi}{d\tau}+\frac{5a^3}{24}\operatorname{ctg}^2\varphi_0-\frac{a^3}{512};$$
$$(1-\xi)a\frac{\partial b_2}{\partial\psi}+2a_2=\frac{D\sin\psi}{1+\xi}\frac{d\xi}{d\tau}-\frac{3a^2D\cos\psi}{16(1+\xi)}-\delta. \qquad (82)$$

Solving the equations in (82), we obtain

$$a_2=\frac{D\sin\psi}{(1+\xi)^2}\frac{d\xi}{d\tau}-\frac{Da^2\cos\psi(7-\xi)}{16(1+\xi)^2(3-\xi)};$$
$$b_2=\frac{D\cos\psi}{a(1+\xi)^2}\frac{d\xi}{d\tau}+\frac{Da\sin\psi(5-3\xi)}{16(1+\xi)^2(3-\xi)}-\frac{5a^2}{48}\operatorname{ctg}^2\varphi_0+\frac{a^4}{1024}. \qquad (83)$$

Finally, the sought equation has the form

$$a=a\cos(\eta+\psi)-\frac{a^2}{4}\left[1-\frac{1}{3}\cos 2(\eta+\psi)\right]\operatorname{ctg}\varphi_0-\frac{a^3}{192}\cos 3(\eta+\psi);$$
$$\frac{da}{d\tau}=-\frac{D\cos\psi}{1+\xi}\left[1+\frac{a^2(7-\xi)}{16(1+\xi)(3-\xi)}\right]-\frac{\delta a}{2}+\frac{D\sin\psi}{(1+\xi)^2}\frac{d\xi}{d\tau};$$
$$\frac{d\psi}{d\tau}=1-\xi-\frac{a^2}{16}\left(1+\frac{5}{3}\operatorname{ctg}^2\varphi_0\right)+\frac{a^4}{1024}+$$
$$+\frac{D\sin\psi}{(1+\xi)a}\left[1+\frac{a^2(5-3\xi)}{16(1+\xi)(3-\xi)}\right]+\frac{D\cos\psi}{a(1+\xi)^2}\frac{d\xi}{d\tau}. \qquad (84)$$

We first find the stationary solution, equating the right halves of (84) to zero. Eliminating ψ, we find the algebraic equations relating a with ξ. Figures 35-37 show the results of the numerical solution of this equation. In the interval of the values of a, D, δ, and $d\xi/d\tau$ of interest to us, the terms containing a^4, δ, and $d\xi/d\tau$ do not play any role (as shown by numerical analysis), nor do the second terms in the square brackets of (84). Therefore, for an analytical investigation it is sufficient to use the simplified third-degree algebraic equation (although the numerical calculation can be carried out also with the complete equation):

$$a^3-\frac{16(1-\xi)a}{1+\frac{5}{3}\operatorname{ctg}^2\varphi_0}\mp\frac{16D}{(1+\xi)\left(1+\frac{5}{3}\operatorname{ctg}^2\varphi_0\right)}=0, \qquad (85)$$

where the minus sign corresponds to the stationary phase at $\psi=+\pi/2$ and the plus sign to the stationary phase $\psi=-\pi/2$.

Equation (85) will have three different real roots, if

$$-\frac{16(1-\xi)^3(1+\xi)^2}{D^2\left(1+\frac{5}{3}\operatorname{ctg}^2\varphi_0\right)}<-6{,}75. \qquad (86)$$

If the inequality sign is replaced in (86) by an equal sign, we obtain the condition for the existence of one multiple and one simple real root. If Inequality (86) is not satisfied, then only one real root exists.

For what follows we need to know the value of the multiple and simple roots when the inequality sign in (86) is replaced by the equal sign:

$$|a_{mp}| = \frac{16D^{1/2}}{\left(1+\frac{5}{3}\operatorname{ctg}^2\varphi_0\right)^{1/4}}; \quad |a_{sp}| = 2|a_{mp}|. \qquad (87)$$

Formula (87) has been derived accurate to 1%.

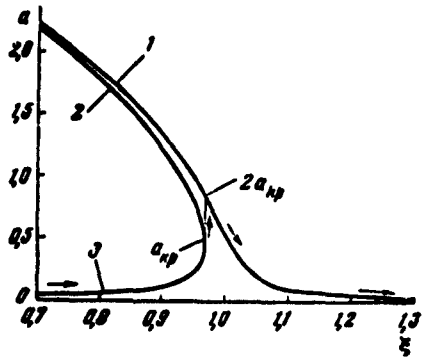

Fig. 35. Stationary resonance curves. The dependence of the amplitude of the phase oscillations a on the ratio ξ of the frequency of the external action to the frequency of the small phase oscillations for D = 0.02 and cos φ_0 = 0. 1) Upper stable branch; 2) upper unstable branch; 3) lower stable branch.

The investigation of the stability of the stationary solution leads to the following results. The upper branch of the curve, corresponding to the stationary phase $\psi = +\pi/2$, is stable. Of the two lower branches, corresponding to the stationary phase $-\pi/2$, one is stable and the other not. The boundary between these regions is $a = a_{kr}$ [see (87)].

Inasmuch as the quantity $\xi = j\Omega/\omega_1$ increases in the proton synchrotron of the USSR Academy of Sciences, the representative point moves over the lowest left curve up to the stability region a_{kr} (see Figs. 35-37). At this point the amplitude increases rapidly (it approximately doubles), and then decreases. We note that the maximum amplitude will occur at $\xi < 1$, i.e., resonance sets in before the frequencies of the small phase and forcing oscillations are equalized.

Inasmuch as the frequency of the small phase oscillations in the

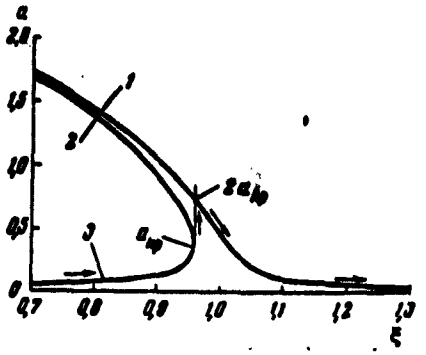

Fig. 36. The same as in Fig. 35, but for D = 0.02 and cos φ_0 = 0.5..

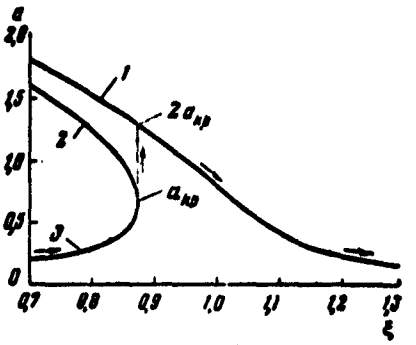

Fig. 37. The same as in Fig. 35, but for D = 0.1 and cos φ_0 = 0.5.

proton synchrotron of the USSR Academy of Sciences changes very slowly, the true resonance curve will be close to the stationary curve. Unfortunately, knowledge of the resonance curve is still not sufficient to judge the motion of the particles with different initial conditions. Only after a very strong perturbation, following the passage through resonance, are the amplitudes of the oscillations of almost all particles equalized. It must be borne in mind that on going over to the unstable branch, damped oscillations with amplitude ~a_{kr} are produced on the stable branch about the new equilibrium position. The amplitude of the oscillations is on the order of one half or two thirds of the distance between the stability limit and the upper stable branch of the curve. The exact form of the curve can be obtained only as a result of numerical integration of (84) for D = 0.04 and δ = 0.0001.

The initial conditions were chosen in such a manner, as to make the amplitude of the oscillations equal to zero away from resonance. Thus, the continuous curve shown in Fig. 38 is the true resonance curve. The dashed curve is obtained for the case when the amplitude of the phase oscillations away from resonance is ~0.2.

We note that were the represented points to be located on the upper curve, then the amplitude would not increase in resonance, but

would decrease monotonically. Such a case can occur for sufficiently large oscillation amplitudes. However, in order for it actually to be realized, it is necessary that the phase of the initial oscillations be equal to $+\pi/2$.

The maximum amplitude in the stationary case is equal to $2a_{kr}$ [see (87)]. In our case the maximum amplitude is somewhat larger (by 25-30%). This is seen in Fig. 38, obtained as a result of numerical integration of (84). We express $2a_{kr}$ in terms of the amplitude $\alpha_{max}^{(lin)}$, calculated in the preceding section, in order to show the extent to which an account of the nonlinearity changes the final result. With the aid of (73), (77), and (87), we obtain:

$$2a_{kp} = \frac{3,2}{\left(1+\frac{5}{3}\operatorname{ctg}^2\varphi_0\right)^{1/5}}\left(\frac{\dot{\omega}_1}{\omega_1^2}\right)^{1/5}\left(\alpha_{max}^{(max)}\right)^{1/5}. \qquad (88)$$

Let us consider an example corresponding to (74) and ctg $\varphi_0 = 0.6$: $2a_{kr} = 0.55(\alpha_{max}^{(lin)})^{1/3}$. Thus, whereas in the linear theory $\alpha_{max}^{(lin)} = 1$, in the nonlinear theory $2a_{kr} = 0.55$. If $\alpha_{max}^{(lin)} = 2$, then $2a_{kr} = 0.69$. We see that the amplitude of the nonlinear oscillations changes within narrower limits.

Thus, the final theoretical formulas for the four cases considered in the end of §7 are:

$$1)\ 2a_{kp} = \frac{3,2}{\left(1+\frac{5}{3}\operatorname{ctg}^2\varphi_0\right)^{1/5}}\left[\frac{k_f\cdot\omega_0}{H(1-n)\omega_1\Pi_0}\right]^{1/5}; \qquad (89)$$

$$2)\ 2a_{kp} = \frac{3,2}{\left(1+\frac{5}{3}\operatorname{ctg}^2\varphi_0\right)^{1/5}}\left[\frac{4\pi R_0^2\Pi_0 k_f\cdot\omega_1}{eV_0\sin\varphi_0}\right]^{1/5}; \qquad (90)$$

$$3)\ 2a_{kp} = \frac{3,2}{\left(1+\frac{5}{3}\operatorname{ctg}^2\varphi_0\right)^{1/5}}(b_f\operatorname{ctg}\varphi_0)^{1/5}; \qquad (91)$$

$$4)\ 2a_{kp} = \frac{3,2}{\left(1+\frac{5}{3}\operatorname{ctg}^2\varphi_0\right)^{1/5}}\left(\frac{C_f}{\omega_1}\right)^{1/5}. \qquad (92)$$

Thus, an examination of the nonlinear case enables us to relax greatly the requirements concerning the size of the field harmonics,

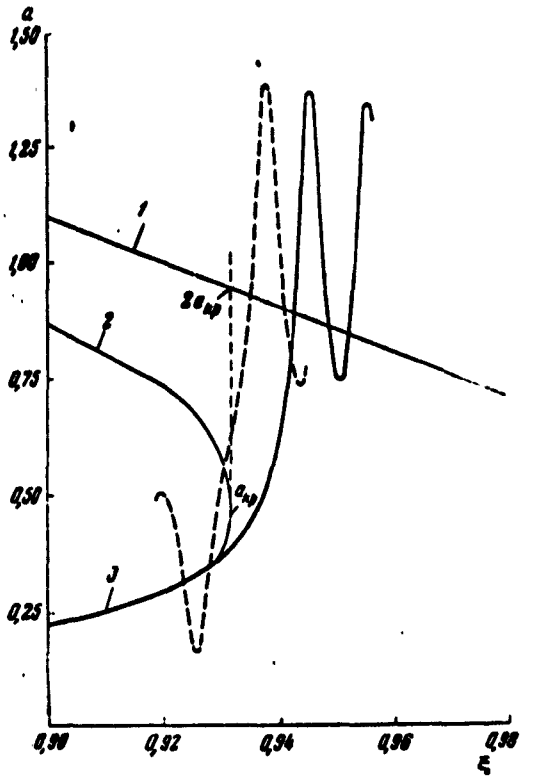

Fig. 38. Dynamic resonance curve obtained from numerical calculations ($D = 0.04$; $\cos \varphi_0 = 0.5$; $\delta = 10^{-4}$). The dashed curve shows the change in the amplitude of the oscillations at initial amplitude $a_{nach} = 0.2$: 1) upper stable branch; 2) unstable branch; 3) lower stable branch.

the frequency of the accelerating field, etc. The major accomplishment of the theory is the possibility of obtaining analytic formulas for the nonlinear oscillations.

Manuscript Page No.

[Footnotes]

119 This was also pointed out in the paper of Blachman and Courant [38].

143 In Barden's calculations, the azimuthal asymmetry was assumed constant. Its variability was taken into consideration in the discussion of the results.

Manu-
script
Page
No.

[List of Transliterated Symbols]

125	ср = sr = sredniy = average
148	эф = ef = effektivnyy = effective
149	нач = nach = nachal'nyy = initial
153	лин = lin = lineynyy = linear
155	кр = kr = kriticheskiy = critical
155	пр = pr = promezhutok = section

Chapter 5

INJECTION THEORY

§1. Introduction

The effectiveness of the injection method determines the intensity of the beam of accelerated particles, since the main particle losses occur during the injection. At the same time, a theoretical analysis of this problem is exceedingly difficult. It is sufficient to state that in spite of the numerous attempts we still have no satisfactory injection theory for the electron accelerators, betatrons, and synchrotrons with betatron triggering. This is connected with the fact that in betatrons and synchrotrons the injection efficiency is determined by the interaction of the particles with one another. In addition, an important role is played by the space charge, secondary-electron emission, etc. From among the large number of particles, only an insignificant fraction enters the acceleration mode. However, the short lifetime of the main mass of the "lost particles" exerts a serious influence on the entire injection process.

The picture is entirely different in the 10-Bev proton synchrotron. The large volume of the chamber, the insignificant inlet proton current (500 microamperes), and the good collimation of the beam enable us to neglect the particle interaction and to stay within the framework of the one-body problem. Indeed, the Coulomb charge would start to play some significant role only if the proton current would increase by 10,000 times compared with the indicated value.

Thus, we have to solve the problem of the motion of a large num-

ber of particles in a specified magnetic control field and electric accelerating field.

Among the aggregate of initial conditions, we must find those that ensure resonant acceleration without collision with the injector and with the chamber walls.

The proton beam emerging from the injector will be assumed specified. An important independent problem is to calculate the motion of the particles from the injector-accelerator, which is 10-12 meters away from the chamber. This problem was solved by A.A. Kolomenskiy [26], and will not be discussed here.

Different variants of injection were developed by the author in 1949-1950. We present here only the final variant, chosen to trigger the 180- and 10,000-Mev installations.

Let us describe the injection method briefly. The particles are introduced from the linear accelerator with the aid of lenses, a turning magnet, and an electrostatic deflector (Fig. 39) into the working region of the magnet, where the magnetic field index is $n \leq 1$.

During the first stage of the injection the accelerating electric field is turned off. The instantaneous particle orbit is gradually pushed from the injector toward the central orbit. The radius of the instantaneous orbit is determined by the energy w_i of the injected particles and by the magnetic field H(R, t):

$$R = \frac{\sqrt{2w_i E_0}}{cH(R, t)}. \qquad (1)$$

Inasmuch as the injection energy is constant, R varies in proportion to 1/H(R, t). The change ΔR in the radius of the orbit during the time T of one particle revolution is

$$\Delta R = R \frac{H_i T}{(1-n) H_i}, \qquad (2)$$

where H_i, $\dot{H}_i$ are the magnetic field and its partial derivative with

respect to time at the instant of injection. At an injection energy 4 Mev we have $T = 7.5$ μsec, $H_1 = 104$ oersted, $\dot{H}_1 = 4000$ oersted/sec, $n = 2/3$, and $\Delta R = 2.4$ cm. The value of ΔR varies in inverse proportion to the injection energy. For example, at a 10-Mev energy $\Delta R = 1$ cm.

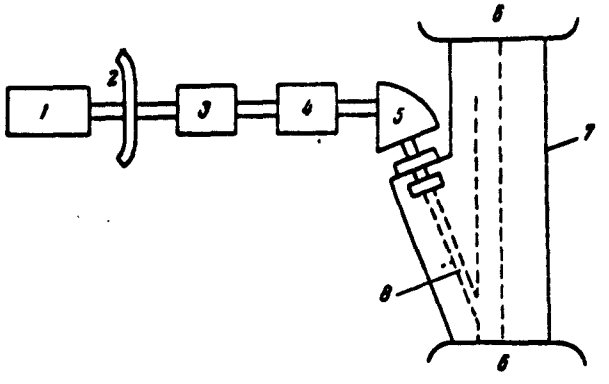

Fig. 39. Diagram for the injection of the particles into the accelerator: 1) linear accelerator; 2) shield; 3) dual magnetic corrector; 4) adjusting capacitor; 5) turning magnet; 6) sector; 7) chamber; 8) inflector.

At the present time, for several reasons connected essentially with the possibility of obtaining the theoretical magnetic field during the instant of injection, the chosen value of energy is $w_1 = 10$ Mev. The contraction of the orbit during one revolution can be regulated between 1 and 3 cm by short-duration forcing of the rate of change of the magnetic field.*

If we denote by ρ_1 the distance from the injector to the central orbit, then the first injection stage (without the accelerating electric field) continues for a time τ_1, where

$$\tau_1 \cong \frac{\rho_1}{\Delta R} T, \qquad \tau_1 = (1-n)\frac{\rho_1}{R_0}\frac{H_1}{\dot{H}_1}. \tag{3}$$

We shall henceforth call the quantity τ_1 the injection time. When $w_1 = 10$ Mev, $\rho_1 = 50$ cm, and $\Delta R = 1$ cm, the injection time is $\tau_1 = 240$ μsec.

After the instantaneous orbit has reached the position of the central orbit, the second injection stage begins: the admission of the particles into the accelerator chamber is stopped and the accelerating electric field is turned on. We shall assume that the second injection stage continues for one period of the phase oscillations (about 500 μsec).

The particles which did not collide during the first injection stage with either the wall or the injector will be called the particles "captured" during the first stage. The capture of the particles during the first stage depends on the angle of departure of the particles from the ejector, γ, the rate of constriction of the orbit, the value of ρ_1, the injector dimensions, the structure of the beam of injected particles, etc.

The particles captured during the first injection stage as a result of the constriction of the instantaneous orbit. Indeed, it can be readily shown that the effect of damping of the oscillations, which is proportional to $H^{-1/2}$, is negligibly small compared with the constriction of the orbit (approximately 50 times smaller).

The particle leaving the injector executes free radial and vertical oscillations about the instantaneous orbit, and the amplitude of the radial oscillations is always larger than or equal to the distance from the point of departure to the instantaneous orbit. The particle does not collide with the injector (with a probability close to unity) if after three to six revolutions the instantaneous orbit is displaced by an amount larger than the difference between the oscillation amplitude and the shortest distance from the injector to the instantaneous orbit, measured at the instant of departure of the particle from the injector.

In order for the particle not to collide with the chamber walls,

the amplitudes of the radial and vertical oscillations should be smaller than the distance from the orbit to the corresponding wall (for more accurate determinations see the next section).

At the second injection stage (called also the transient mode), slow radial-phase oscillations are added to the free oscillations. This raises again the question of collisions between the particles and the injector. It is obvious that the sum of the free and phase oscillations should be less than the distance from the equilibrium orbits to the injector. Moreover, for resonant acceleration in the proton synchrotron mode, the initial phase of the particle (φ_{nach}) and the phase velocity ($\dot{\varphi}_{nach}$) should satisfy certain conditions [see (I, 58)].

If the current from the injector is equal to I, then during the injection time τ_1 the number of protons entering the chamber is $I\tau_1/e$. The number of particles captured during the first stage is $Q_1 = I\tau_1\eta_\rho\eta_z/e$, where η_ρ is the probability that the particle will bypass the injector and the vertical walls of the chamber, and η_z is the probability that the particle will bypass the horizontal walls of the chamber. $\eta_1 = \eta_\rho\eta_z$ is the capture coefficient of the particles during the first stage of injection. In the second stage, some fraction $Q = Q_1\eta_2$ of the Q_1 particles will be captured, where η_2 is the coefficient of the transient mode. The product of both coefficients will be called the injection efficiency. Thus, the efficiency of the injection is equal to the ratio of the captured particles during the injection time to the number of particles admitted into the chamber:

$$\eta = \frac{eQ}{I\tau_1} = \eta_1\eta_2. \qquad (4)$$

Along with the quantity η_ρ we shall use the number of effective revolutions of the particles:

$$n_r = \eta_\rho \frac{\rho_i}{\Delta R} = \frac{eQ_1}{IT\tau_2}. \qquad (5)$$

The quantity η_T is equal to the ratio of the number of particles which do not strike the injector to the number of particles emitted during one period of revolution.

§2. Fundamental Assumptions Made During the Calculations

We are faced with the problem of calculating the injection efficiency, by solving the dynamic problem of the motion of many particles. The efficiency turns out to be quite sensitive to certain parameters of the installation (in particular, to the magnetic field index $\underline{n}$). In practice, however, it is impossible to obtain a definite value of $\underline{n}$ specified with high accuracy. In designing such a tremendous installation as the proton synchrotron of the USSR Academy of Sciences, we are unable to connect the injection method with the attainment of some high accuracy in the value of $\underline{n}$. In the fundamental part of the working region of the chamber, $\underline{n}$ will be within the limits from 0.6 to 0.7.

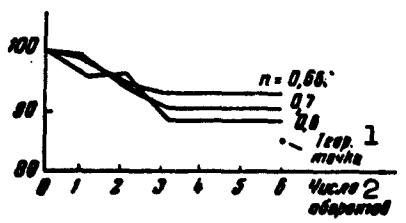

Fig. 40. Percentage of particles not striking the injector after the first six revolutions, for different values of the index $\underline{n}$. The injection energy is $W_i = 4$ Mev, the distance from the injector to the central orbit is $\rho_i = 50$ cm, and the maximum angle of deflection of the particles from the optimal direction is $\gamma_{max} = \pm 0.2^\circ$. The dot denotes the theoretical value obtained from the approximate formula. 1) Theoretical point; 2) number of revolutions.

For practical purposes it is quite essential to determine the dependence of the injection efficiency on the main parameters of the magnet: 1) the size of the magnet gap; 2) the deviation of the magnetic fields from the theoretical value; 3) the characteristics of the injector, namely a) the energy of the injected particles, b) the angular and energy scatter of the particles, and c) the geometry and location of the injector; 4) the characteristics of the high-frequency accelerating device, namely a) the effective accelerat-

ing voltage, b) the multiplicity, i.e., the ratio of the generator frequency to the particle revolution frequency; 5) the rate of change of the magnetic field (the forcing); 6) injection methods.

It turns out that the dependence of η on the foregoing characteristics can be determined with a high degree of accuracy. At the same time, the absolute value of the injection efficiency η needs to be known with an uncertainty amounting to a factor of 1.5-2. It is desirable further that the error result rather in an underestimate of η than in an overestimate.

Starting from the foregoing, we have made the following assumptions: 1) the damping of the free oscillations during the injection time and the damping of the radial-phase oscillations during the phase-oscillation time can be neglected; 2) the particle beam admitted into the chamber is homogeneous in density and in angular spread at any point; 3) the principal losses occur during the third and sixth revolutions after the particle leaves the injector. Were the injection to occur in a constant magnetic field, then 50% of the particles would be lost during the third revolution and the remaining 50% during the sixth revolution.

The first assumption, as indicated above, is easily justified: an account of the attenuation results in a correction amounting to 1-2%. The second assumption is not a principal one. Were we to have experimental data, they could readily be used. Preliminary experiments indicate that the deviations from homogeneity in the beam will not be large.

The most essential is the third assumption. In the installation of the USSR Academy of Sciences, the particles execute during the first injection stage only 20-50 revolutions, so that it is not difficult to determine by numerical calculation the particle loss due to

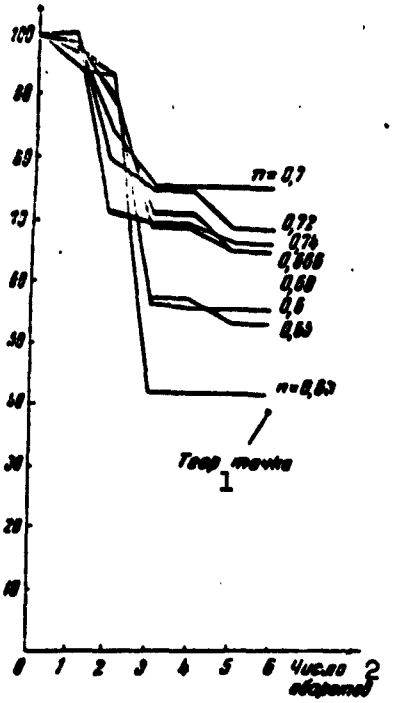

Fig. 41. The same as in Fig. 40, but for $W_1 = 10$ Mev and $\gamma_{max} = \pm 0.1^{\circ}$. 1) Theoretical point; 2) number of revolutions.

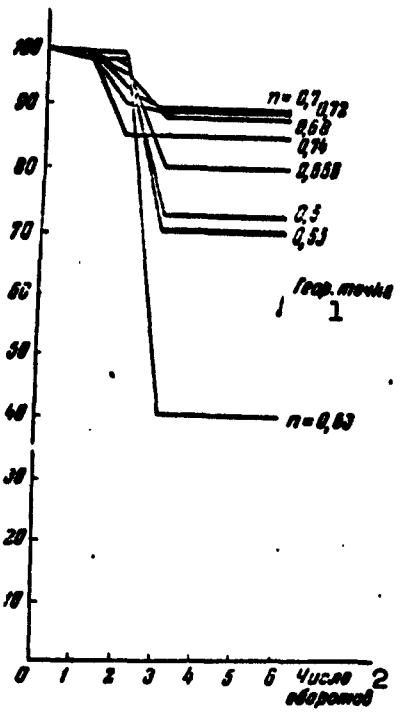

Fig. 42. The same as in Fig. 40, but for $W_1 = 10$ Mev. 1) Theoretical point; 2) number of revolutions.

collisions with the injector. Such calculations were actually carried out in the paper of A.I. Zaboyev [55]. The injection efficiency is a sharply oscillating function of n with many gaps. During the injection period, when the eddy currents and the remanent magnetization play an important role, it is impossible to maintain n constant with a high degree of accuracy. Consequently, the rapid oscillations have no physical meaning.

However, it is possible to obtain with the indicated degree of accuracy analytical formulas which make it possible to choose correctly the accelerator parameters.

Let us consider the following imaginary experiment. Let $n = 0.66 \pm \pm 0.06$ and the magnetic field be constant, and let protons be admitted

into the accelerator chamber. Then, as shown by numerical calculation, no particles are lost at all during the first revolution, from 0 to 20% are lost during the second revolution, and from 30 to 60% on the third revolution. After six revolutions the main bulk of the particles, up to 90%, will be lost, and the main losses occur during the fifth and sixth revolutions, while practically no particles are lost during the fourth revolution.

This picture can be made rougher. In the first approximation we can assume that all 100% of the particles are lost during the third revolution. The second more accurate approximation is the statement that 50% of the particles are lost during the third revolution and 50% during the sixth. If now the magnetic field is varied in time, then some of the particles will avoid collisions with the injector, and furthermore, if we assume our approximate assumption, then the losses will be produced only during the third and sixth revolutions.

Getting ahead of ourselves, we present the results of the numerical calculations in Figs. 40, 41, and 42. The ordinates in these figures are the percentages of the particles that do not collide with the injector after several revolutions, the number of which is laid off on the abscissa axis. The same figures show also the percentage of particles not colliding with the injector, calculated on the basis of the third assumption (the "theoretical point").

From these and many other calculations it is seen that our method gives a sufficient degree of accuracy in all the cases of interest to us.

§3. Capture of Particles During the First Injection Stage

In the first part of the calculation we shall take into account only collision with the injector and vertical walls of the chamber and calculate the value of η_ρ. We then introduce a correction η_z, taking

into account the particle loss due to the collisions with the horizontal walls of the chamber.

Assume that a particle beam with radial dimension 2Δ is admitted into the chamber of the accelerator. The beam subtends an angle $2\gamma_{max}$. The beam axis makes an angle ε with the optimal direction.

The angle of particle emission, relative to the optimal direction, will be denoted by γ. We introduce also symbols for the maximum and minimum angles:

$$\gamma_1 = \gamma_{max} + \varepsilon; \quad \gamma_2 = \gamma_{max} - \varepsilon.$$

These and other symbols are explained in Fig. 43.

In place of the angle γ, which is measured in radians, it is convenient to introduce an angle α, expressed in terms of other dimensionless units:

$$\alpha = \frac{R_0 f \gamma}{\rho_1 \sqrt{1-n}},$$

where the value of f is given in Fig. 21, while ρ_1 is the distance from the injector to the central orbit (see Fig. 43). We shall denote the angle α with the same indices as the angle γ:

$$\gamma_1 \to \alpha_1; \quad \gamma_2 \to \alpha_2; \quad \varepsilon \to \alpha_\varepsilon. \tag{6}$$

The amplitude of the radial oscillations is, in accord with (II, 41)

$$F_c = \sqrt{(u+y)^2 + \alpha^2}, \tag{7}$$

where $u = \rho_0/\rho_1$; $y = x/\rho_1$; F_c = oscillation amplitude$/\rho_1$. (8)

The meaning of $\rho_0 x$ is clear from Fig. 43.

The oscillation amplitude F_c exceeds the distance from the injector to the orbit by an amount

$$\Delta F = \sqrt{(u+y)^2 + \alpha^2} - u. \tag{9}$$

We assume that the collision with the injector occurs at the third and sixth revolutions. Consequently, in order to guarantee the

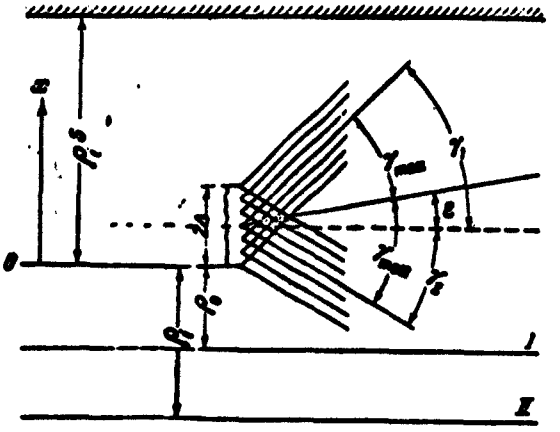

Fig. 43. Notation scheme used in the calculation of the injection efficiency. The hatching denotes the chamber wall, the wavy line the region between the injector plates, the dashed line the optimum beam direction, and the solid line the actual direction of the beam axis. I) Instantaneous orbit; II) average orbit; 0) origin of $\underline{x}$ coordinate.

absence of particle losses, we must stipulate the fulfillment of the following inequalities:

$$\Delta F < \frac{3\Delta R}{N}; \quad \Delta F < \frac{6\Delta R}{N}. \tag{10}$$

In order for the particles not to collide with the chamber walls, we satisfy the condition

$$\Delta F < S \frac{f(\sigma_1)}{f\left(\pi \frac{\pi}{4}\right)}. \tag{11}$$

If $s[f(\sigma_1)/f(\kappa\pi/4)] < 3\Delta R/\rho_1$, all particles which would be lost in the third revolution as a result of collisions with the injector, are actually lost during the first and second revolution, owing to collisions with the chamber walls. We therefore write for the third revolution in place of (10) and (11)

$$\Delta F < a_1, \tag{12}$$

where a_1 is the smaller of the two numbers $3\Delta R/\rho_1$ and $s[f(\sigma_1)/f(\kappa\pi/4)]$.

Analogously, for the sixth revolution we write

$$\Delta F < a_2, \qquad (13)$$

where a_2 is the smaller of the two numbers $6\Delta R/\rho_1$ and $s[f(\sigma_1)/f(\kappa\pi/4)]$.

As shown in Chapter 3, the deviation of the magnetic field from the theoretical value is taken into account in the following manner. First, the size of the magnet region employed is decreased by the amount of the azimuthal asymmetry. The quantity ρ_1 which is contained in our formulas is reduced in proportion to it. Second, the optimal direction for the emission of the particles is changed.

For example, in the 10-Bev proton synchrotron, the working region of the magnet will be 160 cm, of which 40 cm drops out as a result of the azimuthal asymmetry and 10-15 cm is lost because of inaccuracy in the initial frequency of the accelerating field. The value of s_{ρ_1} will be on the order of 10-15 cm. Consequently, the maximum value of ρ_1 does not exceed apparently 50 cm.

1. Parallel particle beam. Let us consider a parallel beam of particles, emitted at an angle α_ε to the optimal direction. The number of particles captured during a time dt from the points of the beam with coordinate x; x + dx is

$$dQ_*' = \frac{I}{e}\, dt\, \frac{dx}{2\Delta}.$$

In place of the time dt we introduce the amount of constriction of the instantaneous orbit $d\rho_0$:

$$dt = \frac{T}{\Delta R}\, d\rho_0,$$

where T is the time of revolution of the particle, and we change over to the dimensionless variables:

$$dQ_*' = 2A\, du\, dy, \qquad (14)$$

where

$$A = \frac{I\rho_1 T}{2e\,(\Delta R)\,\delta},$$

and $\bar{\delta} = 2 \cdot \Delta / \rho_1$ is the dimensionless width of the beam. Let us integrate (14) under the assumption that $\underline{a}$ can assume with equal probability the two values a_1 and a_2, and obtain

$$Q_0'' = A \sum_{i=1}^{2} \iint_{c_i} du\, dy, \tag{15}$$

where the integration regions c_1 and c_2 will be determined by the inequalities given below. The first two inequalities are obvious

$$0 < y < \bar{\delta}, \tag{16}$$

$$\sqrt{(u+y)^2 + a_i^2} - u < a_i. \tag{17}$$

The next inequality takes into account the fact that the instantaneous orbit is constricted only to the central orbit, and then the accelerating field is turned on. Therefore the oscillation amplitude F_c cannot exceed unity:

$$\sqrt{(u+y)^2 + a_i^2} < 1. \tag{18}$$

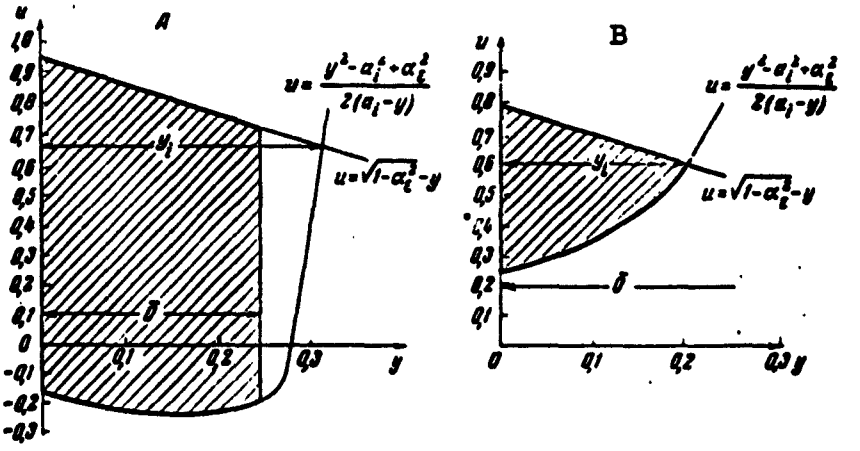

Fig. 44. Domains of integration (cross hatched) of the integrals (15) for two cases:

A) $u_i > \bar{v}$, $a_i < a_i$; B) $u_i < \bar{v}$, $a_i > a_i$

The lower boundary is in accord with Eq. (17); the upper boundary is in accord with Eq. (18); the right-hand boundary for case A is in accord with Eq. (16).

Figure 44 shows the domain of integration for two different cases.

It is seen from this figure that the maximum possible value of y is determined by the intersection of the boundaries of domains (17) and (18), and is equal to

$$y_i = a_i - 1 + \sqrt{1 - a_i^2}. \tag{19}$$

The actual width of the beam $\overline{0}$ can be either larger or smaller than y_1. We introduce the quantity $\overline{y}_1$, which is equal to the smaller of the two numbers $\overline{0}$ and y_1. If we integrate first with respect to u, then the limits of integration are

$$\frac{a_i^2 - a_i^2 + y^2}{2(a_i - y)} < u < \sqrt{1 - a_i^2} - y, \qquad 0 < y < \overline{y}_1. \tag{20}$$

After simple integration we obtain

$$Q_a^{\prime} = A \sum_{i=1}^{2} \left[\left(\sqrt{1 - a_i^2} + \frac{a_i}{2} - \frac{\overline{y}_i}{4} \right) \overline{y}_i + \frac{a_i^2}{2} \ln \frac{a_i - \overline{y}_i}{a_i} \right]. \tag{21}$$

Let us consider two particular cases. Let the beam width $\overline{0}$ be larger than y_1. Then

$$Q_a^{\prime} = \frac{I \rho_i T}{4 e \Delta H 0} \sum_{i=1}^{2} \left[1 + \frac{a_i^2}{2} - \frac{3}{2} a_i^2 - (1 - 2a_i) \sqrt{1 - a_i^2} + a_i^2 \ln \frac{1 - \sqrt{1 - a_i^2}}{a_i} \right]. \tag{22}$$

or approximately

$$Q_a^{\prime} \approx \frac{I \rho_i T}{2 e \Delta H 0} \sum_{i=1}^{2} a_i \left[1 + \frac{a_i}{4} - \frac{a_i^2}{2 a_i} \ln \frac{2 \bar{e} a_i}{a_i^2} \right], \tag{23}$$

where $\bar{e}$ is the base of the natural logarithms. From (22) we can readil obtain the maximum permissible angle $\alpha_\varepsilon = \alpha_{gi}$. It depends on the value of a_1:

$$a_{gi} = \sqrt{a_i (2 - a_i)} \sim \sqrt{2 a_i}. \tag{24}$$

In order for the number of captured particles to be large, it is necessary to have

$$a_i < \sqrt{2 a_i}. \tag{25}$$

Let us consider a second particular case. Let the width of the beam be smaller than y_1. This case is realized if

$$a_1 < \sqrt{\bar{a}_1(2-\bar{a}_1)} = a_{g1}, \qquad (26)$$

where

$$\bar{a}_i = a_i - \bar{\delta}. \qquad (27)$$

It is then necessary to substitute $\bar{\delta}$ in Eq. (21) in place of $\bar{y}_1$

$$Q''_u = \frac{I_{pi}T}{2e\Delta R}\sum_{i=1}^{2}\left[\sqrt{1-a_i^2} + \frac{a_i+\bar{a}_i}{4} + \frac{a_i^2}{\bar{\delta}}\ln\frac{\bar{a}_i}{a_i}\right]. \qquad (28)$$

The quantity η_p, introduced in §2, can be readily obtained from (22) and (28):

$$\eta''_p = \frac{Q''_u e\Delta R}{IT p_i}. \qquad (29)$$

2. Beam with angular scatter. In order to find the number of particles captured during the first injection stage, it is sufficient to multiply (21) by $d\alpha_\varepsilon/2\alpha_{max}$ and integrate from the minimum to the maximum angle $(-\alpha_2; +\alpha_1)$. Since only the square of the angle is contained in all the formulas we get

$$Q_u = \sum_{i=1}^{2}\int_0^{\alpha_i} Q''_u \frac{d\alpha}{2\alpha_{max}} \qquad (30)$$

(we leave out the indices of ε and α). Each integral in (30) breaks up into two parts: when $\alpha < \bar{\alpha}_{gi} = \sqrt{\bar{a}_i \cdot (2 - \bar{a}_i)}$ it is necessary to use Expression (28) for Q''_u, and if $\alpha > \bar{\alpha}_{gi}$ Expression (22) should be used.

If the angle α_k is larger than the maximum permissible angle α_{gi} (24), then the integration must be carried out to α_{gi}. If the angle α_k is smaller than α_{gi}, the integration is carried out to the angle α_k.

Taking into account the foregoing remarks, the integration is quite simple to carry out. To write down the final result in the most concise fashion, we introduce a function of the two independent variables:

$$\Phi(a, \alpha)=\frac{\alpha}{2}\left[1+\frac{a^2}{2}-\frac{11}{18}a^2-\frac{1-3a}{3}\sqrt{1-a^2}+\right.$$
$$\left.+\frac{a^2}{3}\ln\frac{1-\sqrt{1-a^2}}{a}\right]-\frac{1-\frac{3}{2}a}{3}\arcsin a, \qquad (31)$$

where

$$a=\begin{cases}a, & \text{if } a<\sqrt{\alpha(2-\alpha)};\\ \sqrt{\alpha(2-\alpha)}=\alpha_{gi}, & \text{if } a>\sqrt{\alpha(2-\alpha)}.\end{cases}$$

Let us investigate the behavior of the function Φ. If $a > \alpha_{gi}$ then

$$\Phi(a;\ \alpha)=\Phi(a;\ \sqrt{\alpha(2-\alpha)})=$$
$$=\frac{1}{3}\left[\sqrt{\alpha(2-\alpha)}\left(1+\frac{a^2}{6}+\frac{\alpha}{6}\right)-\left(1-\frac{3}{2}\alpha\right)\arcsin\sqrt{\alpha(2-\alpha)}\right]. \qquad (32)$$

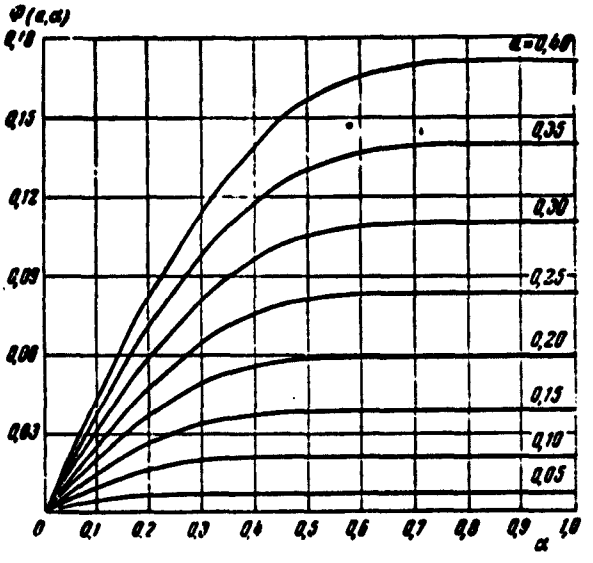

Fig. 45. Plot of the function $\Phi(a, \alpha)$ in accord with Formula (31) for the calculation of the number of particles captured during the first injection stage.

When $a \ll 1$ we have approximately

$$\Phi(a, \sqrt{\alpha(2-\alpha)})=\frac{4\sqrt{2}}{9}a^{3/2}\left(1+\frac{3}{20}a\right). \qquad (33)$$

The difference between the two values of the functions is

$$\Phi(a, a_1)-\Phi(\bar{a}, a_1)=\frac{a_1}{2}\left[(a-\bar{a})\sqrt{1-a_1^2}+(a-\bar{a})\arcsin a_1+\right.$$
$$\left.+\frac{a^2-\bar{a}^2}{2}+\frac{a_1^2}{3}\ln\frac{\bar{a}}{a}\right]. \qquad (34)$$

We can now write down an expression for the number of particles captured during the first stage, in general form:

$$Q_u = \frac{I_0 N T}{4 e \Delta R \bar{\delta} \alpha_{max}} \sum_{i=1}^{2} \sum_{k=1}^{2} [\Phi(a_i;\ \alpha_k) - \Phi(\bar{a}_i;\ \alpha_k)]. \tag{35}$$

Plots of the function $\Phi(a, \alpha)$ for different values of a are shown in Fig. 45, where the abscissas are the values of α.

Let us consider several particular cases.

1. Assume that we have a broad beam with large angular scatter. Then for $\bar{\delta} > a_1$ ($\alpha_k > \sqrt{a_1(2 - a_1)}$) we have

$$\eta_\varphi = \frac{1}{6\bar{\delta}\alpha_{max}} \sum_{i=1}^{2} \left[a_{\varphi i}\left(1 + \frac{a_i}{6} + \frac{a_i^2}{6}\right) - \left(1 - \frac{3}{2} a_i\right) \arcsin a_{\varphi i} \right], \tag{36}$$

$$\eta_\varphi \approx \frac{2\sqrt{2}}{9\bar{\delta}\alpha_{max}} \sum_{i=1}^{2} a_i^{3/2} \left(1 + \frac{3}{20} a_i\right), \tag{37}$$

when $a_1 \ll 1$.

From (37) it follows that the intensity increases in proportion to $\rho_1^{3/2}$; $(\Delta R)^{1/2}$, and $(N)^{3/2}$, where N is a parameter of the theory (the number of "effective revolutions" without colliding with the injector). Since the width of the beam and the angular scatter are large, the intensity is inversely proportional to the angle subtended $2\alpha_{max}$ and to the beam width $\bar{\delta}$.

2. If the width of the beam is $\bar{\delta} < a_1$ ($\alpha_k > \sqrt{a_1(2 - a_1)}$), then

$$\eta_\varphi \approx \frac{2\sqrt{2}}{9\alpha_{max}} \sum_{i=1}^{2} \left[\frac{a_i^{5/2} - (a_i - \bar{\delta})^{5/2}}{\bar{\delta}} \left(1 + \frac{3}{20} a_i\right) + \frac{3}{20} (a_i - \bar{\delta})^{5/2} \right]. \tag{38}$$

3. In the limit as $\bar{\delta} \to 0$ we obtain

$$\eta_\varphi = \frac{\sqrt{2}}{3\alpha_{max}} \sum_{i=1}^{2} a_i^{3/2} \left(1 + \frac{a_i}{4}\right). \tag{39}$$

The intensity increases in this case as

$\rho_1^{3/2}$; $(\Delta R)^{-1/2}$ and $N^{1/2}$.

4. Let us consider the case of small angles but a broad beam:

$$\bar{\delta} > a_i - 1 + \sqrt{1 - a_{i\min}^2},$$

where α_{min} is the minimum value of the angle α. In this case

$$Q_u = \frac{I\tau_i T}{\beta_0 \Delta R \bar{\delta} a_{max}} \sum_{i=1}^{2} \sum_{k=1}^{2} a_k \left[1 + \frac{a_i^2}{2} - \frac{11}{8} a_k^2 - \right.$$

$$\left. - \frac{1 - 2a_i}{3} \sqrt{1 - a_k^2} + \frac{a_k^2}{3} \ln \frac{1 - \sqrt{1 - a_k^2}}{a_i} - \frac{2 - 3a_i}{3a_k} \arcsin a_k \right]. \qquad (40)$$

Approximately we have (for $a_1 \ll 1$; $\alpha_1 \ll 1$)

$$\eta_\rho \approx \frac{1}{4\bar{\delta} a_{max}} \sum_{i=1}^{2} \sum_{k=1}^{2} \left[a_i a_k \left(1 + \frac{a_i}{4} \right) - \frac{5}{9} a_k^2 \left(1 - \frac{3}{5} \ln \frac{a_k^2}{2a_i} \right) \right]. \qquad (41)$$

5. When the angle subtended and the width of the beam are small, then

$$\eta_\rho \approx \frac{1}{\bar{\delta} \cdot a_{max}} \left\{ \frac{1}{4} \sum_{i=1}^{2} \sum_{k=1}^{2} \left[a_i a_k \left(1 + \frac{a_i}{4} \right) - \right. \right.$$

$$\left. \left. - \frac{5}{9} a_k^2 \left(1 - \frac{3}{5} \ln \frac{a_k^2}{2a_i} \right) \right] - \frac{2\sqrt{2}}{9} \sum_i \bar{a}_i^{3/2} \left(1 + \frac{3}{20} a_i \right) \right\}, \qquad (42)$$

when

$$\sqrt{\bar{a}_i (2 - \bar{a}_i)} < a_k < \sqrt{a_i (2 - a_i)}$$

and

$$\eta_\rho \approx \frac{1}{4a_{max}} \sum_{i=1}^{2} \sum_{k=1}^{2} a_k \left[\sqrt{1 - a_k^2} + \arcsin a_k + \right.$$

$$\left. + \frac{a_i + \bar{a}_i}{2} + \frac{a_k^2}{3\bar{\delta}} \ln \frac{\bar{a}_i}{a_i} \right], \qquad (43)$$

when

$$a_k < \sqrt{\bar{a}_i (2 - \bar{a}_i)}.$$

We have considered all the particular cases encountered in practice, with the exception of the so-called "mixed" cases, i.e., we assumed that both angles α_1 and α_2 satisfy identical conditions for both values of a_1. The method of writing down the expression for η_ρ or Q_u in the mixed cases is obvious: one of the terms in the double sums should be replaced by a corresponding term from the sums (37)-(43). To save space we shall not write out these expressions, all the more since

Formula (35) covers all the possible cases. The application of the obtained relations to the proton synchrotron of the USSR Academy of Sciences will be given below.

3 Calculation of the corrections for collisions with the horizontal walls of the chamber. Inasmuch as the angles in the radial (γ) and vertical (ζ) directions are small, we can consider motion in the two directions independently.

We denote the beam dimension in the vertical direction by 2χ, the angle subtended by the beam by $2\zeta_m$, the vertical working dimension of the chamber by $2D_z$, and the displacement of the beam axis from a direction parallel to the central magnetic plane by ε_z. The amplitude of the oscillations has a maximum at the center of the sector and is equal to

$$B=\frac{f_z\left(\frac{\sigma_\nu}{2}\right)}{f_z(\sigma_1)}\sqrt{z_1^2+\frac{f_z^2(\sigma_1)R_0^2}{n}(\zeta-\zeta_0)^2},$$

where $f_z(\sigma_\nu/2)$ and $f_z(\sigma_1)$ is the value of the function f at the center of the sector and at the point of the injector (see Fig. 21) for the vertical oscillations (z_1 is the coordinate of the particle emitted from the injector). The optimal angle ζ_0 is small and ranges between 0 and 1', so that it can be henceforth neglected.

We introduce the notation

$$\frac{f_z\left(\frac{\sigma_\nu}{2}\right)}{f_z(\sigma_1)}\chi=\chi_\nu,\quad \frac{f_z\left(\frac{\sigma_\nu}{2}\right)R_0}{n}\zeta_m=a_{\zeta m},$$
$$\frac{f_z\left(\frac{\sigma_\nu}{2}\right)}{f_z(\sigma_1)}z_1=z_\nu,\quad \frac{f_z\left(\frac{\sigma_\nu}{2}\right)R_0}{n}\zeta=a_\zeta. \qquad (44)$$

Then the amplitude of the oscillations can be expressed more simply as

$$B=\sqrt{z_\nu^2+a_\zeta^2}. \qquad (45)$$

In order to prevent collisions with the chamber walls, we must have

$$\sqrt{z_\nu^2+a_\zeta^2}<D_z \text{ or } a_\zeta<\sqrt{D_z^2-z_\nu^2}=a_{\zeta\beta}. \qquad (46)$$

where α_{zg} is the maximum permissible angle. For different points of the injector (z_ν) this angle assumes different values.

The probability of not colliding with the chamber walls is obviously

$$\eta_\nu = \int_{-\chi_\nu}^{+\chi_\nu} \int_{-\alpha_{z_2}}^{\alpha_{z_1}} \frac{d\alpha_z\, dz_\nu}{2\alpha_{zm} 2\chi_\nu}, \qquad (47)$$

where α_{z_1} and $-\alpha_{z_2}$ are the maximum and minimum vertical angles, expressed in the units defined in (44).

Let us consider three cases.

Case 1. Let the angles of emission of the particle be sufficiently large, i.e., $|\alpha_{z_1}| > D_z$; $|\alpha_{z_2}| > D_z$, and $\alpha_{z_1} > 0$. In this case the domain of integration in (47), on the plane (α_z; z_ν), is a circle of radius D_z, truncated by two symmetrical chords: $z_\nu = \chi_\nu$ and $z_\nu = -\chi_\nu$. Calculating the area of this figure

$$2s = 2\left[\chi_\nu \sqrt{D_z^2 - \chi_\nu^2} + D_z^2 \arcsin \frac{\chi_\nu}{D_z}\right], \qquad (48)$$

we obtain

$$\eta_\nu = \frac{s \pm s}{2\alpha_{zm}\chi_\nu}, \qquad (49)$$

where the upper sign is for α_{z_1}, $\alpha_{z_2} > 0$ and the lower one for α_{z_1}, $\alpha_{z_2} < 0$.

Case 2. Let the angles of emission be small, i.e.,

$$\sqrt{D_z^2 - \chi_\nu^2} < |\alpha_{z_1}| < D_z \text{ and } \sqrt{D_z^2 - \chi_\nu^2} < |\alpha_{z_2}| < D_z \ (\alpha_{z_1} > 0).$$

In this case two segments are cut off from the integration domain considered in the preceding case by two parallel chords $\alpha_z = \alpha_{z_1}$ and $\alpha_z = -\alpha_{z_2}$.

Let us introduce the coordinates $z_1 = \sqrt{D_z^2 - \alpha_{z_1}^2}$ and $z_2 = \sqrt{D_z^2 - \alpha_{z_2}^2}$, for which the maximum permissible angle is, respectively, α_{z_1} and α_{z_2}. Then

$$\eta_\nu = \frac{\left[s + \alpha_{z_1} z_1 - D_z^2 \arcsin \frac{z_1}{D_z}\right]}{4\chi_\nu \alpha_{zm}} + \frac{\left[\pm s + \alpha_{z_2} z_2 \pm D_z^2 \arcsin \frac{z_2}{D_z}\right]}{4\chi_\nu \alpha_{zm}}, \qquad (50)$$

where the upper and lower signs are written for the cases $\alpha_{z_2} > 0$ and $\alpha_{z_2} < 0$, respectively.

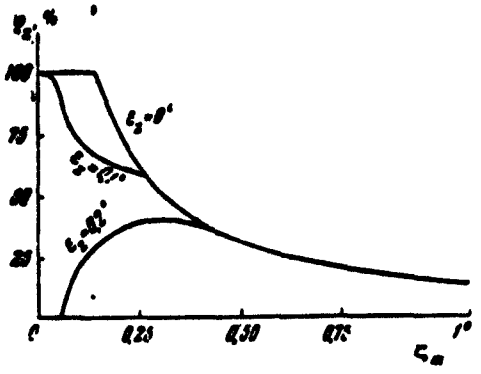

Fig. 46. Percentage of particles colliding with the horizontal walls of the chamber, as a function of the deviation ε_z of the beam axis from the angular half width ξ_m ($2\chi_v$ = = 12.5 cm; $2D_z$ = 25 cm).

Case 3. Let the emission angles be even smaller, i.e.,

$$|\alpha_{z_1}| < \sqrt{D_z^2 - \chi_v^2}$$

and

$$|\alpha_{z_2}| < \sqrt{D_z^2 - \chi_v^2}, \quad \alpha_{z_1} > 0.$$

The integration domain degenerates into a rectangle

$$\eta_v = \frac{2\chi_v \alpha_{z_1} + 2\chi_v \alpha_{z_2}}{4\chi_v \alpha_{zm}} = 1. \qquad (51)$$

Mixed cases. In analogy with the preceding, we can write down also the mixed cases. For example, if

$$\alpha_{z_1} > D_z; \; |\alpha_{z_2}| < \sqrt{D_z^2 - \chi_v^2}$$

then

$$\eta_v = \frac{s + 2\chi_v \alpha_{z_2}}{4\alpha_{zm}\chi_v}. \qquad (52)$$

We see that Formula (52) consists of the first part of (49) and the second part of (51). To facilitate the calculation of the mixed cases, we have purposely broken down the expression in the numerators

of (49) and (51) into two parts, the first of which corresponds to the angle α_{z_1} and the other to the angle α_{z_2}.

A plot of η_z for different values of ζ_m and ε_z is shown in Fig. 46.

4. Application to the USSR Academy of Sciences proton synchrotron. Figures 47-50 show four groups of curves of η_T for different values of the parameters of the 10,000-Mev installation of the USSR Academy of Sciences.

If the beam has a sufficiently large angle scatter, then it is easy to obtain satisfactory intensity even when the error upon injection is large.

In the case of a parallel or nearly parallel beam and a very small value of the error ε, the value of η_T is of course even larger. However, for any appreciable value of ε the intensity immediately tends to zero. For example, when $\rho_i = 30$ cm, $dH/dt = 4000$ oersted/sec, and $\varepsilon \sim 0.2^\circ$ we obtain for an almost parallel beam $\eta_T = 0$. A parallel beam with error $\varepsilon = 0.15^\circ$ yields the same intensity as a beam with a larger angular divergence ($\gamma_{max} \sim 1^\circ$) with error $\varepsilon = 0.8^\circ$.

A certain improvement is obtained for a parallel beam with erroneous injection direction by forcing the derivative of the magnetic field. For example, for $dH/dt = 12{,}000$ oersted/sec, a parallel beam, and an error $\varepsilon = 0.3^\circ$ the intensity still remains different from zero.

From this we draw two conclusions.

1. In order to adjust the apparatus it is necessary to use a beam with large angle scatter. Generally speaking, owing to the negligible aperture of the inlet unit, the beam will be almost parallel. One of the possible ways of increasing the beam entrance angle is to apply to one of the pair of plates used for the admission of the particles an alternating voltage with frequency larger than the particle revolution frequency. It is obvious that the obtained beam with varying direc-

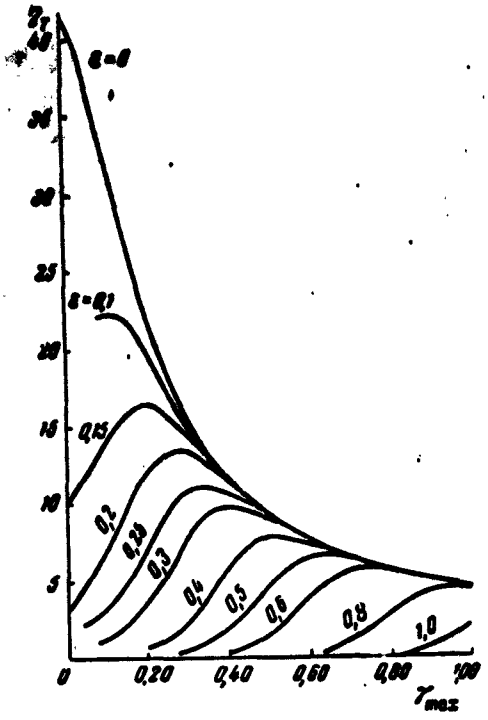

Fig. 47. Number of effective revolutions η_T as a function of the deviation ε of the beam axis from the optimal direction and of the angular half width γ_{max} of the beam (the angles are given in degrees). The injection energy is W_i = = 10 Mev, the distance from the injector to the central orbit is ρ_i = 50 cm, the beam width is 5 cm, and the change in the magnetic field is dH/dt = 4000 oersted/sec.

tion is equivalent to a beam with large angular spread.

2. To adjust the machine it may be useful to force the derivative of the magnetic field, although if the apparatus is in stable operation and the injection is at correct angles, this forcing will not be necessary. Forcing is also useful if the injector increases the intensity while decreasing the injection time.

Thus, in spite of the fact that the value of ΔR_0 (the constriction

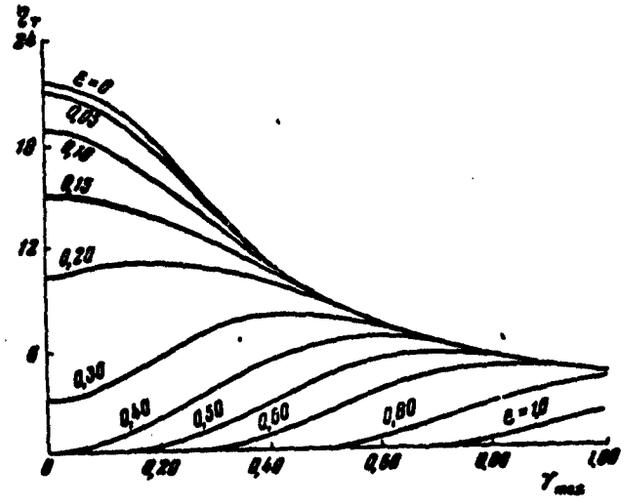

Fig. 48. The same as in Fig. 47, but for dH/dt = 10,000 oersted/sec.

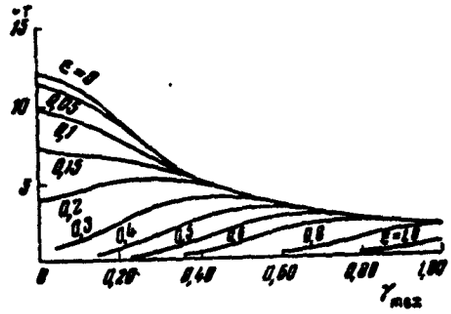

Fig. 49. The same as in Fig. 47, but for ρ_1 = 30 cm and dH/dt = 12,000 oersted/sec.

of the orbit) is large compared with ΔR for medium scale accelerators, the problem of particle capture in a 10,000-Mev installation encounters a difficulty of its own. A 7-9' deviation of the angle of particle emission from the specified direction causes the particle to strike the injector.

Attention must be called also to another unfavorable circumstance. During the first stage of the injection, the capture is most effective if the deviation of the instantaneous orbit from the injector is large.

Therefore most particles which do not collide with the injector have a large amplitude of free oscillations and will be poorly captured in the second stage of the injection (see the next section).

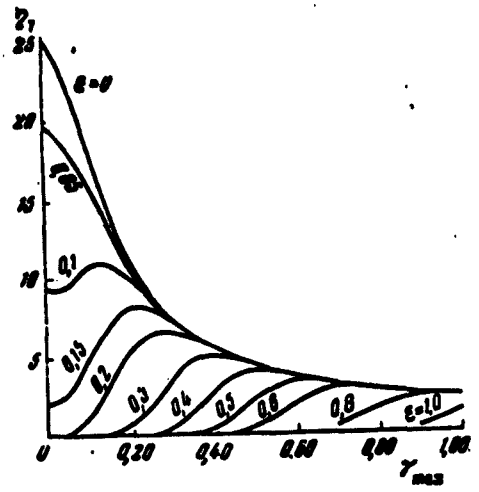

Fig. 50. The same as in Fig. 47 but for $\rho_1 = 30$ cm.

The most convenient would be powerful but brief injection with a favorable position of the instantaneous orbit, using a forced value of dH/dt.

On examining the plots in Figs. 47-50 we can make the unequivocal conclusion that the overwhelming majority of particles will be captured during the first stage. For this purpose it is necessary to stabilize the direction of the particle admitted into the chamber with an accuracy of several minutes, which apparently is feasible.

§4. Distribution of the Particles among the Oscillation Amplitudes after the First Injection Stage

In the present section we consider the auxiliary problem of the distribution of the particles among the oscillation amplitudes after the first stage of injection. As will be shown below, this greatly facilitates the calculation of the second stage of injection. As in the preceding section, we consider first a parallel beam.

1. Parallel particle beam. In order to find the distribution of the particles among the oscillation amplitudes, it is necessary to introduce the amplitude F_c in the integral (15) in place of one of the variables (u or y) and integrate with respect to the second variable. For example:

$$du = \frac{F_c dF_c}{u+y} = \frac{F_c dF_c}{\pm\sqrt{F_c^2 - a_i^2}}, \tag{53}$$

where the sign of the root coincides with the sign of (u + y),

$$Q_u^{\circ} = A \sum_{i=1}^{2} \int\int_{c_i'} \frac{dy F_c dF_c}{\pm\sqrt{F_c^2 - a_i^2}}. \tag{54}$$

The integration domain c'_i is plotted on the (y, F) plane for different cases (Fig. 51). Let $a_i > \alpha_\varepsilon$, and

$$a_i - \frac{a_i^2}{a_i} < \bar{0} < a_i - 1 + \sqrt{1 - a_i^2} = y_i.$$

$$Q_u^{\circ} = A \sum_{i=1}^{2} \left[\int_{a_i}^{F_c'} \frac{F_c dF_c}{\sqrt{F_c^2 - a_i^2}} \left(2 \int_{0}^{a_i - F_c + \sqrt{F_c^2 - a_i^2}} dy + \int_{a_i - F_c - \sqrt{F_c^2 - a_i^2}}^{a_i - F_c + \sqrt{F_c^2 - a_i^2}} dy \right) + \right.$$

$$\left. + \int_{F_c'}^{F_c''} \frac{F_c dF_c}{\sqrt{F_c^2 - a_i^2}} \int_{0}^{a_i - F_c + \sqrt{F_c^2 - a_i^2}} dy + \int_{F_c''}^{1} \frac{F_c dF_c}{\sqrt{F_c^2 - a_i^2}} \int_{1}^{\bar{0}} dy \right], \tag{55}$$

where

$$F_c' = \frac{a_i^2 + a_i^2}{2a_i};$$
$$F_c'' = \frac{a_i^2 + a_i^2}{2a_i}; \tag{56}$$
$$\bar{a}_i = a_i - \bar{0}.$$

From this we obtain immediately the distribution of the particles among the oscillation amplitudes:

$$a_i - \frac{a_i^2}{a_i} < \bar{0} < y_i;\ a_i < a_i.$$

$$Q_{F_c}^{\circ} dF_c = A dF_c \sum_{i=1}^{2} \begin{cases} \frac{2F_c(a_i - F_c)}{\sqrt{F_c^2 - a_i^2}}, & \text{when } a_i < F_c < F_c'; \\ \frac{F_c(a_i - F_c)}{\sqrt{F_c^2 - a_i^2}} + F_c, & \text{when } F_c' < F_c < F_c''; \\ \frac{\bar{0}F_c}{\sqrt{F_c^2 - a_i^2}}, & \text{when } F_c'' < F_c < 1. \end{cases} \tag{57}$$

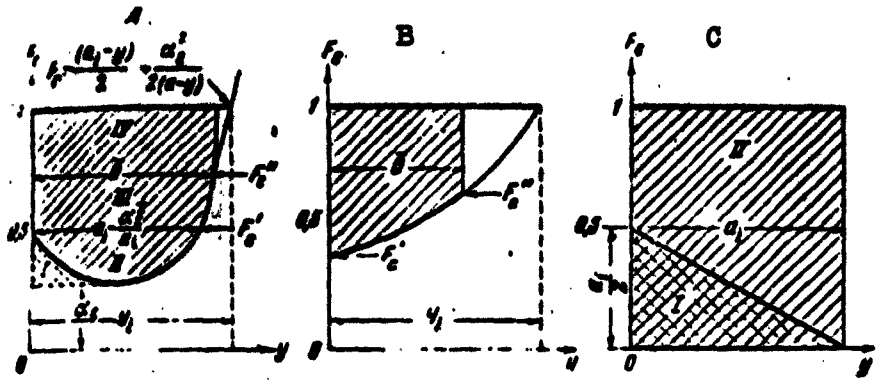

Fig. 51. Integration domains (cross hatched) of the integrals (55) for different cases:

A) $y_1 > \bar{0}$, $\alpha_\varepsilon < \alpha_1$; B) $y_1 > \bar{0}$, $\alpha_\varepsilon > \alpha_1$; C) $\alpha_\varepsilon = 0$, $\alpha_1 < 0$.

Integration is carried out twice over the domain I.

Expression (57) remains valid also when $\bar{0} > y_1$ and $\alpha_\varepsilon > a_1$ (for arbitrary $\bar{0}$), if the following rules are employed: 1) if $F''_c > 1$ it is necessary to assume $F''_c = 1$; 2) if any expression in (57) becomes negative, it should be assumed equal to zero.

On the other hand, if $\alpha_\varepsilon < a_1$ and $\bar{0} < a_1 - (\alpha_\varepsilon^2/a_1)$, then

$$Q''_{F_c}dF_c = AdF_c \sum_{i=1}^{4} \begin{cases} \frac{2F_c(a_i - F_c)}{\sqrt{F_c^2 - a_i^2}}, \text{when } a_i < F_c < F''_c \text{ и } \bar{0} > a_i - a_i; \\ \frac{2\bar{0}F_c}{\sqrt{F_c^2 - a_i^2}}, \text{when } a_i < F_c < F''_c \text{ и } \bar{0} < a_i - a_i; \\ \frac{F_c(a_i + \bar{0} - F_c)}{\sqrt{F_c^2 - a_i^2}} - F_c, \text{when } F''_c < F_c < F'_c; \\ \frac{F_c\bar{0}}{\sqrt{F_c^2 - a_i}}, \text{when } F'_c < F_c < 1. \end{cases} \quad (58)$$

The values of F'_c and F''_c are determined in (56).

It follows from (57) and (58) that as the angle α_ε decreases, the particle distribution among the oscillation amplitudes for $F_c \gg a_i$ becomes more and more uniform. This is particularly clearly seen in Fig. 52, which shows the probability density Q''_{F_c}/Q''_u as a function of the amplitude F_c:

$$\psi(F_c) = \frac{Q''_{F_c}}{Q''_u} \approx 1 \text{ for } \begin{matrix} a_i \ll d_i, \\ \bar{0} > y_i. \end{matrix} \quad (59)$$

2. Beam with angle scatter. In order to obtain the distribution of the particles among the oscillation amplitudes in the presence of an angle scatter of the particles, it is sufficient to multiply Formulas (57) and (58) by $d\alpha_\varepsilon/2\alpha_m$ and integrate over all possible angles α_ε taking account of all the inequalities presented above.

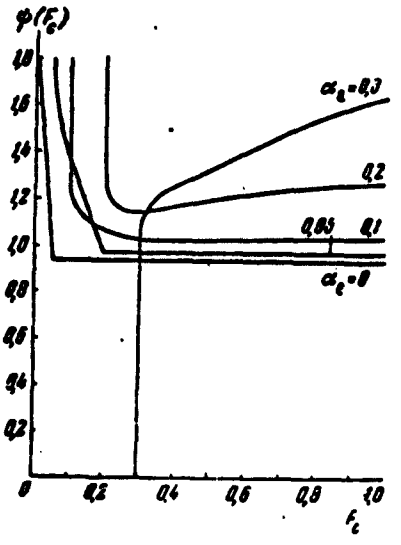

Fig. 52. Distribution of particles among the oscillation amplitudes for a parallel beam and various errors α_ε in the direction of the beam axis, a_1 = = 0.1; a_2 = 0.3 (the value of α_ε for each curve is indicated on the right side).

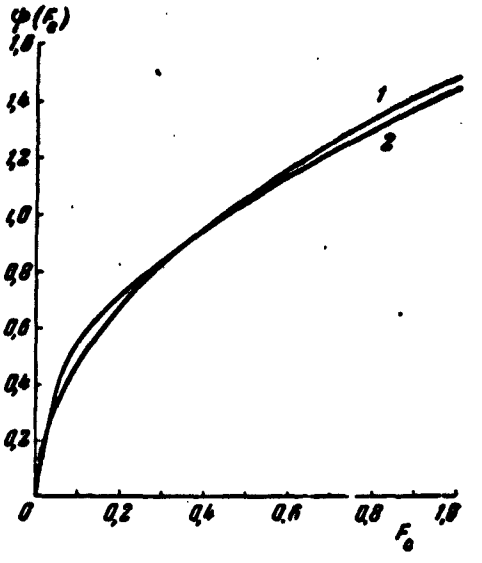

Fig. 53. Distribution of particles among the oscillation amplitudes for a broad beam with large angle scatter. Curve 1 is in accord with the approximate formula (63), while curve 2 is in accord with the exact formula (62). a_1 = 0.1; a_2 = 0.3; $\bar{\sigma} \geq 0.3$.

Assume that we have a beam with a large angle spread. Then we obtain after integration

$$Q_{F_\varepsilon}dF_\varepsilon = \frac{A}{\alpha_{max}}dF_\varepsilon \sum_{i=1}^{2} \begin{cases} \pi\bar{\sigma}F_\varepsilon, & \text{when } 0 < F_\varepsilon < \frac{a_i}{2}; \\ \pi(a_i - F_\varepsilon)F_\varepsilon - \Phi_1(\bar{a}_i), & \text{when } \frac{a_i}{2} < F_\varepsilon < \frac{a_i}{2}; \\ \Phi_1(a_i) - \Phi(\bar{a}_i), & \text{when } \frac{a_i}{2} < F_\varepsilon < 1, \end{cases} \qquad (60)$$

where

$$\Phi_1(x) = F_c\left[\sqrt{x(2F_c - x)} - (F_c - x)\arccos\frac{F_c - x}{F_c}\right], \qquad (61)$$

$$\Phi_1(x) \approx \frac{2\sqrt{2}}{3} x^{3/2}\sqrt{F_c}\left(1 - \frac{x}{16F_c} + \ldots\right),$$

when $F_c \gg x$.

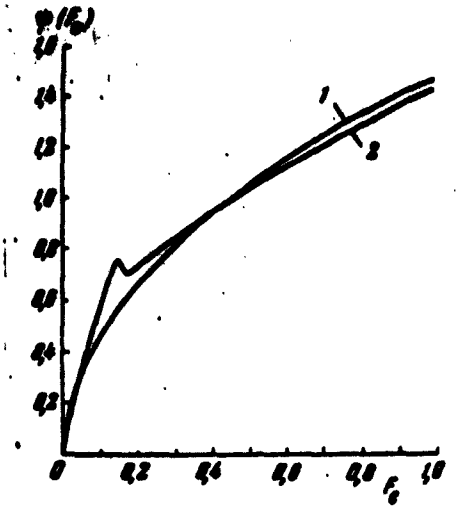

Fig. 54. The same as in Fig. 63, but for a narrow beam ($\theta = 0$).

Let us calculate the probability density

$$\psi(F_c) = \frac{Q_u}{Q_\infty}, \qquad (62)$$

where Q_u is given by Formula (35). At approximately $F_c \gg a_1$ we have [see Formulas (33) and (37)]

$$\psi(F_c) = \frac{3}{2}\sqrt{F_c}. \qquad (63)$$

A comparison of Formulas (62) and (63) is shown in Fig. 53 for different values of a_1 and for a broad beam. It is clear from this figure that the approximate formula (63) represents well the probability density $\psi(F_c)$ over almost the entire interval of variation of F_c.

For a narrow beam, a comparison of Formulas (62) and (63) is shown in Fig. 54. We again reach the conclusion, which is important for what follows, that the width of the beam influences only the oscillation amplitude distribution of order a_1.

The form of the function $\psi(F_c)$ is more greatly influenced by the character of the angular scatter of the beam. We can roughly assume that all the possible values of the probability density $\psi(F_c)$ lie between the two extreme values given in (59) and (63). The only exception from this rule is the case when the particle beam is very narrow but the error in the emission angle is large. Then the distribution is, roughly speaking, also close to (59), but with $F_c \gg \alpha_s$. This case,

although it can arise in the adjustment and starting of the machine, is nevertheless an exception in the case of a normally operating machine. It will also be considered below.

§5. Transient Mode with Accurate Switching on of the Accelerating Field for a Monoenergetic Particle Beam

During the time of the second injection stage, radial-phase oscillations arise. The particle will not collide with the injector during the second stage if

$$F_c + \Phi_c < 1, \tag{64}$$

where $\Phi_c = \rho_A/\rho_1$, and ρ_A is the amplitude of the radial-phase oscillations.

In addition, as shown in Chapter 1, the amplitude of the radial-phase oscillations is uniquely related with the swing of the phase oscillations $\varphi_2 - \varphi_1$. Figure 9 shows a plot of the function

$$\varphi_2 - \varphi_1 = s\left(\frac{\rho_1}{\bar{\rho}}\right)2\pi, \tag{65}$$

where $\bar{\rho}$ is the maximum amplitude of the radial-phase oscillations. The connection between $\bar{\rho}$ and the parameters of the installation is given in Formula (I, 40).

At first we consider for simplicity accurate turning on of the accelerating field in the absence of an energy spread of the particles. By definition, in "accurate turning on of the accelerating field" the frequency of particle revolution equals the frequency of the accelerating field, i.e.,

$$\dot{\varphi}_{nach} = 0. \tag{66}$$

The amplitude of the accelerating field is established rapidly (within 10-15 μsec) compared with the period of the phase oscillations (~500 μsec), and therefore we can assume with good degree of accuracy that the amplitude is established instantaneously. In this case, if Condition (66) is satisfied, the initial phase of the particle $\varphi_{nach} >$

$> (-\varphi_0)$ is equal to one of the two maximum values of the phase (φ_1 or φ_2). Inasmuch as $(\varphi_2 - \varphi_1)/2\pi$ is always smaller than unity, not all of the particles will be subjected to proton-synchrotron acceleration.

If the amplitude of the free oscillations is equal to $F_0\rho_1$, then the amplitude of the radial-phase oscillations should be less than $\rho_1(1 - F_0)$. Multiplying the probabilities of these two events and integrating over all possible values of F_0 we obtain the transient-mode coefficient:

$$\eta_2 = \int_0^1 \varepsilon\left(\frac{\rho_1(1-F_0)}{\rho}\right)\psi(F_0)\,dF_0 = \int_0^1 \varepsilon_1(F_0)\,\psi(F_0)\,dF_0. \qquad (67)$$

where $\psi(F_0)$ is the probability density of the given value of the amplitude F_0 after the first injection stage, determined in the preceding section. An analytic expression for the quantity η_2 cannot be obtained in the general case, if for no other reason than the fact that there is no analytic expression for the function ε. A numerical integration of Formula (67) entails no difficulty.

However, for many important particular cases we obtain an approximate expression for η_2. For this purpose it is necessary to approximate the function ε. It is possible, of course, to expand the function in powers of ρ_A/ρ, but this series converges poorly. We shall therefore seek an approximating function using as guidance the following principles: the approximation must be quite accurate for small ρ_A/ρ and approximate for $\rho_A/\rho \sim 1$. Indeed, as follows from Inequality (64) and Formula (67), the particles subjected to proton-synchrotron acceleration are those for which ρ_A/ρ is small. Figure 55 shows plots of the function $2\pi\varepsilon(\rho_A/\rho) = \varepsilon_0(\rho_A/\rho)$ (dashed) and of the two approximate functions $\varepsilon_0(\rho_A/\rho)$ (solid lines) for the values of $\cos\varphi_0$ of practical importance:

$$\varepsilon_{1,2} = \frac{\varepsilon_0}{\varepsilon_{\max}} = \frac{2(1-\varphi_0 \operatorname{ctg}\varphi_0)^{1/2}\rho_A}{\pi\bar{\rho}}\left[1 + k_{1,2}\left(\frac{\rho_A}{\bar{\rho}}\right)^2\right]; \qquad (68)$$

$$\varepsilon_{\max} = \frac{2(1-\varphi_0 \operatorname{ctg}\varphi_0)^{1/2}}{\pi}(1 + k_{1,2}),$$

where $k_1 = 0.2$ and $k_2 = 0.25$. Further calculations have shown that at both values of the constant k we obtain the same expression for η_2 in the region of values of φ_0 of practical interest. In general, the second term in the square brackets of (68) gives rise as a rule to only a small correction.

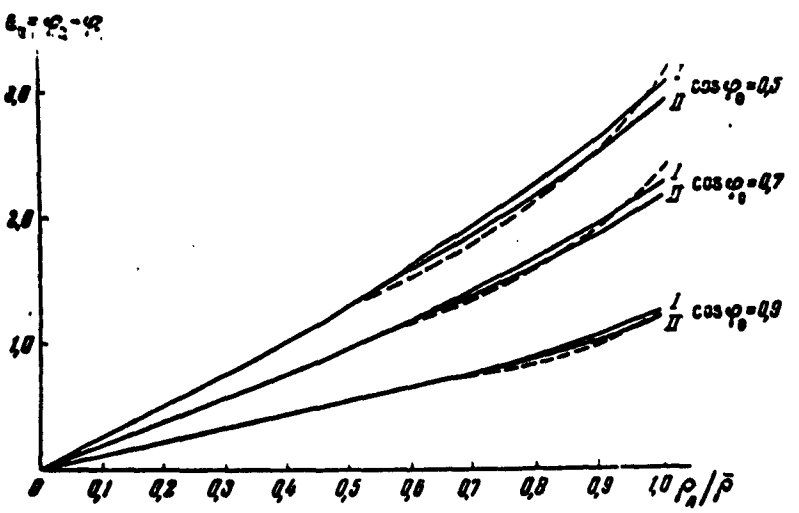

Fig. 55. Comparison of the exact (dashed) and approximate (I and II) curves for the function $\varepsilon_0(\rho_A/\bar{\rho})$ given by Formula (68). Curve I: $\varepsilon_0 = 4\sqrt{1 - \varphi_0 \operatorname{ctg}\varphi_0}\,(a + 0.25\,a^3)$, curve II: $\varepsilon_0 = 4\sqrt{1 - \varphi_0 \operatorname{ctg}\varphi_0}\,(a + 0.2\,a^3)$; for the curve I, $k = 0.25$ while for curve II, $k = 0.2$.

1. Let us calculate η_2 for the case of uniform distribution of the amplitudes after the first injection stage. This case corresponds to a monoenergetic parallel beam. With this simple example we can also analyze the computation technique. If the beam deviates from the optimal direction, then approximately all the amplitudes from α_ε to 1 are represented:

$$\eta_0 = \int_{a_0}^{1} \varepsilon\left[\frac{\rho_i}{\beta}(1-F_0)\right] dF_0 = \frac{3(1-\gamma_0 \operatorname{ctg}\gamma_0)^{1/2}\rho_i}{\pi(1-a_0)\beta} \times$$

$$\times\left[\int_{a_0}^{1}(1-F_0)\,dF_0 + \frac{k\rho_i^2}{\beta^2}\int_{a_0}^{1}(1-F_0)^2\,dF_0\right].$$

In the course of integration it must be borne in mind that if the argument of the function $\varepsilon(x)$ exceeds unity, then ε must be regarded as equal to ε_{max} in accord with (68):

$$\eta_0 = \frac{(1-\gamma_0 \operatorname{ctg}\gamma_0)^{1/2}}{\pi\beta}\left[1-a_0+\frac{k}{2\beta^2}(1-a_0)^2\right], \text{ when } \beta > \rho_i - a_0\rho_i;$$

$$\eta_0 = \frac{3(1-\gamma_0 \operatorname{ctg}\gamma_0)^{1/2}}{\pi(1-a_0)}\left[1-a_0-\frac{x}{2}+\frac{5k\rho_i}{4}\left(1-\frac{4}{5}a_0-\frac{4}{5}x\right)\right], \qquad (69)$$

when $\bar{\rho} < \rho_1 - \alpha_\varepsilon\rho_1$; here $x = \bar{\rho}/\rho_1$.

2. Let us consider a monoenergetic beam with large angle divergence. In this case

$$\eta_0 = \frac{3}{2}\int_0^1 \varepsilon\left[\frac{\rho_i}{\beta}(1-F_0)\right]\sqrt{F_0}\,dF_0. \qquad (70)$$

Integrating, we obtain

$$\eta_0 = \frac{4\rho_i(1-\gamma_0 \operatorname{ctg}\gamma_0)^{1/2}}{5\pi\beta}\left[1+\frac{8\rho_i^2 k}{21\beta^2}\right], \text{ when } \frac{\beta}{\rho_i} = x > 1;$$

$$\eta_0 = \frac{4\rho_i(1-\gamma_0 \operatorname{ctg}\gamma_0)^{1/2}}{5\pi\beta}\left\{1-(1-x)^{5/2}+\right. \qquad (71)$$

$$\left.+\frac{8\rho_i^2 k}{21\beta^2}\left[1-(1-x)^{7/2}\left(1+\frac{3}{2}x+\frac{21}{8}x^2-\frac{35}{8}x^3\right)\right]\right\},$$

when $x < 1$.

If we assume that we have a distribution

$$\psi(F_0) = 2F_0, \qquad (72)$$

which is a poorer representation of reality, we obtain a simpler expression:

$$\left.\begin{aligned}
\eta_0 &= \frac{2}{3}\frac{\rho_i(1-\gamma_0 \operatorname{ctg}\gamma_0)^{1/2}}{\pi\beta}\left[1+\frac{3\rho_i^2 k}{10\beta^2}\right], \text{ if } x > 1;\\
\eta_0 &= \frac{2}{3}\frac{\rho_i(1-\gamma_0 \operatorname{ctg}\gamma_0)^{1/2}}{\pi\beta}\left[1-(1-x)^3+\frac{3\rho_i^2 k}{10\beta^2}(1-2(1-x)^3\times\right.\\
&\left.\times(3-x+3x^2))\right], \text{ if } x < 1.
\end{aligned}\right\} \qquad (73)$$

Comparing (71) and (73) on Figs. 56a and 56b, we can verify that the difference does not exceed 15%. We make use of this fact in what follows.

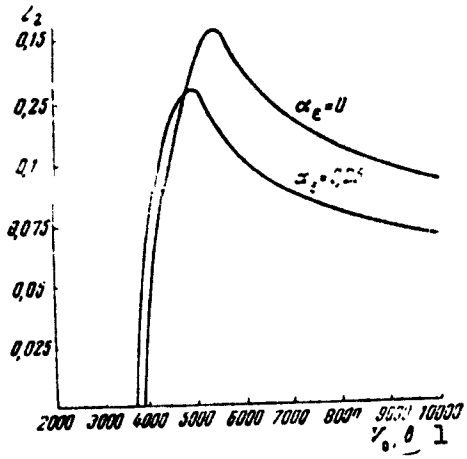

Fig. 56a. Transient mode coefficient η_2 for a monoenergetic parallel beam as a function of the voltage V_0. The upper curve is for accurate injection; the lower is for the case of an error $\alpha_\varepsilon = 0.25$. The injection energy is $W_1 = 4$ Mev; distance to the central orbit is $\rho_1 = 50$ cm. 1) v.

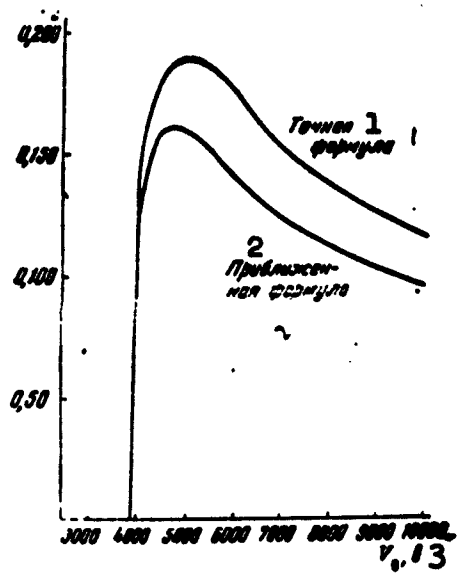

Fig. 56b. Same as in Fig. 56a, but for a monoenergetic beam with injection energy 10 Mev. The upper curve is for a particle distribution $\psi(F_c) = (3/2)\ F_c$; lower – for $\psi(F_c) = 2F_c$. 1) Exact formula; 2) approximate formula; 3) v.

§6. Transient Mode with Error in Turning on the Accelerating Field and for a Nonmonoenergetic Particle Beam

In turning on the accelerating field, an error may arise: either the accelerating field is not turned on on time, or the beam energy does not have the correct value. In practice these two factors cause one and the same result and can therefore be represented theoretically by one and the same parameter.

Assume that at the instant when the accelerating field is turned on the instantaneous orbit is a distance $\rho_1 M$ away from the central or-

bit (by definition, on the central orbit the frequency of revolution is equal to the frequency of the accelerating field or is a multiple of the latter). The value of M is connected with the "error" in the energy ΔE_1:

$$\rho_1 M = R_0 \frac{\Delta E_1}{2(1-n)w_1}, \quad \beta^2 \sim 0 \tag{74}$$

or with the "error" in the turning-on instant:

$$\rho_1 M = R_0 \frac{\Omega_1 \Delta t}{H_1 (1-n)}. \tag{75}$$

The phase velocity of the particles at the instant of turning on

$$\dot{\varphi}_{нач} = \frac{\rho_1 M}{R_0} \omega \left(n - \frac{L}{2\pi R_0 H_0}\right) \tag{76}$$

differs from zero.

The amplitude of the radial-phase oscillations ρ_A depends on the initial phase $\varphi_{нач}$ and on the initial phase velocity $\dot{\varphi}_{нач}$ (i.e., on $\rho_1 M$). With the aid of (76) and (I, 38-40) we write

$$2\left[\left(\frac{\rho_A}{\bar{\rho}}\right)^2 - \left(\frac{M\rho_1}{\bar{\rho}}\right)^2\right] = (\sin\varphi_0 - \varphi_0\cos\varphi_0)^{-1/3}(\sin\varphi_0 - \varphi_0\cos\varphi_0 - \sin\varphi_{нач} + \varphi_{нач}\cos\varphi_0). \tag{77}$$

As can be seen from (77), $\varphi_{нач}$ is a multiple-valued function of $(\rho_A/\bar{\rho})^2 - (M\rho_1/\bar{\rho})^2$. We find for each value $(\rho_A/\bar{\rho})^2 - (M\rho_1/\bar{\rho})^2$ two values $\varphi_{нач}$: $\varphi_{1_{нач}} < \varphi_0$ and $\varphi_{2_{нач}} > \varphi_0$, and set up the function

$$\frac{\varphi_{2нач} - \varphi_{1нач}}{2\pi} = s_M\left(\sqrt{\left(\frac{\rho_A}{\bar{\rho}}\right)^2 - \left(\frac{M\rho_1}{\bar{\rho}}\right)^2}\right). \tag{78}$$

We call attention to the fact that when M = 0 the function (78) goes over into the function (65), the form of which is known to us. Since M enters into (77) only as part of the combination $[(\rho_A/\bar{\rho})^2 - (M\rho_1/\bar{\rho})^2]$, we get

$$s(x) = s_M(x). \tag{79}$$

Let us call attention to one difference between (65) and (78). In (78) $\varphi_{2_{нач}} - \varphi_{1_{нач}}$ is no longer the swing of the phase oscillations,

when the amplitude of the radial-phase oscillations is equal to ρ_A. In this case $\varphi_{2_{nach}} - \varphi_{1_{nach}}$ is equal to the region of initial phases, for which the amplitude of the radial-phase oscillations for specified M is smaller than or equal to ρ_A. It is obvious that it is precisely this quantity that interests us in the calculation of the efficiency of the second stage of injection (the transient mode).

The approximate expression for ε_M has in this case the form [see (68)]:

$$\varepsilon_M\left(\frac{\rho_A}{\beta}\sqrt{u_A^2-M^2}\right)=\frac{2(1-\varphi_0 \operatorname{ctg}\varphi_0)^{1/n}\rho_A}{\pi\beta}\times$$
$$\times\left[\sqrt{u_A^2-M^2}+\frac{k}{x^3}(u_0^2-M^2)^{3/2}\right], \qquad (80)$$

where

$$u_A=\frac{\rho_A}{\rho_M};\quad x=\frac{\beta}{\rho_M};\quad k\approx 0{,}2 \text{ or } 0{,}25.$$

The maximum value is obtained when $\rho_A = \bar{\rho}$, i.e., when $u_A = x = \bar{\rho}/\rho_1$:

$$\varepsilon_{M;max}=\frac{2(1-\varphi_0 \operatorname{ctg}\varphi_0)^{1/n}\rho_A}{\pi\beta}\times\left[\sqrt{x^2-M^2}+\frac{k}{x^3}(x^2-M^2)^{3/2}\right]. \qquad (81)$$

The coefficient of the transient mode is in this case equal to

$$\eta_2=\int_0^{1-M}\varepsilon_M\left(\frac{\rho_A}{\beta}\sqrt{(1-F_c^2)-M^2}\right)\psi(F_c)\,dF_c. \qquad (82)$$

During the integration it must be remembered that if $(1 - F_c) > x$ then $\varepsilon_M = \varepsilon_{M;max}$. In Formula (82) we take into account automatically that when an error arises in the energy or in the instant of turning on, there will be fewer particles after the first stage than in the case of accurate turning on. Actually, in (82) we integrate with respect to F_c not to unity, but to $1 - M$. Thus, we sift out all the particles that are captured after $\underline{u}$ increases to $1 - M$ ($u \leq F_c$).

Let us calculate the coefficient η_2 for a uniform particle distribution ($\psi(F_c) = 1$):

$$\eta_2=\frac{2\rho_A(1-\varphi_0 \operatorname{ctg}\varphi_0)^{1/n}}{\pi\beta(1-a_1)}\left[\Phi_1(x)+\frac{k\rho_A^2}{\beta^2}\Phi_2(x)\right]+\frac{\varepsilon_{M;max}}{1-a_1}(1-x-a_1), \qquad (83)$$

where

$$\Phi_1(x) = \frac{1}{2}\left[x\sqrt{x^2 - M^2} + M^2 \ln\left|\frac{M}{x + \sqrt{x^2 - M^2}}\right|\right];$$
$$\Phi_2(x) = \frac{1}{8}\left[x(2x^2 + 5M^2)\sqrt{x^2 - M^2} - 3M^4 \ln\left|\frac{M}{x + \sqrt{x^2 - M^2}}\right|\right]. \quad (84)$$

By definition, if $x_1 > 1 - \alpha_g$ we must put in Formula (84) $x = 1 - \alpha_g$.

We see from Expressions (83) and (84) that in order for the coefficient η_2 to be different from zero it is necessary that M be smaller than x and smaller than $1 - \alpha_g$. The case described by Formula (83) is realized when an electrostatic generator is used as a source. Indeed, in this case we have an almost monoenergetic beam with small angle scatter. However, the average energy of the beam is subject to large slow oscillations. Therefore $M \neq 0$.

If the injector employed is a linear accelerator, then the energy scatter is large and in each cycle we have an entire set of values of M. In order to obtain the value of η_2 it is necessary to average Formula (83) over all possible values of M:

$$\eta_2 = \frac{1}{M_2 - M_1}\int_{M_1}^{M_2} \eta_2 dM.$$

In the case of accurate switching-on and a nonmonoenergetic beam, $M_2 = -M_1 = M_0$.

Carrying out the averaging in (83) we replace the functions $\Phi_1(x)$, ε_M, and $\Phi_2(x)$ by their mean values:

$$\overline{\Phi_1(x)}^{cp} = \frac{1}{M_2 - M_1}\left[\frac{M^2}{6}\ln\frac{|M|}{x + \sqrt{x^2 - M^2}} + \frac{Mx}{3}\sqrt{x^2 - M^2} + \right.$$
$$\left. + \frac{x^2}{6}\arcsin\frac{M}{x}\right]_{M_1}^{M_2};$$
$$\overline{\Phi_2(x)}^{cp} = \frac{1}{40(M_2 - M_1)}\left[-3M^4\ln\frac{|M|}{x + \sqrt{x^2 - M^2}} + \right.$$
$$\left. + \frac{Mx}{4}\sqrt{x^2 - M^2}(23x^2 - 22M^2) + 3x^4\arcsin\frac{M}{x}\right]_{M_1}^{M_2};$$
$$\overline{\varepsilon_{x,max}}^{cp} = \frac{(1 - \alpha_g \operatorname{ctg}\varphi_0)^{1/n}}{x(M_2 - M_1)}\left[M\sqrt{x^2 - M^2} - x^2\arcsin\frac{M}{x} - \right.$$
$$\left. + \frac{k}{4x^3}(M\sqrt{x^2 - M^2}(5x^2 - 2M^2)) + 3x^4\arcsin\frac{M}{x}\right]_{M_1}^{M_2}. \quad (85)$$

In using Formulas (85), the following should be borne in mind. The symbol $\Big]_{M_1}^{M_2}$ denotes that it is necessary to subtract from the value of the expression in the square bracket at $M = M_2$ the value of the same expression at $M = M_1$. If it turns out that M_1 or M_2 are larger than $\underline{x}$ (or $1 - \alpha_\varepsilon$), then we must set M in the square bracket equal to $\underline{x}$ (or $1 - \alpha_\varepsilon$).

For $\bar{\eta}_2$ we obtain a very simple expression in the case of the large energy spread (i.e., when $M_2 > x$ and $-M_1 > x$):

$$\eta_2 = \frac{(1-\varphi_0 \operatorname{ctg} \varphi_0)^{1/2} \varphi_i x^3}{(1-\alpha_\varepsilon)(M_2 - M_1)\rho} \left\{ 1 - \frac{2}{3} x + A_1 + \frac{3kx^2 \rho_i^2}{4\rho^2} \left(1 - \frac{4}{5} x + A_1 \right) \right\};$$
$$A_1 = \alpha_\varepsilon (\alpha_\varepsilon - 2 + x); \qquad (86)$$
$$\psi(F_c) = \begin{cases} 1, & \text{when } \alpha_\varepsilon < F_c < 1 \\ 0, & \text{when } F_c < \alpha_\varepsilon. \end{cases}$$

By way of another example it would be necessary to analyze the distribution of the particles among the oscillation amplitudes for a large aperture angle of the cone of the particle beam, which is proportional to $\sqrt{F_c}$ with great degree of accuracy. However, the integrals obtained in this case cannot be evaluated in terms of elementary functions.* We must therefore use the less accurate distribution (72), which gives an undervalued result for the coefficient η_2 (by approximately 15%).

In this case

$$\eta_2 = \frac{4\rho_i (1-\varphi_0 \operatorname{ctg} \varphi_0)^{1/2}}{\pi \rho} \left\{ \Phi_1(x) - \frac{1}{3}(x^3 - M^2)^{3/2} + \right.$$
$$\left. + \frac{\rho_i^2 k}{\rho^2} \left[\Phi_2(x) - \frac{1}{5}(x^3 - M^2)^{5/2} \right] \right\} + \varepsilon_{M;\max} (1-x)^2, \qquad (87)$$

where $\Phi_1(x)$ and $\Phi_2(x)$ are defined in (84). We recall that if $\underline{x}$ is greater than unity, we must set $\underline{x}$ equal to unity in (87).

If the particles are admitted into the chamber with an energy spread, then Expression (87) must be averaged over M. In the simplest case we have

$$\eta_2 = \frac{4\rho_1(1-\gamma_0\operatorname{ctg}\gamma_0)^{1/2}}{\pi\beta(M_2-M_1)}\left\{\overline{\Phi_1}^{cp} - \overline{\frac{1}{3}(x^2-M^2)^{3/2}}^{cp} + \right.$$
$$\left. + \frac{4\rho_1^2}{\beta^2}\left[\overline{\Phi_2}^{cp} - \overline{\frac{1}{5}(x^2-M^2)^{5/2}}^{cp}\right]\right\} + \overline{\varepsilon_{M;\max}}^{cp}(1-x)^2, \qquad (88)$$

where $\overline{\Phi_1}^{cr}$; $\overline{\Phi_2}^{cr}$; $\overline{\varepsilon_{M;\max}}^{cr}$ were determined above in (85), and

$$\overline{\frac{1}{3}(x^2-M^2)^{3/2}}^{cp} = \frac{1}{2\pi(M_2-M_1)}\left[M\sqrt{x^2-M^2}(5x^2-2M^2) + \right.$$
$$\left. + 3x^4 \arcsin\frac{M}{x}\right]_{M_1}^{M_2}; \qquad (89)$$

$$\overline{\frac{1}{5}(x^2-M^2)^{5/2}}^{cp} = \frac{1}{240(M_2-M_1)}\left[M\sqrt{x^2-M^2}(33x^4-26x^2M^2+8M^4) + \right.$$
$$\left. + 15x^6 \arcsin\frac{M}{x}\right]_{M_1}^{M_2}.$$

Formula (88) greatly simplifies in the case of a large energy spread, i.e., when $|M| > x$:

$$\eta_2 = \frac{4x^2(1-\gamma_0\operatorname{ctg}\gamma_0)^{1/2}}{\beta(M_2-M_1)}\left[1-\frac{4}{3}x+\frac{x^2}{2} + \right.$$
$$\left. + \frac{3\rho_1^2x^2}{\beta^2}\left(1-\frac{8}{5}x+\frac{2}{3}x^2\right)\right]. \qquad (90)$$

As already mentioned, the results of Formulas (88) and (90) can be improved by multiplying them by 1.15.

So far we have based all our arguments on the assumption that the frequency of the accelerating field and the frequency of particle revolution coincide. If the revolution frequency is q times smaller than the frequency of the accelerating field, then $\overline{\rho}$ in all the expressions for η_2 and $\overline{\eta}_2$ should be taken $\sqrt{q}$ times smaller than for $q = 1$.

§7. Transient Mode Coefficient at Injection Energies 4 or 10 Mev

In the preceding sections we have considered several factors influencing the magnitude of the transient mode coefficient η_2. Among these factors were: the amplitude of the voltage v_0 on the accelerating gap; the character of the first stage of injection [form of the function $\psi(F_0)$]; the distance from the injector to the central orbit ρ_1; the energy scatter of the particles Δw_1; the injection energy w_1; and the multiplicity q.

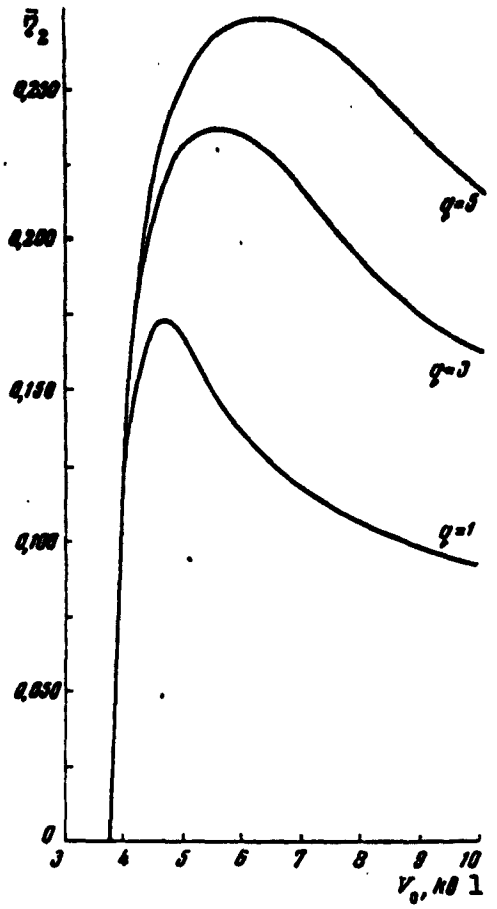

Fig. 57. Transient mode coefficient as a function of the voltage V_0 and the multiplicity q at injection energy $W_i = 4$ Mev with distance from the injector to the central plane $\rho_i = 50$ cm, energy spread $\Delta W_i/W_i = 0\%$ and particle distribution $\psi(F) = 1$.
1) kv.

The influence of all the foregoing factors on this quantity can be traced on the 12 plots presented in the present section. In particular, the amplitude of the accelerating voltage was varied from 4 to 10 kv. The distance from the injector to the central orbit was chosen equal to 50 and 30 cm. The energy spread was assumed uniform (values of $\Delta W_i/W_i$ were 0%; $\pm 0.5\%$; $\pm 1\%$). The multiplicity was varied between 1

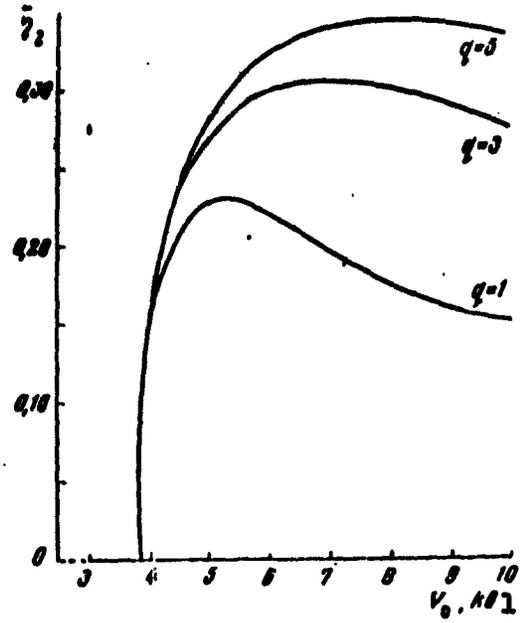

Fig. 58. The same as in Fig. 57, but for W_1 = 10 Mev. 1) kv.

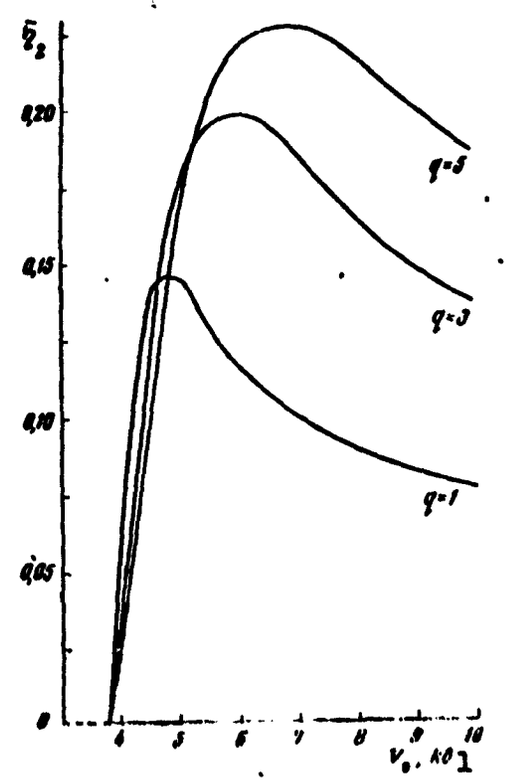

Fig. 59. The same as in Fig. 57, but for $\Delta W_1/W_1 = \pm 0.5\%$. 1) kv.

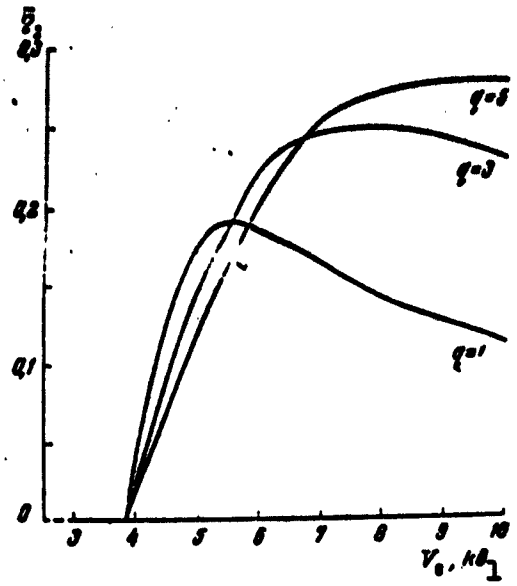

Fig. 60. The same as in Fig. 57, but for W_1 = 10 Mev and $\Delta W_1/W_1$ = = $\pm$0.5%. 1) kv.

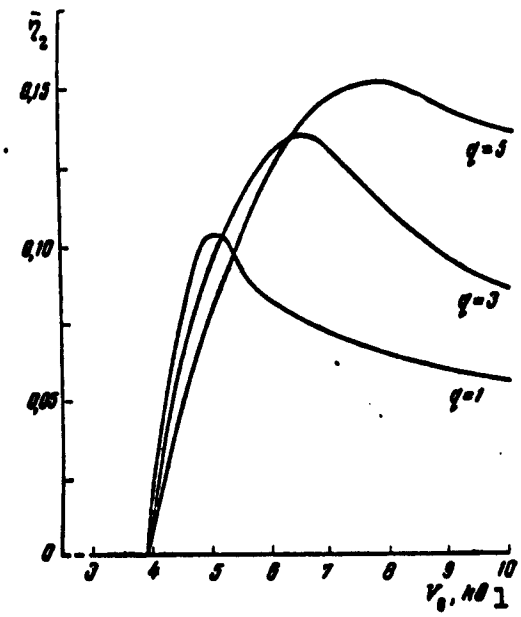

Fig. 61. The same as in Fig. 57, but for $\Delta W_1/W_1 = \pm 1\%$. 1) kv.

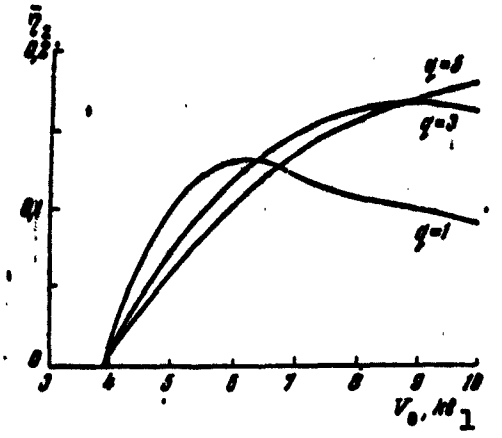

Fig. 62. The same as in Fig. 57, but for W_1 = 10 Mev and $\Delta W_1/W_1$ = = $\pm$1%. 1) kv.

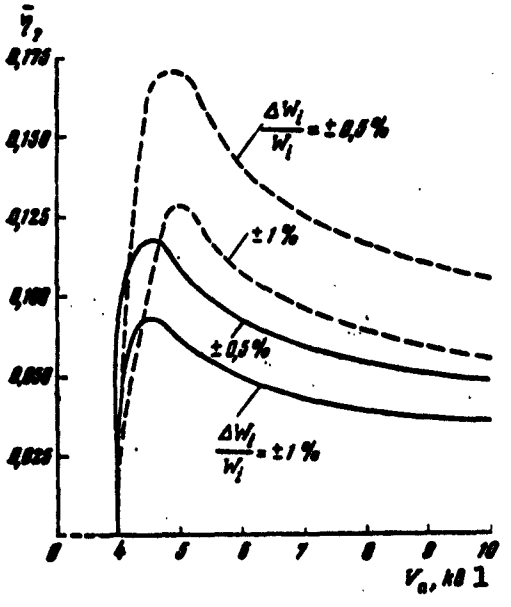

Fig. 63. Comparison of the curves for η_2 at injection energy W_1 = 4 Mev, multiplicity q = 1, and distribution $\psi(F)$ = 1 for two different distances from the injector to the central orbit, ρ_1 = 50 cm (dashed curves) and ρ_1 = 30 cm (solid curves). 1) kv.

and 5. All the numerical calculations were made for two injection energies, 4 and 10 Mev. The rate of change of the magnetic field intensity was taken at $6.5 \cdot 10^3$ oersted/sec.

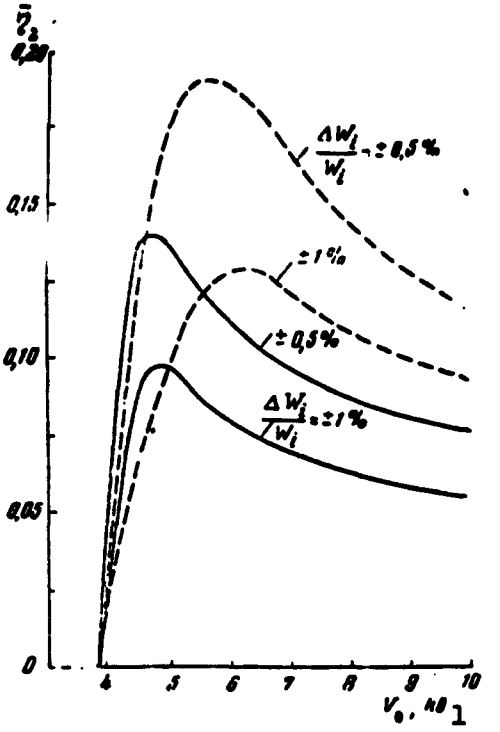

Fig. 64. The same as in Fig. 63, but for injection energy W_1 = 10 Mev. 1) kv.

The character of the injection in the first stage was taken into account in the following fashion. The transient mode coefficient depends on the form of the function $\psi(F_c)$, of the particle distribution among the oscillation amplitudes after the first stage of the injection. We can use here arbitrary variants, but at this stage of the calculation it is meaningful to consider only the extreme cases: uniform distribution among the amplitudes ($\psi(F_c) = 1$), corresponding to a parallel beam, and a linear distribution ($\psi(F_c) = 2F_c$), which represents approximately a particle beam with a large angle spread ($2\gamma_{max} > 0.5^\circ$). The true value of the coefficient $\bar{\eta}_2$ lies somewhere between

these two values, depending on the injection conditions. The computational accuracy obtained in this case is sufficient to determine the intensity of the beam of accelerated particles and to choose the parameters of the installation.

The numerical values which we have chosen for the plots correspond to the "normal" operation of the installation. For example, we assume that the error in the angle α_ε and the error in the instant of turning on are sufficiently small. If α_ε is very large or the turning-on error is large, then η_2 tends rapidly to zero. Thus, we do not present here the so-called "adjustment graphs," which we have calculated, since they do not characterize the intensity that can be attained in the 10-Bev proton synchrotron, although one could not get along without these curves to adjust the machine during its startup.

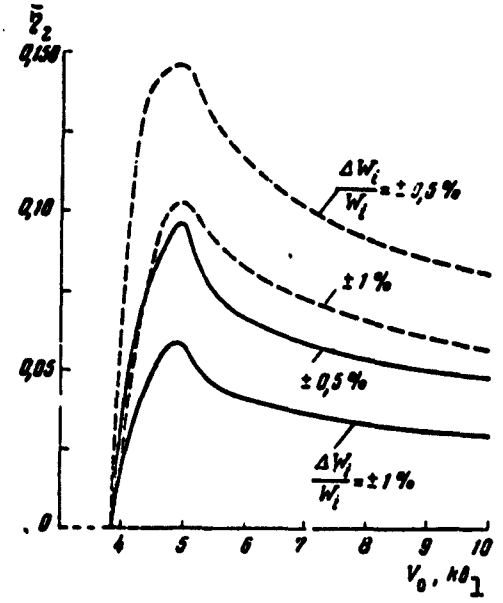

Fig. 65. Comparison of the curves for η_2 at injection energy $W_1 = 4$ Mev, $\rho_1 = 50$ cm, multiplicity $q = 1$, for two particle distributions among the amplitudes of the free oscillations, $\psi(F) = 1$ (dashed curves) and $\psi(F) = 2F$ (solid curves). 1) kv.

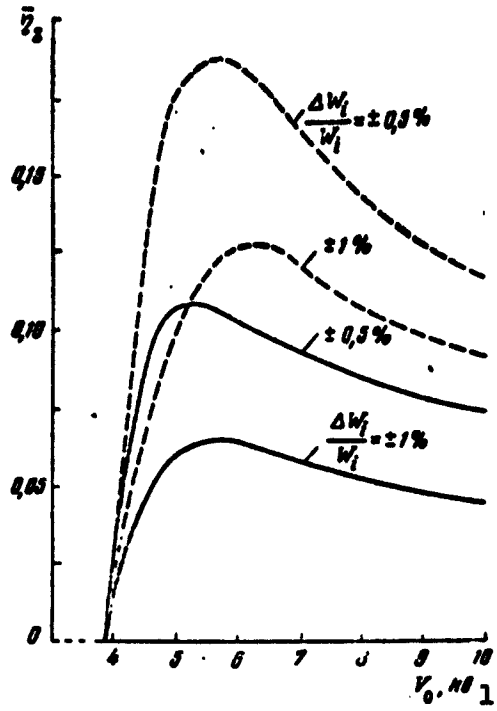

Fig. 66. The same as in Fig. 65, but for W_1 = 10 Mev. 1) kv.

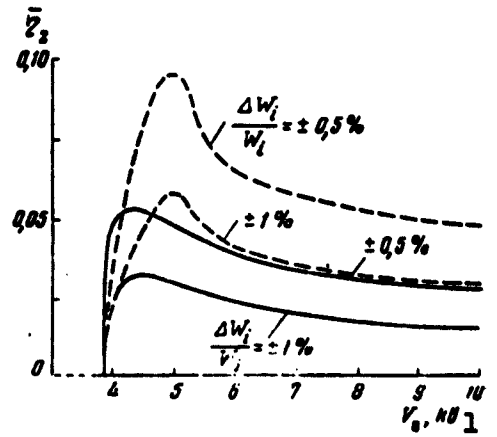

Fig. 67. The same as in Fig. 63, but for a different distribution function ($\psi(F) = 2F$). 1) kv.

Let us proceed to a specific description of the plots.

1. Parallel particle beam. Figures 57 and 58 show plots of η_2 for different values of v_0 and q with zero energy scatter and a parallel particle beam. For $w_1 = 4$ Mev the maximum value of η_2 is 0.17 at $q = 1$, 0.23 at $q = 3$, and 0.27 at $q = 5$. At a 10-Mev injection energy these figures increase to 0.23, 0.30, and 0.34, respectively. The optimal values of v_0 range between 5 and 8 kv for all these cases.

In the case of a uniform energy spread of $\pm 0.5\%$ (Figs. 59 and 60) the values of the coefficient η_2 differ very little from those given above. However, if a 0.5% energy drift were to occur in the monoenergetic beam, the coefficient η_2 would decrease by many times. Therefore particles with deviation of $\pm 0.5\%$ from the average energy are poorly captured in the acceleration mode, and when the deviation from the average energy exceeds $\pm 0.6\%$ they are not captured at all.

Indeed, Figs. 61 and 62 show plots for an energy spread of $\pm 1\%$. The maximum value of $\bar{\eta}_2$ decreases by almost a half. Particles with a spread within the limits of $\pm 0.5\%$ are effectively captured in the acceleration mode, while those having a spread between 0.5 and 1% are practically not captured. Therefore the coefficient η_2 decreases by approximately one half.

The requirement with regard to the monoenergetic nature of the beam becomes much more stringent if an error exists in the particle emission angle α_ε. As a crude approximation, when the energy spread is large $\bar{\eta}_2$ decreases by a factor $(1 - \alpha_\varepsilon)/[1 - 3\alpha_\varepsilon(1 - \alpha_\varepsilon)]$ [see (86)], while the effective capture energy range decreases by a factor $1/(1 - \alpha_\varepsilon)$. To save space we confine ourselves to these remarks and do not present the plots.

Figures 63 and 64 show the influence that the distance from the central orbit to the injector ρ_1 exerts on the coefficient $\bar{\eta}_2$. The need

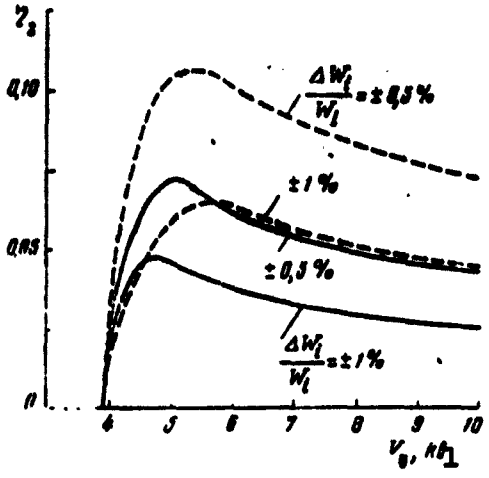

Fig. 68. The same as in Fig. 64, but for a different distribution function ($\psi(F) = 2F$). 1) kv.

for reducing ρ_i can be related, in particular, with the increase in the azimuthal asymmetry. In this case the coefficient $\bar{\eta}$ decreases sharply (by 40-50%) and assumes at 4 Mev values 0.1 ($\Delta w_1/w_1 = \pm 0.5\%$) and 0.06 ($\Delta w_1/w_1 = \pm 1\%$). At 10 Mev, $\bar{\eta}_2$ is somewhat larger: 0.13 ($\Delta w_1/w_1 = \pm 0.5\%$) and 0.08 ($\Delta w_1/w_1 = \pm 1\%$).

2. Beam with large angle spread. Figures 64, 65, and 66 show a comparison of the transient mode coefficients for a parallel beam and one with large angle spread. In the latter case the value of the coefficient $\bar{\eta}_2$ is approximately 50% smaller. It must be borne in mind, however, that this value is closer to reality, for in the first case the error in the angle α_ε can greatly exceed $\bar{\eta}_2$.

Figures 67 and 68 show clearly that in the case of a large angle spread in the beam the value of $\bar{\eta}_2$ changes with changing distance from the injector to the central orbit.

The main results are listed in the table.

Thus, in the worst case when $\rho_i = 30$ cm and $\Delta w_1/w_1 = 1\%$ the coefficient is $\bar{\eta}_2 = 0.05$ at 10 Mev and $\bar{\eta}_2 = 0{:}03$ at 4 Mev ($q = 1$).

TABLE

Maximum Value of $\bar{\eta}_2$ (in %) at Injection Energies 4 and 10 Mev

1	2 Кратность	3 Характеристика первого этапа инжекции	$\bar{\eta}_2$, % 5 при W_0=4 Мэв: 4 энергетический разброс, %			5 при W_0=10 Мэв: 4 энергетический разброс, %		
			0	0,5	1	0	0,5	1
R_0=50	q=1	ψ=1	17	15	10	23	19	13
		ψ=2F_c	—	10	6	—	11	7
	q=3	ψ=1	24	20	14	30	25	17
		ψ=2 F_c	—	—	—	—	—	—
	q=5	ψ=1	27	23	15	34	28	18
		ψ=2 F_c	—	18	8	—	16	10
R_0=80	q=1	ψ=1	—	9	7	—	14	10
		ψ=2 F_c	—	5	3	—	7	5
	q=5	ψ=1	—	—	—	—	—	—
		ψ=2 F_c	—	10,2	6	—	18,2	7,7

1) Distance from injector to central orbit, cm; 2) multiplicity; 3) characteristic of first injection stage; 4) energy spread, %; 5) when.

Manuscript Page No.

[Footnotes]

161 For a short time, 50-200 μsec, $\dot{H}_1$ can be increased to 12000 oersted/sec.

196 The first integration (with respect to F_c) can be reduced to elliptic integrals, but the formulas obtained are not convenient for calculations. The averaging over M must in this case be carried out numerically.

Manuscript Page No.

[List of Transliterated Symbols]

163 нач = nach = nachal'nyy = initial

197 ср = sr = sredniy = average

Chapter 6

STRONG FOCUSING

§1. Introduction

At the end of 1952, Livingston, Courant, and Snyder proposed a method for producing powerful focusing in accelerators designed for the production of protons with energies up to 50-100 Bev. It turned out later on that similar work was done in 1950 by N. Christofilos, but was not published.

As is well known, in ordinary accelerators the focusing force in the vertical (z) and radial (r) directions varies in inverse proportion to the radius of the magnet

$$F_z = -nH_z \frac{ev}{c} \frac{z}{R} \qquad (1)$$

$$F_r = -(1-n) H_z \frac{ev}{c} \frac{\rho}{R}, \qquad (2)$$

where H_z is the vertical component of the magnetic field, $\underline{e}$ and $\underline{v}$ are the charge and velocity of the particles, while $\underline{z}$ and ρ are the deviations of the particle from the orbit in the vertical and radial directions. In particular, if the radius of the magnet is increased it becomes necessary therefore to increase the linear dimensions of the employed region of the magnet gap.

The decrease in the focusing forces makes it difficult to obtain an intense beam of accelerated particles, particularly during the particle injection and in the initial stage of acceleration.

This can be illustrated by means of the following example. If the particle is injected into the accelerator chamber not at the correct

angle, but with an angle error γ, then the amplitudes of the radial F_ρ and vertical F_z oscillations increase by

$$\left.\begin{aligned}\Delta F_\rho &= \sqrt{\rho_1^2 + \frac{F_1^2}{1-n}} - \rho_1,\\ \Delta F_z &= \sqrt{z_1^2 + \frac{F_1^2}{n}} - z_1,\end{aligned}\right\} \qquad (3)$$

where ρ_1 and z_1 are the coordinates of the injected particle expressed in the variables ρ and z. It is clear from these formulas that the increase in the oscillation amplitude increases strongly with increasing radius of the particle orbit. This makes it necessary to increase either the dimensions of the magnet gap or the accuracy with which the particles are injected into the chamber. Both methods are usually employed.

There exist methods which make it possible to increase the efficiency of the focusing forces with the aid of various combinations of electric and magnetic fields, and thereby decrease the necessary aperture of the magnet gap.

Among the other possibilities, Livingston, Courant, and Snyder [58] considered the most effective way of increasing the focusing, that of alternating sectors with opposite signs of n.

The present calculation was undertaken in order to explain the shortcomings and advantages of the procedure indicated above for improving the focusing. We have therefore tried to simplify the problem as much as possible without attempting to design any particular accelerator, but merely clarify the characteristic features of the phenomenon, without obscuring it by extraneous effects.

§2. Free Oscillations and Stability Region

Let us assume that we have 2N identical sectors (see Fig. 69) subtending an angle v. In the odd sectors the magnetic field index is $n_1 < 0$, while for the even sectors $n_2 > 0$. Let us assume that on the

boundary between sectors n changes abruptly from n_1 to n_2. In addition, we assume that linear sections exist. If we do not design a specific accelerator, but are interested in the singularities of the motion, these two assumptions are not essential. It is easy to take into account the linear sections, and also the transition region between n_1 and n_2. In such a case, however, the formulas and the calculation become much more complicated, although the character and the singularities of the motion do not change.

When $n\chi/R \ll 1$ the equation of motion has the form

$$\chi'' + \varkappa_1^2 \chi = 0, \quad \chi'' - \varkappa_2^2 \chi = 0, \tag{4}$$

where

$$\varkappa_1 = \begin{cases} \sqrt{1-n_1} - & \text{for radial motion} \\ \sqrt{n_2} - & \text{for vertical motion} \end{cases}$$
$$\varkappa_2 = \begin{cases} \sqrt{n_2-1} - & \text{for radial motion} \\ \sqrt{-n_1} - & \text{for vertical motion} \end{cases}$$

Generally speaking, Eqs. (4) have a small range of applicability with respect to χ/R in the case of very large n. However, if the law governing the fall-off of the magnetic field is specially chosen, the range of applicability of (4) will be appreciably larger. The nonlinear terms become significant only in the investigation of resonances.

The solution of Eqs. (4) has the form

$$\begin{aligned} \chi_1 &= A \sin \varkappa_1 \theta + B \cos \varkappa_1 \theta; \\ \chi_2 &= C \operatorname{sh} \varkappa_2 \theta + D \operatorname{ch} \varkappa_2 \theta, \end{aligned} \tag{5}$$

where χ_1 and χ_2 are the solutions for the focusing and defocusing sectors, respectively. The constants A; B; $\overline{C}$; $\overline{D}$ are interrelated by the conditions for the continuity of the solution. The angle θ ranges from 0 to ν in each sector:

$$C = p(Ac - Bs); \quad D = As + Bc, \tag{6}$$

where

$$c = \cos \varkappa_1 \nu; \quad s = \sin \varkappa_1 \nu; \quad p = \frac{\varkappa_1}{\varkappa_2}. \tag{7}$$

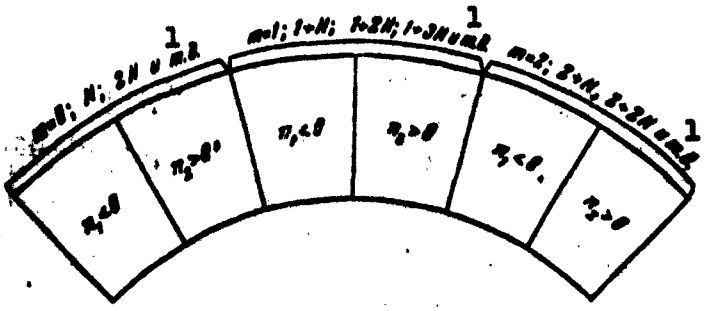

Fig. 69. Arrangement of the accelerator magnets in strong focusing. 1) etc.

Let us introduce a variable m, which changes by unity on going from one pair of sectors to the other (see Fig. 69). We shall assume that A; B; $\overline{C}$; $\overline{D}$ are functions of this variable. Then the continuity conditions yield the following two difference equations:

$$\begin{aligned} A_m[s\cdot c_2+pc\cdot s_2]+B_m[c\cdot c_2-ps\cdot s_2]&=B_{m+1};\\ A_m[s\cdot s_2+pc\cdot c_2]+B_m[c\cdot s_2-ps\cdot c_2]&=pA_{m+1}; \end{aligned} \tag{8}$$

We shall henceforth use the notation:

$$s_i=\operatorname{sh}\varkappa_i\nu;\quad c_i=\operatorname{ch}\varkappa_i\nu. \tag{9}$$

The solution of (8) is sought in the form

$$A_m=De^{i\mu m}+\text{c.c.};\quad B_m=fDe^{i\mu m}+\text{c.c.} \tag{10}$$

We substitute (10) in (8) and equate the determinate to zero, obtaining

$$\cos\mu=c\cdot c_2+\frac{(1-p^2)s\cdot s_2}{2p}. \tag{11}$$

Expanding cos μ in powers of ν, we obtain

$$\cos\mu=1-\nu^2(\varkappa_1^2-\varkappa_2^2)-\nu^4\left[\frac{\varkappa_1^2\varkappa_2^2}{6}-\frac{(\varkappa_1^2-\varkappa_2^2)^2}{8}\right]+\ldots, \tag{11'}$$

where

$$\varkappa_1^2-\varkappa_2^2=\begin{cases}2(1-n_{cp}) & \text{for radial motion}\\ 2n_{cp} & \text{for vertical motion.}\end{cases}$$

It is seen from (8) that

$$f=f_1-f_2e^{i\mu}, \tag{12}$$

where $$f_1=\frac{s\cdot s_2+pc\cdot c_2}{pc\cdot c_2-s\cdot s_2};\quad f_2=\frac{p}{pc\cdot c_2-s\cdot s_2}.$$

The solution of (8) can thus be written in the form

$$\chi_m = D e^{i m \varphi} \psi(\theta) + D^* e^{-i m \varphi} \psi^*(\theta) = F_0(\theta) \cos[\nu m + \varepsilon(\theta)], \tag{13}$$

where

$$F_0(\theta) = 2|D\psi(\theta)|; \quad \varepsilon = \arg D\psi;$$

$$\psi(\theta) = \sqrt{\frac{2}{\varkappa_1 l (\varkappa_1 + \varkappa_2)}} \begin{cases} \sin \varkappa_1 \theta + f \cos \varkappa_1 \theta & \text{for the focusing sector} \\ p(e - f/e) \operatorname{sh} \varkappa_2 \theta + & \\ + (e + f/e) \operatorname{ch} \varkappa_2 \theta & \text{for the defocusing sector.} \end{cases}$$

The normalizing coefficient of the function ψ is chosen such as to make the Wronskian of the functions ψ and ψ^* equal to 2/i.

The condition for the stability of the solution (13) is the inequality

$$|\cos \mu| < 1. \tag{14}$$

If the number of sectors 2N tends to infinity, then the condition (14) is equivalent to the ordinary condition (1), written out for n_{sr}:

$$n_{cp} = \frac{n_1 + n_2}{2}$$
$$0 < n_{cp} < 1. \tag{15}$$

This condition can be obtained from (11') and (14) by discarding from (11') the terms with powers ν^4 and above.

When N is finite and the values of κ_1 and κ_2 are large, the limits of the inequality (15) broaden appreciably:

$$\delta_{np} < n_{cp} < \delta_{np}. \tag{16}$$

When $n^2\nu^4 < 6$ we get approximately

$$\delta_{np} = -\frac{n^2\nu^2}{12\left(1 - \frac{n^2\nu^4}{45}\right)}; \quad \delta_{np} = 1 + \frac{n^2\nu^2}{12\left(1 - \frac{n^2\nu^4}{45}\right)}, \tag{17}$$

where

$$n = \frac{-n_1 + n_2}{2} = \frac{|n_1| + |n_2|}{2}.$$

If $6 < n^2\nu^4 < 12.3$, then

$$\delta'_{np} = 1 - \frac{\frac{1}{\nu^2} - \frac{n^2\nu^2}{12}}{1 - \frac{n^2\nu^4}{45}}; \quad \delta'_{np} = \frac{\frac{1}{\nu^2} - \frac{n^2\nu^2}{12}}{1 - \frac{n^2\nu^4}{45}}. \tag{17'}$$

When $12.3 < n^2\nu^4 < 22$ there is no common stability region for the vertical and radial oscillations. The stability region (16) reaches a maximum at approximately

$$n^2\nu^4 \approx 6.$$

A plot of the stability region is shown in Fig. 70.

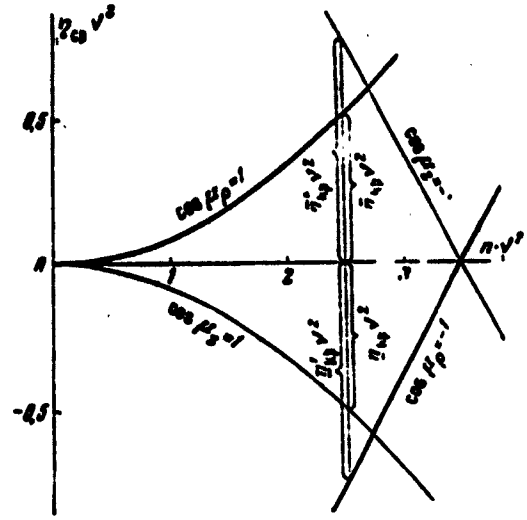

Fig. 70. Principal region of stability of the free oscillations.

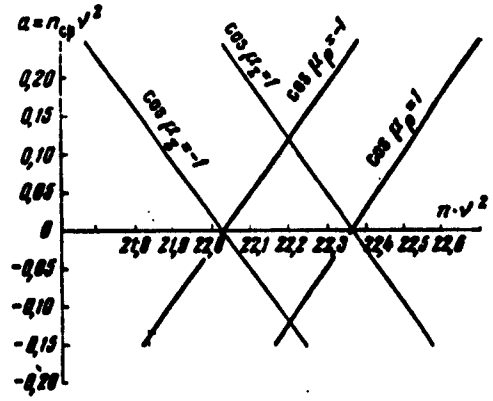

Fig. 71. One of the stability regions for large values of $n\nu^2$.

In addition to the region of stability with respect to n, which is common to the radial and vertical oscillations, we introduce a region for the separate stability of the vertical and radial oscilla-

tions, Δn_z and Δn_p:

$$\Delta n_z = \frac{}{\left(1-\frac{n^2\nu^4}{48}\right)\nu^2} = a_{np} - a_{np}; \quad \Delta n_p = A_{np} - b_{np}.$$

We then have approximately, for $n^2\nu^4 < 12.3$:

$$\cos\mu_z = 1 - 2\frac{(n_{np}-a_{np})}{\Delta n_z}, \quad \sin\mu_z = \frac{2}{\Delta n}\sqrt{(n_{op}-a_{np})(A_{np}-n_{op})};$$
$$\cos\mu_p = 1 - 2\frac{(A_{np}-n_{op})}{\Delta n_p}, \quad \sin\mu_p = \frac{2}{\Delta n_p}\sqrt{(A_{np}-n_{op})(n_{op}-a_{np})}. \qquad (18)$$

For very large n, there exists an infinite series of stability regions in the places where $\cos\sqrt{n}\nu = 0$. Figure 71 shows one such region. The practical significance of such a region was clarified later on for one of the types of strong-focusing accelerators [20], proposed by A.A. Kolomenskiy, V.A. Petukhov, and M.S. Rabinovich.

§3. Envelope of Particle Trajectory

Knowledge of the stability boundary is still not sufficient to determine the extent to which the use of the proposed method of improving stability is advantageous. For a correct understanding of the character of the phenomena it is necessary to calculate the envelope of the particle trajectory.

As indicated in Chapter 2 (page 96), the amplitude of the particle oscillations at an azimuth θ is*:

$$F_\theta = \sqrt{\frac{f(\theta)}{f(\theta_i)}\left[\gamma_{nach}^2 + f(\theta_i)(\gamma-\gamma_{otn})^2\right]}, \qquad (19)$$

where γ is the angle of entry of the particle into the accelerator chamber, χ_{nach} is the initial deviation of the particle from the equilibrium orbit, and θ_i is the azimuth of the injector. We shall show that for the accelerator under consideration Relation (19) is also applicable.

With the aid of Relation (19) we can answer several important questions.

1. The influence of the deviation of the angle of emission of the

particle from the optimal direction on the amplitude of the oscillations must be known so as to calculate the collisions between the particles and the injector. This influence is determined by the factor $f(\theta_1)$.

2. The injection efficiency is also determined by the change in the angle γ_{opt} during the course of the injection, provided the angle γ_{opt} is not very small.

3. The dimension of the accelerator chamber depends also on the function $\Phi(\theta)$, which determines the collisions between the particles and the chamber walls.

Let us proceed to determine the envelope. Assume that the injector is placed at a certain azimuth $\theta_1 = 0$; m = 0. The initial deviation from the equilibrium orbit was denoted χ_{nach} and the angle of particle emission by γ:

$$\gamma = \frac{\chi'_{нач}}{R} = \frac{1}{R}\left(\frac{d\chi}{d\theta}\right)_{нач}.$$

Then we have, in accordance with (13),

$$\begin{aligned} &D\psi(0_i) + D^*\psi^*(0_i) = \chi_{нач}; \\ &D\psi'(0_i) + D^*\psi'^*(0_i) = R\gamma, \text{ где } \psi' = \frac{d\psi}{d\theta}. \end{aligned} \tag{20}$$

From (20) we readily obtain

$$D = \frac{i}{2}[\chi_{нач}\psi'^*(0_i) - R\gamma\psi^*(0_i)].$$

The oscillations at a certain azimuth θ are, in accordance with (13), sinusoidal with frequency $N\mu$. The square of the oscillation amplitude is

$$F_0^2(0) = 4|D\psi(0)|^2 = |\chi_{нач}\psi'(0_i) - R\gamma\psi(0_i)|^2\psi(0)\psi^*(0). \tag{21}$$

Recognizing that the Wronskian of the functions ψ and ψ^* is equal to 2/i, we transform (21) into

$$F_0^2(0) = \frac{\psi(0)\psi^*(0)}{\psi(0_i)\psi^*(0_i)}\left\{\chi_{нач}^2 + \right.$$

$$\left. + \left[R\gamma\psi(0_i)\psi^*(0_i) - \frac{\chi_{нач}}{2}(\psi'(0_i)\psi^*(0_i) - \text{c.c.})\right]\right\}. \tag{22}$$

The optimal angle of emission of the particle from the injector will be defined as the emission angle for which the amplitude of the oscillations is minimal. It is seen from (22) that

$$R\gamma_{corr}=\frac{\chi_{max}}{2}\left[\frac{\psi'(\theta_i)}{\psi(\theta_i)}+\frac{\psi'^{*}(\theta_i)}{\psi^{*}(\theta_i)}\right]=\frac{\chi_{max}}{2}\left[\frac{d\ln\Phi(\theta)}{d\theta}\right]_{\theta_i}, \tag{23}$$

where we introduce the notation

$$\Phi(\theta)=\psi(\theta)\psi^{*}(\theta); \tag{24}$$

$\Phi(\theta)$ is the modulus of the Floquet functions. Substituting (23) and (24) into (22), we obtain the sought-for formula (19), if we put

$$f(\theta_i)=R\Phi(\theta_i). \tag{25}$$

Thus, to determine all the properties of the envelope it is necessary to calculate only one function, $\Phi(\theta)$. Indeed, the equation of the envelope (19) can now be rewritten in the form

$$F_e^2(\theta)=\frac{\Phi(\theta)}{\Psi(\theta_i)}\left[\chi_{max}^2+R^2|x|^2(\theta_i)\left(\gamma-\frac{\chi_{max}}{2R}\frac{d\ln\Phi(\theta_i)}{d\theta_i}\right)^2\right]. \tag{26}$$

The expressions for $\Phi(\theta)$ will be obtained with the aid of (24) and (13). We first consider $\Phi_1(\theta)$ in a focusing sector.

After several transformations we obtain

$$\Phi_1(\theta)=\Phi_1(0)+\frac{s_2(1+p^2)}{2\varkappa_1 p\sin\mu}[\cos\varkappa_1(\nu_1-2\theta)-c], \tag{27}$$

where

$$\Phi_1(0)=\frac{s\cdot c_2+pc\cdot s_2}{\varkappa_1\sin\mu}. \tag{28}$$

In the derivation of (27) and (28) we used the following identities, obtained from (12):

$$\frac{f+f^{*}}{ff^{*}-1}=\frac{s}{c};\quad \frac{ff^{*}}{f_2}=s\cdot c_2+p\cdot s_2\cdot c. \tag{29}$$

As can be seen from (27), $\Phi_1(\theta)$ has a maximum at the center of the focusing sector:

$$\Phi_1\left(\frac{\nu}{2}\right)=\Phi_1(0)+\frac{s_2(1-c)(1+p^2)}{2\varkappa_1 p\sin\mu}. \tag{30}$$

Let us call attention to the fact that $\Phi_1(0)=\Phi_1(\nu)$.

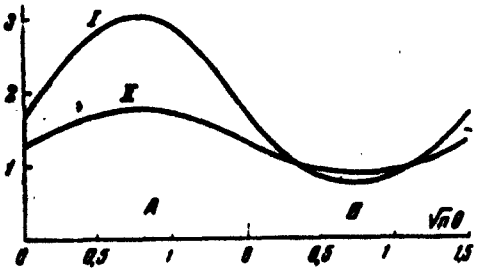

Fig. 72. Modulus of the Floquet function of the free-oscillation equation in the center of the stability region ($\kappa v = 1.5$; $n_1 + n_2 = n_{sr} = 0$): A) focusing sector; B) defocusing sector; I) $\Phi(\theta)/v$; II) $\sqrt{\Phi(\theta)/v}$.

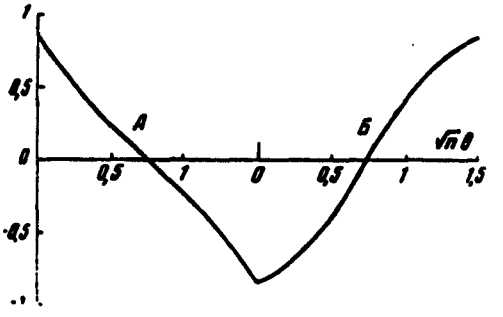

Fig. 73. Plot of the function $2F_3(1, 5, 0, \theta) = 1/\eta v[d \ln \Phi(\theta)/d\theta]$ vs. the azimuth θ in the center of the stability region ($\kappa v = 1.5$; $n_{sr} = 0$): A) focusing sector; B) defocusing sector.

Let us consider the envelope in the defocusing sector.

$$\Phi_2(\nu) = \Phi_1(0) - \frac{s(1+\rho^2)}{2\varkappa_1 \sin\mu}\,|c_2 - \operatorname{ch}\varkappa_2(\nu_2 - 2\delta)|. \tag{31}$$

In the derivation of (31) from (24) we used the identity

$$\frac{|\rho(l+l^*)|}{ll^*+\rho^2} = \frac{c_2}{c_2}. \tag{32}$$

As can be seen from (31), $\Phi_2(\theta)$ has a minimum at the center of the defocusing interval. The minimum value is

$$\Phi_2\left(\frac{\nu}{2}\right) = \Phi_1(0) - \frac{s(c_2-1)(1+\rho^2)}{2\varkappa_1 \sin\mu}. \tag{33}$$

A plot of the function $\Phi(\theta)$ is shown in Fig. 72 for the case when $n_{sr} = 0$ and $\nu\sqrt{n} = 1.5$. Figure 73 shows the values of the logarithmic derivative of $\Phi(\theta)$ for the same case.

The ratio of the maximum of $\Phi(\theta)$ to its minimum is

$$\alpha = \frac{e_1[1+\rho^2-e(1-\rho)^2]+2e\cdot e_2}{e[1+\rho^2+e_2(\rho-\rho^2)]+2\rho e\cdot e_2}. \qquad (34)$$

For the values of the function $\Phi(\theta)$ and α given above we can present several approximate expressions, which are convenient for estimating purposes; this will be done below.

If the particles are injected into the chamber from the start of some sector, then in calculating the collisions with the injector it is necessary to take into account the value of $\Phi(0)$. In the problem of collisions with the walls, the quantity $\Phi_1(\nu/2)$ assumes the same role. But these two problems are closely related with each other. Indeed, we should place the injector at such distances from the orbit, as to make the particle not collide with the wall. The change in distance between the orbit and the injector also greatly influences the number of particles colliding with the injector. Therefore, by way of an estimate of the "convenience" of the focusing method proposed, we introduce the concept of "effective radius of the accelerator."

This "effective radius" will have a somewhat different value for radial than for vertical oscillations. In ordinary accelerators we have

$$R_{eff} = \frac{R}{\nu} = \begin{cases} \frac{R}{\sqrt{n}} & \text{for vertical oscillations} \\ \frac{R}{\sqrt{1-n}} & \text{for radial oscillations} \end{cases} \qquad (35)$$

which is always somewhat larger than the geometrical radius R.

The quantity $\Phi_1(\nu/2)$ can be represented in the form:

$$\Phi_1\left(\frac{\nu}{2}\right) = \nu F_1(x; a); \quad \begin{matrix} x^2 = n\nu^2 \\ a = n_{cp}\nu^2. \end{matrix} \qquad (36)$$

The focusing is the same vertically and radially, if $n_{sr} = 1/2$

and $a = 1 \cdot \nu^2/2 \approx 0$. Let us consider therefore the function

$$F_1(x; 0) = \frac{2\sqrt{3}\left(1 + \frac{x^2}{4} - \frac{x^4}{80} + \ldots\right)}{x^2\sqrt{1 - \frac{x^4}{12} + \ldots}}.$$

A plot of the function $F_1(x; 0)$ is shown in Fig. 74. The function $F_1(x; 0)$ reaches a minimum when $x^2 = n\nu^2 = 2.25$. The minimum value of $F_1(x; 0)$ is

$$\min F_1(x; 0) = 3{,}026. \qquad (37)$$

Near the minimum, the function $F_1(x; 0)$ changes very little. For example, in the interval

$$1{,}2 < n\nu^2 < 3. \qquad (38a)$$

the function $F_1(x; 0)$ changes by not more than 30%, while in the interval

$$1{,}7 < n\nu^2 < 2{,}8 \qquad (38b)$$

it changes by not more than 10%. Outside of these intervals, particularly toward larger values of $n\nu^2$, the function $F_1(x; 0)$ increases rapidly. For example, when $n\nu^2 = 3.497$ the function is $F_1 = 16.6$ and it becomes infinite when $n\nu^2 = 3.516$.

Thus, if we choose $x^2 = n\nu^2$, say in the interval (38b), we get

$$R_{ef} \approx 3\nu R.$$

For example, for the accelerator first proposed for the Brookhaven laboratory ($\nu = 2.62 \cdot 10^{-2}$), $R_{ef} \approx R/13$, if $2500 < n < 4100$. In an ordinary accelerator with $n = 0.6$ we have

$$R_{ef} = \begin{cases} 1.6\ R \text{ for radial oscillations} \\ 1.3\ R \text{ for vertical oscillations} \end{cases}$$

Thus, the effective radius of a strong-focusing accelerator is approximately 17-20 times smaller than for an ordinary accelerator (for the data of the hypothetical Brookhaven accelerator). Later on it became necessary to reduce somewhat the focusing in the projected strong-focusing accelerators, so as to decrease the required accuracy

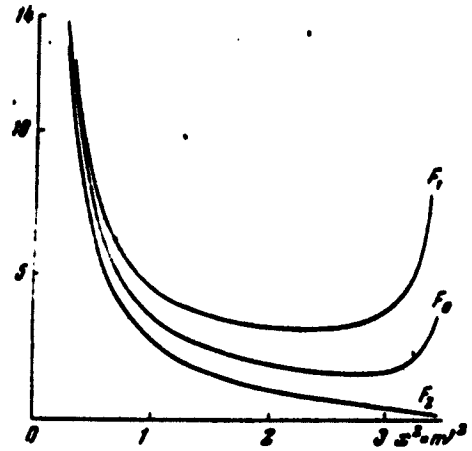

Fig. 74. Plot of the functions F_0, F_1, and F_2 for $n_{sr} = 0$.

with which the magnet had to be manufactured. In these projects R_{ef} is nearly five or six times smaller than R. Let us assume that the sector subtends an angle ν which varies in inverse proportion to the radius R, and then R_{ef} remains constant, and the optimum value of $\underline{n}$ along with the stability region varies in inverse proportion to the square of R.

The oscillation frequency in the range of values (38b) is approximately $N\mu = N\pi/2 = \pi^2/2\nu$, i.e., N/4 times larger than the revolution frequency.

In analogy with the preceding, the functions $\Phi_2(\nu/2)$ and $\Phi_1(0)$ can be written in the form

$$\Phi_1(0) = \nu F_0(x;\ a);\ \Phi_2\left(\frac{\nu}{2}\right) = \nu F_2(x;\ a). \qquad (39)$$

A plot of the functions $F_0(x;\ 0)$ and $F_2(x;\ 0)$ is shown in Fig. 74. The function $F_0(x;\ 0)$ has a minimum at $n\nu^2 = 2.75$:

$$\min F_0(x;\ 0) = 1{,}545.$$

The function $F_2(x;\ 0)$ drops to zero at the limiting value $x = \sqrt{n}\cdot\nu = 1.875$.

The angle γ_{opt}, defined in (23), can be represented in the form

$$\gamma_{opt} = \frac{\gamma_{max}}{R} x_1,\ F_2(x;\ a;\ 0). \qquad (40)$$

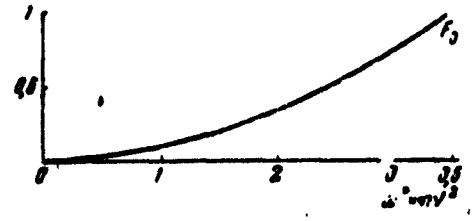

Fig. 75. Dependence of the function F_3 on $x^2 = n\nu^2$ for $n_{sr} = 0$ and $\theta = 0$.

Figure 73 shows a plot of the function F_3 vs. the angle θ for $x = \sqrt{n} \cdot \nu = 1.5$; $a = 0$. Figure 75 shows a plot of F_3 as a function of $x^2 = n\nu^2$, when $a = n_{sr}\nu^2 = 0$ and $\theta = 0$. If the injector is placed halfway between the sectors, then in the Brookhaven accelerator γ_{opt} will change during the process of injection* from 0 to 0.5°. If the beam has a small angle scatter, of the order of several minutes, then the particles will be captured only during a small fraction of the time of the injection process (i.e., the process when the orbit is constricted from the injector to the center of the accelerating chamber). This phenomenon can be avoided by placing the end of the injector in the middle of some sector, preferably in the middle of the sector where $n_1 < 0$. Indeed, at any azimuth we have

a) $\frac{\partial F_r^2(\psi)}{\partial \Phi(\psi_i)} > 0$, when $\chi_{max} < R_{eff}\gamma$;

b) $\frac{\partial F_r^2(\psi)}{\partial \Phi(\psi_i)} < 0$, when $\chi_{max} > R_{eff}\gamma$.

Case "b" is realized for the radial oscillations, and case "a" for the vertical oscillations. Consequently, the amplitude of the vertical oscillations is minimal if $\Phi(\theta_1)$ is minimal, and the amplitude of the radial oscillations is minimal when $\Phi(\theta_1)$ is maximal. This is precisely the situation in the middle of the sector where $n_1 < 0$.

In practice, it becomes necessary to forego prolonged injection in strong-focusing accelerators. The particle is captured in the accel-

eration mode only during one particle revolution.

§4. Azimuthal Asymmetry

If the magnetic field along the equilibrium radius depends on the azimuth θ

$$0<\theta<2\pi;\quad H(R_0;\ \theta)=H_0(R_0)[1+h(\theta)], \tag{41}$$

then, as is well known, in first approximation the equations (4) assume the form

$$\chi''+\varkappa^2(\theta)\chi=-R_0h(\theta), \tag{42}$$

where

$$\varkappa^2(\theta)=\begin{cases}\varkappa_1^2 & \text{in focusing sectors}\\ -\varkappa_2^2 & \text{in defocusing sectors.}\end{cases}$$

Let us consider the Sturm-Liouville equation

$$\chi''+[\varkappa^2(\theta)+\lambda]\chi=0, \tag{43}$$

Let us find the eigenfunctions and the eigenvalues λ from the condition of the periodicity of the solutions

$$\chi(0)=\chi(2\pi);\quad \chi'(0)=\chi'(2\pi).$$

We can use the general solution obtained in §2 if we make everywhere the following substitution:

$$\varkappa_1^2\to\varkappa_1^2+\lambda;\quad \varkappa_2^2\to\varkappa_2^2-\lambda.$$

The periodicity conditions stipulate that $\mu = 2\nu k$, i.e.,

$$\cos\mu=\cos 2\nu k=\cos\sqrt{x^2+\Lambda_k}\operatorname{ch}\sqrt{x^2-\Lambda_k}-\frac{\Lambda_k\sin\sqrt{x^2+\Lambda_k}\cdot\operatorname{sh}\sqrt{x^2-\Lambda_k}}{\sqrt{x^4-\Lambda_k^2}}, \tag{44}$$

where

$$\Lambda_k=(\lambda_k+n_{cp})\nu^2,\qquad x=\sqrt{n}\nu. \tag{45}$$

Solving the transcendental equation (44) we obtain the spectrum of the eigenvalues λ_k.

For the case $\Lambda_k \ll 1$ and $x^2 < 12$ we obtain approximately with the aid of Formulas (18) or (11') a total of N values of λ_k:

$$+\lambda_k = -n_{sp} + \Delta n_\rho \sin^2 \nu k + n_{sp} =$$
$$= \frac{1}{1 - \frac{n^2 \nu^2}{45}} \left[\frac{\sin^2 \nu k}{\nu^2} - 1 - \frac{n^2 \nu^2}{12} \right] + n_{sp}. \qquad (46)$$

When $\nu \to 0$ the eigenvalue $-\lambda_k$ goes over into the ordinary denominator in the Fourier coefficients of the distortion of the equilibrium orbit

$$+\lambda_k \to k^2 - 1 + n_{sr}.$$

In ordinary accelerators an important role is played by the smallest value λ_1. In our case other smallest λ_k play an appreciable role.

We have obtained only N eigenvalues. The others are obtained from (44) graphically. However, they are large and therefore play a small role.

Whereas the first group of N values of λ_k corresponds to the branch $\cos \mu_\rho = 1$ on Fig. 70, the second group of N values of λ_k will correspond to the branch $\cos \mu_\rho = -1$ on Fig. 71, etc.

The periodic solution of the initial equation can be written in the form

$$\chi(\theta) = R_0 \sum_{i=-\infty}^{i=+\infty} \frac{1}{\lambda_i} \frac{\int_0^{2\pi} h(\xi) \psi_i(\xi) d\xi}{\int_0^{2\pi} \psi_i^2(\xi) d\xi} \psi_i(\theta), \qquad (47)$$

where $\psi_i(\theta)$ is the eigenfunction of Eq. (43). As can be seen from (47), an important role is played in this series only by the terms where λ_i is small. The vanishing of λ_i occurs at certain resonant values of $\underline{n}$. Obviously, $\underline{n}$ should be chosen halfway between the successive resonant values.

We note that we are considering here only the first-order resonances, corresponding in an ordinary accelerator to the vanishing of $\underline{n}$. Parametric resonance sets in also under the indicated values of $\underline{n}$ and furthermore halfway between them. There exists also a large number of linear and nonlinear resonances. For their analysis it is most con-

venient to use the method of averaging difference equations, developed in Chapter 4. Calculation shows that as a rule one cannot go through the resonance and that it is necessary to choose and maintain during the acceleration process nonresonant values of $\underline{n}$. The presence of many strong resonances produces specific difficulties in the construction of a strong-focusing accelerator.

Without carrying out detailed calculations, we have explained why the presence of resonances greatly increases the demands on the accuracy with which strong-focusing accelerators must be built. The inventors of strong focusing did not call attention in their papers to the possibility of resonances, so that their preliminary estimates were too optimistic. They chose by way of an accelerator example an accelerator with very large $n = n_{rez}$, at which value the accelerator will obviously not operate. We were the first to call attention, in 1952, to the role of the resonances.

Putting $n_{sr} = 0$, we obtain for $\nu^2 \ll 1$ the resonant values of n_k:

$$\sin \nu k = \frac{\nu^2 n_k}{2\sqrt{3}}.$$

If $n_k \approx \sqrt{6}/\nu^2$, which corresponds to the optimal values of $\underline{n}$, then

$$k_{res} = \frac{N}{4}; \quad \sin \nu k_{res} = \frac{\sqrt{2}}{2},$$

where 2N is the total number of all the sectors. In this region, the neighboring resonant* values are located at distances

$$\Delta n_k = n_{k+1} - n_k = \frac{\sqrt{6}}{\nu}; \quad \frac{\Delta n_k}{n} \approx \nu. \tag{48}$$

The largest value of λ_k in the resonance region will be obtained by assuming that $n = n_k + (\Delta n_k/n)$. In this case

$$\lambda_k = \frac{1}{2\nu}. \tag{49}$$

Thus, λ_k assumes a rather large value in the interval between resonances. For example, for the Brookhaven accelerator we obtain

$\lambda_k = 20.$

However, inasmuch as the distance between the resonances is on the order of ν, this means that n must be held constant to an accuracy much higher than 2.5%. In this case the amplitude of the corresponding "harmonic" in (47) must not exceed 0.1%, since the distortion of the orbit will amount to 1 cm even at this value of the asymmetry, i.e., 20% of the working region at the start of acceleration and 50% of the working region at the end of acceleration. If we take into account the presence of other resonances, the accuracy requirements imposed on the index n should be increased by a factor of several times.

In the accelerator whose parameters were given in the original paper by Livingston, Courant, and Snyder an important role will be played by the asymmetry harmonics in the region $k = 30$. The first harmonics, unlike ordinary accelerators, are immaterial.

When work on the investigation of resonances became known in 1953, it became necessary to decrease appreciably the focusing so as to reduce the role of the resonances, and the index n had to be decreased by almost 10 times. In this case the significant harmonics turn out to be the eighth to the twelfth.

The data given above are sufficient for a rough estimate of the influence of the asymmetry.

A more detailed investigation of the azimuthal asymmetry and of other perturbing phenomena, as well as the calculation of the eigenfunctions, are found in special articles written by many authors.

§5. Instantaneous Orbits

So far we have not considered the instantaneous orbit situated in the center of the chamber. The magnetic field at the center of the chamber does not depend on the azimuth. On circles with other radii the magnetic field depends on the azimuth, inasmuch as the magnetic

field index has opposite signs in neighboring sectors. Therefore only one central instantaneous orbit will be circular in form. Let us assume that the particle energy remained constant but the instantaneous field increased by an amount $\Delta H_0 = h_0 = \text{const}$ and let us consider how the instantaneous orbit changes if it was at the initial instant in the center of the chamber.

To solve this problem we can use Eq. (42), in which we put $h(\Theta) = h_0 = \text{const}$.

We first solve the problem approximately, using the method of the preceding section. In the present case the only nonvanishing coefficients in the series expansion (47) of the solution of Eq. (42) will be those of the functions whose mean values do not equal zero

$$\int_0^{2\pi} \psi_k(\Theta) \cdot d\Theta \neq 0. \tag{50}$$

Condition (50) will be satisfied if

$$\nu = 2\pi k = 0 + 2\pi k_1,$$

where k and k_1 are integers, i.e.,

$$k = 0;\ N;\ 2N;\ 3N, \text{ etc.}$$

It is easy to obtain the smallest eigenvalue $\lambda_0 = \bar{n}_{kr} - n_{sr}$:

$$\lambda_0 \leqslant \lambda_N \leqslant \lambda_{2N} \ldots. \tag{51}$$

Neglecting approximately all the eigenfunctions except ψ_0, we can write

$$\rho = -\frac{R_0 h_0}{\lambda_0} \cdot \frac{\int_0^{2\pi} \psi(\Xi)\, \psi_0(\Theta)\, d\Xi}{\int_0^{2\pi} \psi_0^2(\Xi)\, d\Xi}.$$

Inasmuch as $\psi_0(\Theta)$ differs little from a constant, we have

$$\rho_{ap} \approx -\frac{R_0 h_0}{\lambda_0} = -\frac{R_0 h_0}{1 - n_{ap}}. \tag{52}$$

Formula (52) serves as a definition for n_{ef}:

$$n_{ap} = 1 - \lambda_0 = 1 - n_{sr} + n_{ap} \approx -\frac{n^2 \nu^2}{12\left(1 - \frac{n^2 \nu^2}{45}\right)} + n_{ap}. \tag{53}$$

The introduced quantity n_{ef} plays the role of the usual $\underline{n}$ in circular accelerators in calculations of the shift of the orbit due to changes in the magnetic field, or in the energy, or in the revolution frequency. As can be seen from (53), n_{ef} is a large negative number.

If the field is constant and the energy changed, then we should have in the right half of Eq. (42) $R_0\Delta E/E\beta^2$ in place of $-R_0h_0$. Consequently,

$$\rho_{ep}=R_0\frac{\Delta E}{E\beta^2(1-n_{ef})};\quad \beta=\frac{v}{c}, \tag{54}$$

where E is the total energy of the particle. With the aid of the relation $\omega_0 = c\beta/R$ and Eq. (54) we readily obtain

$$\rho_{ep}=-\frac{\Delta\omega}{\omega_0}\frac{R}{n_{ef}+\beta^2(1-n_{ef})}. \tag{55}$$

Thus, if we introduce n_{ef}, then all the usual formulas for the displacement of the orbit retain their previous form. An accelerator with variable $\underline{n}$ behaves upon shift of the orbit essentially like an accelerator with a constant negative n_{ef}. This fact will be explained below.

The problem posed in the present section can be solved exactly. For this purpose it is necessary either to sum all the terms of the series (47), or solve the problem anew by the joining method. The latter way is the simpler one.

We shall seek a solution of (42) with h_0 = const in the form

$$\rho_1=-R_0h_0\rho^*\cdot\frac{\left[\cos x_1\left(\frac{\nu}{2}-\theta\right)\right]_{x_1\nu}}{(1+\rho^2)\sin x_1\frac{\nu}{2}}-\frac{R_0h_0}{x_1^2} \tag{56}$$

in the focusing sectors and

$$\rho_2=-R_0h_0\rho^*p\cdot\frac{\left[\cos x_2\left(\frac{\nu}{2}-\theta\right)\right]_{x_2\nu}}{(1+\rho^2)\sin\frac{x_2\nu}{2}}+\frac{R_0h_0}{x_2^2} \tag{57}$$

in the defocusing sectors.

It is easy to verify that (56) and (57) are really the solutions of (42) in the focusing and defocusing sectors for arbitrary values of ρ^*. The form of the functions (56) and (57) was chosen such as to make $\rho'_1(\nu) = \rho'_2(0)$ and $\rho'_1(0) = \rho'_2(\nu)$, where the prime denotes differentiation with respect to the angle θ. The value of the constant ρ^* is obtained from the condition

$$\rho_1(\nu) = \rho_2(0).$$

The other necessary equation, $\rho_1(0) = \rho_2(\nu)$, will be satisfied automatically. We readily obtain that

$$\rho^* = \frac{(1+p^2)^2 \operatorname{sh}\frac{\varkappa_2\nu}{2} \cdot \sin\frac{\varkappa_1\nu}{2}}{\nu\varkappa_1^2\left[p\sin\frac{\varkappa_1\nu}{2}\operatorname{ch}\varkappa_2\frac{\nu}{2} - \operatorname{sh}\frac{\varkappa_2\nu}{2}\cos\frac{\varkappa_1\nu}{2}\right]}. \qquad (58)$$

It is also convenient to bear in mind another form for expressing ρ^*:

$$\rho^* = \frac{(1+p^2)^2\left[\varkappa_1(1-c) - p\varkappa_2(1-c_2)\right]}{2p\varkappa_1\nu(1-\cos\mu)}. \qquad (59)$$

Thus, the new instantaneous orbit has a form similar to the envelope calculated in §3. The maximum value is $|\rho|_{max} = |\rho_1(\nu/2)|$ and the minimum $|\rho|_{min} = |\rho_2(\nu/2)|$. The average value ρ_{sr} is

$$\rho_{sr} = -R_0 h_0 \rho^* - (1-p^2)\frac{R_0 h_0}{2\varkappa_1^2}. \qquad (60)$$

From the definition of n_{ef} we have

$$\rho_{sr} = -\frac{R_0 h_0}{1-n_{ef}} = -R_0 h_0\left(\rho^* + \frac{(1-p^2)}{2\varkappa_1^2}\right).$$

Consequently,

$$n_{ef} = 1 - \frac{1}{\rho^* + \frac{1+p^2}{2\varkappa_1^2}} \approx n_{sr} - \frac{n^2\nu^2}{12}.$$

If $\cos\mu = 0$ and $n_{sr} = 0$ then the exact formula yields

$$n_{ef} = 1 - 0{,}2061n; \quad \nu\sqrt{n} = \frac{\pi}{2}. \qquad (61)$$

From the approximate formula (53) we obtain $n_{ef} = 1 - 0.2056n$. We see from this that the approximate formula is quite convenient for

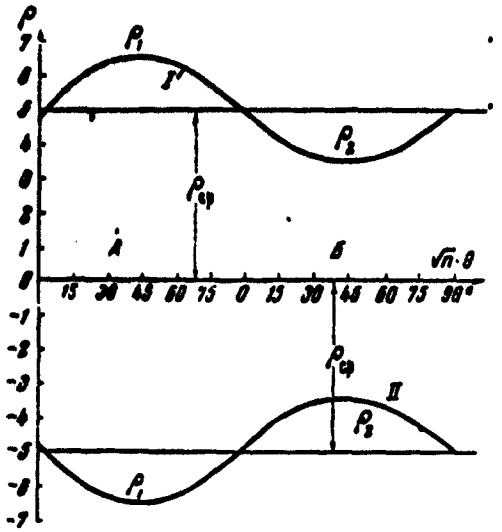

Fig. 76. Instantaneous orbits with radius larger than (I) and smaller than (II) the average radius at the center of the stability region ($\kappa v = \pi/2$ and $n_{sr} = 0$): A) focusing sector; B) defocusing sector.

practical calculations. In this case, i.e., when $\cos \mu = 0$ and $n_{sr} = 0$, we get

$$\rho_1 = \rho_{ср} + \rho_{ср}\left[0{,}8 - 1{,}1\cos\left(\frac{\pi}{4} - \frac{\pi\theta}{2\nu}\right)\right];$$
$$\rho_2 = \rho_{ср} + \rho_{ср}\left[1{,}2 - 0{,}9\mathrm{ch}\left(\frac{\pi}{4} - \frac{\pi\theta}{2\nu}\right)\right]. \qquad (62)$$

As can be seen from (62) and from Fig. 76, the shift in the instantaneous orbit $\rho(\theta)$ differs at the most from ρ_{sr} by approximately $\pm 0.3\ \rho_{sr}$:

$$|\rho(\theta) - \rho_{ср}|_{ср} = 0{,}2\ \rho_{ср}.$$

It is now easy to understand why our formulas for the displacement of the orbit contain not n_{sr} but n_{ef}.

Indeed, the average value of the field on a circle shifted from the central one by an amount ρ_{sr} is determined by the value of n_{sr}:

$$H_{ср}(R_0 + \rho_{ср}) = H(R_0)\left(1 - \frac{n_{ср}\rho_{ср}}{R_0}\right).$$

But the particle does not move along a circle with radius $R_0 + \rho_{sr}$, but moves on a wavy orbit, defined say by Eqs. (56) and (57) or (62) and Fig. 76. In both sectors (focusing and defocusing) the particle deviates from a circle with radius $(R_0 + \rho_{sr})$ toward the direction where the field decreases if $\rho_{sr} > 0$ or increases if $\rho_{sr} < 0$. Thus, at large radii ($\rho_{sr} > 0$), the particle moves effectively in much weaker fields, and at small radii ($\rho_{sr} < 0$) it moves in much stronger fields. For example, in the case considered above ($\cos \mu = 0$) the particle deviates in the mean from a circle with radius $R_0 + \rho_{sr}$ by $0.2\rho_{sr}$.* Consequently, the average field on the orbit is

$$H_{sr} \text{ (on orbit)} = H(R_0)\left[1 - n_{ef}\frac{\rho_{sr}}{R_0} + n\frac{0.2\rho_{sr}}{R_0}\right],$$

and $n_{ef} = n_{sr} - 0.2n$. Thus, we again obtain Formula (61).

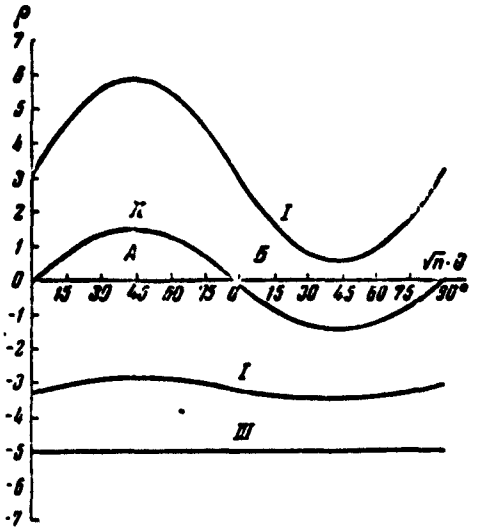

Fig. 77. Envelope of the particle trajectory (I) in the center of the stability region ($\kappa\nu = \pi/2$ and $n_{sr} = 0$) for a shifted instantaneous orbit (II). The average orbit (III) is situated at $\rho = -5$: A) focusing sector; B) defocusing sector.

The results of §3 remain in force if we measure the displacement

from the new orbit, and the angles from the direction tangent to this new orbit. As a result, the form of the envelope becomes distorted. The direction of the optdmal angles of particle emission change. Figure 77 shows the envelope for the case when ρ_{gr} and the amplitude of the oscillations are approximately equal to each other.

§6. The Phase Equation

To derive the phase equation it is essential to know how the revolution period changes with changing particle energy.

In calculating the length of the particle trajectory it is possible to replace the instantaneous wave-like orbit (see §5) by a circle with average radius. Thus, upon change in the average radius by ρ_{gr}, the length of the orbit increases by $2\pi\rho_{gr}$. The resultant error is small. For example, the true increment in the orbit Δs when $\cos \mu = 0$ lies between the two close limits:

$$2\pi\rho_{gr} < \Delta s < 2\pi\rho_{gr}\left(1+0{,}5\frac{\Delta E}{E\beta^2}\right).$$

Neglecting the second-order correction $\pi\rho_{gr}\Delta E/E\beta^2$, we obtain a phase equation which differs from that for an ordinary accelerator in only one respect: n is replaced everywhere by n_{ef}. Indeed, as was shown many times, the phase equation can be derived from the relations:

$$T=\frac{2\pi E}{ecH(E,\ t)};\quad \frac{dE}{dt}=\frac{eV_0\cos\varphi}{T},$$

where T is the period of revolution, V_0 the sum of the voltage amplitudes on all the accelerating electrodes, φ is the phase of the electric field and the instant of passage through the accelerating gap, and $\bar{H}(R, t)$ is the average field along the instantaneous orbit with average radius R. After usual calculations we obtain the phase equation

$$\frac{d}{dt}\left[\frac{E}{e^2K_{n\varphi}}\frac{d\varphi}{dt}\right]-\frac{eV_0\cos\varphi}{2\pi}=-\frac{eV_0\cos\varphi_0}{2\pi}, \qquad (63)$$

where

$$k_{n\varphi}=1+\frac{n_{ef}}{1-n_{ef}}\cdot\frac{1}{\nu^2}, \qquad (64)$$

ω_0 is the frequency of the accelerating electric field;

$$eV_0\cos\varphi_0=\frac{2\pi R_0^2\dot{H}(R_0,t)}{c}(1-\delta)+(1-n_{sf})\frac{\dot{R}_0\dot{H}ET}{R_0}; \qquad (65)$$

$$\dot{H}=\frac{\partial H}{\partial t};\quad \dot{R}_0=\frac{dR_0}{dt}.$$

Here R_0 is the average radius of the orbit, on which the revolution frequency is ω_0. The quantity δ is equal to the ratio of the derivative of the magnetic flux through the orbit with radius R_0 to the quantity $2\pi R_0^2\dot{H}(R_0, t)$.

The entire difference between the phase equation (63) and the ordinary equation lies in the value of K_{ef}. In the nonrelativistic case [$\beta^2 \sim 0$, $|n_{ef}| \gg 1$] we have

$$K_{sf}=-\frac{E_0}{2W}<0,$$

where W is the kinetic energy. In the relativistic case [$(1-\beta^2) \ll 1/|n_{ef}|$] we have

$$K_{sf}=\frac{1}{1-n_{sf}}>0.$$

Thus, for a certain energy E_{kr} the coefficient K_{ef} vanishes:

$$E_{sy}=E_0\sqrt{1-n_{sf}}=E_0\frac{n\nu}{2\sqrt{3}}.$$

If we choose $\underline{n}$ and ν such as to make $\cos\mu = 0$ and $n_{sr} = 0$, then

$$E_{sy}=4{,}54\sqrt{n}E_0=\frac{7{,}13}{\nu}E_{0}. \qquad (66)$$

As was already pointed out by us [10], when $k_{ef} < 0$ the stable phasing point is the phase $-\varphi_0$ (on the rising portion of the accelerating voltage), and the unstable phase is $+\varphi_0$. When the sign of k_{ef} reverses, $+\varphi_0$ and $-\varphi_0$ interchange their roles. The unstable phase is $-\varphi_0$, and the stable one $+\varphi_0$.

Equation (63), as is well known, is the equation of the pendulum with "effective mass" $m_{ef} = E/\omega_0^2 k_{ef}$. At the start of the acceleration process the "effective mass" of the pendulum has a negative value. This

means that in the present case any instability point becomes stable for positive "mass" and vice versa. As the acceleration increases, the absolute value of the "effective mass" of the pendulum increases. This causes the oscillation frequency to decrease and to tend to zero when the total particle energy tends to a value E_{kr}. Simultaneously, the amplitudes of the phase oscillations become rather strongly attenuated. Consequently, when the particles reach energies E_{kr}, all the particle phases freeze in place, so to speak, in the region of the point $-\varphi_0$. Owing to the small value of the phase velocity, the swing of the radial-phase oscillations increases strongly, since the averaging of the particle energy occurs only over the period of the phase oscillations, which is very long. With further increase in energy, the particles gradually begin to move. Those particles which were in the stability region, begin to execute rather large phase oscillations about a new equilibrium point $+\varphi_0$. At the same time, inasmuch as the "effective mass" of the pendulum, which has become positive, decreases strongly, the amplitudes of the phase oscillations, which are large enough as it is, build up strongly.

The indifferent equilibrium position of the pendulum involves, as the energy increases to E_{kr}, additional hidden dangers connected with various perturbations, which can cause strong particle losses owing to the absence of a potential well for the pendulum.

It is therefore desirable to have the maximum energy for a given accelerator lower than E_{kr}, or else to get rid completely of the realignment of the phase region with the aid of special sectors with magnetic fields directed opposite to the main field.

If this cannot be done for some reason, it is necessary to change at the corresponding instant of time the phase of the accelerating field by $2\varphi_0$. Inasmuch as the frequency of the phase oscillations is

very small at that instant, the change in phase can be carried out sufficiently slowly.

In addition, as will be indicated below, it is necessary that the rate of change of the energy be large at that instant of time.

As is known from the theory of the proton synchrotron, an error $\Delta\omega$ in the frequency shifts the equilibrium radius of the orbit by an amount ΔR_0, with

$$\frac{\Delta R_0}{R_0} = -\frac{\Delta\omega/\omega_0}{k_{ef}(1-n_{ef})\beta^2} = -\frac{\Delta\omega/\omega}{n_{ef}+\beta^2(1-n_{ef})}. \qquad (67)$$

The denominator in the right half of (67) is large if $(1 - \beta^2) \gg 1/n_{ef}$. This means that at low energies larger deviations of the frequency from the exact law are permissible. However, later on the denominator of (67) decreases and vanishes when $E = E_{kr}$. The change in the radius of the orbit at that point is determined by the value of $\partial n_{ef}/\partial R$. In any case, the requirements imposed on the accuracy of the frequency during that period will be exceedingly high. But even before that, when the denominator is equal to −10, the accuracy with which the frequency is to be maintained in the Brookhaven accelerator should be much lower than 0.1%. We denote the energy at which the denominator of (67) is equal to −k by E_k:

$$E_k = \frac{E_0\sqrt{1-n_{ef}}}{\sqrt{1+k}} = \frac{E_{cr}}{\sqrt{1+k}}. \qquad (68)$$

A plot of the function $n_{ef} + \beta^2(1 - n_{ef})$ is shown in Fig. 78.

The radial dimension $2\bar{\rho}$ of the separatrix separating the stable oscillations from the unstable motion is, as is well known,

$$2\bar{\rho} = 2R_0\sqrt{\frac{2eV_0\sin\varphi_0(1-\varphi_0\operatorname{ctg}\varphi_0)}{\pi E_0\beta^2[n_{ef}+\beta^2(1-n_{ef})](1-n_{ef})}}; \qquad (69)$$

in the nonrelativistic case we have

$$2\bar{\rho} = \frac{2R_0}{|n_{ef}|}\sqrt{\frac{eV_0|\sin\varphi_0|(1-\varphi_0\operatorname{ctg}\varphi_0)}{\pi E_0}}.$$

For example, at energy $W_1 = 4$ Mev and $eV_0 \sin\varphi_0 = 10^5$ ev, $R_0 \approx$

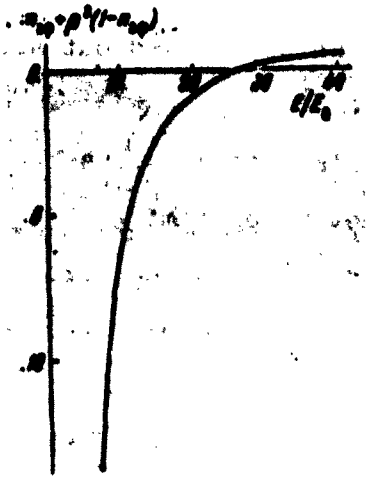

Fig. 78. Dependence of $n_{ef} + \beta^2 (1 - n_{ef})$ on the ratio of the total energy E to the rest energy E_0 ($n_{ef} = -740$).

$\approx 10^4$ cm, and $n_{ef} = -740$, we obtain

$$2\overline{\rho} = 2.5 \text{ cm}.$$

As the energy increases, the size of the separatrix first decreases, and then increases, so that when $E = E_{kr}$ it becomes infinite. The fact that the separatrix becomes infinite in size still means nothing, since the frequency of the phase oscillations vanishes at the same time. However, the rate of change of energy must be sufficiently large, or else particles may be lost near the energy E_{kr} owing to the increase in the radial-phase oscillations. For example, at an energy

$$E_{\pm} \approx E_{s} \pm |n_{s}| W_1,$$

where W_1 is the injection energy, the size of the separatrix will be equal to its size at the start of acceleration.

Let us consider small phase oscillations. Their amplitude α_{max}, as is well known, varies in proportion to $1/\sqrt[4]{n_{ef}}$:

$$\alpha_{max} = \sqrt{\frac{[n_s + \beta^2 (1 - n_s)] \sin \varphi_s}{E}}. \qquad (70)$$

This formula is valid only away from the energy E_{kr}, since near E_{kr} the adiabaticity condition

$$\frac{1}{\omega_1^2} \frac{d\omega_1}{dt} < 1, \qquad (71)$$

is not satisfied, where ω_1 is the frequency of the small phase oscillations

$$\omega_1 = \omega_s \sqrt{\frac{eV_0 K_s \cos \varphi_s}{2\pi E}}.$$

In calculating the change in the amplitude of the oscillations in

the region of E_{kr} it is necessary to use other methods, and in particular, the answer may be obtained by the method which uses Airy functions.

The amplitude ρ_A of the small radial-phase oscillations is

$$\frac{\rho_A}{R_0} = \sqrt{\frac{eV_0 \sin\varphi_0}{2\pi E\beta^2 [n_{ef} + \beta^2(1-n_{ef})](1-n_{ef})}}\,\varepsilon_{max}.$$

Thus, the amplitude of the radial-phase oscillations changes in proportion to

$$\sqrt[4]{\frac{1}{[n_{ef} + \beta^2(1-n_{ef})]\,E^3\beta^4 \sin\varphi_0}}.$$

Consequently, the amplitude of the radial-phase oscillations first decreases rapidly and then, in the region of E_{kr}, increases.

A more detailed investigation of the phase equation in the region of E_{kr} has been the subject of many recent papers [21].

In 1953 the author, together with A.A. Kolomenskiy and V.A. Petukhov, has shown that it is possible to build a strong-focusing system without a critical energy. In particular, there is no critical energy in one of the versions of the annular synchrocyclotron.

From the discussions given above it follows that there is no critical energy if k_{ef} does not reverse sign. Inasmuch as k_{ef} is negative at sufficiently low energies and large n_{ef}, it should be negative also when $\beta^2 = 1$. This is possible if $n_{ef} > 1$.

A large positive n_{ef} denotes that in the given magnetic field the particles with the higher energy move along an orbit with a smaller perimeter. It is particularly convenient to change the perimeter in the desired direction by introducing sectors in which the magnetic field has an opposite direction.

This problem is treated in the papers by A.A. Kolomenskiy [25], V.V. Vladimirskiy and Ye.K. Tarasov [31]. In particular, the latter was able to find the most effective variants for the elimination of

the critical energy, wherein the perturbing sectors with oppositely directed fields are installed with a period which is approximately equal to the period of the free oscillations.

Manuscript Page No.

[Footnotes]

214 Inasmuch as we are not considering the linear sections here, it is convenient to introduce the angle θ in place of the dimensionless length σ.

221 The change in γ_{opt} during the injection process will actually be even larger if one takes into account the form of the displaced instantaneous orbit, as was done in §5.

224 In the general case $\frac{\Delta a_k}{a} = \nu \operatorname{ctg} \pi\nu$ and the maximum value of λ_k in the resonance region is $\frac{\operatorname{ctg} \pi\nu}{2\nu\left(1-\frac{\nu^2}{15}\right)}$.

230 This quality is obtained by averaging one of the expressions in the square brackets in (62).

Manuscript Page No.

[List of Transliterated Symbols]

211 ср = sr = sredniy = average

214 нач = nach = nachal'nyy = initial

214 опт = opt = optimal'nyy = optimal

224 рез = rez = rezonansnyy = resonant

226 кр = kr = kriticheskiy = critical

226 эф = ef = effektivnyy = effective

REFERENCES

1. V.I. Veksler, DAN SSSR [Proc. Acad. Sci. USSR], 43, 346 (1944).
2. V.I. Veksler, DAN SSSR [Proc. Acad. Sci. USSR], 44, 393 (1944).
3. V.I. Veksler, Journ. of Phys. USSR 9, 153 (1945).
4. M.S. Rabinovich, Journ. of Phys. USSR 10, 523 (1946).
5. M.S. Rabinovich, Journ. of Phys. USSR 10, 530 (1946).
6. M.S. Rabinovich, Teoriya sinkhrotrona [Synchrotron Theory], FIAN [Institute of Physics of the Academy of Sciences USSR (im. P.N. Lebedev)], 1946.
7. M.S. Rabinovich, Intensivnost' puchka ionov v fazotrone [Intensity of Ion Beam in a Synchro-Cyclotron], FIAN, 1947.
8. M.S. Rabinovich. Teoriya sovremennykh rezonansnykh uskoriteley [Theory of Modern Resonance Accelerators], FIAN, 1948.
9. S.M. Rytov, K teorii sinkhrotrona [Synchrotron Theory], FIAN, 1947.
10. E.L. Burshteyn and A.A Kolomenskiy, Dvizheniye zapryazhennykh chastits v bystroperemennykh magnitnykh polyakh [Motion of Charged Particles in Rapidly Alternating Magnetic Fields], FIAN, 1947.
11. E.L. Burshteyn, K raschetu intensivnosti v betatrone [Calculating Intensity in a Betatron], FIAN, 1948.
12. O.D. Kazachkovskiy, Dvizheniye chastits v sinkhrofazotrone s lokal'nym uskoryayushchim polem [Motion of Particles in a Proton-Synchrotron with Local Accelerating Field], 1948.
    O.D. Kazachkovskiy, Gorizontal'naya inzhektsiya v sinkhrofazotrone s variatsiyey chastoty [Horizontal Injection in a Proton-Synchrotron with Frequency Variation], 1948.
    O.D. Kazachkovskiy, Vertikal'nyy vvod chastits v protonnyy sinkhrotron [Vertical Introduction of Particles into a Proton

Synchrotron], 1948.

L.L. Sabsovich, K teorii sinkhrotrona [Synchrotron Theory], 1948.

L.L. Sabsovich, Bol'shiye fazovyye kolebaniya chastitsy v sinkhrotrone (nelinearizirovannaya teoriya) [Large Phase Oscillations of a Particle in a Synchrotron (Nonlinearized Theory)], 1948.

13. A.A. Kolomenskiy, Teoriya kratnogo rezonansnogo uskoritelya (mikrotrona) [Theory of Multiple Resonance Accelerator (Microtron)], FIAN, 1950.

14. A.A. Kolomenskiy, Dvizheniye elektronov v aksial'no-simmetrichnom magnitnom pole (vneshnyaya molekula) [Motion of Electrons in Axial-Symmetrical Magnetic Field (Outer Molecule)], FIAN, 1949.

15. M.S. Rabinovich, Teoreticheskoye issledovaniye uskoritelya s peremennym pokazatelem magnitnogo polya [Theoretical Investigation of an Accelerator with Variable Index of Magnetic Field], FIAN, 1953.

16. M.S. Rabinovich, Teoriya sinkhofazotrona [Proton-Synchrotron Theory], FIAN, 1947.

17. M.S. Rabinovich, Issledovaniye dvizheniya chastits v sinkhofazotrone s pryamolineynymi promezhutkame [Investigation or Motion of Particles in Proton-Synchrotron with Rectilinear Clearances], FIAN, 1949.

18. M.S. Rabinovich, A.M. Baladin and V.V. Mikhaylov, K teorii svobodnykh kolebaniy v uskoritele s pryamolineynym promezhutkami [A Theory of Free Oscillations in an Accelerator with Rectilinear Clearances], FIAN, 1950.

19. A.M. Baldin, V.V. Mikhaylov and M.S. Rabinovich, Metod ogibayushchikh dlya issledovaniya svobodnykh kolebaniy [Envelopes Method for Investigation of Free Oscillations], ZhETF [Journal of Experimental and Theoretical Physics], 31, 993 (1956).

20. A.A. Kolomenskiy, V.A. Petukhov and M.S. Rabinovich, Kol'tsevoy fazotron [Annular Synchro-Cyclotron], FIAN, 1953 (see also collection entitled Nekotoryye voprosy teorii tsiklicheskikh uskoriteley [Certain Problems in the Theory of Cyclical Accelerators]), Moscow, Izd. AN SSSR, 1955.

21. A.A. Kolomenskiy and L L. Sabsovich, O prokhozhdenii cherez kriticheskuyu energiyu [Passage Through Critical Energy], ZhTF [Journal of Technical Physics], 26, 576, (1956).

22. M S. Rabinovich, Obshchaya teoriya dvizheniya chastits v sinkhrofazotrone s razrezami [General Theory of the Motion of Patticles in a Proton-Synchrotron with Gaps], FIAN, 1950.

23. A.M. Baldin and V.V. Mikhaylov, Vliyaniye na dvizheniye chastits otkloneniya magnitnogo polya ot raschetnogo i dopuska v sinkhofazotrone AN SSSR [Effect on Motion of Particles of Deviation of Magnetic Field from Theory and Tolerance in Proton-Synchrotron of the Acad. Sci. USSR], FIAN, 1950.

24. A.A. Kolomenskiy, Sovmestnoye rassmotreniye fazovykh i svobodnykh kolebaniy v sinkhofazotrone s razreznym magnitom [Joint Consideration of Phase and Free Oscillations in a Proton-Synchrotron with Split Magnet], FIAN, 1950.

25. M.S. Rabinovich, Rezonansy mezhdu medlennymi kolebaniyami [Resonances Between Slow Oscillations], FIAN, 1950.

26. V.I. Veksler et al., Sinkhrofazotron na energiyu 10 Bev AN SSSR [Ten-Bev Proton Synchrotron of the Acad. Sci. USSR], Atomnaya energiya [Atomic Energy], 4, 22 (1956).

27. M.S. Rabinovich, Effektivnost' inzhektsii [Effectiveness of Injection], FIAN, 1950.

28. L.L. Sabsovich, Vyvod chastits iz sinkhrofazotrona AN SSSR [Withdrawal of Particles From Proton-Synchrotron of the Acad. Sci.

USSR], FIAN, 1950.

29. L.L. Sabsovich, Razrabotka i issledovaniye vysokovol'tnykh inzhektiruyushchikh ustroystv [The Development and Investigation of High-Voltage Injector Devices], FIAN, 1950.

30. L.L. Sabsovich, Vliyaniye rasseyannogo polya magnitnogo shunta na effektivnost' vyvoda iz sinkhofazotrona [The Effect of the Scattered Magnetic Field of a Shunt on the Effectiveness of Withdrawal from a Proton-Synchrotron], FIAN, 1951.

31. V.V. Vladimiskiy and Ye.K. Tarasov, O vozmozhnosti ustraneniya kriticheskoy energii v uskoritele s sil'noy fokusirovkoy [The Possibility of Elimination of Critical Energy in Accelerator with Powerful Focusing], Sbornik [Collection], Izd. AN SSSR [Publishing House of the Acad. Sci. USSR], 1955.

32. D.M. Dennison and T.H. Berlin, Phys. Rev. 70, 764 (1946).

33. N.N. Bogolyubov, O nekotorykh statisticheskikh metodakh v matematicheskoy fizike [Certain Statistical Methods in Mathematical Physics], Kiev, 1945.

34. Yu.A. Mitropol'skiy, Medlennyye protsessy v nelineynykh kolebatel'nykh sistemakh so mnogimi stepenyami svobody [Slow Processes in Nonlinear Oscillatory Systems with Many Degrees of Freedom], PMM, 14, 139 (1950).

35. M.A. Markov, Zakhvat protonom elektrona ostatochnogo gaza kamery v nachal'nyy period uskoreniya [Capture by Proton of Residual-Chamber Gas Electron in the Initial Period of Acceleration], FIAN, 1949.

36. N.M. Blachman and E.D. Courant, Phys. Rev. 74, 140 (1948); 75, 315 (1949).

37. N.M. Frank, Phys. Rev. 70, 177 (1946); Rev. Sci. Instr. 20, 1 (1949).

38. N.M. Blachman and E.D. Courant, Rev. Sci. Instr. 20, 596 (1949).
39. A.M. Baldin, Sinkhrofazotron s kratnym rezonansom i pryamolineynymi promezhutkami [Proton-Synchrotron with Multiple Resonance and Rectilinear Gaps], FIAN, 1949.
40. A.M. Prokhorov, Izlucheniye elektronov v sinkhrotrone (doktorskaya dissertatsiya) [Electron Radiation in Proton-Synchrotron (Doctorate Dissertation)], FIAN, 1951.
41. Ya.P. Terletskiy, Journ. of Phys., USSR 9, 159 (1945).
42. V.V. Mikhaylov, Vliyaniye magnitnogo polya v promezhutke na dvizheniye chastits [Influence of Gap Magnetic Field on the Motion of Particles], FIAN, 1949.
43. A.M. Prokhorov and S.M. Rytov, Rezonans pri n = 0.2 [Resonance with n = 0.2], FIAN, 1949.
44. E.D. Courant, J. Appl. Phys., 20, 611 (1949).
45. T. Teichman, J. Appl. Phys., 21, 1251 (1950).
46. N.M. Blachman, Rev. Sci. Instr., 21, 908 (1950).
47. M.S. Rabinovich, Teoreticheskoye issledovaniye rezonansnykh yavleniy v sinkhrofazotrone AN SSSR [Theoretical Investigation of Resonance Phenomena in Proton-Synchrotron of the Acad. Sci. USSR], 1952.
48. N.M. Blachman, Rev. Sci. Instr. 22, 269 (1951).
49. L.I. Mandel'shtam and N.D. Papaleski, Ob yavleniyakh rezonansa n-roda [Resonance Phenomena of "Kind" n], Collected Works, Vol. 1, p. 13.
50. V.A. Fok, Tablitsy funktsiy Eyri [Tables of Airy Functions], Moscow, 1946.
51. S.E. Barden, Proc. Phys. Soc., B 64, 85 (1951).
52. A.B. Kuznetsov, K voprosu rezonansnogo zakhvata elektronov v betatronnyy rezhim uskoreniya [The Problem of Resonance Capture

or Electrons in Betatron Acceleration Mode], FIAN, 1951.

53. N.M. Krylov and N.N. Bogolyubov, Vvedeniye v nelineynuyu mekhaniku [Introduction to Nonlinear Mechanics], Kiev, 1937.

54. N.M. Blachman, Rev. Sci. Instr. 23, 250 (1952).

55. A.I. Zaboyev, Effektivnost' inzhektsii v modeli sinkhrofazotrona (diplomnaya rabota) [The Effectiveness of Injection in a Model Synchro-Positron (Thesis)], FIAN, 1950.

56. N.F. Nelipa, Vliyaniye assimetrii polya na dvizheniye elektronov v betatrone [The Influence of Field Asymmetry on the Motion of Electrons in a Betatron], FIAN, 1949.

57. N.F. Nelipa, Rezonansy mezhdu bystrymi kolebaniyami [Resonances Between Fast Oscillations, FIAN, 1950.

58. E.D. Courant, M.S. Livingston and H. Snyder, Phys. Rev. 88, 1190 (1952).

DISTRIBUTION LIST

DEPARTMENT OF DEFENSE	Nr. Copies
HEADQUARTERS USAF	
AFCIN-3D2	1
ARL (ARB)	1
OTHER AGENCIES	
CIA	1
NSA	6
DIA	9
AID	2
OTS	2
AEC	2
PWS	1
NASA	1
ARMY	3
NAVY	3
RAND	1
NAFEC	1
SPECTRUM	1
PGE	12

MAJOR AIR COMMANDS	Nr. Copies
AFSC	
SCFDD	1
ASTIA	25
TDBTL	5
TDBDP	5
AEDC (AEY)	1
SSD (SSF)	2
AFFTC (FTY)	1
AFSWC (SMF)	1

UNCLASSIFIED